
ANALYTICA CHIMICA ACTA

An international journal devoted to all branches of analytical chemistry

EDITORS

HARRY L. PARDUE (West Lafayette, IN, U.S.A.)

ALAN TOWNSHEND (Hull, Great Britain)

J.T. CLERC (Berne, Switzerland)

WILLEM E. VAN DER LINDEN (Enschede, The Netherlands)

PAUL J. WORSFOLD (Plymouth, Great Britain)

Editorial Advisers

F.C. Adams, Antwerp
M. Aizawa, Yokohama
J.F. Alder, Manchester
C.M.G. van den Berg, Liverpool
A.M. Bond, Bundoora, Vic.
S.D. Brown, Newark, DE
J. Buffle, Geneva
P.R. Coulet, Lyon
S.R. Crouch, East Lansing, MI
R. Dams, Ghent
L. de Galan, Vlaardingen
M.L. Gross, Lincoln, NE
W. Heineman, Cincinnati, OH
G.M. Hieftje, Bloomington, IN
G. Horvai, Budapest
T. Imasaka, Fukuoka
D. Jagner, Gothenburg
G. Johansson, Lund
D.C. Johnson, Ames, IA
A.M.G. Macdonald, Birmingham
D.L. Massart, Brussels
P.C. Meier, Schaffhausen
M.E. Meyerhoff, Ann Arbor, MI

J.N. Miller, Loughborough
H.A. Mottola, Stillwater, OK
M.E. Munk, Tempe, AZ
M. Otto, Freiberg
D. Pérez-Bendito, Córdoba
C.F. Poole, Detroit, MI
S.C. Rutan, Richmond, VA
J. Ruzicka, Seattle, WA
A. Sanz-Medel, Oviedo
S. Sasaki, Toyohashi
T. Sawada, Tokyo
K. Schügerl, Hannover
M.R. Smyth, Dublin
M. Thompson, Toronto
G. Tölg, Dortmund
Y. Umezawa, Tokyo
E. Wang, Changchun
J. Wang, Las Cruces, NM
H.W. Werner, Eindhoven
O.S. Wolfbeis, Graz
Yu.A. Zolotov, Moscow
J. Zupan, Ljubljana

ANALYTICA CHIMICA ACTA

Scope. *Analytica Chimica Acta* publishes original papers, preliminary communications and reviews dealing with every aspect of modern analytical chemistry. Reviews are normally written by invitation of the editors, who welcome suggestions for subjects. Preliminary communications of important urgent work can be printed within four months of submission, if the authors are prepared to forego proofs.

Submission of Papers

Americas

Prof. Harry L. Pardue
Department of Chemistry
1393 BRWN Bldg, Purdue University
West Lafayette, IN 47907-1393
USA
Tel: (+ 1-317) 494 5320
Fax: (+ 1-317) 496 1200

Computer Techniques

Prof. J.T. Clerc
Universität Bern
Pharmazeutisches Institut
Baltzerstrasse 5, CH-3012 Bern
Switzerland
Tel: (+ 41-31) 654171
Fax: (+ 41-31) 654198

Other Papers

Prof. Alan Townshend
Department of Chemistry
The University
Hull HU6 7RX
Great Britain

Tel: (+ 44-482) 465027
Fax: (+ 44-482) 466410

Prof. Willem E. van der Linden
Laboratory for Chemical Analysis
Department of Chemical Technology
Twente University of Technology
P.O. Box 217, 7500 AE Enschede
The Netherlands

Tel: (+ 31-53) 892629
Fax: (+ 31-53) 356024

Prof. Paul Worsfold
Dept. of Environmental Sciences
University of Plymouth
Plymouth PL4 8AA
Great Britain

Tel: (+ 44-752) 233006
Fax: (+ 44-752) 233009

Submission of an article is understood to imply that the article is original and unpublished and is not being considered for publication elsewhere. *Anal. Chim. Acta* accepts papers in English only. There are no page charges. Manuscripts should conform in layout and style to the papers published in this issue. See inside back cover for "Information for Authors".

Publication. *Analytica Chimica Acta* appears in 14 volumes in 1993. The subscription price for 1993 (Vols. 267-280) is Dfl. 4214.00 plus Dfl. 462.00 (p.p.h.) (total approx. US\$ 2672.00). *Vibrational Spectroscopy* appears in 2 volumes in 1993. The subscription price for *Vibrational Spectroscopy* (Vols. 4 and 5) is Dfl. 700.00 plus Dfl. 66.00 (p.p.h.) (total approx. US\$ 437.75). The price of a combined subscription (*Anal. Chim. Acta* and *Vib. Spectrosc.*) is Dfl. 4592.00 plus Dfl. 528.00 (p.p.h.) (total approx. US\$ 2925.75). All earlier volumes (Vols. 1-266) except Vols. 23 and 28 are available at Dfl. 259.50 (US\$ 148.25), plus Dfl. 18.00 (US\$ 10.25) p.p.h., per volume. The Dutch guilder price is definitive. The U.S. dollar price is subject to exchange-rate fluctuations and is given only as a guide. Subscriptions are accepted on a prepaid basis only, unless different terms have been previously agreed upon.

Our p.p.h. (postage, packing and handling) charge includes surface delivery of all issues, except to subscribers in the U.S.A., Canada, Australia, New Zealand, China, India, Israel, South Africa, Malaysia, Thailand, Singapore, South Korea, Taiwan, Pakistan, Hong Kong, Brazil, Argentina and Mexico, who receive all issues by air delivery (S.A.L.-Surface Air Lifted) at no extra cost. For Japan, air delivery requires 25% additional charge of the normal postage and handling charge; for all other countries airmail and S.A.L. charges are available upon request.

Subscription orders. Subscription orders can be entered only by calendar year and should be sent to: Elsevier Science Publishers B.V., Journals Department, P.O. Box 211, 1000 AE Amsterdam, The Netherlands. Tel: (+31-20) 5803 642, Telex: 18582, Telefax: (+31-20) 5803598, to which requests for sample copies can also be sent. Claims for issues not received should be made within six months of publication of the issues. If not they cannot be honoured free of charge. Readers in the U.S.A. and Canada can contact the following address: Elsevier Science Publishing Co. Inc., Journal Information Center, 655 Avenue of the Americas, New York, NY 10010, U.S.A. Tel: (+1-212) 6333750, Telefax: (+1-212) 6333990, for further information, or a free sample copy of this or any other Elsevier Science Publishers journal.

Advertisements. Advertisement rates are available from the publisher on request.

Detailed "Instructions to Authors" for *Analytica Chimica Acta* was published in Volume 256, No. 2, pp. 373-376. Free reprints of the "Instructions to Authors" of *Analytica Chimica Acta* and *Vibrational Spectroscopy* are available from the Editors or from: Elsevier Science Publishers B.V., P.O. Box 330, 1000 AH Amsterdam, The Netherlands. Telefax: (+31-20) 5862845.

US mailing notice - *Analytica Chimica Acta* (ISSN 0003-2670) is published biweekly by Elsevier Science Publishers (Molenwerf 1, Postbus 211, 1000 AE Amsterdam). Annual subscription price in the USA US\$ 2672.00 (subject to change), including air speed delivery. Second class postage paid at Jamaica, NY 11431. *USA Postmasters:* Send address changes to *Anal. Chim. Acta*, Publications Expediting, Inc., 200 Meacham Av., Elmont, NY 11003. Airfreight and mailing in the USA by Publication Expediting.

ANALYTICA CHIMICA ACTA

An international journal devoted to all branches of analytical chemistry

(Full texts are incorporated in CJELSEVIER, a file in the Chemical Journals Online database available on STN International; Abstracted, indexed in: Aluminum Abstracts; Anal. Abstr.; Biol. Abstr.; BIOSIS; Chem. Abstr.; Curr. Contents Phys. Chem. Earth Sci.; Engineered Materials Abstracts; Excerpta Medica; Index Med.; Life Sci.; Mass Spectrom. Bull.; Material Business Alerts; Metals Abstracts; Sci. Citation Index)

VOL. 274 NO. 2

CONTENTS

MARCH 15, 1993

Sensors

- Herbicide biosensor based on photobleaching of the reaction centre of *Rhodobacter sphaeroides*
R. Jockers, F.F. Bier, R.D. Schmid (Braunschweig, Germany), J. Wachtveitl and D. Oesterheld (Martinsried, Germany) 185
- Modification of electrode surfaces with oxidised phenols to confer selectivity to amperometric biosensors for glucose determination
I.M. Christie, P. Vadgama (Salford, UK) and S. Lloyd (London, UK) 191
- Amperometric enzyme electrode with fast response to glucose using a layer of lipid-modified glucose oxidase and Nafion anionic polymer
F. Mizutani, S. Yabuki and T. Katsura (Ibaraki, Japan) 201
- Resonant frequency of a piezoelectric quartz crystal in contact with solutions
S. Kurosawa, H. Kitajima, Y. Ogawa (Sapporo, Japan), M. Muratsugu (Asahikawa, Japan), E. Nemoto (Katsuta, Japan) and N. Kamo (Sapporo, Japan) 209

Electroanalytical Chemistry

- Ultratrace measurements of selenium by cathodic stripping voltammetry in the presence of rhodium
J. Wang and J. Lu (Las Cruces, NM, USA) 219
- Polarographic studies of metal ion complexes of Ampicillin and Amoxycillin
S.J. Lyle and S.S. Yassin (Dhahran, Saudi Arabia) 225

Atomic Spectrometry

- Atomization of tin in saline water media in graphite furnace atomic absorption spectrometry with a tungsten-coated tube using palladium as a chemical modifier
E. Iwamoto, H. Shimazu, K. Yokota and T. Kumamaru (Higashi-Hiroshima, Japan) 231
- Application of inductively coupled plasma atomic emission spectrometry for the certificate analysis of uranium certified reference material: determination of trace impurity elements in U_3O_8 by extraction chromatography
X.J. Yang and J.S. Guan (Beijing, China) 237

Environmental Analysis

- Determination of butyltin compounds in sediment using gas chromatography-atomic absorption spectrometry: comparison of sodium tetrahydroborate and sodium tetraethylborate derivatization methods
Y. Cai, S. Rapsomanikis and M.O. Andreae (Mainz, Germany) 243
- Determination of fluorine and iodine in biological materials
M. Langenauer, U. Krähenbühl (Berne, Switzerland) and A. Wytttenbach (Villigen, Switzerland) 253
- Determination of platinum in environmental and geological samples by radiochemical neutron activation analysis
D. Wildhagen and V. Krivan (Ulm, Germany) 257

Flow-Injection Analysis

- Direct determination of benzene in gasoline by flow-injection Fourier transform infrared spectrometry
M. Gallignani, S. Garrigues and M. De la Guardia (Valencia, Spain) 267

(Continued overleaf)

มหาวิทยาลัยเทคโนโลยีพระจอมเกล้าธนบุรี

74 ค.ศ. 2536

Contents (continued)

Entrapped copper(II) carbonate for indirect determination of glycine by flow injection atomic absorption spectrometry J.V. Garcia Mateo and J. Martínez Calatayud (Valencia, Spain)	275
Extraction of dicyanoaurate(I) using supported liquid membranes in a flow-injection manifold: evaluation of extractants D.E. Barnes, M.J.C. Taylor, G.D. Marshall (Randburg, South Africa) and J.F. Van Staden (Pretoria, South Africa)	283
<i>Ion Exchange</i>	
Preparation of an anion-exchange resin with quaternary phosphonium chloride and its adsorption behaviour for noble metal ions M. Fujiwara, T. Matsushita (Otsu, Japan), T. Kobayashi, Y. Yamashoji and M. Tanaka (Suita, Japan)	293
Determination of urinary fluoride by ion chromatography Y. Michigami, Y. Kuroda, K. Ueda and Y. Yamamoto (Kanazawa, Japan)	299
<i>Chemometrics</i>	
Structure–activity relationship study on paraffin inhibitors for crude oils (INIPAR model II) M. Cristante, J.-L. Selves, G. Grassy (Toulouse, France) and J.P. Colin (Saint Martory, France)	303
<i>Activation Analysis</i>	
Determination of sub-ng g ⁻¹ concentrations of thorium and uranium in microelectronic materials by radiochemical neutron activation analysis M. Franek and V. Krivan (Ulm, Germany)	317
<i>Mass Spectrometry</i>	
Influence of operating parameters on ion intensity in glow discharge mass spectrometry M. Saito (Tokyo, Japan)	327
<i>Organic Reagents</i>	
3,5,6-Trisubstituted 1,2,4-triazines as analytical reagents. Part I. Compounds containing the ferrioxime functional group or iron(II)–methine chromophore W.I. Stephen (Birmingham, UK) and M.A. Islam (Dhaka, Bangladesh)	335
3,5,6-Trisubstituted 1,2,4-triazines as analytical reagents. Part II. Compounds containing the cuproine functional group W.I. Stephen (Birmingham, UK) and M.A. Islam (Dhaka, Bangladesh)	347
<i>Other Techniques</i>	
Membrane inlet manometry for the measurement of water activity in aqueous and organic solutions H. Degn and N.-U. Frigaard (Odense, Denmark)	355
A study of the effect of chain length on nearest neighbour interactions of immobilized species J.L. Alves and M.A. Ditzler (Worcester, MA, USA)	361
Numerical treatment of titrations with the formation of a reasonably stable complex: titration of thiocyanate with Hg(II) V. Rodríguez Martín and O. Jiménez de Blas (Salamanca, Spain)	367
<i>Author Index</i>	371

Herbicide biosensor based on photobleaching of the reaction centre of *Rhodobacter sphaeroides*

Ralf Jockers, Frank F. Bier and Rolf D. Schmid

Department of Enzyme Technology, GBF – Gesellschaft für Biotechnologische Forschung, Mascheroder Weg 1,
W-3300 Braunschweig (Germany)

Josef Wachtveitl and Dieter Oesterhelt

Department of Membrane Biochemistry, Max-Planck-Institut für Biochemie, W-8033 Martinsried (Germany)

(Received 19th June 1992; revised manuscript received 30th October 1992)

Abstract

A fast and simple measuring device for the detection of photosystem-II herbicides is presented. Herbicides are monitored by absorption changes at 860 nm after photobleaching for 2 s. This system can be easily miniaturized and consists of three components, sample cell, light source and detector for absorption measurements, and a computer data processing unit. Detection ranges and limits were determined for several herbicides. Plans for further miniaturization are discussed.

Keywords: Biosensors; Herbicides; Photobleaching

Pesticides are of major importance in modern agriculture. Most pesticides are herbicides, and among them photosystem-II (PS-II) herbicides hold the strongest position in the agricultural market [1]. However, their application over a number of decades has led to increasing problems for maintaining water quality. As a consequence, a European Directive for drinking water was passed [2,3]. This has resulted in a high demand for continuous control systems, especially for drinking water from supply stations. Detection methods currently used (LC, GC-MS) [4] are not suitable as rapid screening methods, as they are time consuming and provide only discontinuous analysis. Several attempts have been made

to introduce biological detection systems such as biosensors or enzyme-linked immunosorbent assays (ELISA) to overcome these problems. Detection of PS-II herbicides has been reported using either photosynthetically active cells (*Synechococcus sp.*) [5], chloroplast membranes [6,7] or antibodies directed against herbicides [8–10]. Antibodies allow the specific detection of only one substance, whereas photosystem-based sensors are able to determine all compounds affecting light-induced electron flow. The European Directive for pesticides in drinking water sets maximum concentrations for each individual pesticide and for the sum of all pesticides present. Therefore, sensors for the detection of single compounds and whole classes of pesticides are needed.

In this work, the isolated reaction centre (RC) of *Rhodobacter sphaeroides*, belonging to purple

Correspondence to: R. Jockers, ICGM, Laboratoire d'Immuno-Pharmacologie Moléculaire, 22 rue Méchain, 75014 Paris (France) (present address).

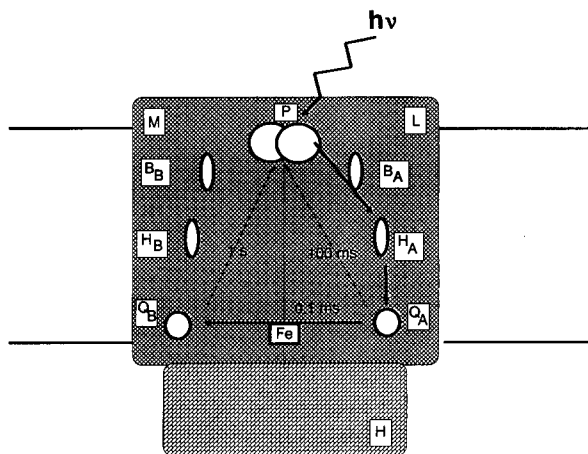


Fig. 1. Schematic representation of the photochemistry and arrangement of the chromophores in the reaction centres of *Rhodobacter sphaeroides*. H, L, M = protein subunits; P = bacteriochlorophyll dimer; B = bacteriochlorophyll; H = bacteriopheophytin; Q_A = primary quinone; Q_B = secondary quinone; Fe = iron; 100 ms = half-time of electron transfer from Q_A to P; 1 s = half-time of electron transfer from Q_B to P; 0.1 ms = electron transfer time from Q_A to Q_B .

bacteria, was selected for the detection of PS-II herbicides. The stability of the bacterial RC was suitable for biosensor application, whereas the stability of the plant system was not. X-ray structural analysis of crystallized RC from purple bacteria and the homology in the primary structure of PS-II from plants and purple bacteria not only indicated similarities in structure and folding but also helped to explain similarities found in function and herbicide binding [11–14]. Herbicide detection was based on the photobleaching of the bacteriochlorophyll dimer (P) (Fig. 1). Photobleaching results in the oxidation of P to P^+ . This process can be monitored by measuring the decrease in absorption at 860 nm; at this wavelength P absorbs but P^+ does not. Apart from the physiological electron transfer pathway via Q_B to other macromolecular complexes, electrons can recombine directly with P^+ . Recombination processes are well known and have been discovered at all the intermediate states between P and Q_B [15] (Fig. 1). Where the Q_B site contains a ubiquinone a recombination rate of 1 s^{-1} is observed, because the transfer from Q_A to Q_B is fast and virtually irreversible. If the Q_B site is empty or

occupied via herbicide binding, the only possible recombination from a Q-site is that from Q_A , with a half-life of 100 ms [16,17]. This sets the basis for measuring the competitive binding of ubiquinone and herbicides to the Q_B site seen as an increase in the recombination rate between 1 and 10 s^{-1} .

Until now, recombination processes were usually initiated by flash excitation and followed by subsequent time-resolved absorption measurements. Here, a measuring method is described in which recombination processes are initiated and followed by continuous irradiation with weak actinic light, resulting in stationary bleaching of the isolated RC. The level of bleaching under constant irradiation reflects the integral of recombination from Q_A and Q_B and hence the occupation of the Q_B sites by herbicides. Irradiance has to be controlled in a way that allows a maximum difference in bleaching levels, obtained between herbicide-filled or -empty and ubiquinone-filled Q_B sites. Recombination experiments with flash excitation were carried out as a control and proved to be an essential method for functional characterization of RCs.

Finally the influence of PS-II herbicides on continuous photobleaching was observed and sensitivity limits were determined.

EXPERIMENTAL

Chemicals

Terbutryn and atrazine were purchased from Riedel-de Haën (Hanover, Germany) and diuron and *o*-phenanthroline from Sigma (Munich, Germany). *N*-Thiazole 3983 was a generous gift from J.F. Kluth (Bayer, Monheim, Germany).

Reaction centre isolation

Growth of *Rhodobacter sphaeroides* and isolation of reaction centres were carried out according to previous work [18].

Removal of ubiquinone

The bound quinone was depleted from the Q_B site of bacterial RC according to the procedure outlined by Okamura et al. [19].

Recombination measurements

Recombination was monitored by time-resolved absorption changes at 860 nm for 2 s. The following components were arranged sequentially on a linear axis: 50-W halogen lamp, 860-nm interference filter, NG5 filter, sample cell and photodiode connected to the data processing unit. Data could be collected every millisecond with an absorbance resolution of about 10^{-4} . Data collection and processing were performed with the program Curveking and Dataqueen [20] using an Atari-ST-1040 personal computer. Measurements were performed with and without dye laser flash excitation (595 nm, 10 ns, 2 mJ per pulse; FL 3001/2 from Lambda Physik GmbH, Göttingen, Germany) at 90° to the axis of the measuring light. When measurements with laser flash excitation were performed, controls without laser flashes were subtracted. The assay contained 180 nM RC, 0.7 mM ubiquinone-0 (UQ_0) in 600 μ l of buffer {20 mM Trizma buffer [tris-(hydroxymethyl)aminomethane] (pH 8.0)}, 0.08% *N,N*-dimethyldodecylamine *N*-oxide (LDAO) and 6 μ l of ethanol or ethanolic herbicide solution.

RESULTS

Normally, photobleaching is induced by a strong actinic flash, exciting all RCs simultaneously. Subsequent recombination is monitored by absorption measurements with non-actinic, i.e., low-intensity light (Fig. 2, curves A). In the present experiments no flash was used, but the continuous absorption measuring light at 860 nm was strong enough to produce complete accumulation of P^+ (Fig. 2, curve B). Under these standard conditions recombination occurs via the Q_B site and is therefore slow (1 s). If electron flow between Q_A and Q_B is blocked, the faster recombination from Q_A dominates and P^+ accumulation is increasingly reduced. This is observed in RCs with a ubiquinone-depleted Q_B site. For example, during RC isolation most of the Q_B ubiquinone was lost. External quinone had to be added to reconstitute the whole electron transfer pathway up to Q_B , to reach maximum steady-state bleaching. Addition of herbicides, binding to Q_B ,

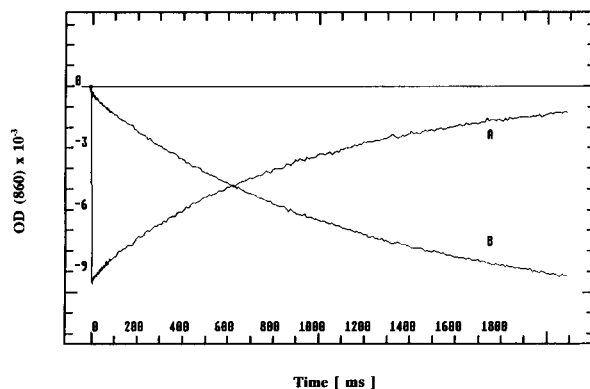


Fig. 2. Bleaching of the bacteriochlorophyll dimer by either (A) excitation at 595 nm (Q_x transition band) with a saturating flash and subsequent recombination at 860 nm (Q_y transition band) or (B) continuous illumination at 860 nm (light intensity in front of the sample cell was 0.5 mW cm^{-2}) in the presence of saturating ubiquinone concentrations (1 mM UQ_0).

produced the same phenomenon because ubiquinone is competitively removed. A sensor was developed that is based on the reduction of the amplitude of P^+ in the photostationary state and which therefore correlates with the strength of herbicide binding.

In most experiments room temperature was chosen as the assay temperature. Heating or cooling of the measuring device between 15 and 30°C caused no observable variation of signal amplitude or sensitivity under these conditions.

Giangiaco and Dutton [21] have shown that the Q_B site binds and functions with a wide variety of different quinones. However, a proper function is strongly dependent on the free-energy difference for electron transfer between Q_A and Q_B . If Q_A is occupied by native ubiquinone-10 (UQ_{10}), functional reconstitution of Q_B is only possible with ubiquinone derivatives [21]. Therefore, only native UQ_{10} and UQ_0 were tested. Concentrations of $1 \mu\text{M}$ UQ_{10} and $100 \mu\text{M}$ UQ_0 were necessary for reconstituting 50% of the slow recombination, indicating 50% occupation of the Q_B site. The reconstitution time was also determined following the recovery of the slow recombination phase. With UQ_{10} this was completed after incubation for 2 min, but for UQ_0 about 120 min were needed. For sensor application UQ_0

was chosen for reconstitution because of its higher water solubility, greater stability in aqueous solution and lower price compared with UQ_{10} . The standard concentration for reconstitution was 0.7 mM UQ_0 , which was sufficient to reconstitute 90% of slow recombination.

The irradiation intensity and measuring time were optimized to give the maximum discrimination between a herbicide-filled and a ubiquinone-filled Q_B site. The level of RC, bleached to a maximum, was determined by saturating flash excitation (Fig. 2, curve A). The light intensity of the continuous measuring light was adjusted so that after 2 s of stationary photobleaching, the maximum value determined by flash excitation was reached. Simultaneously decreasing the measuring light intensity and increasing the measuring time did not enhance the sensitivity of the system towards herbicides. Therefore, 2 s of continuous irradiation with 0.5 mW cm^{-2} in front of the sample cell was chosen with regard to the development of a rapid sensor assay.

The system was tested under various conditions. First, as a control experiment, RC with a quinone-depleted Q_B site and RC incubated with 4 mM *o*-phenanthroline (herbicide) were used. The standard irradiance resulted in no bleaching because under these conditions electron transfer between Q_A and Q_B is totally blocked [19,22]. Both control experiments were also performed with laser flash excitation and recombination from Q_A was observed as expected with proper functioning of the RC (data not shown).

Herbicides were monitored with the same irradiation but in the presence of 0.7 mM UQ_0 . The result for terbutryn, as the absorption changes at 860 nm, is shown in Fig. 3. Figure 4 illustrates the titration curves obtained using different herbicide concentrations. In addition to terbutryn, several other herbicides were chosen for evaluation of this assay system. Classical herbicides such as atrazine (belonging to the class of *s*-triazines [23]) and diuron (belonging to the class of phenylureas) were tested. Both are known to be strong inhibitors of plant photosynthesis but weak inhibitors of bacterial photosynthesis [23]. *o*-Phenanthroline (a phenanthrene derivative) and several recently introduced potent inhibitors of

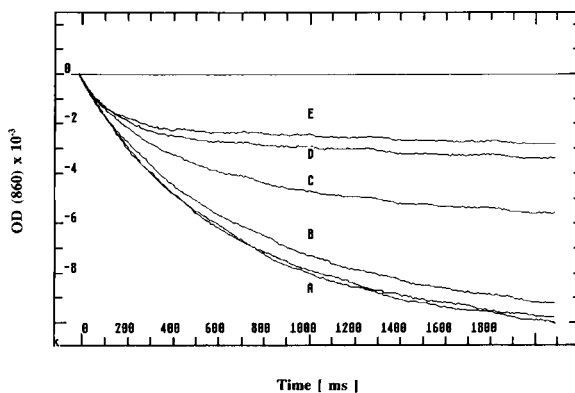


Fig. 3. Time-resolved absorption changes at 860 nm in the presence of different terbutryn concentrations. Continuous illumination for 2 s with 180 nM reaction centre and weak actinic light at 860 nm (intensity as in Fig. 2) in the presence of 0.7 mM UQ_0 were observed. (A) 0 and 0.01 μM terbutryn; (B) 0.1 μM ; (C) 1 μM ; (D) 10 μM ; (E) 100 μM .

both bacterial and plant photosynthesis such as *N*-thiazoles were also tested (Fig. 4) [24]. The results are summarized in Table 1. Whereas atrazine, diuron and *o*-phenanthroline are weak inhibitors of bacterial photosynthesis, terbutryn and *N*-thiazole 3983 are potent inhibitors and could be detected with high sensitivity.

The same RC sample could be used several times without adding new reagents. The standard

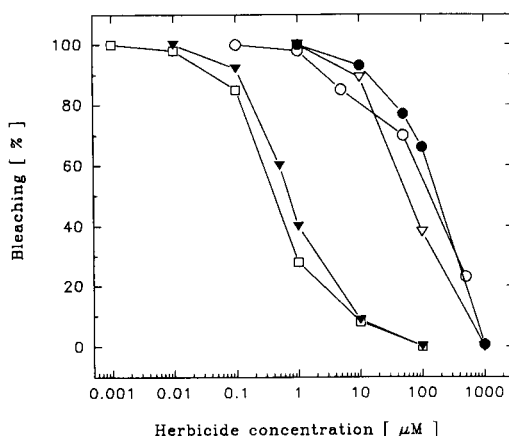


Fig. 4. Titration curves for different photosystem-II herbicides. Herbicide concentrations versus percentage bleaching of bacterial reaction centres at 860 nm. Conditions as in fig. 3. \circ = Atrazine; \bullet = diuron; ∇ = *o*-phenanthroline; \blacktriangledown = terbutryn; \square = *N*-thiazole 3983.

TABLE 1

 I_{50} values and detection limits for PS-II herbicides tested^a

Compound	I_{50} (μM)	Detection limit	
		μM	$\mu\text{g l}^{-1}$
Terbutryn	0.7	0.04	10
Atrazine	150	3	650
<i>o</i> -Phenanthroline	70	10	2300
Diuron	200	20	3960
<i>N</i> -Thiazole 3983	0.4	0.02	7

^a I_{50} = herbicide concentration at which 50% stationary photobleaching was observed in isolated reaction centres of *R. sphaeroides*; 95% bleaching was set as the detection limit.

deviation for 20 repeated measurements with the same RC was less than 2%. The dark adaptation time between subsequent measurements of the same RC sample had to be at least 30 s to allow recovery of the ground state of RC via charge recombination. When high concentrations of herbicide had been applied, poisoned RCs were replaced with fresh ones, because regeneration was time consuming.

Solubilized RCs stored at 4°C showed no change in herbicide binding over more than 6 months. At room temperature the stability did not decrease during the first 60 h.

DISCUSSION

A very simple and rapid measuring device for PS-II herbicides has been developed. Results are available within 2 s by reading the absorption change. A minimum amount of reagent is required. The system is self-regenerating because of electron cycling within the RC. An alternative method would be to test the amount of photobleachable RC, using flash excitation. Work on this approach was discontinued because it required a high-voltage power supply and did not allow the construction of a compact system. As miniaturization is always of interest in the field of biosensor technology, a new prototype further simplified by using an LED with maximum light emission at 860 nm, instead of a halogen lamp and interference filter, is under development. Until now the system has been run in the discontinuous mode, but the new prototype will work in the continuous mode. RCs will be immobilized behind an ultrafiltration membrane and can be quickly exchanged after they have been poisoned with an excess of herbicide.

The bacterial RC proved to be suitable for the detection of several PS-II herbicides. In addition, the remarkable stability of the isolated bacterial RC fulfils the requirements for biosensor application. However, the detection of some agriculturally important herbicides such as atrazine could not be achieved. Recently, mutation at the Q_B site of the RC of *Rhodospseudomonas viridis* has created a high sensitivity towards diuron [25]. In addition to broadening the herbicide specificity of bacterial RCs, the sensitivity has to be enhanced even for herbicides with high affinity to be able to detect the concentrations specified in the European Directive for drinking water [2]. With the help of the detailed structural knowledge of the Q_B site [13] and the availability of genetic manipulation systems for bacterial RC [26], it is hoped in the future to increase the sensitivity towards herbicides by mutation.

The authors thank J.F. Kluth (Bayer, Monheim, Germany) for the generous gift of the *N*-thiazole. Special thanks are due to W. Oettmeier (University of Bochum, Germany) for valuable advice.

REFERENCES

- 1 A. Woodburn and J. McDougall, CountyNatWest Wood Mac (CNWN) Estimates, Agrochemical Service, Update of the Agrochemical Products Section, The Natwest Investment Bank Group, March 1989.
- 2 European Communities, Council Directive of 15th July 1980 Relating to the Quality of Water Intended for Human Consumption, 80/778/EEC, Drinking Water Directive No. L229, Commission of the European Community, Brussels, 1980, p. 11.
- 3 Trinkwasserverordnung, Bundesgesetzblatt, Germany, 1 (1986) 760.
- 4 J. Scherma, Anal. Chem., 61 (1989) 153R.
- 5 D.M. Rawson, A.J. Willmer and A.P.E. Turner, Biosensors, 4 (1989) 299.
- 6 R. Carpentier, C. Loranger, J. Chartrand, M. Purcell, Anal. Chim. Acta, 249 (1991) 55.

- 7 B. Hirschwald, G.M. Zimmermann, S. Normann and K. Haberer, *Z. Wasser Abwasser Forsch.*, 23 (1990) 184.
- 8 C. Wittmann and B. Hock, *Food Agric. Immunol.*, 1 (1989) 211.
- 9 F.F. Bier, W. Stöcklein, M. Böcher, U. Bilitewski and R.D. Schmid, *Sensors Actuators*, B7 (1992) 509.
- 10 P.M. Krämer and R.D. Schmid, *Pestic. Sci.*, 32 (1991) 451.
- 11 J. Deisenhofer, O. Epp, K. Miki, R. Huber and H. Michel, *Nature*, 318 (1985) 618.
- 12 J.P. Allen, G. Feher, T.O. Yeates, H. Komiya and D.C. Rees, *Proc. Natl. Acad. Sci. U.S.A.*, 84 (1987) 5730.
- 13 W. Draber, J.F. Kluth, K. Tietjen and A. Trebst, *Angew. Chem.*, 103 (1991) 1650.
- 14 A. Trebst, *Z. Naturforsch., Teil C*, 41 (1986) 240.
- 15 M.Y. Okamura, R.J. Debus, D. Kleinfeld and G. Feher, in B.L. Trumpower (Ed.), *Function of Quinones in Energy Conserving Systems*, Academic, New York, 1982, p. 299.
- 16 C.A. Wraight, *Isr. J. Chem.*, 21 (1981) 348.
- 17 R.R. Stein, A.L., Castellvi, J.P. Bogacz and C.A. Wraight, *J. Cell. Biochem.*, 24 (1984) 243.
- 18 K.A. Gray, J.W. Farchaus, J. Wachtveitl, J. Breton and D. Oesterheld, *EMBO J.*, 9 (1991) 2061.
- 19 M.Y. Okamura, R.A. Isaacson and G. Feher, *Proc. Natl. Acad. Sci. U.S.A.*, 72(9) (1975) 3491.
- 20 R. Uhl, B. Meyer and H. Desel, *J. Biochem. Biophys. Methods*, 10 (1985) 35.
- 21 K.M. Giangiacomo and P.L. Dutton, *Proc. Natl. Acad. Sci. U.S.A.*, 86 (1989) 2658.
- 22 R.K. Clayton and T. Yamamoto, *Photochem. Photobiol.*, 24 (1976) 67.
- 23 W. Oettmeier and S. Preusse, *Z. Naturforsch., Teil C*, 42 (1987) 690.
- 24 A. Trebst, J. Kluth, K. Tietjen and W. Draber, in H. Frese (Ed.), *Pesticide Chemistry, Advances in International research, Development and Legislation*, VCH, Weinheim, 1991, p. 111.
- 25 I. Sinning, H. Michel, P. Mathis and A.W. Rutherford, *FEBS Lett.*, 256 (1989) 192.
- 26 E.J. Bylina, R.V.M. Jovine and D.C. Youvan, *Biotechnology*, 7 (1989) 69.

Modification of electrode surfaces with oxidised phenols to confer selectivity to amperometric biosensors for glucose determination

I.M. Christie and P. Vadgama

Department of Clinical Biochemistry, University of Manchester, Hope Hospital, Eccles Old Road, Salford M6 8HD (UK)

S. Lloyd

London Hospital Medical College, Turner St., London E1 2AD (UK)

(Received 9th March 1992; revised manuscript received 21st September 1992)

Abstract

The preparation of electrochemical coatings on a platinum anode, using phenol and dopamine solutions, are described. In the amperometric mode, the modified electrode displayed a high degree of selectivity to H_2O_2 and against ascorbate, urate, serum and paracetamol. Such selectivity is superior to that of conventional cellulose acetate membranes used in oxidase based biosensors. Most significantly, with a coated electrode surface, the decrease in paracetamol response while a large H_2O_2 signal is retained, is shown to alleviate the problem of paracetamol interference in a glucose sensor. This glucose sensor based on glucose oxidase is free from any significant paracetamol interference and represents a major advance over existing cellulose acetate membrane devices. The influence of both the phenolic used, and the degree of coating, on the linear response range, response time and lifetime are discussed, and compared with a cellulose acetate membrane.

Keywords: Amperometry; Biosensors; Glucose determination; Modified electrodes; Phenols; Selectivity

Amperometric electrodes themselves do not discriminate between signal and interference currents when used in conjunction with enzymes to form biosensors. During clinical use, the main interferents encountered in patients' serum samples are ascorbate, urate, small peptides and amino acids, and in some cases paracetamol [1].

Means must be found to eliminate the electrode response due to these interfering species. The use of the lowest polarising voltage sufficient

for the intended reaction, is an important factor in reducing the current from undesired electrochemical oxidations [2]; but for many sensors, particularly those based on oxidase enzymes producing hydrogen peroxide [3], this is not sufficient screening. Membranes, such as cellulose acetate, have been developed as permeability barriers to physically exclude interferents, while permitting the product of the enzyme reaction to reach the electrode surface [3,4].

This work considers electrochemical coating as a means of modifying the electrode surface, in order to prevent a range of biological interferents reacting, while permitting the desired reaction to

Correspondence to: I.M. Christie, Department of Clinical Biochemistry, University of Manchester, Hope Hospital, Eccles Old Road, Salford M6 8HD (UK).

occur. The preparation and selectivity properties of such layers are described. With a view to biosensor applications, a glucose sensor is described, with such a coating applied to the electrode surface, and the responses to glucose and interferents are compared to the conventional cellulose acetate membrane device.

Considerable interest has recently been shown in a wide variety of techniques for modification of electrode surfaces [5]. Fouling was encountered during work on the oxidation of phenol by Hedenberg and Freiser [6], using a platinum electrode, and subsequently other metals were investigated by other workers [7]. The inhibition of Br^- and I^- oxidation at a platinum electrode in the presence of phenol [8], was ascribed to virtually complete coverage by phenoxy radicals ($\text{PhO}\cdot$), adsorbed by a charge transfer process. A higher voltage was required for this process (0.9 V vs. SCE) than for the adsorption of neutral molecules (0.3 V vs. SCE). Self inhibition of phenol oxidation was also noted [9]. Oxidation occurred faster than absorption, but as the latter became more complete, both processes tended to zero.

A discussion of the properties of 2,6-xyleneol coatings, and a model for their formation, was given by Bruno et al. [10]. The films were adherent and continuous, of thickness 50–100 nm, and were found to be very hydrophobic. Alternating ionic and radical steps were thought to be involved in polymerisation to poly(2,4,6-dimethyl-1,4-phenylene ether).

Bejerano and Gileadi [11] found electrochemical inhibition with 2,4,6-trimethylphenol, which has all polymerisation sites blocked. They concluded that absorption of radicals not polymerisation was the primary process.

By incorporating reactive aldehyde and ketone groups into the phenolic, a polyphenylene oxide (PPO) layer has enabled grafting of other chosen molecules onto a coated electrode [12].

Polyphenylene oxide derived coatings on platinum have also displayed selectivity for H^+ over Fe^{2+} , on the basis of size [13,14]. Casting polyphenylene oxide from solution, by evaporating solvent, was found to yield inferior coatings [13]. Wang et al. [15] have utilised phenolic coat-

ings in amperometric detection of H_2O_2 and paracetamol, in the presence of ascorbate, urate and NADH. The selectivity achieved was attributed to exclusion on the basis of molecular size. Sasso et al. [16] have used a diaminobenzene coating as part of a glucose biosensor, applied over glucose oxidase immobilised on an electrode, to exclude ascorbate and urate, but with unknown selectivity against paracetamol. Paracetamol exclusion was achieved in a flow injection system by Geise et al. [17] by means of a diaminobenzene/resorcinol coating.

Platinum, electrochemically coated with a phenolic material, has also been used in the potentiometric mode as a pH sensor [18].

EXPERIMENTAL

Apparatus and membranes

The electrochemical cell consisted of a platinum anode and silver cathode, acting as a pseudoreference (Rank Bros, Bottisham, Cambridge) [4]. Polarisation at 0.65 V vs. Ag, was achieved with a variable voltage source, also equipped to measure current in the range 0.1 nA to 2.0 mA (Department of Chemistry Workshop, University of Newcastle-upon-Tyne). A recorder output was connected to a Goertz Metrawatt SE120 (Vienna) strip chart recorder. Membranes used to cover the electrode surface were secured with an O-ring, held in place by the sample chamber when the cell was assembled.

Polycarbonate membranes (PCM) of 0.03- and 0.05- μm pore sizes were obtained from Nuclepore (Pleasanton, CA). Coatings were compared with cellulose acetate membranes, positioned beneath a polycarbonate membrane. Cellulose acetate membranes (CA) were cast from 1 ml of 2% solution in acetone, spread on a 5.6-cm square glass plate, which was rotated by hand for several minutes while the solvent evaporated, and then left for at least two hours before use. When a coating was performed without a covering membrane over the anode, an annular piece of PCM was placed under the O-ring of the Rank cell, to allow a liquid path to prevent the electrodes becoming electrically insulated from each other.

Glucose sensors incorporated a layer of glucose oxidase immobilised beneath a covering 0.05- μm PCM. This same composite preparation was used directly on the platinum electrode, or above the electrode and a covering cellulose acetate membrane or phenol coating, when the cell was assembled. 10 μl of a solution containing 30 mg ml^{-1} glucose oxidase (117000 U gm^{-1} , Sigma, Poole) and 200 mg ml^{-1} bovine serum albumin (Sigma) were mixed with 5 μl of a 5% solution of glutaraldehyde (BDH, Poole). 3 μl of the mixture were spread with a pipette on to 1 cm^2 of a 0.05- μm PCM, and allowed to set before use on the electrode.

Coating and measurement procedures

Experiments were performed in stirred buffer at pH 7.4, containing 2.44 g $\text{NaH}_2\text{PO}_4 \cdot 4 \text{H}_2\text{O}$, 7.5 g Na_2HPO_4 , 3 g NaCl and 0.6 g disodium EDTA per litre. This has been the buffer previously used in enzyme based glucose sensors, and since the coatings were evaluated as the selective layer in such sensors, the same buffer was utilised throughout. Before use, electrodes were cleaned by placing a drop of concentrated nitric acid on the anode for 15 min, rinsing, and scrubbing with alumina, then conditioning for several hours in buffer at +0.65 V vs. Ag, until a steady baseline current was achieved.

Coatings were formed through a covering PCM by continued polarisation of the anode (+0.65 V) in the presence of 5 mM buffered solutions of the coating species. Coating was initiated by replacement of the buffer in the cell with the phenolic solution, and terminated when the solution was replaced with buffer. Coating times were one or two hours, depending on the extent of signal suppression required from the coated electrode. The signal in response to 1 mM ascorbate was used as a marker to assess the integrity of the coated electrodes. Coatings were removed by polishing the electrodes with alumina, and recovery of the original signal from ascorbate was taken as an indication of a "clean" electrode surface.

When coating was interrupted at short time intervals, the electrode was depolarised to prevent continuation of coating while the cell was rinsed and filled with buffer, before the responses

from the electrode were assessed. The electrode was repolarised and exposed to fresh coating solution to continue the coating procedure.

Responses to glucose, hydrogen peroxide and interferents were determined by adding stock solutions to buffers in the cell.

RESULTS

The exposure of a clean PCM covered platinum anode, polarised at +0.65 V vs. Ag, to stirred solutions of phenol and dopamine resulted in a current, Fig. 1, due to electrochemical oxidation of the phenolic species. This signal rapidly decreased until it became stable at a low value. Both dopamine and phenol exhibited similar behaviour, the difference in current being attributed to the effect of the substituent group of dopamine facilitating the electrochemical oxidation. The original signal size was restored when the electrode was cleaned with alumina, suggesting a modification to the surface during exposure to the phenol.

In addition to the loss of response to the modifying species, Fig. 1, the responses obtained with other known electroactive species were in-

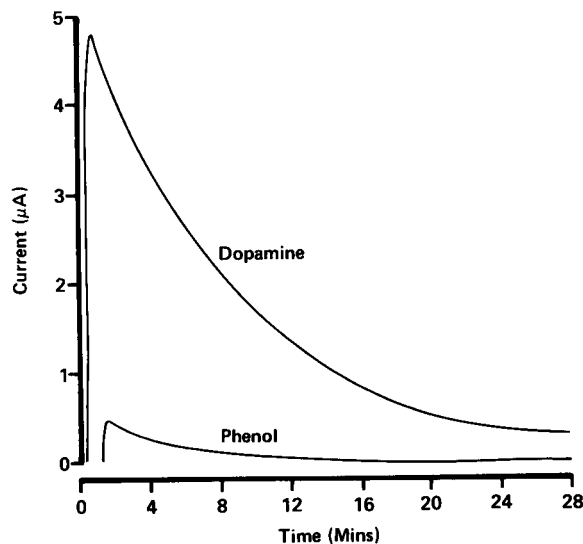


Fig. 1. Current vs. time curves during coating of platinum anode from 5 mM dopamine and phenol solutions (+0.65 V vs. Ag, pH 7.4 phosphate buffer, 0.05- μm PCM).

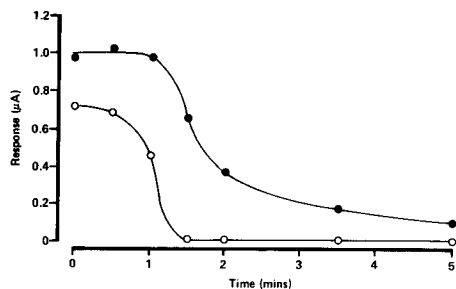


Fig. 2. Responses to 1 mM 4-aminophenol (●), and 1 mM ascorbate (○) solutions during continued re-exposure of polarised platinum anode to 5 mM phenol solution (+0.65 V vs. Ag, pH 7.4 phosphate buffer, 0.03- μ m PCM).

investigated, Fig. 2. Exposure to phenol was seen to progressively reduce the signals from the oxidation of 4-aminophenol and ascorbate. Although both curves were similar, the ascorbate signal decayed before that from the 4-aminophenol. The effect of a short term coating is shown in Table 1. This modification in signal ratio confers selectivity to the sensor. The duration of phenol exposure required to bring about such a reduction in ascorbate signal was variable from 1.5 min to 60 min. This was attributed to variation in the condition of the platinum surface at which the coating occurred. Monitoring the current resulting from the phenol oxidation itself, was found to give an indication of the degree of signal attenuation that would result in response to other species, were the electrode to be tested at that particular time. After long periods of exposure, the change in current with time was small, and exact exposure time was not critical in electrode modification.

To clarify whether the modification to the signals noted above, is an electrode phenomenon,

TABLE 1

Changing ratios of responses 4-aminophenol:ascorbate, between continued coating of electrode by exposure to 5 mM phenol^a

Time (min)	4AP:ASC
0	1.3:1
1.5	40 :1
3.5	21 :1
5.0	51 :1

^a +0.65 V vs. Ag, pH 7.4 phosphate buffer.

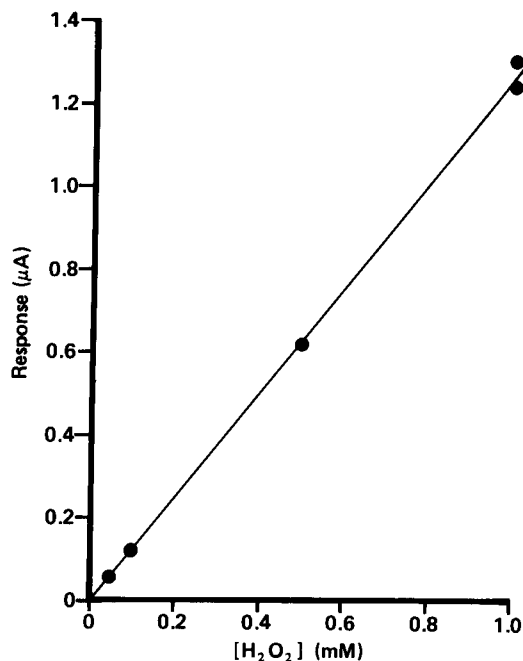


Fig. 3. Response to unstirred, buffered H_2O_2 (pH 7.4 phosphate), obtained at a platinum anode (+0.65 V vs. Ag). Electrode (no PCM) precoated by 2-h exposure to 5 mM phenol (+0.65 V vs. Ag, pH 7.4 phosphate buffer).

and not a membrane fouling effect, a polarised electrode was exposed to a 5 mM phenol solution for two hours, with no covering PCM. No stirring was employed, to prevent scratching of any coating on the electrode. Figure 3 shows the signals obtained in response to hydrogen peroxide for this system. A linear response up to at least 1.0 mM resulted for hydrogen peroxide. The response of this electrode to 1.0 mM ascorbate was 2.5 nA, confirming that the electrode surface was indeed modified. Scratching of the electrode surface with a pipette, however, destroyed the selectivity against ascorbate, suggesting the modification took the form of a coated layer on the electrode. Consequently, non-selective polycarbonate membranes continued to be employed to protect the coated surface. A PCM covered electrode, previously tested for ascorbate responses, was then exposed to 5 mM phenol for one hour while unpolarised. No attenuation of signal size was seen when the electrode was subsequently polarised and tested with ascorbate solution, con-

firming that the electrode modification was an electrochemical phenomenon.

The response times of phenolic coated electrodes were dependent on the protecting PCM. For a one-hour phenol coating with a 0.03- μm PCM, 4-aminophenol responses took the form of a step change from a baseline to a plateau, within 1.5 min for concentrations up to 1 mM. However, when a 0.05 μm PCM was used, this response became transient, showing an initial peak before decreasing to a stable value, at concentrations above 0.2 mM. With a cellulose acetate membrane below the PCM, slow responses (30 min) were seen. Use of 0.03- or 0.05- μm PCM alone with no coatings, gave rapid step changes from zero up to 1 mM.

With 0.03- or 0.05- μm PCM over uncoated electrodes, similar rapid step change responses to peroxide were seen for concentrations up to 1 mM. At an electrode protected by a 0.03- μm PCM and coated in phenol for one hour, rapid (≤ 1 -min) step changes were noted in response to peroxide up to 0.2 mM, above which, response times were markedly increased, a rapid initial response being followed by a slower prolonged increase in signal. Two-hour coatings only gave rapid responses below 0.05 mM. In contrast, the use of a cellulose acetate membrane, also below a 0.03- μm PCM, resulted in rapidly attained plateau responses for peroxide concentrations up to at least 1 mM. At a phenol coated electrode without a PCM, the responses to unstirred peroxide showed current peaks before attaining plateaux within two minutes, the plateau values being shown in Fig. 3.

The effect of 5 mM dopamine as a modifying agent is shown in Fig. 4. Responses to 0.1 mM solutions through a 0.05- μm PCM are shown in Fig. 4a, and for the modified electrode and PCM, in Fig. 4b, (1.0 mM solutions). All signals were reduced by the dopamine treatment, but particularly highly attenuated were ascorbate and urate responses, and also 4-aminophenol and paracetamol responses were reduced relative to that of hydrogen peroxide.

Similar experiments, using one- or two-hour phenol exposure, compared with a cellulose acetate membrane in addition to the PCM, are

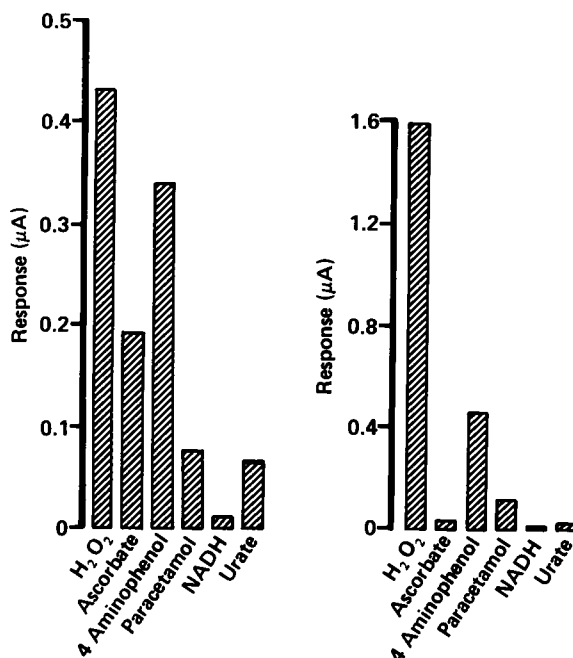


Fig. 4. Responses at a platinum anode (+0.65 V vs. Ag, pH 7.4 phosphate buffer, 0.03- μm PCM). (a) 0.1 mM solutions prior to electrode coating. (b) 1.0 mM solutions after coating of anode by 1-h exposure to 5 mM dopamine (+0.65 V vs. Ag, pH 7.4 phosphate buffer, 0.03- μm PCM).

shown in Fig. 5. Signal sizes in response to 1 mM solutions were much less than with the dopamine coating described above. The responses to hydrogen peroxide were similar for each composite (Fig. 5). A one hour phenol coating reduced paracetamol responses considerably more than did a cellulose acetate membrane, although ascorbate responses were similar. The results of a two-hour exposure to phenol showed a further decrease in signal size for ascorbate, paracetamol, NADH and urate. The 4-aminophenol response was much reduced compared to that with the cellulose acetate membrane, but a large response to hydrogen peroxide was retained. The ratios of hydrogen peroxide response to those of ascorbate and paracetamol are shown in Table 2. A two-hour phenol coating gave a higher response ratio than cellulose acetate for H₂O₂: ascorbate, and a greatly enhanced selectivity against paracetamol.

The responses obtained with the glucose electrode are shown in Fig. 6. Both the cellulose

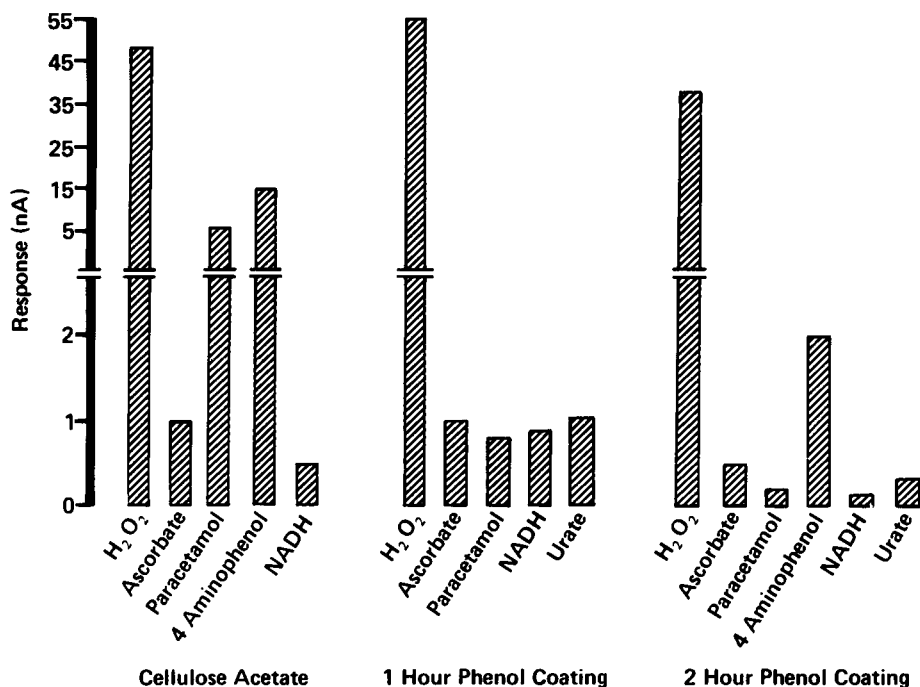


Fig. 5. Responses at a platinum anode (+0.65 V vs Ag, pH 7.4 phosphate buffer, 0.1 mM solutions). (a) 0.03- μ m PCM and cellulose acetate membrane over electrode. (b) 0.03- μ m PCM and anode modified by 1-h coating in 5 mM phenol (+0.65 V vs. Ag, pH 7.4 phosphate buffer). (c) 0.03- μ m PCM and anode modified by 2-h coating in 5 mM phenol (+0.65 V vs. Ag, pH 7.4 phosphate buffer).

acetate membrane and phenol coating attenuated the signal obtained when no selective barrier was employed beneath the enzyme. Responses obtained with the cellulose acetate were double those with the phenolic coating. No significant difference in linear range was noted, between the two approaches to selectivity.

Figure 7 shows the responses to glucose and some common interferences, resulting from the use of alternative, selective barriers. For the glucose:

TABLE 2

Comparison of selectivity ratios for responses H_2O_2 :interferent, for membrane + coating combinations

	0.05 PCM only	0.03 PCM + CA	0.03 PCM + 1 h phenol	0.03 PCM + 2 h phenol	0.03 PCM + 1 h dop ^a
H_2O_2 : ASC	2.2:1	48:1	55:1	76:1	40:1
H_2O_2 : PMOL	5.0:1	8:1	79:1	190:1	13:1

^a dop = dopamine.

paracetamol ratio, a cellulose acetate membrane gave 1:2, and the phenolic coating gave 21:1, though reduced glucose signals led to lower ratios

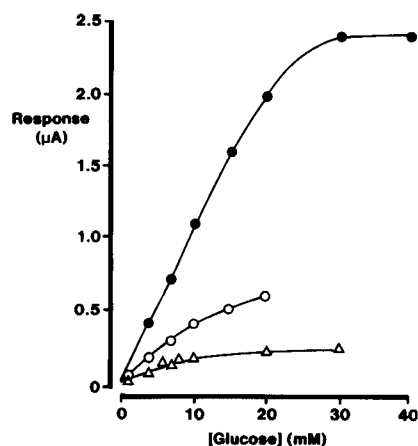


Fig. 6. Responses to glucose obtained with PCM/glucose oxidase composite overlying either (●) the platinum anode direct, or (○) above a cellulose acetate membrane, (Δ) or phenolic coating, 5 mM, 18 h (+0.65 V vs. Ag, pH 7.4 phosphate buffer).

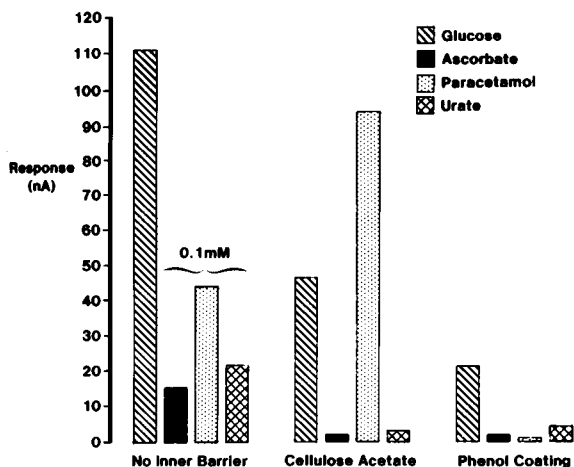


Fig. 7. Responses to glucose and interferent species, with platinum anode directly below enzyme/PCM composite, or with interposed cellulose acetate membrane or phenolic coating, 5 mM, 18 h (1 mM solutions except as stated, pH 7.4 phosphate buffer, +0.65 V vs. Ag).

against the residual signals from urate and ascorbate, though modifying coating times could be advantageous.

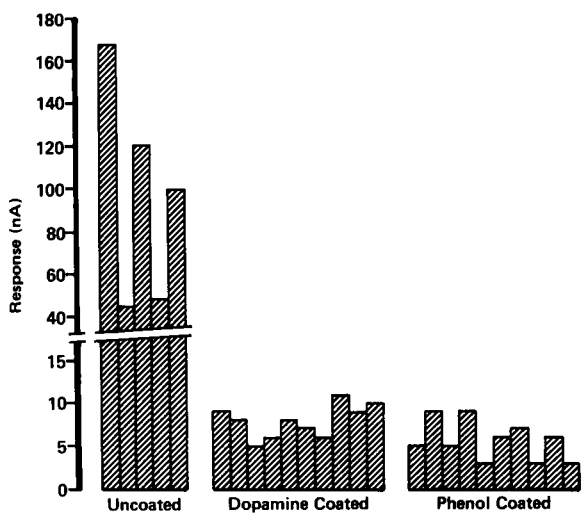


Fig. 8. Responses to undiluted serum at platinum anode (+0.65 V vs. Ag). (a) 0.03- μ m PCM, no coating; samples from 5 patients. (b) 0.03- μ m PCM and anode coated by 1-h exposure to 5 mM dopamine (+0.65 V vs. Ag, pH 7.4 phosphate buffer); samples from 10 different patients. (c) 0.03- μ m PCM and anode coated by 1-h exposure to 5 mM phenol (+0.65 V vs. Ag, pH 7.4 phosphate buffer); samples from another 10 patients.

Practical use of such modified electrodes in biosensors, would challenge the selective layer with the range of small molecules found in serum; macromolecules being excluded by the covering membrane. The results in Fig. 8a, obtained with a 0.03- μ m PCM shows the current responses generated by a random set of five patients' serum samples, with signals ranging from 44–168 nA. Ten different samples in each case were used to test dopamine (Fig. 8b) and phenol (Fig. 8c modified electrodes, with covering PCM). Serum interference was greatly reduced when coated electrodes were employed. The dopamine treatment appeared slightly less effective (5–11 nA signals) than the phenol treated electrode (3–9 nA signals). Signals showed variation between individuals, this variation was restricted to a much smaller range within the diminished interference signal.

On storage (polarised) in unstirred buffer, dopamine treated electrodes lost selectivity progressively after several hours, although phenol coatings retained their selectivity for several days.

DISCUSSION

The loss of signal found with dopamine and phenol was an electrochemical coating occurring at the electrode surface not on the membrane, and appeared to be the same effect as noted previously [6,7,9]. The +0.65 V polarising voltage used here would indicate involvement of neutral molecules, according to Bejerano et al. [8], ionic participation requiring polarisation at +0.9 V. They claimed a very large surface coverage, however the extent of coverage here is unknown. For use in a biosensor, the application and method of use will determine the optimum extent of signal suppression, to combine adequate selectivity with a measurable signal. It was not part of this study to determine whether adsorption of radicals [8,11] or polymerisation [10] was involved.

However, the interaction of radicals on the surface, noted by Gileadi [19], as a sudden onset of inhibition, may account for the sigmoidal curves seen in Fig. 2, for the attenuation of oxidation currents. Such a shape was not seen for the

coating species itself, but may have been masked by the rapid current changes on initial exposure to a high concentration of phenolics.

The duration of coating affected the signal size and signal:interference ratio (Fig. 2, Table 1) and is best optimised for each individual sensor application. Signal current decreases rapidly on coating with prolonged exposure leading to a relatively unchanging low value; the point at which coating should be optimally terminated depending on a trade off between sensitivity and selectivity. The signal:interference ratio did not increase continuously with time (Table 1) but was dependent on the shape of the curves involved.

The degree of selectivity of the dopamine coating against the charged species ascorbate, NADH and urate, shown in Fig. 4, is consistent with previous observations [8,9], and also with the work of Wang et al. [15], though they believed size exclusion to be the predominant mechanism involved. 4-Aminophenol responses also decreased, as this molecule is charged, but were attenuated to a lesser extent, possibly owing to its aromatic character. The retention of relatively large H_2O_2 signals is a consequence of the molecule being small and uncharged, and likewise paracetamol is uncharged and produced a significant signal.

For phenol coatings, the pattern was similar, but paracetamol signals were reduced to a relatively greater extent than for dopamine coatings. Such a high degree of paracetamol exclusion was not noted by Wang et al. [15] or Sasso et al. [16], though significant paracetamol exclusion was reported by Geise et al. [17].

The use of cellulose acetate resulted in a similar pattern of responses for H_2O_2 , ascorbate and NADH, but poorer selectivity against paracetamol. This species has been a serious interferent in glucose monitoring [1]. The H_2O_2 :paracetamol ratio was much greater for the phenol coating (Table 2), and this represents the most important improvement in selectivity that would be gained by the use of coated electrodes.

The large responses to 4-aminophenol, using cellulose acetate, were however very slow, and not a suitable response for kinetic alkaline phosphatase measurement. This problem would not be encountered with the phenolic coatings, al-

though a smaller signal size (Fig. 5) could be a disadvantage.

The interference from serum was drastically reduced by phenolic coating, particularly by phenol itself. Hence the electrode modification allows H_2O_2 signals to be detected with little interference from serum or paracetamol, which is the desired performance from the selective component of a biosensor.

The use of a phenolic coating below glucose oxidase/PCM layers gave a glucose response of a magnitude such that the device would give a feasible measure of glucose while being essentially free of paracetamol interference. This is shown to be unattainable with the cellulose acetate membrane currently in use for such sensors, and represents a significant advance in this type of biosensor.

The main disadvantage to the use of the phenolic coatings is their instability. The relatively low voltage for obtaining the coating could account for this, the favouring of adsorption or polymerisation mechanism being voltage dependent, Bejerano et al. [8]. Other workers have described strongly adhering polymerised layers [17], obtained at higher voltages [10]. A long lifetime is essential before coatings can be considered a viable alternative to cellulose acetate membranes.

The electrode responses, during loss of the phenolic, mirror their time profile during the coating (Fig. 2), then prolonged coating may yield a layer displaying relatively unchanging character during initial loss of material, with an apparently extended lifetime. The possible loss of loosely attached material may lead eventually to a more stable, but less selective layer of strongly adsorbed molecules.

Conclusion

Phenolics have been electrochemically coated on to platinum anodes, such that the resulting modified electrodes have shown a degree of selectivity when used for amperometric detection of H_2O_2 , from glucose oxidase based sensors, with the elimination of signals from the common serum interferents encountered in clinical monitoring. An important advance over existing selectivity

barriers of cellulose acetate, is the almost complete removal of paracetamol interference from glucose measurement, while an adequate response to the H_2O_2 generated by glucose oxidase is retained. However, before such coatings can be accepted as an alternative to classical membranes, their lifetime must be much extended.

The authors wish to express their gratitude for financial support from the SERC and ICI plc.

REFERENCES

- 1 G. Palleschi, M.A.N. Rahni, G.J. Lubrano, J.N. Ngwainbi and G.G. Guilbault, *Anal. Biochem.*, 159 (1986) 114.
- 2 H.T. Tang, C.E. Lunte, H.B. Halsall and W.R. Heineman, *Anal. Chim. Acta*, 214 (1988) 187.
- 3 W.H. Mullen, F.H. Keedy, S.J. Churchouse and P.M. Vadgama, *Anal. Chim. Acta*, 183 (1986) 59.
- 4 Z. Koochaki, I. Christie, P. Vadgama, *J. Membr. Sci.*, 57 (1991) 83.
- 5 R.W. Murray, A.G. Ewing and R.A. Durst, *Anal. Chem.*, 59 (1987) 379A.
- 6 J.F. Hedenburg and H. Freiser, *Anal. Chem.*, 25 (1953) 1355.
- 7 S.S. Lord and L.B. Rogers, *Anal. Chem.*, 26 (1954) 284.
- 8 T. Bejerano, C. Forgacs and E. Gileadi, *J. Electroanal. Chem.*, 27 (1970) 69.
- 9 E. Zeigerson and E. Gileadi, *J. Electroanal. Chem.*, 28 (1970) 421.
- 10 F. Bruno, M.C. Pham and J.E. Dubois, *Electrochim. Acta*, 22 (1977) 451.
- 11 T. Bejerano and E. Gileadi, *J. Electroanal. Chem.*, 38 (1972) 137.
- 12 M.C. Pham, P.C. Lacaze and J.E. Dubois, *J. Electroanal. Chem.*, 86 (1978) 147.
- 13 T. Ohsaka, T. Hirokawa, H. Miyamoto and N. Oyama, *Anal. Chem.*, 59 (1987) 1758.
- 14 Y. Ohnuki, H. Matsuda, T. Ohsaka and N. Oyama, *J. Electroanal. Chem.*, 158 (1983) 55.
- 15 J. Wang, S. Chen and M.S. Lin, *J. Electroanal. Chem.*, 273 (1989) 231.
- 16 S.V. Sasso, R.J. Pierce, R. Walla and A.M. Yacynych, *Anal. Chem.*, 62 (1990) 1111.
- 17 R.J. Geise, J.M. Adams, N.J. Barone and A.M. Yacynych, *Biosensors Bioelectron.*, 6 (1991) 151.
- 18 W.R. Heineman, J.H. Wieck and A.M. Yacynych, *Anal. Chem.*, 52 (1980) 347.
- 19 E. Gileadi, *Isr. J. Chem.*, 9 (1971) 405.

Amperometric enzyme electrode with fast response to glucose using a layer of lipid-modified glucose oxidase and Nafion anionic polymer

Fumio Mizutani, Soichi Yabuki and Tatsuo Katsura

National Institute of Bioscience and Human-Technology, 1-1 Higashi, Tsukuba, Ibaraki 305 (Japan)

(Received 21st August 1992; revised manuscript received 12th October 1992)

Abstract

An amperometric enzyme electrode for glucose was prepared by using a lipid-modified glucose oxidase and a perfluorinated ionomer (Nafion). First, a glassy carbon base electrode was dipped into a benzene solution of the modified enzyme and dried, then the electrode was dipped into a Nafion solution and dried. The water-insoluble, modified enzyme was thus immobilized on the electrode surface with a strongly adhering, thin polymer coating. The anodic current (at 0.9 V vs. Ag/AgCl) of this electrode increased immediately after the addition of glucose and the response time was shorter than 2 s. A linear response to glucose was observed up to 3 mM with a detection limit of 0.2 μ M. The enzyme electrode was applied to the determination of glucose in fruit juices; the Nafion coating was effective in suppressing the electrochemical interference by L-ascorbate in the samples. The electrode could be used for at least 6 weeks.

Keywords: Amperometry; Enzymatic methods; Enzyme electrodes; Glucose

Analytical devices combining the specificity of enzymatic reactions with high sensitivity of electrochemical transduction have attracted increasing interest in the last decade [1,2]. Particular efforts in this field have been directed to the realization of an amperometric sensor for the analytically significant substrate glucose by using glucose oxidase (GOD) [3]. In conventional amperometric glucose-sensing electrodes, three membranes are attached on the surface of base electrode: the first is used for protecting against fouling of electrode, the second for immobilizing GOD and the third for eliminating electroactive interferents. Various approaches to developing simple, rapid and reproducible procedures for

the construction of glucose-sensing electrodes have been presented. For immobilizing GOD easily and effectively, incorporation of GOD by mixing the enzyme with carbon paste matrices [4–8], electrodeposition of GOD during the anodic growth of polymers [9–16] and that during the cathodic growth of platinum black [17,18] have been examined.

Most recently, Wang et al. [19] developed a unique method for immobilizing GOD on an electrode surface with the use of an aqueous solution containing the enzyme and a poly-(ester-sulphonic acid) (AQ-55D, Eastman): the solution is placed on an electrode and then dried with a heat gun to form a GOD-polymer-coated electrode. They also reported the use of a perfluorinated ionomer (Nafion, DuPont) as the matrix for enzyme immobilization [20]. Anionic polymers such as Nafion and AQ polymers have been re-

Correspondence to: F. Mizutani, National Institute of Bioscience and Human-Technology, 1-1 Higashi, Tsukuba, Ibaraki 305 (Japan).

ported to serve as protective and selective coatings on enzyme electrodes [5,21,22]: the polymer coating is effective for protecting the electrode surface from fouling agents present in biological and food samples [5], and also for excluding anionic interferents (e.g., L-ascorbate) in these samples [21–27]. The use of such a functional polymer layer as the matrix for enzyme immobilization [19,20] is an interesting approach to realizing enzyme electrodes with a simple membrane structure. A simple and thin enzyme membrane-based system would give a fast response and high sensitivity in electrochemical measurements [15,28]. However, an electrode using a GOD–anionic polymer system [19] showed poor stability owing to leaching of GOD out of the polymer matrix. It seems natural that water-soluble, negatively charged [29] GOD molecules will leach out of the layer of an anionic linear polymer. In order to circumvent this stability problem, the use of a lipid-modified GOD [30], instead of native GOD, is considered to be suitable: the water-insoluble, modified enzyme would be far more stably immobilized in the polymer matrix.

In this paper, the preparation and use of an enzyme electrode based on such a lipid-modified GOD and an anionic polymer coating is described. The lipid-modified GOD was placed on an electrode surface by dip-coating from a benzene solution of the modified enzyme, then the polymer coating was applied by dip-coating from a Nafion solution. The resulting electrode exhibited high performance characteristics such as rapid response (100% response, less than 2 s), high sensitivity (detection limit lower than 0.2 μM) and high stability (usable for at least 6 weeks).

EXPERIMENTAL

Materials

The enzymes used were GOD (EC 1.1.3.4, from *Aspergillus* sp., Grade II, Toyobo, Osaka) and peroxidase (EC 1.11.1.7, from horseradish, Grade I-C, Toyobo). An amphiphile, *N*-(α -trimethylammonioacetyl)didodecyl-L-glutamate chloride [$(\text{C}_{12})_2\text{gluN}^+\text{Cl}^-$], was obtained from

Sogo Pharmaceutical (Tokyo) and Nafion [5% (w/v) solution, 1100 equiv. wt.], from Aldrich (Milwaukee, WI). F-kits (Boehringer Mannheim, Indianapolis, IN) were used for the spectrophotometric measurement of glucose and L-ascorbate. The kit for glucose uses the enzyme pair hexokinase–glucose-6-phosphate dehydrogenase. Other reagents were of analytical-reagent grade. Deionized, doubly distilled water was used throughout.

Lipid-modified enzyme

GOD modified with $(\text{C}_{12})_2\text{gluN}^+$ was prepared according to the procedure of Okahata et al. [30]. A buffer solution (5 ml, 0.02 M potassium acetate buffer plus 0.1 M KCl, pH 6) containing 25 mg of GOD was mixed with an aqueous dispersion (50 ml) of 100 mg of $(\text{C}_{12})_2\text{gluN}^+\text{Cl}^-$. The precipitate formed after incubation of the mixture at 4°C for 24 h was lyophilized. A light yellow powder (ca. 100 mg) was obtained.

The GOD content in the modified enzyme was determined by measuring the absorption of flavin adenine dinucleotide (FAD) in a benzene solution of the lyophilized product at 450 nm. The enzyme activities of the unmodified and modified GOD were measured spectrophotometrically by using a peroxidase–phenol–4-aminoantipyrine chromogenic system [31]. The solution (or dispersed medium in the case of the modified enzyme) used for measuring the GOD activity was a 0.1 M potassium phosphate buffer (pH 7.0, 25°C).

Enzyme electrode system

A glassy carbon disc electrode (GCE) (Bioanalytical Systems, West Lafayette, IN) 3 mm in diameter was polished with a 0.05- μm alumina slurry, rinsed with water and then sonicated in water for 2 min. The electrode was activated by anodization at 1.5 V vs. Ag/AgCl for 30 min in a 0.05 M potassium phosphate buffer solution (pH 7.5) [32], rinsed with water and dried. After the pretreatment, the GCE was dipped into a benzene solution of the modified GOD [2% (w/v)] and the solvent was allowed to evaporate at room temperature for 5 min. Finally, Nafion membrane coatings were made by dip-coating the enzyme-attached GCE in 0.5% (w/v) Nafion solution, which was prepared by diluting the 5% solution

as received with a mixture of 2-propanol [50% (v/v)] and water [21], and the electrode was allowed to dry with the surface facing down [5] at room temperature for at least 1 h. The Nafion coating and drying process was repeated three times unless stated otherwise. The thickness of the resulting modified GOD–Nafion layer obtained in this way was determined as ca. 0.5 μm by using a stylus-type apparatus (Talystep, Taylor-Hobson, Leicester).

Other enzyme electrodes, an electrode with a native GOD–Nafion layer and one with a modified GOD–acetylcellulose layer, were prepared as follows. The electrode based on native GOD was made by casting 5 μl of GOD solution [0.5% (w/v)] on the GCE surface, allowing the enzyme solution to dry for 1 h and by coating three times with the 0.5% Nafion solution. The electrode with an acetylcellulose coating was prepared by the use of an acetone solution of 0.5% (w/v) acetylcellulose instead of 0.5% Nafion solution.

A potentiostat (HA-502, Hokuto Denko, Tokyo) was used in a three-electrode configuration for amperometric measurements: the enzyme electrode, an Ag/AgCl reference electrode (Bio-analytical Systems) and a platinum auxiliary electrode were immersed in 10 ml of a test solution of 0.1 M potassium phosphate buffer (pH 7) in a cylindrical cell. The solution was saturated with air and stirred by using a magnetic bar. The temperature of the solution was kept at 25°C.

RESULTS AND DISCUSSION

Properties of modified enzyme

The GOD content in the lyophilized powder of the modified enzyme was calculated to be 33%. In neutral media, GOD is highly anionic (expressed as GOD^{80-}) [28]; hence it is assumed that n molecules of lipid attached on the surface of GOD form a complex expressed as $n[(\text{C}_{12})_2\text{gluN}^+] \cdot \text{GOD}^{80-} \cdot (n - 80)\text{Cl}^-$. From the GOD content in the complex and the molecular weight of native GOD (1.5×10^5), n is calculated to be 490. The cross-sectional area of $(\text{C}_{12})_2\text{gluN}^+$ can be calculated to be 0.45 nm^2 , as that of an analogue, N -(α -trimethylammonioacetyl)dihexade-

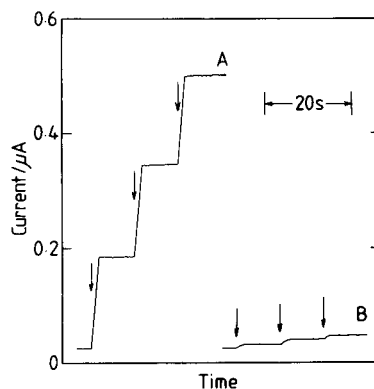


Fig. 1. Current–time curves for (A) the GCE coated with a modified GOD–Nafion layer and (B) that with a native GOD–Nafion-layer, obtained on increasing the glucose concentration in 0.2 mM steps.

cyl-L-glutamate [$(\text{C}_{16})_2\text{gluN}^+$], has been evaluated as 0.45 nm^2 from the surface pressure–area isotherm of $(\text{C}_{16})_2\text{gluN}^+$ on a water subphase [30]. GOD is a globular protein with a diameter of 8 nm [33]; hence the number of $(\text{C}_{12})_2\text{gluN}^+$ that can be directly attached to the GOD surface is calculated to be 450. This value is compatible with the n value obtained; $(\text{C}_{12})_2\text{gluN}^+$ molecules are considered to form a monolayer on the GOD surface.

The GOD activity of the modified enzyme was determined to be 38 U mg^{-1} solid, which corresponded to 115 U mg^{-1} GOD. The GOD activity of the unmodified enzyme was determined to be 110 U mg^{-1} . These results show that the enzyme activity does not decrease during the modification process and that the enzyme substrates, glucose and oxygen, permeate easily into the lipid layer to reach the active site of the enzyme.

Glucose response of enzyme electrode

Figure 1 shows the current–time curves for the GCE coated with the modified GOD–Nafion layer and that with the native GOD–Nafion layer. The potential of each electrode was set at 0.9 V vs. Ag/AgCl. The current on each electrode increased immediately after the addition of glucose and reached another steady state within 2 s. As the Nafion layer is thin, the glucose added is expected to diffuse quickly through the layer so

as to be oxidized by the enzymatic reaction. Hydrogen peroxide produced through the GOD reaction in the vicinity of the GCE surface is immediately oxidized to give an anodic current. These rapid processes of substrate diffusion and electrochemical oxidation result in a fast response on the enzyme electrodes.

As shown in Fig. 1, the glucose response of the electrode based on the modified GOD was far larger than that on the electrode using native GOD. When native GOD was used, the enzyme readily leaked out of the Nafion matrix and only a small amount of GOD remained immobilized in the matrix. After the GCE coated with the native GOD–Nafion layer had been immersed in the test solution for 30 min, the solution exhibited an enzyme activity of 0.27 U, which corresponded to the amount of native GOD used for preparing the enzyme electrode (2.5 μg), and the GOD activity on the GCE surface was lower than 1 mU cm^{-2} . In contrast, such a significant leakage of the enzyme from the GCE surface was not observed with the modified GOD–Nafion system. About 20% of the modified GOD placed on the electrode surface leaked out of the enzyme–Nafion layer within 30 min after soaking the electrode in the test solution, but the leakage of the enzyme was almost negligible after the 30-min soaking. The GOD activity retained in the modified enzyme–Nafion layer was as high as 200 mU cm^{-2} . The much higher enzyme activity on the GCE coated with the modified GOD–Nafion layer is responsible for the larger glucose response than that with the electrode using native GOD.

Figure 2 shows the relationship between the steady-state current response for 1 mM glucose and the potential of the GCE coated with a modified GOD–Nafion layer. The current–potential profile obtained with the same electrode in the glucose-free test solution is also shown in Fig. 2. The current response for glucose increased with increasing electrode potential applied and reached a plateau above 1.0 V vs. Ag/AgCl. On the other hand, the background (residual) current increased appreciably above 1.0 V vs. Ag/AgCl. Subsequent experiments were therefore done at 0.9 V vs. Ag/AgCl. The shape

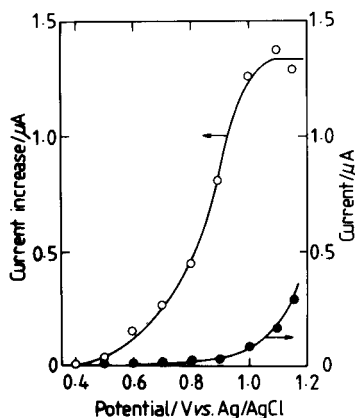


Fig. 2. Effect of potential on (○) the current response for 1 mM glucose of the GCE coated with a modified GOD–Nafion-layer and (●) the background current of the same electrode.

of the glucose response–potential profile shown in Fig. 2 was almost identical with that of the current–potential curve for the oxidation of hydrogen peroxide on the same electrode, as expected. For the construction of the present glucose-sensing system, glassy carbon was selected as the base electrode material because the hydrophobic surface of the material was considered to be suitable for immobilizing the hydrophobic lipid-coated enzyme. On the other hand, carbon electrodes are known to show poor activity for the oxidation of hydrogen peroxide [34,35]. A high electrode potential is hence required for operating the present enzyme electrode as compared with conventional glucose sensors based on platinum electrodes, the operating potential of which is usually in the range 0.6–0.7 V vs. Ag/AgCl.

The relative standard deviation for ten successive measurements of 0.2 mM glucose on the modified GOD–Nafion-coated GCE was 1.3%. Figure 3 shows a calibration graph obtained with the modified GOD–Nafion-coated GCE. The enzyme electrode gave a linear current response up to 3 mM glucose, and a significant increase in the response with an increase in the glucose concentration was observed in the range 3–10 mM. The detection limit was as low as 0.2 μM (signal-to-noise ratio = 5).

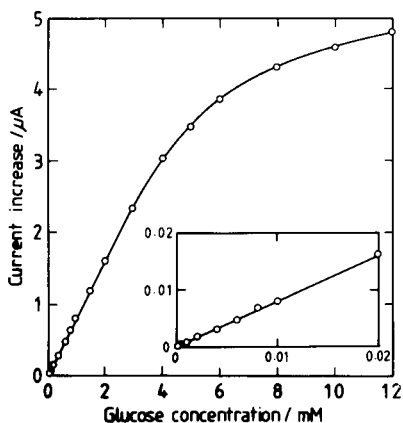


Fig. 3. Calibration graph for glucose on the GCE coated with a modified GOD-Nafion layer. The inset shows an enlargement of the initial part of the graph.

Determination of glucose in beverages

Figure 4 shows the enzyme electrode responses for the successive addition of 0.2 mM glucose and 0.1 mM L-ascorbate, which is a typical electroactive interferent present in biological and food samples. The enzyme electrodes used were (a) the electrode coated three times with 0.5% Nafion solution, (b) that coated once with 0.5% Nafion solution and (c) that coated three times with 0.5% acetylcellulose solution. As shown, the use of a Nafion layer was very effective in reducing the ratio of L-ascorbate response to glucose response as compared with the use of

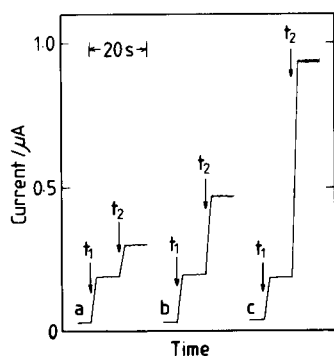


Fig. 4. Current-time curves for the enzyme electrodes: (a) electrode coated three times with 0.5% Nafion solution; (b) electrode coated once with 0.5% Nafion solution; (c) electrode coated three times with 0.5% acetylcellulose solution. t_1 and t_2 are the time points when 0.2 mM glucose and 0.1 mM L-ascorbate were added, respectively.

TABLE 1

Comparison of results obtained for glucose in fruit juices by different methods ^a

Sample	Glucose concentration (mM)		x/y
	proposed method (x)	F-kit method (y)	
Orange juice 1	155	155	1.00
Orange juice 2	148	145	1.02
Orange juice 3	142	138	1.03
Apple juice	144	142	1.01
Mixed fruit juice 1	175	171	1.02
Mixed fruit juice 2	160	160	1.00

^a L-Ascorbate concentrations in the samples were determined to be in the range 0.3–2.1 mM by using the F-kit.

acetylcellulose, and repetition of the Nafion coating brought about a decrease in the ratio, as expected. The ratio of response for glucose to that for the same concentration of L-ascorbate on electrode (a) was 1.4.

The concentrations of glucose and L-ascorbate in normal sera are ca. 5 and ca. 0.05 mM, respectively, and those in fruit juice are reported to be 100–200 [36,37] and lower than 3 mM [38], respectively; the L-ascorbate concentration is less than 2% of the glucose concentration in these samples. For measuring glucose in such samples with electrode (a), the level of electrochemical interference by ascorbate is expected to be within a few percent of the signal output.

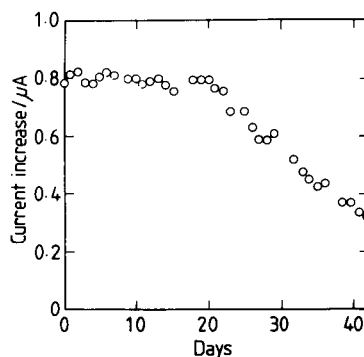


Fig. 5. Long-term stability of the modified GOD-Nafion-coated GCE. The electrode response for 1 mM glucose was measured 30 times a day. The average value of the 30 measurements is plotted against the number of days after the preparation of the electrode.

Table 1 gives the results for the determination of glucose in fruit juices from the current increase on electrode (a). Each sample (50 μ l) was added to the test solution without any pretreatment. The results were compared with those given by the F-kit method. The agreement was excellent; the regression equation between the results obtained by the present electrode method (x) and those by the F-kit method (y) was $y = 1.003x - 2.573$ and the correlation coefficient was 0.989 for the six samples given in Table 1. These results show that the present enzyme electrode is useful for the simple and rapid determination of glucose concentration. The use of a pair of electrodes, the present enzyme electrode and a deactivated enzyme-based electrode, for differential measurement of electrode current would be a suitable approach to the more accurate determination of glucose.

Stability of modified GOD–Nafion-attached GCE

The long-term stability of the GCE coated with the modified GOD–Nafion layer was examined by determining 1 mM glucose 30 times a day each day for 6 weeks. The average value of the electrode responses for the 30 measurements did not decrease for 3 weeks, as shown in Fig. 5. The electrode responses gradually decreased after 3 weeks, but they are still measurable until the end of 6 weeks. The detection limit was lower than 1 μ M even on the 42nd day. The modified GOD–Nafion-coated GCE thus showed a high stability.

Conclusion

The combination of a water-insoluble, lipid-modified GOD with a thin coating of Nafion anionic polymer provided a glucose-sensing electrode with high performance characteristics such as rapid response, high sensitivity and high stability. These characteristics are particularly promising for the application of the electrodes in flow injection systems. Work in this direction is in progress. The simple procedure for the preparation of enzyme electrodes is another attractive feature of the present enzyme electrodes; the dip-coating procedure may be of particular interest because it is highly suitable for preparing

micro-enzyme electrodes. Such a micro-enzyme sensor has already been prepared with the use of an ultramicro GCE (diameter 10 μ m) as the base transducer.

REFERENCES

- 1 F.W. Scheller, F. Schubert, R. Renneberg, H.-G. Muller, M. Janchen and H. Weise, *Biosensors*, 1 (1985) 135.
- 2 F. Mizutani and M. Asai, in D.L. Wise (Ed.), *Bioinstrumentation*, Butterworths, Boston, 1990, p. 317.
- 3 R. Wilson and A.P.F. Turner, *Biosensors Bioelectron.*, 7 (1992) 165.
- 4 W. Matsuzewski and M. Trojanowicz, *Analyst*, 113 (1988) 735.
- 5 L. Gorton, H.I. Karan, P.D. Hale, T. Inagaki, Y. Okamoto and T.A. Skotheim, *Anal. Chim. Acta*, 228 (1990) 23.
- 6 J. Wang, L.-H. Wu, Z. Lu, R. Li and J. Sanchez, *Anal. Chim. Acta*, 228 (1990) 251.
- 7 A. Amine, J.-M. Kaufmann and G.J. Patriache, *Talanta*, 38 (1991) 107.
- 8 F. Mizutani, S. Yabuki, A. Okuda and T. Katsura, *Bull. Chem. Soc. Jpn.*, 64 (1991) 2849.
- 9 M. Umana and J. Waller, *Anal. Chem.*, 58 (1986) 2979.
- 10 N.C. Foulds and C.R. Lowe, *J. Chem. Soc., Faraday Trans. 1*, 82 (1986) 1259.
- 11 P.N. Bartlett and R.G. Whitaker, *J. Electroanal. Chem.*, 224 (1987) 37.
- 12 C. Iwakura, Y. Kajiyama and H. Yoneyama, *J. Chem. Soc., Chem. Commun.*, (1988) 1019.
- 13 N.C. Foulds and C.R. Lowe, *Anal. Chem.*, 60 (1988) 2473.
- 14 S. Yabuki, H. Shinohara and M. Aizawa, *J. Chem. Soc., Chem. Commun.*, (1989) 945.
- 15 C. Malitesta, F. Palmisano, L. Torsi and P.G. Zamboni, *Anal. Chem.*, 62 (1990) 2735.
- 16 Y. Kajiyama, H. Sugai, C. Iwakura and H. Yoneyama, *Anal. Chem.*, 63 (1991) 49.
- 17 K. Ikariyama, S. Yamauchi, T. Yukihashi and H. Ushioda, *Anal. Lett.*, 20 (1987) 1791.
- 18 K. Ikariyama, S. Yamauchi, T. Yukihashi and H. Ushioda, *J. Electrochem. Soc.*, 136 (1989) 702.
- 19 J. Wang, D. Leech, M. Ozsoz, S. Martinez and M.R. Smyth, *Anal. Chim. Acta*, 245 (1991) 139.
- 20 J. Wang, E. Dempsey, M. Ozsoz, and M.R. Smyth, *Analyst*, 116 (1991) 997.
- 21 D.J. Harrison, R.F.B. Turner and H.P. Baltes, *Anal. Chem.*, 60 (1988) 2002.
- 22 S. Dong, B. Wang and B. Liu, *Biosensors Bioelectron.*, 7 (1991) 215.
- 23 G.A. Gerhardt, A.F. Oke, F. Nagy, B. Moghaddam and R.N. Adams, *Brain Res.*, 290 (1984) 390.
- 24 F. Nagy, G.A. Gerhardt, A.F. Oke, M.E. Rice, R.N. Adams, R.B. Moore, M.N. Szentirmay and C.R. Martin, *J. Electroanal. Chem.*, 188 (1985) 85.
- 25 J. Wang and P. Tuzhi, *Anal. Chem.*, 58 (1986) 3257.

- 26 A. Aoki, T. Matsue and I. Uchida, *Denki Kagaku*, 56 (1988) 1120.
- 27 T. Matsue, A. Aoki, T. Abe and I. Uchida, *Chem. Lett.*, (1989) 133.
- 28 J. Voet and E.C. Andersen, *Biochem. Biophys.*, 233 (1984) 88.
- 29 P.W. Carr and L.D. Bowers, *Immobilized Enzymes in Analytical and Clinical Chemistry*, Wiley, New York, 1980, p. 197.
- 30 Y. Okahata, T. Tsuruta, K. Ijiro and K. Ariga, *Thin Solid Films*, 180 (1989) 65.
- 31 B.B. Bauminger, *J. Clin. Pathol.*, 27 (1974) 1015.
- 32 J. Wang and P. Tuzhi, *Anal. Chem.*, 58 (1986) 1787.
- 33 S. Nakamura, S. Hayashi and K. Koga, *Biochim. Biophys. Acta*, 445 (1976) 294.
- 34 L. Gorton, *Anal. Chim. Acta*, 178 (1985) 247.
- 35 L. Gorton and T. Svensson, *J. Mol. Catal.*, 38 (1986) 49.
- 36 K. Matsumoto, H. Kamikado, H. Matsubara and Y. Osajima, *Anal. Chem.*, 60 (1988) 147.
- 37 F. Mizutani and M. Asai, *Anal. Chim. Acta*, 236 (1990) 245.
- 38 K. Matsumoto, K. Yamada, and Y. Osajima, *Anal. Chem.*, 53 (1981) 1974.

Resonant frequency of a piezoelectric quartz crystal in contact with solutions

Shigeru Kurosawa¹

Faculty of Pharmaceutical Sciences, Department of Physical Chemistry and Biophysics, Hokkaido University, Sapporo 060 (Japan)

Hideo Kitajima and Yoshihiko Ogawa

Faculty of Engineering, Department of Electronic Engineering, Hokkaido University, Sapporo 060 (Japan)

Makoto Muratsugu

Department of Laboratory Medicine, Asahikawa Medical College, Asahikawa 078 (Japan)

Eiji Nemoto

Department of Mechanical Engineering, Ibaraki National College of Technology, Katsuta 312 (Japan)

Naoki Kamo

Faculty of Pharmaceutical Sciences, Department of Physical Chemistry and Biophysics, Hokkaido University, Sapporo 060 (Japan)

(Received 10th June 1992; revised manuscript received 29th September 1992)

Abstract

The resonant frequency of a piezoelectric crystal was determined by transmission measurements. The simple principle of this resonance method is that a transmission is measured at varying frequencies with a two-port transmission line system containing parallel resistance. Previous workers formulated the resonant frequency of a quartz crystal and the equation derived indicated that the frequency is dependent on $(\rho\eta)^{1/2}$ and F_b^3 , where ρ , η and F_b are the density and viscosity of the solution and the fundamental frequency of the quartz crystal, respectively. The resonance method was applied to solutions of varying $(\rho\eta)^{1/2}$, and it is concluded that the equation holds for a wide range of different solutions. The resonance method is advantageous in solutions over the widely used conventional oscillation method because the range of $(\rho\eta)^{1/2}$ for possible measurements is much wider.

Keywords: Piezoelectric sensors; Sensors; Quartz crystals

The oscillating frequency of a piezoelectric quartz crystal is changed by adsorption of sub-

stances on the crystal surface. The frequency change is expressed by the following equation:

$$\Delta F = -2.26 \times 10^{-6} F_b^2 \Delta m \quad (1)$$

where ΔF is the frequency change, F_b the fundamental frequency of the crystal and Δm the mass adsorbed on the surface per unit area of the electrode [1]. The detection is very sensitive: a

Correspondence to: N. Kamo, Faculty of Pharmaceutical Sciences, Department of Physical Chemistry and Biophysics, Hokkaido University, Sapporo 060 (Japan).

¹ Present address: National Chemical Laboratory for Industry, Tsukuba, 305 (Japan).

frequency decrease of 1 Hz corresponds to an adsorbed mass of 5.46 ng cm^{-2} when the fundamental frequency of the quartz is 9 MHz. Piezoelectric quartz crystals have therefore been used for mass measurements, and many gas sensors have been reported [2–5]. When the crystal is dipped into a solution, the oscillating frequency depends on the solvent used [6–8]. Several applications have been published, including the determination of ions [9], immunoassays [10–12], liquid chromatography [13,14], an electrochemical microbalance [15] and others [16,17]. In these applications, the crystal is used in a solution. The factors that determine the frequency are important from the standpoint of understanding the mechanism of the oscillation of the crystal in solution and from the practical standpoint of increasing its applicability as a sensor in a solution.

Other workers have measured the frequency in various solvents and developed experimental equations. Bruckenstein and Shay [18] proposed the following theoretical equation describing the oscillating frequency in solutions:

$$\Delta F = -2.26 \times 10^{-6} n F_b^{3/2} (\rho \eta)^{1/2} \quad (2)$$

where η is the viscosity of the solution, ρ the density of the solution and n the number of surfaces of the crystal contacting the solution ($n = 1$ or 2). Kanazawa and Gordon [19] also derived an equation for ΔF from a model that couples the stress wave in the quartz to a damped stress wave in the liquid. Hager [20] derived a similar relationship from an automatic gain control circuit system. We earlier reported on an experimental test of Eqn. 2 with a wide variety of solutions [8,21]. The oscillating frequencies in various solutions were measured. The quartz crystal was used as one of the elements in an oscillating electronic circuit, and this method is referred to as the oscillation method in this paper. With the oscillation in pure water as a reference, the change in frequency from that in pure water was denoted ΔF_w . Proportionality between ΔF_w and $(\rho \eta)^{1/2} - (\rho_w \eta_w)^{1/2}$ was observed for various solutions except electrolyte and polymer solutions (ρ_w and η_w are the density and viscosity, respectively of pure water). This linear relationship held

for every crystal tested, but the slope was dependent on the crystal used. This is presumably due to the coating treatment necessary for stable oscillation in solutions; the amount of sealant varied from one crystal to another, giving rise to the variations in the weight of the crystal. It was therefore not possible to examine Eqn. 2 quantitatively. In addition, the oscillating frequency was dependent on values of the resistance (R) and capacitance (C) of the electronic circuit (using transistor–transistor logic circuit, TTL), implying that this is another obstacle to the rigorous testing of Eqn. 2 in addition to the coating.

In this paper, the development of the resonance method, which measures an transmission for a two-port transmission line system, is reported. “Transmission” of the quartz crystals is defined as determining the frequency giving the largest transmission (series resonant point, F_s) and giving the smallest transmission (parallel resonant point, F_p). The differences in these values from the reference state (unloaded in air) are denoted ΔF_s and ΔF_p , respectively. When polystyrene of various weights was imposed on the electrodes in air, ΔF_s and ΔF_p were equal to each other and they followed Eqn. 1 exactly. The same frequency changes were obtained with the oscillating method. On the other hand, in solution, only ΔF_s was proportional to $(\rho \eta)^{1/2}$ and followed Eqn. 2. For large values of $(\rho \eta)^{1/2}$, however, large deviations were observed. The range of $(\rho \eta)^{1/2}$ where measurements of ΔF_s and ΔF_p were possible was wider than that using the oscillating method. Hence the proposed resonance method has advantages over the previous oscillation method.

EXPERIMENTAL

Materials

AT-cut crystals of varying fundamental frequencies were used; crystals of 3, 6, 9, 12, 15 and 18 MHz were obtained from Yakumo Tsushin (Tokyo). When necessary, one side of the quartz crystal surface was coated with a silicone sealant (Shin-etsu Kagaku, Tokyo). As reported previously, the coating was effective for stable oscillation in solutions with high $(\rho \eta)^{1/2}$ values [8,21].

Sucrose and glycerol were of guaranteed-reagent grade from Wako (Osaka). Polystyrene (PSt) and tetrahydrofuran were obtained from Nacalai Tesque (Kyoto). PSt was cast on the crystal electrodes by application with a microsyringe of a 0.1% (w/v) solution in tetrahydrofuran. Water was purified with a Milli-Q system (Millipore, Tokyo) and its specific resistance was more than 18 M Ω cm. To test Eqn. 2, values of $(\rho\eta)^{1/2}$ were necessary, and were determined with a pycnometer and Ostwald viscometer. Other physical constants were taken from the literature [22,23].

Resonance method

Figure 1a shows a schematic diagram of the experimental set-up. A signal source (HP-3325A) generated a 500-mV sinusoidal waveform at a desired frequency. R_s (50 Ω) represents the source resistance and R_p (50 Ω) is the load resistance. R_p is a high-precision resistor (0.1%) purchased from Vishay Kyowa (Tokyo). The output voltage across R_p was measured with an HP Model 8405A Vector volt meter. The procedure was as follows: first, the quartz crystal was temporarily replaced with a short lead and the applied voltage was adjusted to 500 mV. This adjustment was done at one frequency (e.g., 9 MHz) as preliminary experiments showed no frequency dependence of the output voltage of the HP-3325A (signal source). Next, a quartz crystal was inserted and the output voltage [root-mean-square (RMS), denoted $|V|$] across R_p was measured. After a change in the frequency of the signal

source of 10 or 100 Hz, $|V|$ was measured. $|V|$ was plotted as a function of the frequency; these plots are called transmission curves. This plot corresponds to the admittance (Y) of the crystal at various frequencies, as the input voltage is constant. Obtaining the value of the parameters described in the following equivalent electric circuit is referred to as characterizing the transmission curve, or transmission characteristics.

If 50 or 100 mV was employed instead of 500 mV as the input voltage, the same results were obtained, at least in solutions of medium viscosity or in air. In highly viscous solution, however, the peaks in the transmission curve were so insignificant that 500 mV was employed for all these experiments.

The crystal was installed in a Pyrex cell and immersed in a test solution (20 ml). Before measurement the crystal and the inside of the cell were rinsed three times with the test solution. Test solutions were changed with an aspirator, and their temperature was kept at $25 \pm 0.1^\circ\text{C}$ by circulating thermostated water; room temperature was maintained at $25 \pm 1^\circ\text{C}$.

Equivalent electric circuit of a piezoelectric quartz crystal

The essential properties of the crystal can be represented by an equivalent electric circuit (Fig. 1b), which consists of a capacitance C_1 , inductance L and resistance R in series, shunted by a capacitance C_0 . The assumption of the transmission measurement is as follows: under series reso-

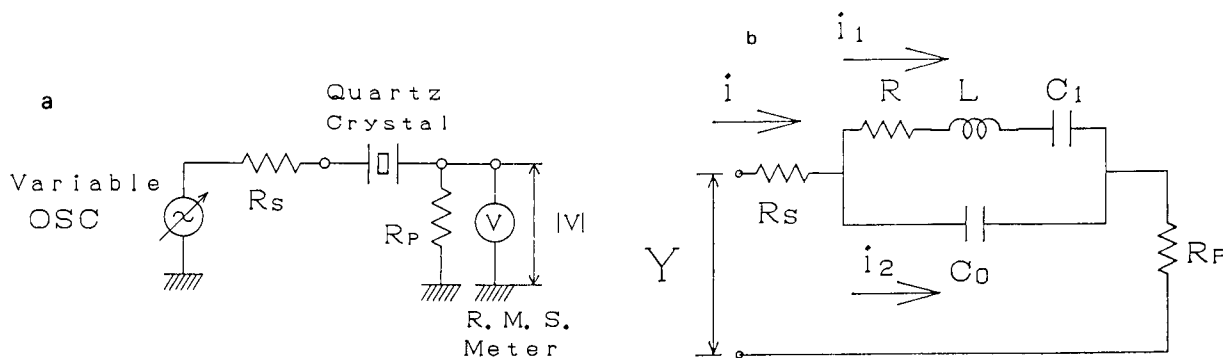


Fig. 1. (a) Schematic diagram of the resonance method. (b) Electrical equivalent circuit for the resonance measurement. For details, see text.

nant conditions, the current flowing through L is dominant ($i_1 \approx i$) and the current through the parallel capacitance is negligible ($i_2 \approx 0$). On the other hand, under parallel resonant conditions, the parallel capacitance plays an important role. The series and parallel frequencies are related to various values of the elements in the equivalent circuit as follows [24,25]:

$$F_s = (1/2\pi)(1/LC_1)^{1/2} \quad (3)$$

$$F_p = (1/2\pi) \left[(1/LC_1) + (1/LC_0) + (R^2/L^2) \right]^{1/2} \quad (4)$$

$$Q_L = F_s/F_{bw} \quad (5)$$

where F_{bw} is the band width at $1/\sqrt{2}$ relative response. Therefore, the loaded quality factor, Q_L , can be calculated from the transmission curve. $|V|_o$ and $|V|_{max}$ are the input voltage (RMS) and maximum voltage at output (RMS) of the transmission curves, respectively. The parallel capacitance of the crystal C_0 was measured with a Yokogawa–Hewlett-Packard 4261 LCR meter with a 16061A Test Fixture at 1 kHz.

The oscillation method

The method by which the quartz is incorporated into the oscillating electric circuit for measurements of oscillating frequencies is referred to

as the oscillation method. The oscillating circuit was made of TTL gates (SN7400); the resistances and capacitances were the same as described previously (circuit II in [8]). Sometimes, using the same crystal, both the oscillation and resonance methods were applied.

RESULTS AND DISCUSSION

Transmission characteristics of the quartz crystal in air

When polystyrene in various amounts was applied to the crystal surface of the electrode by the casting method, the transmission curves of the quartz crystal were obtained using 9 MHz as the fundamental oscillating frequency. Typical examples, shown in Fig. 2a, indicate that the transmission curves were sharp. From these curves, resonant characteristics such as F_s , F_p and Q_L were determined. When the loaded mass was increased, broadening of the curve and a decrease in the peak values became evident; the loaded quality factor, Q_L and $|V|_{max}$ decreased with increase in the loaded mass. The parallel capacitance, C_0 , was nevertheless unchanged at 5 pF. F_s and F_p were shifted to lower frequencies; ΔF_s and ΔF_p were increased and were almost identical.

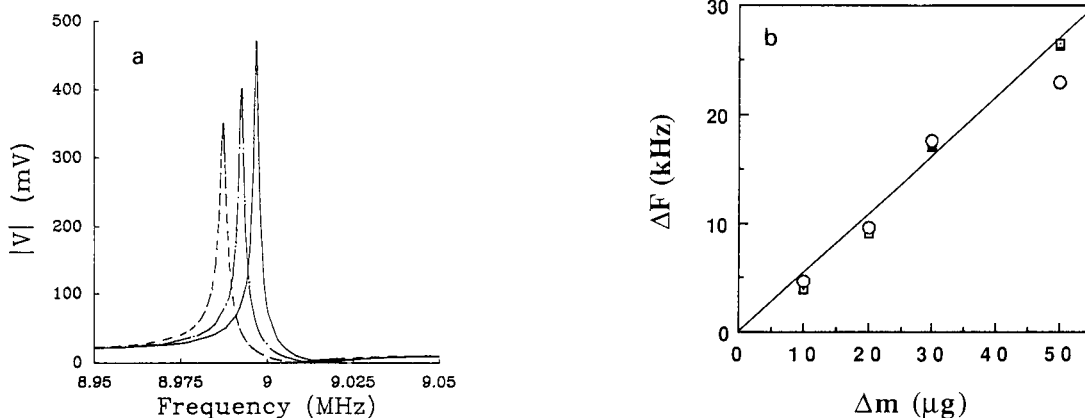


Fig. 2. Resonance method for experiments in air. A piezoelectric quartz crystal of 9 MHz was loaded with various amounts of polystyrene. (a) Transmission curves obtained when the coated amounts of polystyrene, Δm , were (solid line) 0, (dot-dashed line) 10 μg and (dashed line) 20 μg . (b) Correlation of ΔF (ΔF_s , ΔF_p and ΔF_{osc}) with Δm . ■ = ΔF_s series resonant shifts; □ = ΔF_p parallel resonant shifts; ○ = ΔF_{osc} , oscillating frequency shifts using the oscillation method. The straight line represents the theoretical plot of Eqn. 1.

Comparison with the oscillation method and test of Eqn. 1

The fundamental oscillating frequency of the crystal used was 9 MHz, the same as in the resonance method. Figure 2b shows the relationship between ΔF (ΔF_s , ΔF_p and ΔF_{osc}) and the loaded mass, Δm , revealing that the proportional relationship holds, although deviation of ΔF_{osc} is observed at a higher Δm of 50 μg . The solid line represents the theoretical line of Eqn. 1. It is concluded that in air, the previous oscillation method and the present resonance method give the same results and the results follow the theoretical relationship (Eqn. 1). When the loaded mass is large, deviation of ΔF_{osc} is observed. The resonance method is therefore superior to the oscillation method, at least using the TTL electric circuit.

Transmission characteristics of the crystal in solutions

When the quartz crystal was immersed in various solutions, the transmissions were measured and some of the curves are shown in Fig. 3a–c. Transmission characteristics of 9-MHz quartz crystal are given in Tables 1 and 2. Table 1 gives those when one surface of the crystal is covered with sealant (referred to as the one-side opened crystal), and Table 2 those when both sides of the crystal are in contact with the solution (two-side opened crystal). With increase in the sucrose or glycerol concentration [increase in $(\rho\eta)^{1/2}$], broadening of the curve was observed; the evident decreases in Q_L and increases in F_{bw} were observed. As expected from Eqn. 2, both $|\Delta F_s|$ and $|\Delta F_p|$ increased, although they were not identical with each other, which is in sharp contrast to the values in air.

Oscillation method in solutions and comparison with the resonance method

The frequency changes in the oscillation method with solutions with various concentrations of sucrose and glycerol were obtained with the one- and two-side opened crystals are given in Table 3. The oscillation method failed to measure the frequency change in solutions of high concentration with both the two-side and one-side

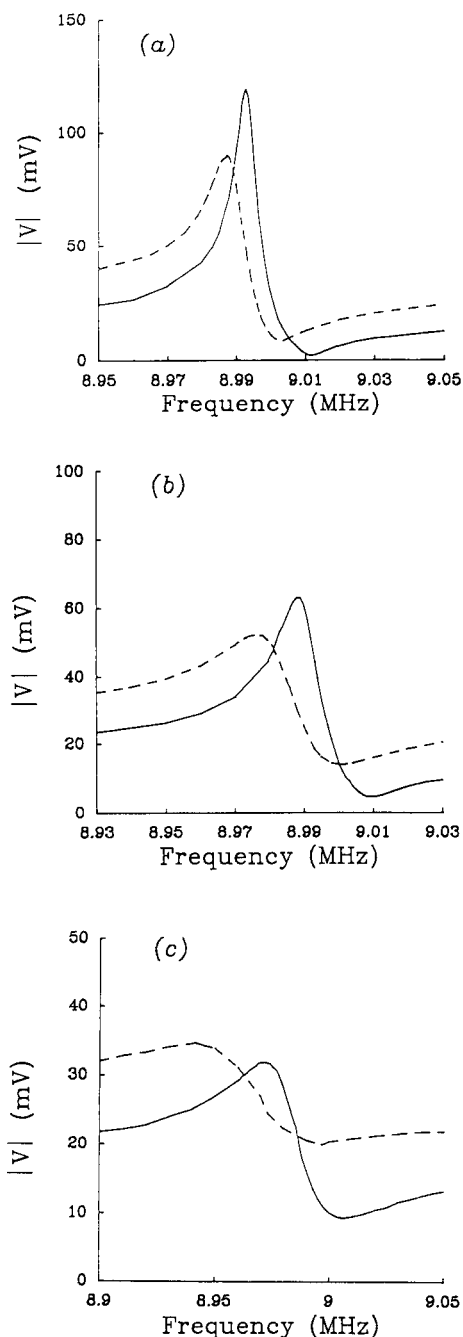


Fig. 3. Transmission curves in various solutions. Piezoelectric crystals of 9 MHz were used. Solid curves are those obtained with the one-side opened crystal and the dashed curves those with the two-side opened crystal. Solutions: (a) water; (b) 40 wt.% sucrose; (c) 60 wt.% sucrose. As described in the text, the top of the peak is the series resonant point and the bottom of the curve is the parallel resonant point.

TABLE 1

Transmission characteristics of the one-side opened quartz crystal in various solutions ^a

Solution	F_s (Hz)	F_p (Hz)	F_{bw} (Hz)	Q_L	$ \Delta F_s $ (Hz)	$ \Delta F_p $ (Hz)	V_{max} (mV)	C_0 (pF)
None	8 996 734	9 016 650	1657	5430	0	0	381.0	5.0
Water	8 992 900	9 011 680	6010	1496	3834	4970	119.0	6.5
20 wt.% sucrose	8 991 740	9 011 200	7830	1148	4994	5450	94.8	6.6
40 wt.% sucrose	8 988 360	9 009 390	13 570	662	8374	7260	63.2	6.6
60 wt.% sucrose	8 972 400	9 005 800	71 690	125	24 334	10 850	32.0	6.6
20 wt.% glycerol	8 991 600	9 011 190	7500	1199	5134	5460	98.9	6.7
40 wt.% glycerol	8 989 860	9 010 310	10 200	881	6874	6340	77.0	6.5
60 wt.% glycerol	8 986 090	9 008 530	17 230	522	10 644	8120	53.8	6.3
80 wt.% glycerol	8 972 850	9 006 300	57 940	155	23 884	10 350	32.9	5.7
100 wt.% glycerol	8 924 900	9 005 300	990 000	9	71 834	11 350	22.0	5.6

^a One side of the crystal (9 MHz) was covered with silicone sealant, then the other side was contacted with the solution.

opened crystals. The oscillation method was limited to the useful concentration range below 60 wt.% of glycerol or 40 wt.% of sucrose [below $3.556 (\rho\eta)^{1/2}$ in $\text{g}^{1/2} \text{cm}^{-3/2} \text{cP}^{1/2}$] when the one-side opened crystal was used, and the range was greatly limited to below 20 wt.% when the two-side opened crystal was used. The resonance method, in contrast, was applicable under both of these conditions.

Examination of the validity of Eqn. 2

According to Eqn. 2, $|\Delta F|$ ($|\Delta F_s|$, $|\Delta F_p|$ and $|\Delta F_{osc}|$) should be proportional to $(\rho\eta)^{1/2}$ of the

solution. In Fig. 4, $|\Delta F|$ is plotted against $(\rho\eta)^{1/2}$, showing that $|\Delta F_s|$ almost follows a linear relationship whereas $|\Delta F_p|$ and $|\Delta F_{osc}|$ do not. At large values of $(\rho\eta)^{1/2}$, however, deviation of $|\Delta F_s|$ from the theoretical value was evident; when $(\rho\eta)^{1/2}$ was $34.667 \text{ g}^{1/2} \text{cm}^{-3/2} \text{cP}^{1/2}$, an appreciable decrease from the values expected from Eqn. 2 was observed. Higher terms in the derivation of Eqn. 2 should be considered for solutions with large $(\rho\eta)^{1/2}$ values. The reason why $|\Delta F_p|$ does not follow the equation is not clear, but it is noted that parallel capacitance C_0 changes with increase in $(\rho\eta)^{1/2}$ of the solution

TABLE 2

Transmission characteristics of the two-side opened quartz crystal in various solutions ^a

Solution	F_s (Hz)	F_p (Hz)	F_{bw} (Hz)	Q_L	$ \Delta F_s $ (Hz)	$ \Delta F_p $ (Hz)	V_{max} (mV)	C_0 (pF)
None	8 996 707	9 016 850	1415	6358	0	0	440.0	5.0
Water	8 987 330	9 003 040	12 650	710	9377	13 810	90.0	6.5
20 wt.% sucrose	8 984 300	9 002 290	18 890	476	12 407	14 560	72.1	6.6
40 wt.% sucrose	8 976 540	9 001 140	46 670	192	20 167	15 710	52.1	6.6
60 wt.% sucrose	8 941 300	8 996 900	597 200	15	55 407	19 950	34.7	6.6
20 wt.% glycerol	8 985 130	9 002 250	17 000	529	11 577	14 600	75.0	5.3
40 wt.% glycerol	8 980 600	9 000 980	28 920	311	16 107	15 870	60.1	5.3
60 wt.% glycerol	8 971 860	8 999 940	74 530	120	24 847	16 910	46.0	5.3
80 wt.% glycerol	8 943 940	8 996 140	751 000	12	52 767	20 710	34.0	7.7
100 wt.% glycerol	8 822 900	– ^b	– ^b	– ^b	173 807	– ^b	24.9	7.7

^a The crystal (9 MHz) was not coated with sealant so that both sides were contacted with the test solution. ^b The parallel resonant point could not be found.

TABLE 3

Oscillation frequency of one- and two-side opened quartz crystals by the oscillation method in various solutions ^a

Crystal	Solution	F_{osc} (Hz)	$ \Delta F_{\text{osc}} $ (Hz)
One-side opened	None	9000262	0
	Water	8995412	4850
	20 wt.% sucrose	8994357	5905
	40 wt.% sucrose	8992010	8252
	20 wt.% glycerol	8994585	5677
	40 wt.% glycerol	8993292	6970
	60 wt.% glycerol	8991068	9194
Two-side opened	None	9000437	0
	Water	8991738	8699
	20 wt.% sucrose	8990534	9903
	20 wt.% glycerol	8990588	9849

^a The crystals used were the same as those in Tables 1 and 2.

(see Tables 1 and 2). On the other hand, however, C_0 remains constant in air, and $|\Delta F_s|$ and $|\Delta F_p|$ are almost equal.

Another aspect in the examination of Eqn. 2 is consideration of n , the number of opened surfaces ($n = 1$ or 2). As shown in Tables 1 and 2, the change in $|\Delta F_s|$ for the two-side opened crystal ($n = 2$) is approximately twice than that for the one-side opened crystal ($n = 1$).

Equation 2 indicates that a linear relationship between $|\Delta F_s|$ and $F_b^{3/2}$ should hold. Figure 5 shows the plots of $|\Delta F_s|$ against $(\rho\eta)^{1/2}$ using

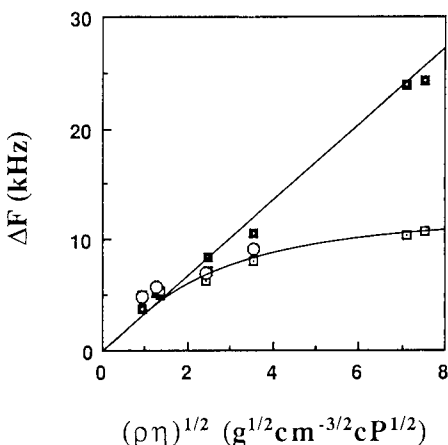


Fig. 4. ΔF versus $(\rho\eta)^{1/2}$ relationship. The $(\rho\eta)^{1/2}$ values were changed with glycerol and sucrose. ■ = ΔF_s ; □ = ΔF_p ; ○ = ΔF_{osc} .

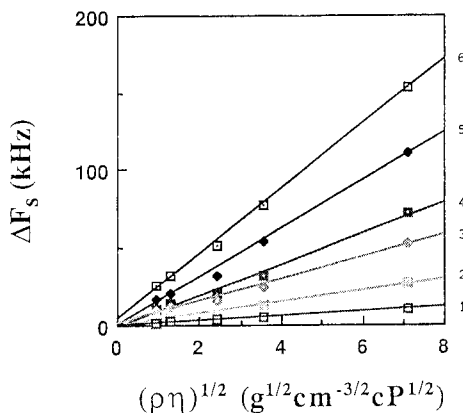


Fig. 5. Plots of ΔF_s versus $(\rho\eta)^{1/2}$ using crystals of various fundamental oscillating frequencies with both sides in contact with glycerol solutions at 25°C. Fundamental oscillating frequencies used: (1) 3; (2) 6; (3) 9; (4) 12; (5) 15; (6) 18 MHz.

crystals of various F_b , indicating that for every crystal the linear relationship holds. Linear regression gave the following: for 3 MHz, $|\Delta F_s| = 0.245 + 1.4344(\rho\eta)^{1/2}$, $R^2 = 0.989$ ($R = 0.994$); for 6 MHz, $|\Delta F_s| = -0.292 + 3.7488(\rho\eta)^{1/2}$, $R^2 = 0.986$ ($R = 0.993$); for 9 MHz, $|\Delta F_s| = 1.1954 + 7.0626(\rho\eta)^{1/2}$, $R^2 = 0.989$ ($R = 0.994$); for 12 MHz, $|\Delta F_s| = -0.6873 + 10.005(\rho\eta)^{1/2}$, $R^2 = 0.989$ ($R = 0.994$); for 15 MHz, $|\Delta F_s| = -0.0164 + 15.407(\rho\eta)^{1/2}$, $R^2 = 0.995$ ($R = 0.997$); and for 18 MHz, $|\Delta F_s| = 4.438 + 20.853(\rho\eta)^{1/2}$, $R^2 = 0.998$ ($R = 0.999$). The intercepts are very small, indicating that $|\Delta F_s|$ is proportional to $(\rho\eta)^{1/2}$ as in Eqn. 2. The slope of these linear lines, $d|\Delta F_s|/d(\rho\eta)^{1/2}$ is plotted against $F_b^{3/2}$ in Fig. 6, revealing clearly that the linear relationship between $|\Delta F_s|$ and $F_b^{3/2}$ holds. We previously failed to show the validity of Eqn. 2 by the oscillation method [8]. Similarly, the failure of the oscillation method is evident in Fig. 4. The slope of the straight line in Fig. 6 is $2.7 \times 10^{-6} \text{ Hz}^{-1/2} \text{ g}^{-1/2} \text{ cm}^{3/2} \text{ P}^{-1/2}$, which is close to the theoretical value of Eqn. 2.

An impedance analyser has been used to measure the resonant frequency and resistance of the equivalent circuit of the quartz crystal [26,27]. The network analyser method has recently been used [28] and the validity of Eqn. 2 was tested. Most recently, Martin et al. [29] were able to combine an equivalent circuit model for the elec-

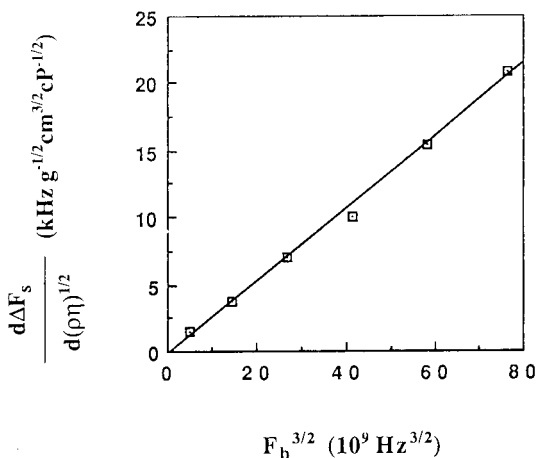


Fig. 6. Correlation of $F_b^{3/2}$ with the slope of Fig. 5. The regression equation is $y = -0.32349 + 0.27117x$, $R^2 = 0.995$ ($R = 0.997$).

trical behaviour of the quartz crystal with liquid-phase properties. The present method does not require measurement of the phase angle or computational calculations such as the admittance locus method.

Comparison of proposed method with the oscillation method

From the above discussion, the present method is obviously superior to the oscillation method. Moreover, the principle of the present measurement is simpler than that of the oscillation method. The crystal in the oscillating circuit has an internal resistance ($R + r$, where r represents the weight loaded or the viscous friction resistance). It is cancelled by a negative resistance ($-R$) which is generated by a positive feedback circuit; The condition for sustained oscillation is $|R + r| \leq |-R|$ [30]. In addition, the frequency of oscillation should be between F_s and F_p , where the quartz crystal works as an inductor [31]. In fact, oscillation does occur in the frequency range between F_s and F_p , as shown in Tables 1–3. If the difference between F_s and F_p is large (e.g., in experiments in solutions), the actual oscillating frequency is difficult to fix as the rest of the circuit significantly affects it. The present method of obtaining the transmission characteristics does not depend on negative resistance elements; a

broad working range can therefore be expected, and has actually been demonstrated.

Conclusions

The resonance method is superior to the usual oscillation method, especially for solution experiments. The resonance method has further advantages in quantitative measurements. Equation 2 has been proved experimentally, but deviations are observed when $(\rho\eta)^{1/2}$ is large. The single surface coating is useful in solution experiments. Only with the resonance method, could the depolymerization of carp actomyosin be monitored; no change could be observed with the oscillation method (using TTL). Details will be reported elsewhere. Further detailed analysis of the transmission characteristics with the equivalent circuit is being made.

The authors are grateful to S. Wakamatsu (Hokkaido University) for technical support and Y. Kunitoh and K. Hirama (Toyo Communication Equipment) for useful discussions. This work was partially supported by the Shimadzu Science and Technology Foundation.

REFERENCES

- 1 J. Hlavay and G.G. Guilbault, *Anal. Chem.*, 49 (1977) 1890.
- 2 G.G. Guilbault, in C.S. Lu and A.W. Czanderna (Eds.), *Application of Piezoelectric Quartz Crystal Microbalances*, Vol. 7, Elsevier, New York, 1984, Chap. 8 and 10.
- 3 J. Janata and A. Bezegh, *Anal. Chem.*, 60 (1988) 62R.
- 4 J.J. McCallum, *Analyst*, 114 (1989) 1173.
- 5 S. Kurosawa, N. Kamo, D. Matsui and Y. Kobatake, *Anal. Chem.*, 62 (1990) 353.
- 6 T. Nomura, M. Watanabe and T. S. West, *Anal. Chim. Acta*, 175 (1985) 107.
- 7 S. Yao and T. Zhou, *Anal. Chim. Acta*, 212 (1988) 61.
- 8 S. Kurosawa, E. Tawara, N. Kamo and Y. Kobatake, *Anal. Chim. Acta*, 230 (1990) 41.
- 9 T. Nomura, F. Tanaka, T. Yamada and H. Itoh, *Anal. Chim. Acta*, 243 (1991) 273.
- 10 H. Muramatsu, J.M. Dicks, E. Tamiya and I. Karube, *Anal. Chem.*, 59 (1987) 2760.
- 11 K.A. Davis and T.R. Leary, *Anal. Chem.*, 61 (1989) 1227.
- 12 S. Kurosawa, E. Tawara, N. Kamo, F. Ohta and T. Hosokawa, *Chem. Pharm. Bull.*, 38 (1990) 1117.
- 13 P.L. Konash and G.J. Bastiaans, *Anal. Chem.*, 52 (1980) 1929.

- 4 T. Nomura, F. Tanaka, T. Yamada and H. Itoh, *Anal. Chim. Acta*, 246 (1991) 300.
- 5 M.D. Ward and D.A. Buttry, *Science*, 249 (1990) 1000.
- 6 D.A. Buttry, in A.J. Bard (Ed.), *Electroanalytical Chemistry*, Vol. 17, Dekker, New York, 1990, pp. 1–85.
- 7 M. Thompson, A.L. Kipling, W.C. Duncan-Hewitt, L.V. Rajaković and B.A. Čavić-Vlasak, *Analyst*, 116 (1991) 881.
- 8 S. Bruckenstein and M. Shay, *Electrochim. Acta*, 30 (1985) 1295.
- 9 K.K. Kanazawa and J.G. Gordon, II, *Anal. Chim. Acta*, 175 (1985) 99.
- 10 H.E. Hager, *Chem. Eng. Commun.*, 43 (1986) 25.
- 11 S. Kurosawa, E. Tawara, N. Kamo, and H. Kitajima, *Proceedings of 178th Meeting of the Electrochemical Society*, October 1990, Extended Abstracts, The electrochemical Soc. Fall Meeting, Seattle, WA, 1990, Abstract No. 798, p. 1136.
- 12 G. Barr, *A Monograph on Viscometry*, Oxford University Press, Oxford, 1931, Appendix III; E.C. Bingham and R.F. Jackson, *Sci. Pap. Natl. Bur. Stand.*, No. 298 (1917).
- 23 J.F. Swindells, J.R. Coe and T.B. Godfrey, *J. Res. Natl. Bur. Stand.*, 48, No. 1 (1952).
- 24 C.F. Franklin, *Transistor Circuit Analysis and Design*, Van Nostrand, New York, 1960.
- 25 C. Lu and A.W. Czanderna, *Applications of Piezoelectric Quartz Crystal Microbalances*, Elsevier, Amsterdam, 1984.
- 26 H. Muramatsu, E. Tamiya and I. Karube, *Anal. Chem.*, 60 (1988) 2142.
- 27 T. Zhou, L. Nie and S. Yao, *J. Electroanal. Chem.*, 293 (1990) 1.
- 28 A.L. Kipling and M. Thompson, *Anal. Chem.*, 62 (1990) 1514.
- 29 S.J. Martin, V.E. Granstaff and G.C. Frye, *Anal. Chem.*, 63 (1991) 2272.
- 30 J.R. Herbert, *Theory and Application of Electron Tubes*, McGraw-Hill, New York, 1955.
- 31 F.T. Frederick, *Electronic and Radio Engineering*, McGraw-Hill, New York, 1955.

Ultratrace measurements of selenium by cathodic stripping voltammetry in the presence of rhodium

Joseph Wang and Jianmin Lu¹

Department of Chemistry, New Mexico State University, Las Cruces, NM 88003 (USA)

(Received 19th August 1992; revised manuscript received 26th October 1992)

Abstract

A remarkably sensitive cathodic stripping voltammetric procedure for ultratrace measurements of selenium in the presence of added rhodium is described. The method is based on the accumulation and subsequent reduction of a Rh_2Se_3 layer on the hanging mercury drop electrode. Optimum experimental conditions were established, including the use of a 0.1 M sulfuric acid solution containing $10 \mu\text{g l}^{-1}$ rhodium, and preconcentration at -0.2 V followed by a fast linear scan. Such conditions yield an extremely low detection limit of 0.5 ng l^{-1} ($6 \times 10^{-12} \text{ M}$) selenium following a 3-min preconcentration. The improved sensitivity (over earlier cathodic stripping voltammetric schemes) is coupled to high selectivity and precision. Applicability to assays of groundwater and river water samples is illustrated.

Keywords: Stripping voltammetry; Rhodium; Selenium

Trace measurements of selenium have received much attention in recent years because of the biological significance of this element. In particular, the narrow concentration range between deficient and toxic levels of selenium has stimulated the development of ultrasensitive methods for its determination [1]. Electroanalytical techniques, particularly stripping voltammetry, have been shown by several workers to be extremely useful for this task [1–8]. While anodic stripping procedures (at gold electrodes) were used in previous years [3], cathodic stripping schemes (at the static mercury electrode) have been adapted recently for routine applications because of the ease of attaining renewable and

reproducible surfaces [4–7]. Various variants of the cathodic stripping techniques for trace selenium have thus been proposed based on the preconcentration and subsequent reduction of HgSe [4] and Cu_2Se [6] layers.

The present paper describes an extremely sensitive cathodic stripping voltammetric procedure for the determination of selenium in the presence of rhodium. The procedure relies on the formation of an insoluble layer of Rh_2Se_3 on the mercury surface during the preconcentration step. The sharp cathodic stripping response, resulting from the reduction of the accumulated Rh_2Se_3 species, is significantly (ca. 10- to 50-fold) larger than the analogous Cu_2Se or HgSe peaks, respectively. The corresponding lowering of the detection limit (down to $6 \times 10^{-12} \text{ M}$) is coupled with high selectivity and precision. The performance characteristics of the resulting procedure for selenium are elucidated in the following sections.

Correspondence to: J. Wang, Department of Chemistry, New Mexico State University, Las Cruces, NM 88003 (USA).

¹ Permanent address: Department of Chemistry, Shandong Normal University, Jinan, Shandong (China).

EXPERIMENTAL

Apparatus and reagents

An EG & G PAR voltammetric analyzer (Model 264A) was used in connection with the AG&G PAR Model 303 static mercury drop electrode and a EG&G PAR Model 305 stirrer. A medium-size hanging mercury drop electrode (HMDE), with an area of 0.016 cm², was employed, in connection with Ag/AgCl (Sat. KCl) reference and platinum wire counter electrodes. Data were displayed on an EG&G PAR Model 0073 X-Y recorder.

All solutions were prepared from double-distilled water. Stock solutions of selenium, rhodium and other metals (1000 mg l⁻¹, AA standard, Aldrich) were diluted daily as required. Bovine albumin and dodecyl sodium sulfate were obtained from Sigma and Baker, respectively. A 0.1 M H₂SO₄ solution served as the supporting electrolyte. The groundwater and river water samples were collected at the Hanford site (Richland, WA) and Rio Grande (Las Cruces, NM), respectively, and used without pretreatment.

Procedure

The supporting electrolyte solution (10 ml), containing 10 μg l⁻¹ rhodium was pipetted into the cell, and purged with nitrogen for 8 min. The preconcentration potential (usually -0.2 V) was applied to a fresh mercury drop while the solution was stirred. Following the preconcentration period, the stirring was stopped, and after a 15-s equilibration the voltammogram was recorded by applying a negative-going linear scan (at 50 mV s⁻¹) to -1.25 V. Some preliminary experiments employed the differential pulse waveform. The deposition/stripping cycle was repeated at a new mercury drop after standard additions. All experiments were performed at a room temperature.

RESULTS AND DISCUSSION

Figure 1 shows cyclic voltammograms for 0.5 μg l⁻¹ selenium, in a sulfuric acid media containing 10 μg l⁻¹ rhodium, obtained after 0 (A) and 60 (B) s stirring at -0.20 V. While no distinct

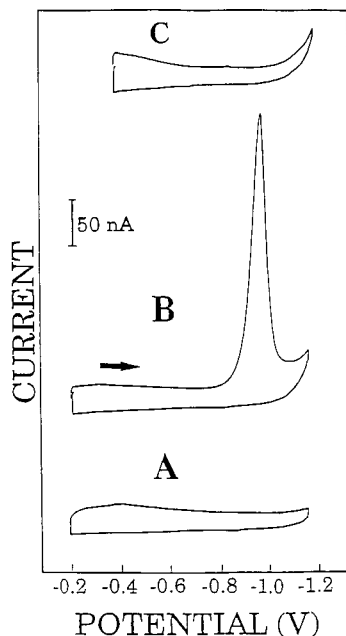


Fig. 1. Cyclic voltammograms for 0.5 μg l⁻¹ selenium (in the presence of 0.1 M H₂SO₄ and 10 μg l⁻¹ rhodium) after (A) 0 and (B) 60 s stirring at -0.20 V. Also shown (C), is the corresponding voltammogram for 0.5 μg l⁻¹ selenium (in the presence of 0.02 M HCl and 2.5 mg l⁻¹ copper) after 60 s stirring at -0.40 V. Scan rate, 50 mV s⁻¹.

peak is observed without accumulation a well-defined response is observed (at -0.97 V vs. Ag/AgCl) following the stirring period. Subsequent scans yielded substantially smaller peaks (not shown), indicating a rapid removal of the Rh₂Se₃ layer from the surface. Maximum surface coverage was observed following a 10-min stirring. The maximum charge obtained by integrating the reduction current was found to be 5.3 μC. The selenium peak increased in a non-linear fashion with the scan rate (over the 10–200 mV s⁻¹ range). No peak was observed in analogous measurements without the rhodium (not shown). Figure 1 displays also the corresponding voltammogram in the presence of added copper (under the optimum conditions of Ref. 6) (C). An extremely small reduction peak, due to the reduction of copper in the Cu₂Se deposit [6], is observed at -0.84 V.

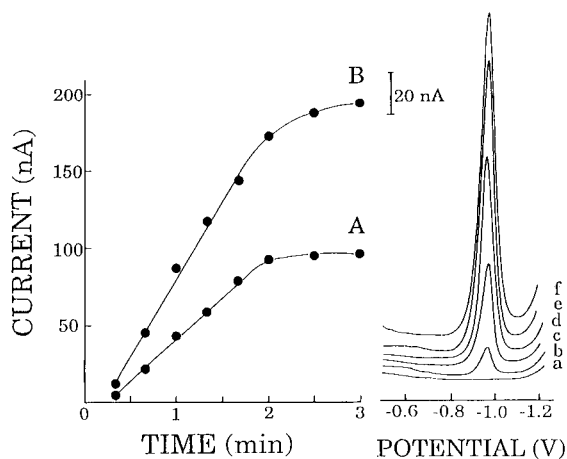
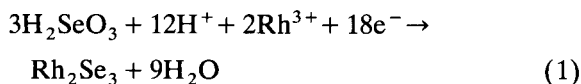


Fig. 2. Stripping voltammograms for 250 ng l^{-1} selenium after different pre-concentration periods: (a) 0, (b) 20, (c) 40, (d) 60, (e) 80 and (f) 100 s. Pre-concentration at -0.20 V with 400 rpm stirring. Linear scan at 50 mV s^{-1} . Also shown, current-time plots for (A) 100 and (B) 250 ng l^{-1} . Solution conditions as in Fig. 1 (A, B).

The deposition process, in the acidic medium, appears to involve the reduction of Se(IV) to Se(II) (in a manner analogous to that suggested for other cathodic stripping procedures [5,6]), coupled with the formation of the Rh_2Se_3 deposit. The net reaction is thus likely to be:



The voltammetric peak is attributed to the reduction of rhodium in the Rh_2Se_3 surface layer. The fact that a well-defined cyclic voltammetric response is observed for sub- $\mu\text{g l}^{-1}$ concentrations indicates the remarkable sensitivity of rhodium-based selenium measurements. Full analytical exploitation of these enhancement effects is accomplished through the use of a cathodic stripping operation, as illustrated below.

Figure 2 illustrates linear scan voltammograms for 250 ng l^{-1} ($3.1 \times 10^{-9} \text{ M}$) selenium after different accumulation periods (0–100 s, a–f). Despite the extremely low (ppt) concentration and the short pre-concentration times, well defined peaks are observed ($E_p = -0.97 \text{ V}$, $b_{1/2} = 56 \text{ mV}$). The peak increases rapidly with increasing accumulation time, indicating (again) a signif-

icant enhancement of the selenium concentration on the electrode surface. For example, ca. 11-fold enhancement of the peak is observed by extending the pre-concentration period from 20 to 60 s (compare b and d). A selenium peak is not detected without pre-concentration. Also shown in Fig. 2 are plots of the resulting current vs. accumulation time for 100 and 250 ng l^{-1} . At both levels, the current increases linearly with the time at first (up to 2 min), and then starts to level off. Overall, the inherent sensitivity of this scheme allows convenient measurements of sub-nM concentrations of selenium following very short pre-concentration times.

The dependence of the stripping peak current on the pre-concentration potential was examined over the -0.05 to -0.60 V range (Fig. 3A). The peak rises rapidly between -0.05 and -0.20 V , and then decreased sharply. All subsequent work used a potential of -0.20 V . The selenium response increases linearly with the rhodium concentration, until it levels off at $10 \mu\text{g l}^{-1}$ (Fig. 3B). While highly sensitive stripping measurements were carried out in different mineral acids (HCl , HNO_3 , HClO_4 and H_2SO_4), best performance was observed in the sulfuric acid medium. The stripping peak increased gradually with the sulfuric acid concentration until 0.05 M , and then more slowly (Fig. 3C). The high sensitivity in acidic media is consistent with the literature on other cathodic stripping procedures [4–6]. Both differential pulse and linear scan stripping modes exhibited remarkable sensitivity. However, the linear scan mode offered higher signal-to-background characteristics and faster assays, and was thus used in all subsequent work.

Figure 4 shows voltammograms obtained after increasing the selenium concentration in 50 ng l^{-1} steps (a–d). Well-defined peaks are observed using a 90-s pre-concentration period. These four measurements are part of nine concentration increments from 50 to 300 ng l^{-1} . The resulting calibration plots (following 45- and 90-s accumulation) are also shown in Fig. 4. For both periods, the current increases linearly with the concentration up to 200 ng l^{-1} , and then it starts to level off. The linear portion of these plots is characterized with a sensitivity of 179 (A) and 694 (B)

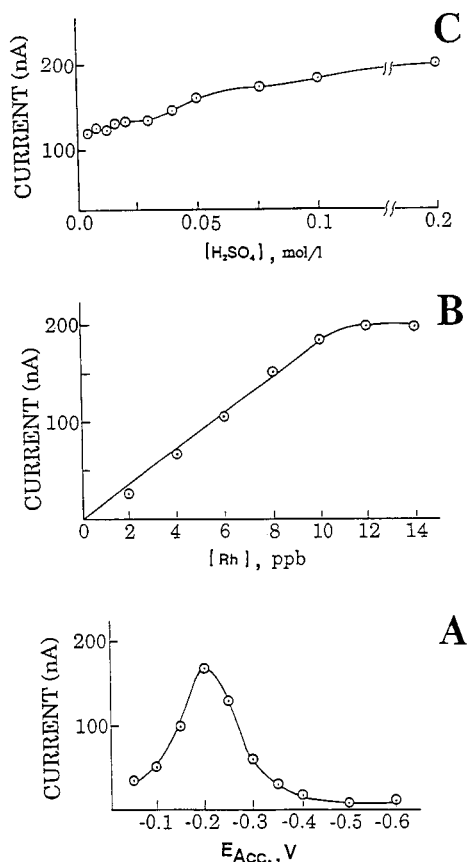


Fig. 3. Effect of pre-concentration potential (A), rhodium concentration (B), and sulfuric acid concentration (C) on the stripping peak current for $0.5 \mu g l^{-1}$ selenium. Preconcentration for 30 s. Differential pulse waveform with $10 mV s^{-1}$ scan rate and 25 mV amplitude. Other conditions as in Fig. 2.

$nA l ng^{-1}$ (correlation coefficients, 0.994 and 0.998, respectively). Non-linear behavior, caused by saturation of the mercury surface, was common to earlier cathodic stripping schemes for selenium (although some of them exhibit a wider linear range) [5,6].

The detectability was estimated from measurements of $25 ng l^{-1}$ ($3.1 \times 10^{-10} M$) selenium after preconcentration for 3 min; the resulting voltammogram is shown in Fig. 5. A detection limit of around $0.5 ng l^{-1}$ ($6 \times 10^{-12} M$) can be estimated based on the signal-to-background characteristics of these data. Hence, 5 pg can be detected in the 10 ml of solution used. A detection limit of $5 ng l^{-1}$ ($6 \times 10^{-11} M$) was reported for analogous measurements in the presence of copper [6]. Even

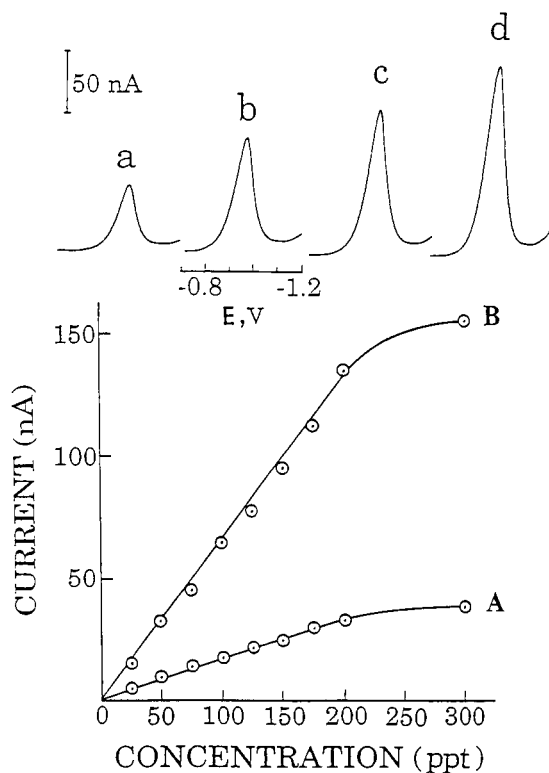


Fig. 4. Stripping voltammograms for solutions of increasing selenium concentrations: (a) 50, (b) 100, (c) 150, and (d) 200 $ng l^{-1}$. Preconcentration for 90 s. Also shown are calibration plots over the 25–300 $ng l^{-1}$ range following (A) 45 and (B) 90 s preconcentration. Other conditions as in Fig. 2.

higher detection limits (of 20–250 $ng l^{-1}$) characterize cathodic stripping procedures based on the formation of mercury selenide [1,4,5]. The signifi-

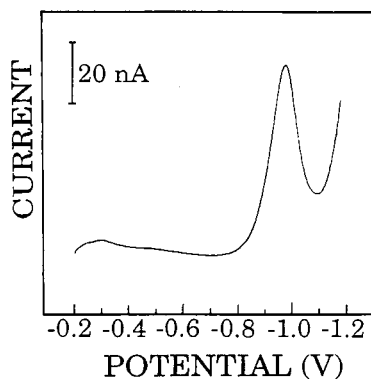


Fig. 5. Stripping voltammogram for $25 ng l^{-1}$ selenium following 3-min preconcentration. Other conditions as in Fig. 2.

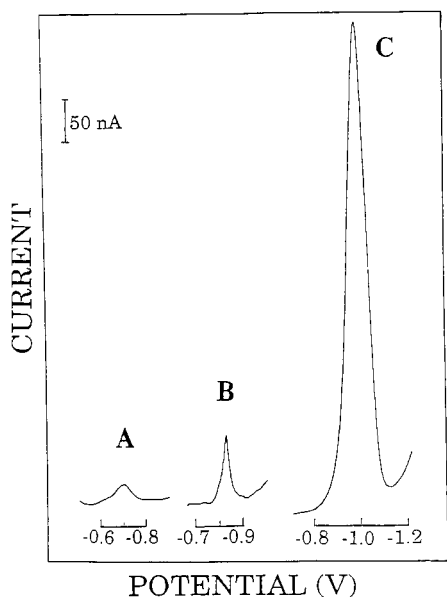


Fig. 6. Stripping voltammograms for $1 \mu\text{g l}^{-1}$ selenium following 1-min preconcentration. Media, hydrochloric acid [0.01 M (A, C), 0.02 M (B)], containing 2.5 mg l^{-1} copper (B) and $10 \mu\text{g l}^{-1}$ rhodium (C). Preconcentration at (A) -0.30 , (B) -0.40 and (C) -0.20 V. Differential pulse waveform as in Fig. 3.

cant improvement in sensitivity offered by the rhodium-based scheme is illustrated in Fig. 6. This figure displays cathodic stripping voltammograms for $1 \mu\text{g l}^{-1}$ selenium, after 1-min preconcentration, using the formation of the HgSe (A), Cu_2Se (B), and Rh_2Se_3 (C) surface layers. (Optimum conditions, in accordance to Refs. 5 and 6, were employed in A and B.) The formation of the Rh_2Se_3 surface species yields a substantially larger stripping peak, of ca. 8.5- and 42-fold higher than the peaks associated with the Cu_2Se and HgSe layers, respectively. The exact reason for the greater response seen with rhodium is not fully clear [but it may be attributed to differences in the solubility of Rh_2Se_3 (vs. HgSe or Cu_2Se)]. The inherent sensitivity of the method also compares favorably to recent non-electrochemical techniques for selenium [9,10].

High reproducibility is another attractive feature of the rhodium-based stripping procedure. A prolonged series of 30 repetitive measurements of 100 ng l^{-1} selenium was used to establish the reproducibility of the data (60 s preconcentra-

tion). The mean peak current found was 44.9 nA , with a range of $42\text{--}48 \text{ nA}$, and relative standard deviation of 3.7% . The high sensitivity and precision are coupled to high selectivity toward selenium. Possible interference from numerous coexisting trace metals (present at 100-fold excess) was investigated. The following metals were tested at the $10 \mu\text{g l}^{-1}$ level and found not to affect the size, potential or shape of the 100 ng l^{-1} selenium peak: Co(II) , Ni(II) , Cu(II) , Zn(II) , Pb(II) , Bi(III) , Mn(II) , Fe(III) , Tl(I) , Cd(II) , As(III) , Mo(VI) , Ti(IV) , V(V) , Cr(VI) , In(III) , Pd(II) , U(VI) , Cd(II) , Pt(II) , Zr(IV) , Ge(IV) , Nb(V) and La(III) . Only Te(VI) yielded a large overlapping peak at these levels. A 5-fold excess of Te exhibited no interference. Interferences due to coexisting Te and Cd were reported for the copper-based cathodic stripping selenium measurements [6]. Coexisting surface-active substances can affect the size of the selenium peak, in a manner common to other cathodic stripping procedures. For example, 30 and 50% depressions of the $0.8 \mu\text{g l}^{-1}$ selenium response were observed in the presence of 2 mg l^{-1} sodium dodecyl sulfate and bovine albumin, respectively (60 s accumulation).

Figure 7 illustrates the applicability of the method to the analysis of groundwater (A) and river water (B) samples. With a short (30 s) preconcentration time, the method yields a well-de-

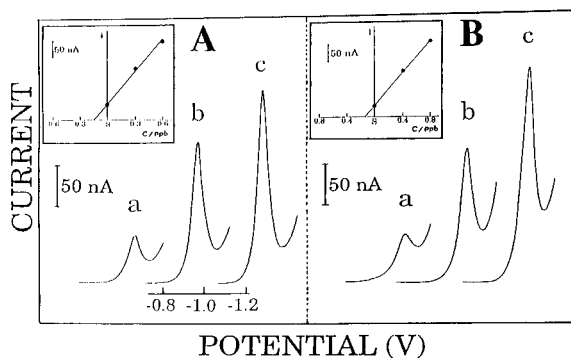


Fig. 7. Determination of selenium in (A) groundwater and (B) river water samples. (A) Scans for the sample (a) and subsequent concentration increments of $0.3 \mu\text{g l}^{-1}$ (b, c). (B) Scans for the sample (a) and subsequent concentration increments of $0.4 \mu\text{g l}^{-1}$ (b, c). Samples contained 0.1 M sulfuric acid and $10 \mu\text{g l}^{-1}$ rhodium. Preconcentration for 30 s. Other conditions as in Fig. 2.

finer selenium peak for these samples (a) and subsequent standard additions (b, c). Selenium levels of 0.09 (A) and 0.16 (B) $\mu\text{g l}^{-1}$ were therefore calculated for the samples. While no pretreatment was required with these water samples, more complex samples (particularly biological materials) would require the use of UV photolysis for the destruction of coadsorbing organic substances.

In conclusion, the method described provides an ultrasensitive and yet a simple approach to the determination of ultratrace levels of selenium. Very short preconcentration periods can be employed for measuring pM–nM concentrations of selenium, thus greatly reducing the total analysis time. The use of rhodium results also in high selectivity, hence addressing the growing needs for a reliable method for determining trace selenium in complex environmental and biological samples. Other stripping strategies, particularly potentiometric stripping analysis, may benefit from the remarkable sensitivity of the new procedure. Additional work may be required for obtaining full understanding of the complex pro-

cesses involved in the deposition/stripping cycles.

This work was supported by grants from Battelle PNL (Subcontract 095985-A-PI) and Lawrence Livermore NL (Subcontract B160617).

REFERENCES

- 1 U. Baltensperger and J. Hertz, *Anal. Chim. Acta*, 172 (1985) 49.
- 2 J. Wang, *Stripping Analysis*, VCH, Deerfield Beach, FL, 1985.
- 3 R.W. Andrews and D.C. Johnson, *Anal. Chem.*, 48 (1976) 1056.
- 4 G. Jarzabek and A. Kublik, *Anal. Chim. Acta*, 143 (1982) 121.
- 5 S. Adeloju, A.M. Bond, M. Briggs and H. Hughes, *Anal. Chem.*, 55 (1983) 2076.
- 6 C.M.G. van den Berg and S. Khan, *Anal. Chim. Acta*, 231 (1990) 221.
- 7 R. Ahmed, J. Hill and R. Magee, *Analyst*, 108 (1983) 835.
- 8 M. Zelic and M. Branica, *Electroanalysis*, 2 (1990) 455.
- 9 P. Shiundu and A. Wade, *Anal. Chem.*, 63 (1991) 692.
- 10 D. Tanzer and K. Heumann, *Anal. Chem.*, 63 (1991) 1984.

Polarographic studies of metal ion complexes of Ampicillin and Amoxycillin

Samuel J. Lyle and Sheikheldin Sami Yassin

Chemistry Department, King Fahd University of Petroleum and Minerals, Dhahran 31261 (Saudi Arabia)

(Received 20th July 1992)

Abstract

A study of the direct current and differential pulse polarographic behaviour of metal complexes, especially nickel(II), of Ampicillin and Amoxycillin at the dropping mercury electrode, is described. In 1 M sodium acetate at pH 8.0, the nickel(II) complex is superior to those of cobalt(II), copper(II), and zinc(II) in providing differential pulse peaks which at -0.865 V and -0.840 V for Ampicillin and Amoxycillin respectively with respect to the Ag/AgCl, sat. KCl reference electrode at 25°C , are well separated from those of excess metal ion. Suitable working conditions of pH, ionic strength in sodium acetate supporting electrolyte, temperature and time of measurement after mixing of reactants were established for the nickel(II) systems. As the temperature of reaction and measurement is increased, the differential pulse peak near -0.850 V decreases roughly exponentially with time at $\geq 25^{\circ}\text{C}$. Tests showed that single electron reversible reduction occurs in the nickel(II) complexes. For quantitative determination by the differential pulse technique, linear calibration graphs were obtained over concentration ranges 3.0×10^{-7} M to 3.0×10^{-5} M and 4.0×10^{-7} M to 2.0×10^{-5} M for Ampicillin and Amoxycillin, respectively, with coefficients of variation from 2 to 3% for 6 determinations in the middle of the calibration ranges. Good agreement was found between results obtained by the differential pulse method and three methods from the British or US Pharmacopoeias.

Keywords: Polarography; Amoxycillin; Ampicillin; Nickel

Ampicillin and Amoxycillin are electrochemically inactive at the dropping mercury electrode (DME) in aqueous solution. However, it has been shown [1] that the related β -lactam antibiotic, cephalexin, forms a complex with nickel(II); this complex is electroactive and can be used [2] for the polarographic determination of the antibiotic. In addition, Ampicillin in dosage forms has been determined quantitatively by polarographic techniques after acid hydrolysis [3]. More recently [4] an amperometric study of nickel(II) and cobalt(II)

complexes of Ampicillin has shown that 1:1 complexes are formed and that they undergo reduction at the DME. The same authors [5] determined the equilibrium constant for the formation of the 1:1 complex of Amoxycillin with nickel(II) and stated without going into details that the antibiotic can be determined by differential pulse polarography (DPP) in the concentration range 4.0×10^{-5} M to 7×10^{-4} M in 0.2 M KNO_3 in the presence of excess nickel(II).

In this paper a detailed study is described of the DPP and direct current (d.c.) polarographic behaviour of Ampicillin and Amoxycillin in the presence of selected bivalent metal ions. The most detailed study involved the nickel(II) com-

Correspondence to: S.S. Yassin, Chemistry Department, King Fahd University of Petroleum and Minerals, Dhahran 31261 (Saudi Arabia).

plexes but copper(II), cobalt(II), and zinc(II) were also examined. Working conditions of pH, ionic strength in sodium acetate supporting electrolyte, temperature and time of measurement after mixing of reactants, were determined. Polarographic reversibility tests were performed and numbers of electrons involved in the reduction processes measured. Interferences, reproducibility in quantitative determination of each of the parent penicillins, and comparison with results derived from methods taken from the British or US Pharmacopoeias are discussed. A procedure for determination is established.

EXPERIMENTAL

Reagents and solutions

Fresh standard solutions in the aqueous medium specified were prepared daily from Ampicillin trihydrate (Fluka, Buchs) and Amoxicillin trihydrate (Smith Kline Beecham, Worthing). Cephalexin was provided by Glaxo (Greenford).

Commercially available capsules containing Ampicillin or Amoxicillin trihydrates, manufactured by Instituto Biochemico Italiano (Milan) and Beecham (Brentford), respectively, were used as supplied. Capsules containing Cephalexin were manufactured by Glaxo.

All other chemicals used were of analytical reagent grade unless specified otherwise.

Apparatus

A Princeton Applied Research Polarographic Analyser, Model 174A with an *X-Y* recorder, Model RE 0074 was used for the d.c. polarography and DPP. The cell was fitted with three electrodes, a DME with mechanical control of drop size and time, a Ag/AgCl reference electrode with a saturated KCl salt bridge and a platinum counter-electrode.

The temperature of the solution in the polarographic cell was controlled thermostatically to $\pm 0.1^\circ\text{C}$ and measured by means of a Chrome-Alumel thermocouple. The pH was measured with a Corning 215 pH meter and "combined" glass electrode assembly.

A Varian-Cary-2390 or a Bausch and Lomb Spectronic 20 spectrophotometer was used for determinations by procedures taken from the British or US Pharmacopoeias.

Recommended quantitative determinations

Standard aqueous solutions of Ampicillin and Amoxicillin were prepared in the range 10^{-7} M to 10^{-4} M. These solutions were made in 0.01 M nickel(II) sulphate, 1.00 M sodium acetate, to a pH of 7.9 to 8.0, adjusted, if necessary, with NaOH or acetic acid. On standing in the polarographic cell for 6 min at 25°C , nitrogen was bubbled through the solution for 4 min before recording a differential polarogram by scanning from -0.4 V to -1.1 V with respect to the reference electrode. A modulation amplitude of 25 mV, drop time of 0.5 s, scan rate of 2 mV s^{-1} and sensitivity setting of $20\ \mu\text{A}$, give satisfactory polarograms. Peak heights at -0.865 V and -0.840 V were measured for Ampicillin and Amoxicillin, respectively. The weighed sample taken from proprietary drug capsules is treated in the same way as the standard, filtering off any insoluble residue if present after the dissolution procedure. For the reversibility tests and measurement of the number of electrons exchanged per molecule in the electrode reductions, where d.c. polarography was used, the antibiotic concentration was 1.0×10^{-3} M, drop time 0.5 s, scan rate 2 mV s^{-1} from -0.4 to -1.2 V at a sensitivity setting of $100\ \mu\text{A}$. Solutions were purged for 4 min.

In carrying out studies on the effects of changing conditions of solution composition, temperature and time of reaction, and examination of the properties of the electrode reduction processes, the basic procedure outlined above was used with appropriate modifications set out with each set of data presented.

Three methods, taken from the British or US Pharmacopoeias, were used for reference purposes; two were spectrophotometric determinations based on (1) the iron(III) complex of a hydroxamic acid derivative [6], and (2) the copper(II) complex of the corresponding penicillenic acid derivative [7], while the third was based on an iodimetric titration [6].

RESULTS AND DISCUSSION

In all of the studies carried out, except where it was necessary to establish that metal complex formation was essential to observe a polarographic response, a large molar excess of bivalent metal ion was present relative to the penicillin or its corresponding degradation products. Polarographic scans from -0.4 to -1.5 V, confirmed earlier published observations that in the presence of Ampicillin [4] or Amoxycillin [5], a new d.c. wave or DPP peak is produced in solutions of nickel(II). The new wave or peak, due to the formation of the nickel(II) complex, is a function of the antibiotic concentration. Conditions for favourable observation of DPP peaks or d.c. polarographic reduction waves were established in the order set out below.

Effect of pH

The base electrolyte was 1.0 M sodium acetate and constant concentrations of Ampicillin and Amoxycillin were used in the DPP studies. The results are depicted in Fig. 1. The electrode depolarization thresholds are about pH 6.0 for Ampicillin and 5.5 for Amoxycillin. Nickel(II) complex maximum response was observed at $\text{pH} \geq 7.9$. The pH could not be taken above 8.3 because of precipitation of the basic nickel(II) salts. The observed form of pH dependence is to be expected if metal complex formation is responsible for the species undergoing electrode reduction. The work of Veselinovic and Kapetanovic [4,5]

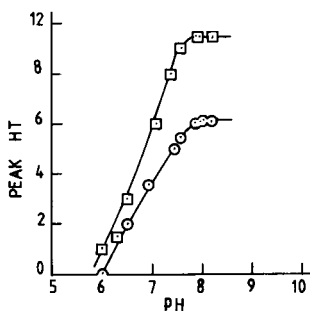
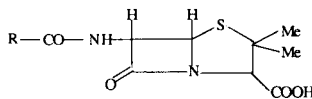
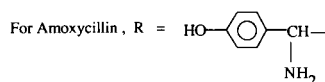
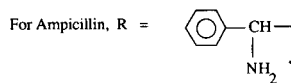


Fig. 1. Peak height (arbitrary units) plotted against pH for (○) Ampicillin, and (□) Amoxycillin, in the presence of 1.0 M sodium acetate and 0.01 M nickel(II) sulphate. Other conditions as for data in Fig. 2.



STRUCTURE I



Scheme 1.

shows that in 0.2 M KNO_3 , 1:1 nickel(II) complexes are formed, and evidence is presented suggesting that the primary amino group attached to the β -lactam side chain, structure I (Scheme 1), coordinates to the metal ion. This amino group is protonated at low pH and coordination will only occur following deprotonation to give the observed peaks near -0.85 V for either penicillin. Steric hindrance would appear to rule out the coordination of both the amino group of R on the side chain and the carboxylic group on the thiazolidine ring, structure I, in a 1:1 complex. Molecular models suggest there is less hindrance in ionized cephalixin, however, and chelation of this type may occur with the cephalosporin.

Effect of sodium acetate

The effect of sodium acetate concentration on peak height in DPP was studied at pH 8.0 and the results are depicted in Fig. 2. The minimum observed for the Ampicillin peak height at about 0.2 M acetate was found also in an earlier study [2] on cephalixin at 0.4 M. It is absent in the Amoxycillin system, Fig. 2, but may occur at concentrations less than 0.1 M. This effect could arise from displacement of hydroxyl by acetate as shown by the reaction,



where P^{2-} represents the ionized penicillin. The polarographic peak height becomes effectively in-

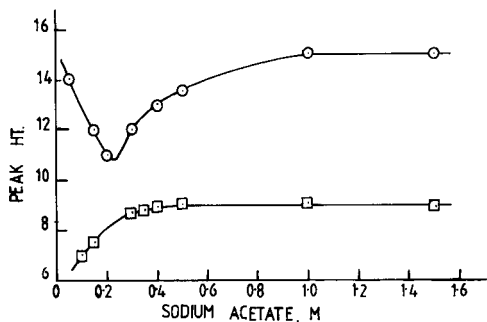


Fig. 2. Peak height (arbitrary units) plotted against acetate concentration for (○) Ampicillin, and (□) Amoxycillin. The pH was maintained at 8.0, each antibiotic was at 6.0×10^{-6} M in the presence of 0.01 M nickel(II) sulphate. Differential pulse polarograms were obtained by scanning from -0.4 to -1.1 V employing 2 mV s^{-1} and sensitivity setting of $20 \mu\text{A}$.

dependent of increasing acetate concentrations greater than 1.0 M for 0.01 M nickel sulphate solutions.

Temperature–time studies

Temperatures from 5 to 40°C were studied by DPP and peak height for a fixed penicillin concentration plotted as a function of time. The data are presented in Figs. 3 and 4. It is seen that the observed polarographic response steadily decreases at operating temperatures greater than 15°C . A further study at 25°C included shorter

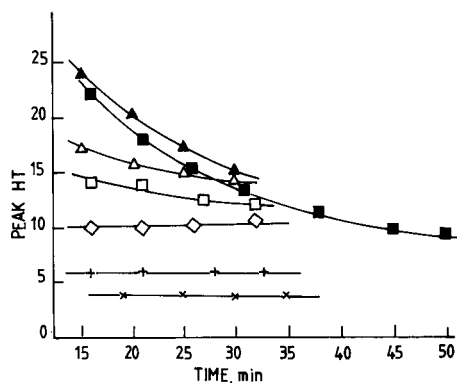


Fig. 3. Effect of temperature and time on peak height in DPP of 5.60×10^{-5} M Ampicillin in 1.0 M sodium acetate and 0.01 M nickel(III) sulphate at pH 8.0. After 15 min each solution was purged with nitrogen for 4 min and readings taken as a function of time at each temperature ($^\circ\text{C}$) (×) 5; (+) 10; (◇) 15; (□) 20; (△) 25; (▲) 35; (■) 40. Operating conditions as described in Fig. 2.

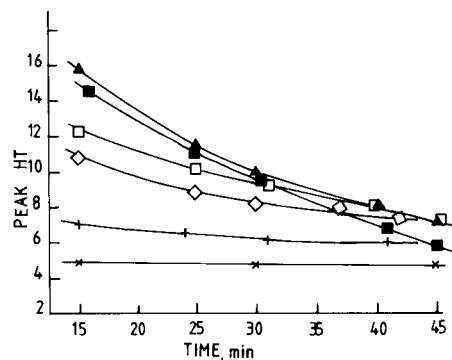


Fig. 4. Effect of temperature and time on peak height in DPP of 1.32×10^{-4} M Amoxycillin under conditions as set out for Ampicillin (Fig. 3). (×) 15; (+) 20; (◇) 25; (□) 30; (▲) 35; (■) 40°C .

reaction times. It showed that decreasing reaction times gave increasing peak heights down to at least 5 min; increases of around 20% for 5 min relative to 15-min reaction times were found for both Ampicillin and Amoxycillin. It was observed that at temperatures $\geq 35^\circ\text{C}$ and reaction times in excess of 15 min, as the polarographic peak near -0.85 V decreased in height, a new peak centred at about -0.695 V and -0.77 V for Ampicillin and Amoxycillin, respectively, appeared and grew. The changes in peak position and height, typified by the polarograms shown in Fig. 5 for Amoxycillin were observed also for Ampicillin. This behaviour is the subject of a further study.

Reversibility test

In DPP the reversibility of the electrode reaction may be evaluated from the ratio between the cathodic and anodic peak currents derived from cathodic and anodic scans respectively. For reversibility this ratio should be unity and the potential difference, $E_c - E_a$, between the peak maxima should be the same as the pulse amplitude, dE [8]. Ratios of 0.99 ± 0.03 for Ampicillin and 0.97 ± 0.04 for Amoxycillin were obtained from six measurements on each (errors quoted are standard deviations). The $E_c - E_a$ values were not of sufficient accuracy to be useful because of the errors involved in location of the E values relative to the experimental $dE = 25$ mV. The half-wave potentials derived from d.c. polaro-

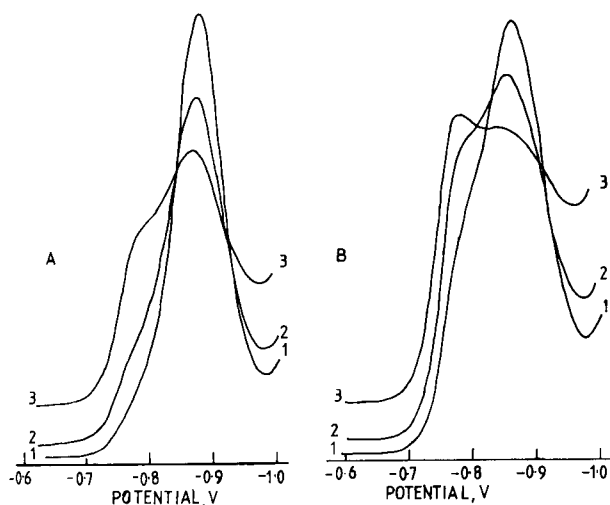


Fig. 5. Differential pulse polarograms of 1.32×10^{-4} M Amoxicillin showing the effect of temperature and time at (A) 35 and (B) 40°C. For A the polarograms were recorded (1) 15, (2) 25, and (3) 45 min from after mixing the reactants. For B the corresponding times were (1) 16, (2) 25, and (3) 41 min. Other conditions as for data in Fig. 3.

graphic cathodic and anodic scans were also equivocal because of the uncertainties in locating the potentials. However, from the peak ratios, it can be concluded that the electrode reactions probably exhibit a high degree of reversibility at 25°C, the temperature of measurement, over short periods of time (about 6 min).

Electron transfer in the electrode reaction

The number of electrons transferred per complex ion in the electrode process was deduced from suitable d.c. polarograms on the assumption that the reaction is reversible in each case. Values of 1.05 and 0.99 were obtained for Ampicillin and Amoxicillin respectively. Similar experiments with cephalexin gave a value of 1.01. Thus the mechanism suggested [2] earlier for the nickel(II) cephalexin reduction is unsatisfactory because it is based on a two-electron reduction by analogy with the behaviour of nickel(II) in the presence of pyridine [9]. Reduction occurring at the ligand, rather than nickel, would probably involve more than one electron. On the other hand, there are well documented examples of the electrode reduction of nickel(II) complexes to the corresponding nickel(I) complexes [10]. It seems likely

that reduction occurs at the metal ion in the complex.

Tests using other metal ions

Other metal ions investigated as replacements for nickel(II) were copper(II), zinc(II) and cobalt(II). For these metal ions the instrumental settings for DPP were, sensitivity $100 \mu\text{A}$, scan rate 2 mV s^{-1} , drop time 0.5 s and modulation amplitude 25 mV. All tests were performed in 1 M sodium acetate at pH 8.0 with an excess of metal ion to drug.

For 1.0×10^{-3} M copper(II) in the absence of Ampicillin, two poorly resolved peaks were observed at -0.125 V and -0.180 V over the scan range of 0.00 and -1.50 V . When 2.7×10^{-4} M Ampicillin was included in this basic system, the two peaks were replaced by a single peak at -0.155 V and two shallow peaks at -0.495 V and -0.895 V , over the same scan range. Because of the complicated polarograms further work was abandoned. For 9.0×10^{-3} M zinc(II), one peak was observed at -1.16 V over the scan range of 0.0 to -1.5 V . Addition of 2.5×10^{-4} M Ampicillin did not produce an additional peak. Therefore the zinc(II) complex, if any, under these conditions is obscured by that of the free zinc ion. It has been shown by amperometric titration that cobalt(II) forms a complex with Ampicillin [4]. The nature of this complex was investigated by DPP in 1 M sodium acetate, pH 8.0 and scan range from -0.60 to -1.80 V . In addition to the free cobalt(II) DPP peak at -1.58 V , a peak at -1.255 V was observed, attributable to a cobalt(II)–Ampicillin complex. This peak tends to shift towards more negative potentials as the pH is increased; it is suitable for the quantitative determination of antibiotic drugs like Ampicillin and Amoxicillin by DPP. However, the cobalt(II) complexes are less satisfactory than the corresponding nickel(II) complexes because resolution of the DPP peaks for the complexed and non-complexed metal ion is smaller for the former.

Quantitative aspects

The procedure developed for the determination of Ampicillin and Amoxicillin is based on

TABLE 1

Summary of quantitative results obtained on the commercial antibiotics

No.	Method (Assay)	Technique	Amount (%)		
			Ampicillin trihydrate ^a	Amoxycillin trihydrate ^a	Cephalexin ^a
1	Iodimetric titration	Titrimetric	99 ± 1	103 ± 1	100 ± 1
2	Hydroxylamine/iron(III)	Spectrophotometric	99 ± 1	102 ± 1	101 ± 1
3	Copper(II) sulphate	Spectrophotometric	99 ± 1	101 ± 1	–
4	Differential pulse Ni(II) complex system	Polarographic	100 ± 1	103 ± 1	100 ± 1

^a Mean ± standard deviation (*n* = 3).

the method for cephalexin devised by Hernandez Mendez et al. [2]. The use of sodium acetate as a supporting electrolyte is preferable to that of KNO₃ [5] because of its buffering role. Further, the acetate assists in the prevention of hydrolysis and subsequent precipitation of the metal ion enabling easier attainment of higher pH values than with KNO₃.

Using the procedure given in Experimental, it was established that linear calibration graphs could be constructed over the concentration ranges 3.0×10^{-7} M to 3.0×10^{-5} M and 4.0×10^{-7} M to 2.0×10^{-5} M for Ampicillin and Amoxycillin, respectively. The coefficient of variation for six measurements on each of 2.18×10^{-6} M Ampicillin and 6.20×10^{-6} M Amoxycillin were 2.0 and 2.9%, respectively indicating that precision is reasonable in each case. Table 1, summarizes the comparative measurements made on the capsules. Values are included for Cephalexin to enable comparison of the results with those of the penicillin antibiotics. It is seen that the values found by DPP are in good agreement with those obtained when the British or US Pharmacopoeias methods are used. Thus it is seen that the contents of the capsules are essentially pure penicillin within errors of measurement. This was confirmed by the analysis of mixtures of capsule content to standard in different ratios. In all instances the predicted peak height from DPP was obtained within experimental error. However, following such a procedure would

enable the detection of interferences in the determination of the drugs in samples of unknown composition.

The authors gratefully acknowledge the support of King Fahd University Of Petroleum and Minerals for this work. They also thank Smith Kline Beecham Pharmaceuticals and Glaxo Group Research for the provision of reference materials.

REFERENCES

- 1 A. Sanchez Perez, J. Hernandez Mendez and M.N. Silva Fernandez, *Cienc. Ind. Farm.*, 2 (1983) 363.
- 2 J. Hernandez Mendez, A. Sanchez Perez, M. Delgado Zamarreno and L. Vega Laso, *Anal. Chim. Acta*, 160 (1984) 335.
- 3 J.A. Squella and L.J. Nunez-Vergara, *Talanta*, 26 (1979) 1039.
- 4 D. Veselinovic and V. Kapetanovic, *J. Pharm. Belg.*, 43 (1988) 163.
- 5 V. Kapetanovic and D. Veselinovic, *Arch. Pharm. (Weinheim)*, 321 (1988) 559.
- 6 United States Pharmacopoeia, 15th edn., 20th revision, US Pharmacopoeial Convention, Rockville, MD, 1980, pp. 1281–1285.
- 7 British Pharmacopoeia, H.M.S.O., London, 1973, p. 30.
- 8 R.L. Birke, M. Kim and M. Strassfeld, *Anal. Chem.*, 53 (1981) 852.
- 9 Ya.I. Turyan and O.N. Malyavinskaya, *J. Electroanal. Chem.*, 23 (1969) 69.
- 10 A.G. Lappin and A. McAuley, in A.G. Sykes (Ed.), *Advances in Inorganic Chemistry*, Vol. 32, Academic Press, London, 1988, p. 241.

Atomization of tin in saline water media in graphite furnace atomic absorption spectrometry with a tungsten-coated tube using palladium as a chemical modifier

Etsuro Iwamoto, Hiromichi Shimazu, Kayoko Yokota and Takahiro Kumamaru

Department of Chemistry, Faculty of Science, Hiroshima University, Higashi-Hiroshima 724 (Japan)

(Received 24th July 1992; revised manuscript received 5th October 1992)

Abstract

The direct atomization of tin in saline water media in graphite furnace atomic absorption spectrometry with a tungsten-coated tube was investigated. The combined use of a tungsten-coated non-pyrolytic graphite tube and palladium as a chemical modifier eliminated salinity in doubly diluted sea water without a serious loss of tin at an ashing temperature of 1700°C. Sulphate interference was also suppressed. When using an injection volume of 20 μ l the sensitivity was 0.0566 ± 0.0043 peak-area absorbance ng^{-1} , and 0.0805 ± 0.0078 without sodium chloride and sulphate. The 3σ detection limit was 0.08 ng.

Keywords: Atomic absorption spectrometry; Sea water; Tin; Waters

The direct determination of tin in saline water by graphite furnace atomic absorption spectrometry (GFAAS) involves a serious difficulty because of interferences from large amounts of chloride and sulphate ions.

Chamsaz and Winefordner [1] attempted to measure tin directly in sea water using various kinds of matrix modifiers, including ammonium nitrate, nitric acid, sucrose, ascorbic acid and oxalic acid, and found that only nitric acid reduced the background absorption to be able to determine inorganic tin, but for organotin compounds there was no measurable signal at levels of 0.1 mg l^{-1} . It is known that sulphate seriously suppresses the tin atomic absorption signal [2–7],

this being attributed to carbon-mediated formation of volatile tin sulphide [4,6]. Therefore, an extraction technique for separation from matrix salts has usually been combined with GFAAS [1].

Previously, a simple tungsten coating method was proposed [8], without soaking in tungstate solution, involving the injection of 100 μ l of a tungstate solution into a non-pyrolytic graphite (NPG) tube, followed by heating the tube according to the atomization temperature programme. The coating process was repeated five times. It was found that the tungsten-coated tube greatly increased the sensitivity for tin in aqueous solutions and gave stable signals for at least 100 firings. This tube was applied to the determination of tin in a fish sample.

In this work, atomization conditions for the direct determination of tin in sea water with the tungsten-coated tube were investigated.

Correspondence to: Takahiro Kumamaru, Department of Chemistry, Faculty of Science, Hiroshima University, Higashi-Hiroshima 724 (Japan).

EXPERIMENTAL

Apparatus and reagents

The apparatus and reagents used, except for palladium(II) solutions as a chemical modifier, were as described previously [8]. Palladium(II) solutions were prepared by dissolving palladium(II) chloride and ammonium palladium(II) chloride (Katayama Chemical Industries, Osaka) of analytical-reagent grade in 0.1 mol l^{-1} hydrochloric acid. A palladium(II) standard solution for atomic absorption spectrometry (1000 mg l^{-1} in 1 mol l^{-1} hydrochloric acid) (Wako, Osaka) was also investigated. It was found that all the palladium(II) solutions contained a detectable tin blank of $8\text{--}10 \mu\text{g l}^{-1}$. Palladium(II) chloride solution, which gave the smallest blank, was selected for subsequent work.

Sea-water samples were collected at Hiroshima Bay in Seto Inland Sea.

Recommended procedure for direct determination of tin

A sea-water sample was filtered with a $0.45\text{-}\mu\text{m}$ membrane filter and the pH was adjusted to 2 by adding hydrochloric acid. The solutions to be analysed were prepared by pipetting 25 ml of the sea-water sample and an aliquot of an aqueous working standard into a 50-ml glass volumetric flask and diluting to volume with deionized water. The chemical modifier palladium(II) solution ($50 \mu\text{l}$) was injected into the graphite tube, followed by the sea-water sample ($20 \mu\text{l}$), and the absorption signals were measured using the atomization temperature programme given in Table 1.

TABLE 1

Atomization temperature program

Parameter	Drying	Ashing	Atomization	Conditioning
Temperature ($^{\circ}\text{C}$)	150	Variable	2700	2700
Ramp time (s)	15	20	0	1
Hold time (s)	10	10	3	1
Internal gas flow-rate (ml min^{-1})	300	300	0	300

RESULTS AND DISCUSSION

Metal-coated tubes, prepared by soaking the tube in a metal salt solution, have been used to overcome the difficulties in the determination of tin in various kinds of samples and to achieve long-term stability with respect to sensitivity. Tungsten, zirconium, tantalum and molybdenum coatings have been reported [5,9,10]. Alternatively, Taga et al. [11] investigated the use of chemical modifiers of $5 \times 10^{-4} \text{ mol l}^{-1}$ potassium tungstate, potassium dichromate and potassium molybdate, and found that tungstate was the most effective for the suppression of interferences from other ions, thereby improving the sensitivity and precision.

Previously it was found that although a tungsten-coated pyrolytic graphite (W-PG) tube gave the highest absorption signal for tin in a simple matrix of 0.05 mol l^{-1} hydrochloric acid, a tungsten-coated-pyrolytic graphite (W-NPG) tube gave the highest and the most stable absorption signal for tin in a fish (sea bass) sample [8].

Elimination of matrix interferences

The large amounts of chlorides present in sea water seriously interfered with the absorption signals when sea-water samples were injected directly into a graphite tube [12,13]. Ediger [12] proposed adding ammonium nitrate to sea-water samples to allow the removal of sodium chloride at lower ashing temperatures at which the analyte element is not yet vaporized. Roe and Froelich [13] tested three chemical modifiers for the determination of barium in sea water, viz., ammonium nitrate, nitric acid and ascorbic acid, and found ammonium nitrate to be the most efficient modifier for eliminating sodium chloride in a slow ashing step at 1400°C .

In this work, the effect of ammonium nitrate as the chemical modifier on the atomic absorption signal of tin in sea water was first investigated. It was found that the background absorbance decreased dramatically at ca. 1100°C , above which the background became low, but no atomic absorption signal of tin was observed with various types of graphite tubes.

Palladium compounds have been shown to be very powerful modifiers [14–17]. Palladium(II) solution was examined as a chemical modifier with tungsten-coated tubes. The effect of ashing temperature on the tin atomic absorbance and background is shown in Fig. 1. A doubly diluted sea-water sample containing inorganic tin (2 ng) was injected and the W-NPG tube was used. The background began to fall at 1100°C, and above 1600°C it became low and stable, being amenable to correction. As shown in Fig. 2, it should be noted that a smooth, stable absorption profile for tin was observed at 1700°C. The tin signal below 1600°C was noise-like because of the high background. For triphenyltin chloride a similar trend was observed. An ashing temperature of 1700°C was selected for subsequent atomization.

No absorption signal of tin was observed when a sea-water sample that was not diluted was injected. The effect of the injection volume of the palladium(II) solution (0.01 mol l⁻¹) was investigated and it was found that above 40 μl constant

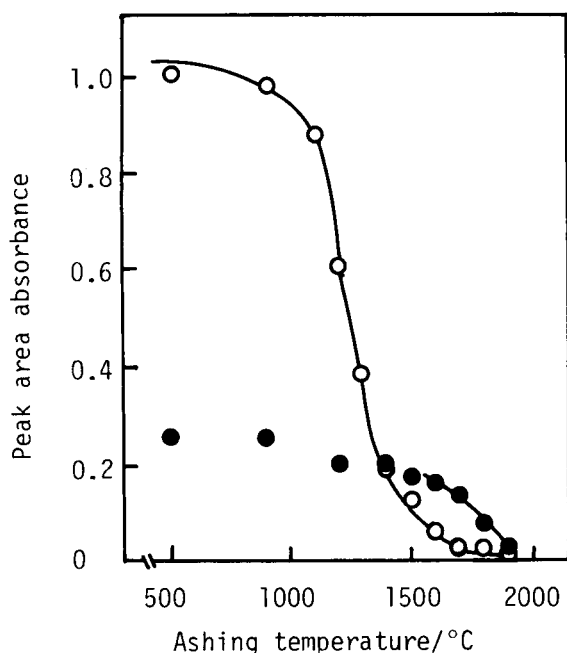


Fig. 1. effect of ashing temperature on (●) tin and (○) background absorbances using Pd (0.01 mol l⁻¹, 50 μl) as a chemical modifier with the W-NPG tube. 2 ng of tin were added to the sea-water sample.

atomic absorbances were observed and a volume of 50 μl was therefore selected. Palladium(II) solutions of concentration less than 0.01 mol l⁻¹ were less effective.

Typical absorption signals for various types of graphite tubes (tungsten-coated tubes, non-coated tubes and L'vov platform tube) are shown in Fig. 2. Only the W-NPG tube gave a stable absorption signal.

Effects of sulphate and magnesium

As shown above, the use of palladium(II) as the chemical modifier with the W-NPG tube was successful for the direct determination of tin in sea water. Sulphate and magnesium ions are dominant species in sea water. Recently, a mixture of magnesium nitrate and palladium nitrate as chemical modifiers was recommended by Schlemmer and Welz [18]. Table 2 shows the effects of sulphate and magnesium, at concentrations similar to those in sea water, on the tin signal. It is seen that when using the NPG tube the presence of magnesium with palladium improves greatly the sensitivity for tin, but when using the W-NPG tube magnesium does not improve the signal. Although sulphate depresses the tin signal, the interference from sulphate is eliminated by the presence of palladium. Hence the good results obtained in this work arise partly from suppression of the interference from sulphate.

Sensitivity and detection limit

Following the recommended procedure, it was found that there was no detectable tin in the sea water collected at Hiroshima Bay. The average sensitivity obtained from the slopes of standard addition plots with inorganic tin for the sea-water samples and aqueous samples without salinity were 0.0566 ± 0.0043 and 0.0805 ± 0.0078 peak-area absorbance ng⁻¹, respectively. The sea-water matrix decreases the sensitivity slightly. In the former instance the 3σ detection limit was 0.08 ng. For triphenyltin chloride in sea water a lower sensitivity of 0.0413 absorbance ng⁻¹ was obtained.

An attempt was made to test the application of this method to the determination of inorganic tin

added to sea-water samples. The results are given in Table 3. The recovery of tin is satisfactory. Therefore, the direct atomization method described above can be applied to the determination of $\mu\text{g l}^{-1}$ levels of tin in, e.g., sea waters polluted by tin compounds or test solutions obtained by leaching ship paint samples with sea water. However, the harmful effects of organotin compounds on many forms of marine life are of

concern even at ng l^{-1} levels [19]. Therefore, extraction of organotin compounds from sea-water samples has been used for preconcentration and the extracts were subjected to GFAAS. Apte and Gardner [9] reported that using furnace tubes pretreated by soaking in sodium tungstate solution a detection limit of 4.0 ng l^{-1} with regard to the tin concentration in sea water, corresponding to a detection limit of 0.016 ng

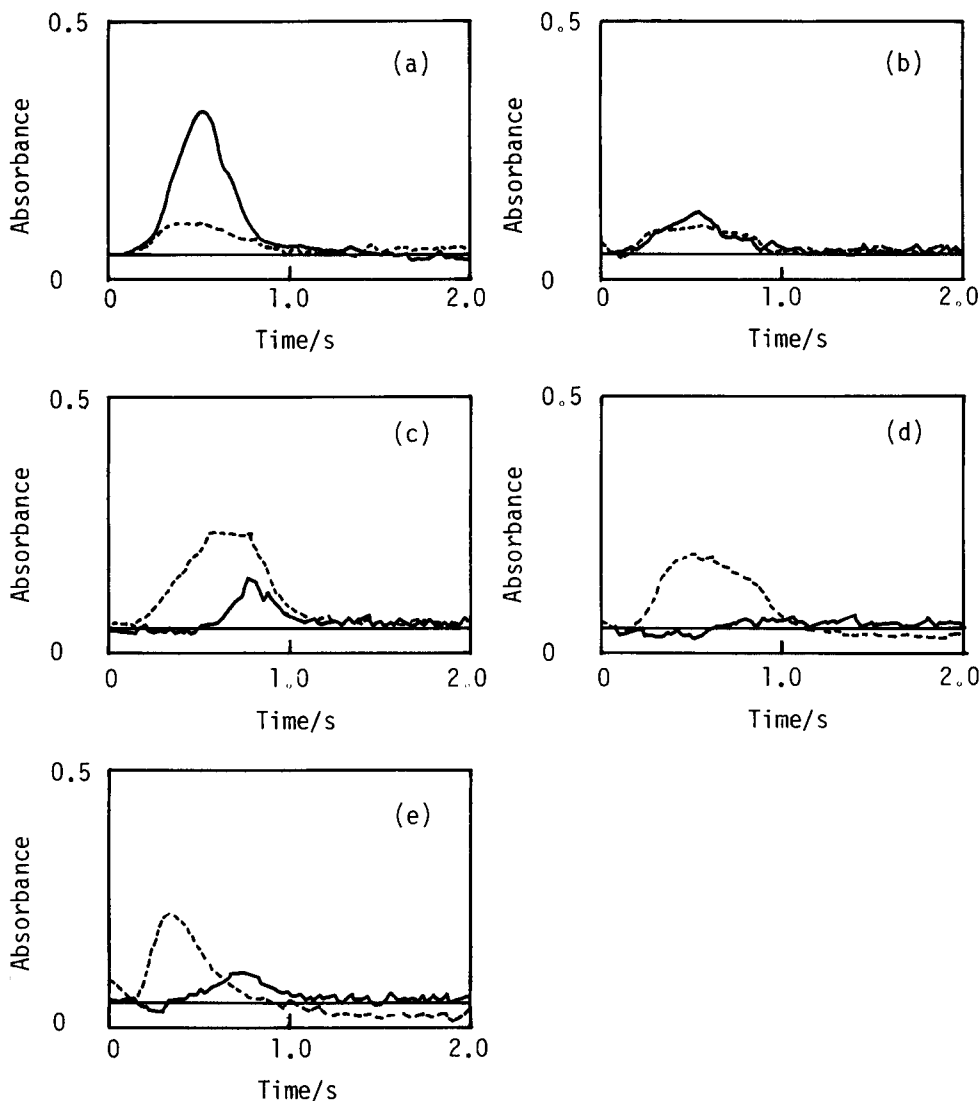


Fig. 2. Atomic absorption profiles for tin using Pd (0.01 mol l^{-1} , $50 \mu\text{l}$) as a chemical modifier with various types of graphite tubes at an ashing temperature of 1700°C . 2 ng of tin were added to the sea-water sample. Solid line, net atomic absorbance; broken line, background absorbance. (a) W-NPG; (b) NPG; (c) W-PG; (d) pyrolytic graphite; (e) L'vov platform tube.

TABLE 2

Effects of sulphate and magnesium on tin peak-area absorbance ^a

Tube	Salt		Modifier		
	Na ₂ SO ₄ ^b	MgCl ₂ ^c	–	PdCl ₂ ^d	PdCl ₂ ^d
NPG	0.035	0.0	0.019	0.015	0.035
W-NPG	0.051	0.0	0.034	0.252	0.212

^a Sample injection volume, 20 μ l (2 ng Sn). ^b 0.028 mol l⁻¹.
^c 0.054 mol l⁻¹. ^d Injection volume, 50 μ l (0.01 mol l⁻¹ in 0.1 mol l⁻¹ HCl).

based on the organic extract, was obtained when extraction of 1-l sea-water samples with 5 ml of toluene was carried out and a 20- μ l sample was injected. Katsura et al. [17] reported that a 19-fold sensitivity enhancement for an ethyl acetate-hexane solution of tri-*n*-butyltin chloride was obtained by addition to the sample solution of organopalladium complexes dissolved in the organic solvent, leading to a detection limit of 0.11 ng. The method was applied to the determination of μ g l⁻¹ levels of total tin leached from ship paints.

Using the present system, toluene extraction of triphenyltin chloride from sea water was also investigated. It was found, however, that no signal-increasing effect of palladium was obtained. The W-NPG tube without palladium gave a stable and higher sensitivity for the organic extract with a detection limit of 0.04 ng.

Conclusion

The direct atomization of tin in sea water in GFAAS is possible only with the combined use of

TABLE 3

Determination of tin in sea water from Hiroshima Bay

Tin (μ g l ⁻¹)	
Added	Found ^a
0	0 \pm 1
20	18 \pm 2
40	41 \pm 2

^a Mean \pm standard deviation ($n = 5$).

a W-NPG tube and palladium as a chemical modifier, and then magnesium which is a dominant species in sea water does not act as a chemical modifier. Although the detection limit of 0.08 ng obtained is not satisfactory for monitoring ng l⁻¹ levels of tin compounds in sea water, this simple method without extraction can be applied to contaminated samples containing tin compounds at levels above μ g l⁻¹ in saline water media.

This work was supported by a grant-in-aid for scientific research (No. 02453034) from the Ministry of Education, Science and Culture of Japan.

REFERENCES

- M. Chamsaz and J.D. Winefordner, *J. Anal. At. Spectrom.*, 3 (1988) 119.
- W.B. Barnett and E.A. McLasaughlin, Jr., *Anal. Chim. Acta*, 80 (1975) 285.
- M. Tominaga and Y. Umezaki, *Anal. Chim. Acta*, 110 (1979) 55.
- P. Hocquellet and N. Laeyrie, *Anal. Chim. Acta*, 3 (1975) 505.
- H. Fritzsche, W. Wegschneider and G. Knapp, *Talanta*, 26 (1979) 219.
- G.D. Rayson and J.A. Holcombe, *Anal. Chim. Acta*, 136 (1982) 249.
- R. Pinel, M. Benabdallah, A. Astruc and M. Astruc, *Anal. Chim. Acta*, 181 (1986) 187.
- E. Iwamoto, H. Shimazu, K. Yokota and T. Kumamaru, *J. Anal. At. Spectrom.*, 7 (1992) 421.
- S.C. Apte and M.J. Gardner, *Talanta*, 35 (1988) 539.
- T.M. Vickery, G.V. Harrison and G.J. Ramelow, *Anal. Chem.*, 53 (1981) 1573.
- M. Taga, H. Yoshida and O. Sakurada, *Bunseki Kagaku*, 36 (1987) 597.
- R.D. Ediger, *At. Absorpt. Newslett.*, 14 (1975) 127.
- K.K. Roe and P.N. Froelich, *Anal. Chem.*, 56 (1984) 2724.
- L.-Z. Jin and Z.-M. Ni, *Can. J. Spectrosc.*, 26 (1981) 219.
- G. Weibust, F.J. Langmyhr and Y. Thomassen, *Anal. Chim. Acta*, 128 (1981) 23.
- L. Ping, W. Lei, K. Matsumoto and K. Fuwa, *Anal. Sci.*, 1 (1985) 257.
- T. Katsura, F. Kato and K. Matsumoto, *Anal. Chim. Acta*, 252 (1991) 77.
- G. Schlemmer and B. Welz, *Spectrochim. Acta, Part B*, 41 (1986) 1157.
- UK Department of the Environment, *Organotin in Anti-fouling Paints: Environmental Considerations*, Pollution Paper No. 94, HM Stationery Office, London, 1986.

Application of inductively coupled plasma atomic emission spectrometry for the certificate analysis of uranium certified reference material: determination of trace impurity elements in U_3O_8 by extraction chromatography

Xiao Jin Yang and Jing Su Guan

Laboratory of Analytical Chemistry, Institute of Atomic Energy, P.O. Box 275(88), Beijing 102413 (China)

(Received 6th August 1992; revised manuscript received 23rd October 1992)

Abstract

Inductively coupled plasma atomic emission spectrometry in combination with tributyl phosphate (TBP) extraction chromatography was applied to the certificate analysis of U_3O_8 samples proposed as certified reference materials (CRMs). A sealed PTFE decomposition vessel was designed for the decomposition of these samples. The chromatographic behaviour of a TBP Levetrel resin column was investigated for the separation of impurity elements from the uranium matrix. In order to assess the accuracy of the analyses for impurity elements, a control sample of U_3O_8 was analysed together with the new proposed CRMs. The results showed good agreement. The precision based on the samples analysed is better than 10%. The proposed method provided excellent and accurate analytical data for the U_3O_8 samples proposed as CRMs.

Keywords: Atomic emission spectrometry; Inductively coupled plasma spectrometry; Sample preparation; Certified reference materials; Extraction; Uranium

Nuclear-grade uranium compounds such as uranium dioxide and U_3O_8 must have certain specifications in order to be suitable for the industrial production of nuclear reactor fuel. The levels of trace impurities in uranium compounds are important because some impurity elements are nuclear poisons and the presence of trace metals affects the overall purity of the enriched product. The determination of trace metal impurities in uranium matrices is of continuing interest in the nuclear industry because of stringent quality control specifications, so methods are needed to provide precise and accurate data that will meet regulatory requirements. Therefore, it is important to develop uranium certified refer-

ence materials (CRMs) in order to evaluate the performance of a laboratory using an accepted method of analysis or to test the accuracy of a new analytical method. The International Atomic Energy Agency (IAEA) has distributed a U_3O_8 CRM (SR-54) [1].

In 1989, the China Nuclear Industry Corporation (CNIC) instigated the development of a series of U_3O_8 CRMs and required the participation of a number of laboratories to establish recommended concentrations of the impurities in these U_3O_8 samples to be proposed as a CRM. In February 1990, this laboratory was invited by CNIC to participate in a collaborative study for the determination of impurities in these developed CRMs. The original protocol required that six independent determinations be done for each sample. In June 1990, the analytical data for these samples were contributed to the study. Af-

Correspondence to: X.J. Yang, Laboratory of Analytical Chemistry, Institute of Atomic Energy, P.O. Box 275(88), Beijing 102413 (China).

ter pooling multi-laboratory and multi-method data, the concentration levels of the impurity elements in these samples were certified by the certifying body. In January 1992, these samples were certified as primary CRMs by the State Bureau of Technical Supervision (SBTS) of China [2]. Certified values were provided for 18 elements.

Several techniques have been used for the determination of trace impurities in a uranium matrix, including carrier distillation [3], spectrochemical analysis [4], atomic absorption spectrometry [5], spark-source mass spectrometry [6] and inductively coupled plasma atomic emission spectrometry (ICP-AES) [7]. ICP-AES, with its excellent analytical characteristics such as low detection limits, high precision and accuracy, wide analytical dynamic range, low chemical and ionization interferences, relative freedom matrix interferences and simultaneous multi-element measurement capability, has developed into a practical trace analysis method and has been successfully applied to the certificate analysis of various CRMs [8–10]. However, if the ICP-AES method is to be employed for the analysis of uranium compounds, the matrix uranium must be separated from the impurity elements analysed prior to the ICP-AES determination because the complex uranium emission spectra will severely interfere with the spectral lines of the analytes, otherwise the determination of trace impurities is impossible. Therefore, liquid–liquid extraction methods for the separation of impurities from uranium such as using tributyl phosphate (TBP) [11–13], tri(2-ethylhexyl)phosphate (TEHP) [14], trioctylphosphine oxide (TOPO) [15] and tri-*n*-octylamine (TNOA) [16] as extractants and ion-exchange chromatography [17,18] combined with ICP-AES have been developed. However, the liquid–liquid extraction method has the disadvantage that it requires multiple extractions.

Recently, the combination of extraction chromatographic separation with ICP detection in the analysis of uranium compounds has become increasingly popular [19–25]. Extraction chromatography, also known as reversed-phase partition chromatography, has a higher separation efficiency and requires less manipulation than liq-

uid–liquid extraction. In early extraction chromatography, Kel-F (polychlorotrifluoroethylene) powder served as the support loading organic extractant [19–23]. However, Kel-F powder used as a support has a small surface area and low affinity for organic extractants, so its capacity for uranium is low and the life of the chromatographic column is short. Levetrel resin [26,27] is another type of extractant–support combination in which the support is styrene–divinylbenzene-based copolymers, which have a high surface area and a high affinity for extractants. This kind of support has been extensively used for loading various extractants [28–30]. Various types of Levetrel resin such as TBP, HDEHP, TOPO, and PMBP types have been developed by the Beijing Research Institute of Chemical Engineering and Metallurgy [28] and are available on request. TBP Levetrel resin has been successfully used for the separation and preconcentration of 25 impurity elements from U_3O_8 using 5 M nitric acid as mobile phase followed by analysis with end-on (axially) viewed ICP in conjunction with a 1-m plane grating spectrograph [31]; the end-on viewed ICP method, however, is not suitable for routine use because a complicated arrangement is required and the precision and speed of this method are lower than those of the direct-reading ICP method. Recently, a reference method for the determination of sixteen trace impurity elements in nuclear-grade UO_2 powder and core involving ICP-AES combined with extraction chromatography using TBP Levetrel resin has been established in China [32].

This work is a continuation of previous studies [32] aimed at providing information on certified nuclear chemical reference materials.

EXPERIMENTAL

Apparatus and equipment

All ICP-AES determinations were made on an Jarrel-Ash 975 ICP direct-reading spectrometer with pneumatic nebulization. The experimental set-up and operating conditions utilized are summarized in Table 1. A PDP 8/E-LA 36 computer controlled all instrument functions.

TABLE 1
Experimental set-up and ICP operating conditions

Monochromator	Jarrel-Ash Model 975, Rowland circle, 0.75 m; 2400 grooves mm^{-1} grating; reciprocal linear dispersion, 0.55 nm mm^{-1}
R.F. generator:	
Frequency	27.12 MHz
Incident power	1.0 kW
Reflected power	< 5 W
Argon gas flow-rates:	
Coolant gas	17 l min^{-1}
Auxiliary gas	1 l min^{-1} , used only for starting plasma
Carrier gas	0.5 l min^{-1}
Nebulizer	Pneumatic nebulizer, stable cross-flow type
Observation height	16 mm above load coil
Integration time	4 s
Integration cycle	3
Solution uptake rate	1 ml min^{-1} , controlled by a peristaltic pump
Computer	PDP 8/E-LA 36

A thermostated oven and a sealed PTFE decomposition vessel were employed for the decomposition of the sample.

Reagents

Distilled, deionized water, prepared using a sub-boiling quartz distillation apparatus, was used throughout. Super-analytical grade nitric acid (Beijing Chemicals) was redistilled prior to use. Stock standard solutions of 1 mg ml^{-1} of individual element were prepared from high-purity or Specpure metals, oxides or salts. Working standard solutions used for ICP-AES calibration were prepared by suitable dilution of the stock standard solutions with 3 M nitric acid.

TBP Leventrel resin (75–120 mesh) was supplied by Beijing Research Institute of Chemical Engineering and Metallurgy.

Preparation of chromatographic column

A borosilicate glass column of i.d. 0.7 cm was packed with the resin using an aqueous suspension. The resin was slightly pressed in the column, any air bubbles should be removed from the

column. The resin bed height was 12 cm. The column was washed with 20 ml of 5% (w/v) sodium carbonate solution followed by sub-boiled distilled water. Any residual impurities in the column were removed prior to use by eluting with 5 M nitric acid. Before separation, the resin in the column was pre-equilibrated with 3 M nitric acid. A separation flow-rate of 0.5 ml min^{-1} was applied.

Sample decomposition and treatment

A 0.3-g sample of U_3O_8 was placed in a PTFE decomposition vessel, to which was added 1.5 ml of redistilled concentrated nitric acid. The cap was tightened to seal the PTFE vessel, which was heated for 6 h in a thermostated oven at 180°C , then removed from the oven and cooled to room temperature. A 2-ml volume of sub-boiled distilled water was added to the vessel; the volume of the solution was then ca. 2.5 ml and the acidity ca. 3 M of nitric acid. This 2.5 ml of solution served as the sample solution for the column separation.

Procedure for sample separation

The 2.5 ml of sample solution was loaded quantitatively on to the TBP Leventrel resin column and eluted with 3 M nitric acid at a flow-rate of 0.5 ml min^{-1} . The uranium was retained on the column while impurity elements remained in the effluent solution. The first 2 ml of effluent solution were discarded and the last 10 ml were collected in a 10-ml volumetric flask and stored until the ICP-AES measurements were carried out.

ICP-AES measurement

A two-point calibration procedure was employed for standardization of the instrument, the two standard solutions being 3 M nitric acid (low standard) and 3 M nitric acid containing $10 \mu\text{g ml}^{-1}$ each of impurity elements (high standard). This calibration procedure has been applied to the certification of trace elements in mussel tissue CRM [8]. The ICP-AES measurements were carried out under the operating conditions given in Table 1.

Column regeneration

The used column was freed from absorbed uranium by stripping the uranium with 30 ml of water at a flow-rate of 0.5 ml min^{-1} and was stored in water until further use.

RESULTS AND DISCUSSION

Sample decomposition

In preliminary experiments, dissolution of the sample was carried out with nitric acid in a quartz beaker. Unfortunately, it was found that the results were significantly lower than those obtained by direct spark-source mass spectrometry without decomposition of the sample. These low results may be attributable to the incomplete decomposition of the samples because in the process of development the uranium compounds used as the matrix of the CRMs were converted into oxide (U_3O_8) by ignition at high temperature (850°C). Therefore, in order to decompose the samples completely, a sealed PTFE decomposition vessel was designed (Fig. 1). The experimental results indicated that the decomposition of 0.3 g of sample with addition of 1.5 ml of concentrated nitric

TABLE 2

Detection limits and lowest quantitatively determinable concentration of impurities in U_3O_8

Element	Wavelength (nm)	DL (2σ) ($\mu\text{g ml}^{-1}$)	LQD (10σ)	
			$\mu\text{g ml}^{-1}$	$\mu\text{g g}^{-1}$ ^a
Ca	317.9	0.012	0.06	1.2
Cd	228.8	0.0014	0.007	0.14
Cr	205.5	0.0034	0.017	0.34
Cu	324.7	0.0048	0.024	0.48
Fe	259.9	0.0044	0.022	0.44
Mg	279.5	0.0002	0.001	0.02
Mn	257.6	0.0016	0.008	0.16
Mo	202.0	0.004	0.02	0.40
Ni	231.6	0.0038	0.019	0.38
Pb	220.3	0.014	0.07	1.4

^a Based on 0.3 g of sample in a volume of 6 ml.

acid in the vessel heated in a thermostated oven at 180°C for 6 h was satisfactory. This sealed PTFE vessel method has the advantage that the risks of contamination and sample leakage are greatly reduced.

Separation of impurities from uranium

The chromatographic behaviour of uranium and impurity elements on a column prepared as described above was examined by separating 3–15 μg of impurities from 0.3 g of high-purity U_3O_8 with nitric acid of different concentrations (2–5 M) as the eluent. It was found that the lengths of the yellow uranium band on the column were about 9, 7 and 6 cm with 2, 3 and 5 M HNO_3 , respectively. The impurity elements passed through the column and occurred in the 3–7 ml fraction of the eluate. Therefore, 6–10 ml of the eluate could be collected for analysis after discarding the first 2 ml. The elution behaviour was observed for the separation of impurities from uranium, with 95–109% recoveries of impurity elements. The eluate was analysed for uranium and the uranium concentration in the eluates was found to be less than $1 \mu\text{g ml}^{-1}$. In subsequent work, 3 M nitric acid was used as the eluent for the separation of impurities from uranium.

Regarding the life of the resin in the column, it was found that the same TBP Levetrel resin column could be used repeatedly over 30 times for separation.

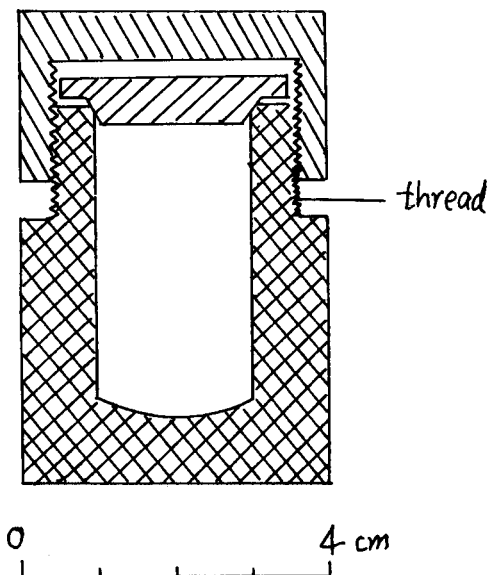


Fig. 1. Schematic diagram of the sealed PTFE decomposition vessel.

TABLE 3

Analytical results ($\mu\text{g g}^{-1}$ U) for trace elements in the proposed U_3O_8 CRMs and a control sample of U_3O_8

Element	GBW 04209			GBW 04210			GBW 04211			Control sample (U_3O_8)	
	Found ^a	R.S.D. (%)	Certified	Found ^a	R.S.D. (%)	Certified	Found ^a	R.S.D. (%)	Certified	Found ^b	R.V. ^c
Ca	38.6	8.2	38.2	62.9	6.6	59.8	100	4.0	95.5	93.1	94.0
Cd	0.55	8.9	0.55	0.90	4.8	0.86	1.50	4.2	1.39	< 0.14	0.02
Cr	32.2	4.6	32.2	49.8	4.9	50.2	85.9	6.3	80.2	7.00	6.50
Cu	39.8	5.0	37.0	59.1	4.8	58.6	99.9	3.9	94.6	3.00	3.30
Fe	63.1	7.2	66.3	99.1	4.4	102.3	166	2.8	162	79.6	78.5
Mg	93.4	4.5	95.0	147.2	4.1	149.5	239	4.6	240	5.50	5.10
Mn	26.3	5.3	25.1	34.3	5.8	39.5	67.6	8.9	63.5	1.00	1.10
Mo	35.2	8.3	37.1	52.9	5.0	49.1	72.1	2.9	79.0	27.8	29.1
Ni	50.4	4.1	50.8	76.8	3.7	79.6	126	5.3	127.6	3.90	3.90
Pb	9.45	6.8	9.60	14.2	6.7	15.0	23.4	5.3	24.0	0.75	0.70

^a Mean of six independent separate analyses. ^b Mean of three independent separate analyses. ^c Recommended value.

Effect of uranium on the determination

The effect of uranium on the ICP-AES determination was examined. The results showed that concentrations of uranium up to $6 \mu\text{g ml}^{-1}$ do not affect the determination of impurity elements. As indicated above, the uranium concentration in the effluent solution containing the analytes was less than $1 \mu\text{g ml}^{-1}$, so the efficiency of the separation is satisfactory.

Detection limits

The detection limit (DL) was calculated as the concentration giving twice the standard deviation (σ) of the blank solution and the lowest quantitatively determinable concentration (LQD) of impurities in U_3O_8 was calculated from 10σ . The results are summarized in Table 2.

Analytical results

For each sample (GBW 04209, 04210 and 04211), each value and the means of six independent separate analyses, standard deviations and relative standard deviations (R.S.D.) were contributed to the certifying body. The mean values, precisions (R.S.D.) and certified values are given in Table 3. In order to assess the accuracy, a control sample (U_3O_8) was analysed together with the proposed CRMs. The results obtained are also given in Table 3.

Conclusions

The proposed sample decomposition with a sealed PTFE vessel and TBP extraction chromatography separation coupled with ICP-AES provided accurate and reliable results for the proposed U_3O_8 CRMs. Extraction chromatography with TBP Levetrel resin is highly efficient for the separation of impurities from uranium. The proposed separation and analysis procedure provide sufficient sensitivity, accuracy, precision and speed to meet the routine quality control requirements of nuclear-grade uranium compounds.

The authors are grateful to Senior Engineer Liu Husheng, Beijing Research Institute of Chemical Engineering and Metallurgy, for providing the necessary facilities.

REFERENCES

- 1 AQCS 1991, Intercomparison Runs Reference Materials, IAEA, Vienna, 1991, p. 14.
- 2 SBTS Standard Reference Materials Catalog 1992, State Bureau of Technical Supervision of China, Beijing, 1992, p. 10.
- 3 H.G. King and C.M. Neff, Appl. Spectrosc., 17 (1963) 51.
- 4 1987 Annual Book of ASTM Standards, Vol. 12.01, ASTM, Philadelphia, 1987, C696–80, Sec. 83–90.
- 5 1987 Annual Book of ASTM Standards, Vol. 12.01, ASTM, Philadelphia, 1987, C696–80, Sec. 112–118.

- 6 T.R. Bangia, K.N.K. Kartha, M. Varghese, B.A. Dhawale and B.D. Joshi, *Fresenius' Z. Anal. Chem.*, 310 (1982) 410.
- 7 K. Kato, *At. Spectrosc.*, 7 (1986) 129.
- 8 K. Okamoto and K. Fuwa, *Analyst*, 110 (1985) 785.
- 9 V. Cheam and A.S.Y. Chau, *Analyst*, 109 (1984) 775.
- 10 R.L. Watters, Jr., *Spectrochim. Acta, Part B*, 46 (1991) 1593.
- 11 J.P. Maney, V. Luciano and A.F. Ward, *Jarrel-Ash Plasma Newsl.*, 2 (1979) 11.
- 12 R.W. Hendrie, K.C. Macleod and B.J. Thompson, *ICP Inf. Newsl.*, 10 (1984) 554.
- 13 J.S. Guan, J.Y. Ji, B.H. Gao and Y.M. Liu, *At. Energy Sci. Technol.*, 19 (1985) 230.
- 14 M.A. Floyd, R.W. Morrow and R.B. Farrar, *Spectrochim. Acta, Part B*, 38 (1983) 303.
- 15 S. Vijayalakshmi, R.K. Prabhu, T.R. Mahalingam and C.K. Mathews, *J. Anal. At. Spectrom.*, 7 (1992) 565.
- 16 T.K. Seshagiri, Y. Babu, M.L.J. Kumar, A.G.I. Dalvi, M.D. Sastry and B.D. Joshi, *Talanta*, 31 (1984) 773.
- 17 J.S. Guan, T.F. Fu, B.H. Gao, Y.Q. Shi, B.S. Song, J.Y. Ji and Y.M. Liu, *Fenxi Huaxue*, 14 (1986) 372.
- 18 P. Burba and P.G. Willmer, *Fresenius' Z. Anal. Chem.*, 323 (1986) 811.
- 19 J.S. Guan, J.Y. Ji and G.Y. Gu, *At. Energy Sci. Technol.*, 17 (1983) 580.
- 20 J.Y. Ji, B.H. Gao and J.S. Guan, *At. Energy Sci. Technol.*, 19 (1985) 233.
- 21 F. Pan, S. You, Q. He, X. Wang, H. Ma, Y. Huang and X. Yu, *Spectrochim. Acta, Part B*, 41 (1986) 1211.
- 22 F. Feng and M. Fang, *Spectrosc. Spectral Anal.*, 5, No. 6 (1985) 28.
- 23 S. Yang and S. Ji, *Spectrosc. Spectral Anal.*, 9, No. 6 (1989) 74.
- 24 H. Liu, B. Fen and Y. Pan, *Fenxi Huaxue*, 19 (1991) 203.
- 25 J.S. Guan, B.H. Gao, W.H. Wang and Y.M. Liu, *At. Energy Sci. Technol.*, 25, No. 6 (1991) 1.
- 26 R. Kroebel and A. Meyer, *Ger. Offen.*, 2162951 (1973).
- 27 H.W. Kauczor, *Hydrometallurgy*, 3 (1978) 65.
- 28 L.Y. Dong, *Uranium Min. Metall.*, 4, No. 3 (1985) 33.
- 29 T. Qian and W. Liu, *Fenxi Shiyanshi*, 8, No. 3 (1989) 28.
- 30 Y. Guan and X. Wu, *Ion Exchange Adsorpt.*, 6 (1990) 60.
- 31 J.S. Guan, Y.Q. Shi and Y.M. Liu, *At. Energy Sci. Technol.*, 25, No. 6 (1991) 8.
- 32 J.S. Guan, H.S. Liu, X.J. Yang, B.H. Gao, B. Fen and Y.M. Liu, *A Reference Method for the Determination of 16 Trace Impurity Elements in UO₂ Powder by ICP-AES Combined with TBP Levetrel Resin Chromatography*, Annual Report of the China Association for Instrumental Analysis, Beijing, 1989, p. 100.

Determination of butyltin compounds in sediment using gas chromatography–atomic absorption spectrometry: comparison of sodium tetrahydroborate and sodium tetraethylborate derivatization methods

Yong Cai, Spyridon Rapsomanikis and Meinrat O. Andreae

Biogeochemistry Department, Max Planck Institute for Chemistry, P.O. Box 3060, Saarstrasse 23, W-6500 Mainz (Germany)

(Received 24th August 1992; revised manuscript received 29th October 1992)

Abstract

Aqueous ethylation and hydride generation, two rapid, convenient speciation techniques used for the determination of butyltin species in river sediments, were compared. After extracting the sediment with methanol containing 0.5 M HCl, the extract was derivatized and analysed by gas chromatography–atomic absorption spectrometry. Monobutyltin and dibutyltin can be determined quantitatively using the hydride generation method; for tributyltin, the analysis suffers from critical interference from the sediment extract. With the ethylation method, quantitative determination of dibutyltin and tributyltin in the sediment can be achieved, while a lower recovery of monobutyltin is observed. The detection limits for butyltins in sediments are significantly improved by this method because no foaming occurs during the ethylation step and because the analytical procedure is not hampered by interference from sediment extracts. The detection limits are 0.20, 0.10 and 0.44 ng Sn g⁻¹ dry sediment for mono-, di- and tributyltin, respectively.

Keywords: Atomic absorption spectrometry; Gas chromatography; Butyltin compounds; Hydride generation; Sediments; Speciation

Organotin compounds comprise one of the most thoroughly studied groups of organometallic chemicals in terms of their industrial and agricultural uses and applications [1]. The butyltin species are under intense scrutiny owing to their significant environmental impact; for example, tributyltin (TBT), the most commonly used organotin compound in the aquatic environment, is by far the most toxic to aquatic organisms, and may be the most acutely toxic chemical to aquatic organisms deliberately introduced into water [2].

Correspondence to: S. Rapsomanikis, Biogeochemistry Department, Max Planck Institute for Chemistry, P.O. Box 3060, Saarstrasse 23, W-6500 Mainz (Germany).

As a result, the use of TBT as an antifoulant is now banned or controlled in many countries [1,3]. However, the TBT controversy is not over and the use of TBT paints continues on many larger vessels [3]. Organotins can enter the aquatic environment not only through their use in antifouling paint, but also through other applications which include disinfection of industrial and electrical generation plant cooling water, slime control in paper mills, as a biocide in preservation of wood, textile, paper or stonework, and as stabilizers of poly(vinyl chloride) (PVC) plastic [4,5]. Recently, the long-term monitoring of TBT in San Diego Bay, CA [6] and in UK estuaries [7] has indicated the possible reduction of TBT concentrations in water and tissue samples following legislative re-

strictions on TBT anti-fouling paint use. In order to evaluate the potential threat to ecosystems from reduced concentrations of TBT (thus assessing the effect and appropriateness of legislation), the development of accurate and sensitive methods for measuring butyltins at extremely low concentrations in various environmental matrices is necessary.

The techniques for the determination of organotin compounds in environmental water samples at trace levels are well documented [8–14]. For tissues and sediments, however, the techniques are less well developed [15,16]. Stephenson et al. [17] found that laboratories agreed within a factor of 2–3 on analyses of butyltins in tissues and sediments in an intercomparison of seven laboratories. The validity of some of the data in the literature concerning butyltin contents in environmental sediments may be doubtful owing to the lack of accurate analytical techniques [18]. Further, the possible invalidity of data may affect proper decisions regarding the regulation of the use of tin-based antifouling paints. It is essential, therefore, to develop a suitable analytical technique (including a procedure for extraction from sediments and tissues) for the determination of butyltin species, especially TBT, in environmental samples. The hydride generation method using sodium tetrahydroborate coupled with cryogenic trapping and separation and detection by atomic absorption spectrometry (HG–AAS) has often been the method chosen because of its speciation analysis capability, high sensitivity and general availability [14,16,19,20]. Unfortunately, the HG–AAS method has the disadvantage when applied to environmental samples that it often suffers from interference from contamination. For example, diesel oil and sulphur compounds have been implicated in the reduction of the organotin hydride signal and they may occur at high levels in environmental samples, particularly in sediments [21–23].

In previous work, the *in situ* aqueous ethylation technique using sodium tetraethylborate (NaBEt_4) [24] was applied to the determination of butyltin species in sediments [25]. The method employs a similar procedure to the hydride generation method; it involves an *in situ* ethylation of

butyltin species in aqueous solution, followed by gas sparging, cryogenic trapping, separation and subsequent detection by AAS.

In this work, the results from these two techniques for the determination of butyltin species in a spiked river sediment employing methanolic hydrochloric acid as extraction solvent were compared. For the analysis of biological samples and sediments, a major consideration is not only the analytical method, but also the procedure for the extraction of these compounds from complex sample matrices. Spiked samples are often used for the evaluation of extraction techniques for butyltin compounds in sediments in the absence of a suitable standard reference material. Some workers use an internal standard added to the spiked sample to justify the recovery evaluation. This is often of no relevance, however, because so far, a reliable method has not been developed for the extraction with the same efficiency of all the organotin compounds present [26,27]. A method based on extracting sediment with a varied volume of solvent has been employed to determine the true concentration of butyltin in sediment. It has proved to be a reliable, quantitative method for determining the recovery of butyltin species [18,25], and was used in this present work.

EXPERIMENTAL

Apparatus

Analyses were performed using a modification of the method described by Schebek et al. [18]. An important modification involves the use of glass instead of Teflon tubing as a cold trap in order to avoid producing gaps in the column during cooling and heating periods. The procedure consists in the following steps: the butyltin species in the sediment extract are first reacted with NaBH_4 or NaBEt_4 to convert the ionic butyltin species into the corresponding butyltin hydride or butylethyltin in a glass reaction vessel; the butyltin hydride or butylethyltins are stripped from solution with a stream of helium and are cold trapped (using liquid nitrogen) on a chromatographic packing; species are separated in order of increasing boiling points by heating the

trap to +200°C, and they are subsequently detected using an electrically heated quartz furnace in an atomic absorption spectrometer.

Reagents and standards

Monobutyltin (MBT), dibutyltin (DBT), tributyltin (TBT) and monomethyltin (MMT), dimethyltin (DMT) and trimethyltin chlorides (TMT) (Alfa-Ventron) and sodium tetraethylborate (Strem) were used as received. Sodium tetrahydroborate was obtained from Fluka. Methanol was of analytical-reagent or “for liquid chromatography” grade. Hydrochloric acid, nitric acid, acetic acid and sodium acetate were of Suprapur grade (Merck). All other chemicals were of analytical-reagent grade or better.

A mixed organotin stock standard solution was prepared at concentrations of ca. 1000 mg l⁻¹ of tin in methanol. It was stored in a refrigerator at 4°C and remained stable for at least 6 months [20]. A mixed organotin working standard solution was prepared daily by diluting the stock standard solution with water obtained from a Milli-Q purification system (Millipore) to a range of 20–80 µg l⁻¹ of tin. A fresh solution of ca. 1% (w/v) sodium tetraethylborate was prepared daily in deionized water and stored in a refrigerator. A solution of 8% (w/v) NaBH₄ in 1% NaOH was also prepared daily with deionized water. Acetic acid–sodium acetate buffer, 1000 ml (pH 4.05), was prepared by mixing 800 ml of 0.2 M acetic acid and 200 ml of 0.2 M sodium acetate and stored in a polyethylene bottle at room temperature.

Sediment sampling and spiking

The river sediment samples were collected from the river Main adjacent to Grosskrotzen-

berg (Germany) using a grab device, and were immediately freeze-dried on arrival in the laboratory, approximately 2 h after sampling. One part of the freeze-dried sample was spiked with MBT, DBT and TBT and the other with TBT alone. The spiking procedure for sediment consisted of the following steps: 100 g of freeze-dried sediment and 180 ml of Milli-Q-purified water were placed in a 500-ml polycarbonate bottle. When the sediment was thoroughly soaked, 3.143 ml of mixed standard solution containing 13.7, 12.0, and 32.0 mg l⁻¹ of tin of MBT, DBT and TBT, respectively, were added to the slurry and mixed well. The suspension was left to equilibrate for 10 days in the dark at room temperature, with shaking for 10 min twice each day. This spiked sediment was then freeze-dried again. The theoretical concentrations of butyltins in the spiked sediment are given in Table 1.

Sediment extraction

A 1.0-g amount of sediment sample was placed in a polycarbonate tube, then a certain volume (15–100 ml) of methanol containing 0.5 M hydrochloric acid was added. The sample was sonicated at 51 kHz for 2 h and then the different steps of the hydride generation and ethylation methods were carried out. For the hydride generation method, the sample was centrifuged for 20 min at 4000 g, then the supernatant solution was decanted and stored in a 30-ml polycarbonate bottle for analysis by HG–AAS. For the ethylation method, the pH of the sample was adjusted to 4.2 with 2.0 M sodium acetate before centrifuging; subsequent operations were the same as those for the hydride generation method. The sediment was extracted and analysed in duplicate using HG–AAS or ethylation–AAS.

TABLE 1

Concentrations of butyltin compounds in unspiked Main River sediment and theoretical concentrations of butyltins in Main River sediment after spiking

Parameter	Concentration (ng Sn g ⁻¹ dry mass)		
	BuSn ³⁺	Bu ₂ Sn ²⁺	Bu ₃ Sn ⁺
Concentration in unspiked sediment	19 ± 3	13 ± 3	ND ^a
Theoretical concentration after spiking	449 ± 3	388 ± 3	1000.0

^a ND = non-detectable (detection limit: 12 ng Sn g⁻¹).

Analytical procedure

Figure 1 is a schematic diagram of the major steps involved in the analytical procedures detailed below.

Hydride generation. A 100-ml volume of water was placed in the reaction flask with 300 μl of HNO_3 and 0.1–0.4 ml of extract was added. The reactor was closed and secured with a stainless-steel clamp. The cold trap was cooled with liquid nitrogen and then 3 ml of NaBH_4 solution were injected into the reaction vessel through a septum. The solution was purged with helium for about 4 min. The helium flow was then switched to by-pass the reaction vessel via a four-way valve, the liquid nitrogen was removed and the integrator was started. At first, the variable transformer heating the cold trap was set at 1.8 A for ca. 1.5 min to allow the column temperature to reach 30°C. The transformer was then turned up to 2.3 A so that the column attained a final temperature of 200°C.

Ethylation. A 10-ml volume of acetic acid-sodium acetate buffer and a Teflon-coated stirring bar were placed in the reaction vessel, then a measured volume of sample material (0.1–0.4 ml) and 130 μl of NaBEt_4 solution were added. The reaction vessel was closed and secured with a stainless-steel clamp. The helium flow was switched to by-pass the reactor via a four-way valve and the reaction continued for 14 min with continuous stirring. The cold trap was cooled with liquid nitrogen to -196°C , then the four-way valve was switched to pass helium through the reactor. After the solution had been purged for 9 min, the helium flow was again switched to by-pass the reactor, then the liquid nitrogen was removed and the temperature programme was started. The heating programme for the elution of these compounds is different from that for the elution of the tin hydrides because of the higher boiling points of the ethyl derivatives. At first, the variable transformer was set at 1.3 A for ca. 3.3 min to heat the column to 120°C. The transformer was then turned up to 2.20 A so that the column reached a final temperature of 200°C. The ethylated derivatives of methyltin and butyltin elute within ca. 4.0 min.

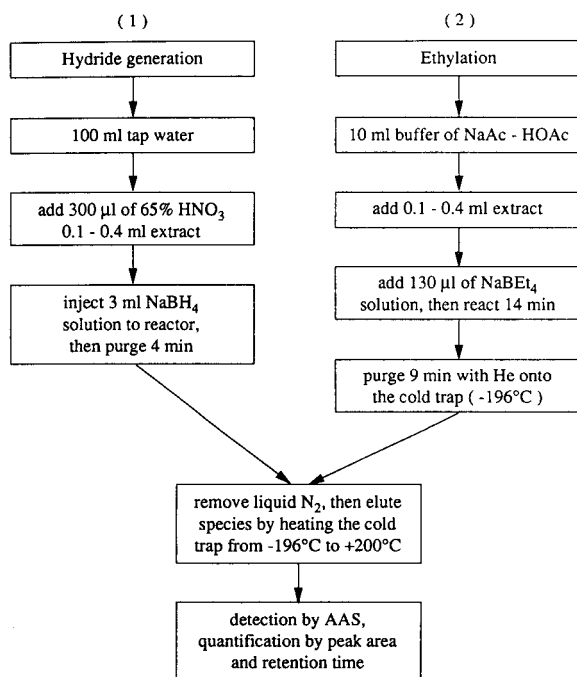


Fig. 1. Schematic diagram of the procedures for the determination of butyltin species using (1) hydride generation and (2) ethylation derivatization techniques.

Quantification

Peak areas were used for quantitative calculations. Peaks in the gas chromatograms were assigned to individual organotin compounds on the basis of retention times and were confirmed by standard additions. For the calculation of organotin compound concentrations in sediment extracts, a three-point standard addition was made to account for the matrix effects. All analyses were carried out at least in duplicate.

RESULTS AND DISCUSSION

Choice of extraction solvent

Methanolic HCl is often used as an extraction solvent for the determination of butyltin species in sediments [16,20]. Varying extraction efficiencies have been reported at different molarities of HCl in methanol for different butyltin species [27]. On the other hand, owing to the complexity

of sediment samples in the aquatic environment, the extraction efficiencies for butyltin species may vary with the type of sediment, despite the use of the same or a similar extraction procedure. Therefore, before carrying out further experiments, it was decided to study the extraction efficiency of TBT from the spiked Main River sediment with different concentrations of HCl in methanol. A 1.5-g amount of sediment and 25 ml of methanol containing HCl at concentrations of 0.17, 0.5, 1.0, 2.0, 3.0, 4.0 and 5.84 mol l⁻¹ were used. The results in Fig. 2 reveal that the less polar extraction solutions extract TBT more efficiently. Methanol containing 0.5 M HCl was therefore chosen as the extraction solvent in the experiments described below.

Determination of butyltins in spiked sediment

Previous results have shown that the variable extraction volume method is a reliable procedure for the assessment of the recoveries and true contents of butyltins in sediments in the absence of a suitable standard reference material [18,25]:

$$C_M M = C_{M_i} M_i + C_L V_L \quad (1)$$

where C_M = true concentration of the analyte in the sediment, M = mass of sediment, C_{M_i} = remaining concentration of the analyte in the sediment, M_i = mass of sediment after extraction,

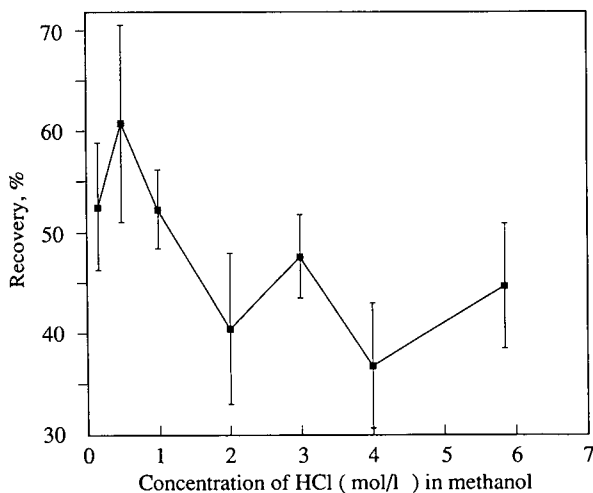


Fig. 2. Dependence of TBT extraction efficiency on the molarity of the methanolic HCl.

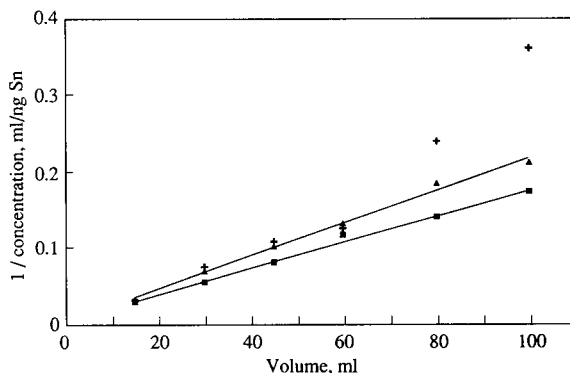


Fig. 3. Results of analysis of a spiked Main River sediment using the hydride generation method. ■ = BuSn³⁺; ▲ = Bu₂Sn²⁺; + = Bu₃Sn⁺.

C_L = concentration of analyte in the extraction solution and V_L = volume of the extraction solution. Assuming a linear adsorption isotherm, where all sites are equivalent, then

$$C_{M_i} = C_L k$$

where k = adsorption constant. With low concentrations of the extracted compounds, one can neglect the difference between M and M_i , and then Eqn. 1 is rearranged to

$$1/C_L = (V_L/C_M)M + k/C_M \quad (2)$$

A series of different volumes of solvent were used to extract an aliquot of sediment and then the true content of the compound was calculated from the slope of the plot of the reciprocal of the concentration against the volume of solvent. For this work, 15, 30, 45, 60, 80 and 100 ml of methanolic HCl were employed in both the hydride generation (Fig. 3) and ethylation (Fig. 4) procedures. For the hydride generation method, MBT and DBT fit a linear equation fairly well, but for TBT the deviation from linearity is more pronounced. Hence it is difficult to achieve a quantitative determination of TBT in the spiked sediment using this procedure. For the ethylation method, however, the assumption of a linear absorption isotherm is valid not only for MBT and DBT, but also for TBT. The true concentrations and recoveries calculated from the linear equation for butyltin species are given in Table 2. The data show that quantitative speciation for TBT

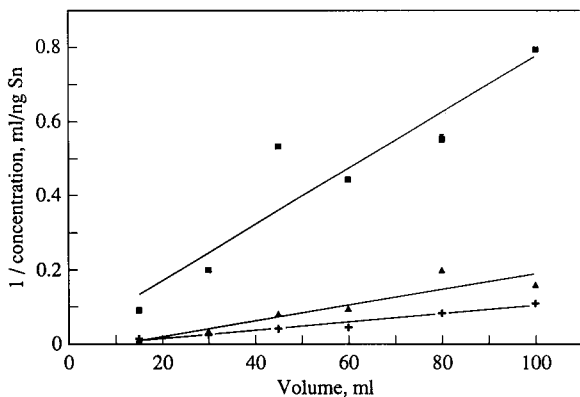


Fig. 4. Results of analysis of a spiked Main River sediment using the ethylation method. ■ = BuSn³⁺; ▲ = Bu₂Sn²⁺; + = Bu₃Sn⁺.

and DBT is possible by means of ethylation. The low recovery of MBT using this method perhaps results from the centrifuge procedure in which the MBT may be coprecipitated with colloidal material [25]. In contrast, MBT and DBT can be determined quantitatively using the hydride generation method. Two typical speciation chromatograms of spiked Main River sediment analysed using the hydride generation and ethylation methods with the same volume of solvent (15 ml) and the addition of the same amount of analyte (0.1 ml) to the reaction vessel are shown in Fig. 5. Clearly, a much better result for TBT is achieved with the ethylation technique, whereas the hydride generation method is more efficient for MBT and DBT.

As mentioned above, with the HG-AAS technique the determination of TBT often suffers from interference from contamination present in the sample [21–23]. The exact cause of this interference in environmental sediments is unknown,

but it clearly depends on the type of sediment. To date, only sample pretreatment methods have reduced the matrix effects (especially in sediments). With the same extraction procedure, critical suppression of signals was also observed during the determination of butyltin species when analysed by the ethylation method, but this interference can be eliminated efficiently by a simple centrifugation step after the pH of the sample has been adjusted to 4.2 [25].

Precision and detection limit

Six replicate analyses of butyltin species in spiked river sediment were conducted using both the hydride generation and ethylation methods. A 1.0-g amount of sediment extracted with 100 ml of solvent yielded the results given in Table 3. The relative standard deviations (R.S.D.s) are 6.2 and 7% for MBT and DBT, respectively, when analysed by the hydride generation method; the precision is lower for TBT (R.S.D. = 13%) because of interference during hydride generation and analysis. With the ethylation method, a better precision is achieved for TBT (R.S.D. = 9%).

Absolute detection limits based on 3σ of baseline noise for butyltin species are given in Table 4. The concentration detection limit is a function of the sample size. For the sediment sample the detection limit depends on the volume of extraction solvent and the amount added to the reaction vessel. In general, better detection limits can be achieved if larger amounts of extract are analysed, but they are often limited by interference resulting from the addition of a large amount of extract. For instance, the maximum volume of extract added to the reactor was 0.5 ml during the hydride generation method as foaming during

TABLE 2

True concentrations of butyltin species in spiked Main River sediment ^a

Method	BuSn ³⁺		Bu ₂ Sn ²⁺		Bu ₃ Sn ⁺	
	C_t	R (%)	C_t	R (%)	C_t	R (%)
Hydride generation	608 ± 24	136 ± 5	482 ± 20	124 ± 5	Nlf ^b	Nlf ^b
Ethylation	132 ± 25	29 ± 6	477 ± 96	123 ± 25	920 ± 108	92 ± 11

^a C_t = true concentration calculated from linear equation (ng g⁻¹ dry mass as tin); R = recovery obtained by comparison with the data in Table 1. ^b Non-linear fit.

TABLE 3

Precision for determination of butyltin species in sediment

Species	Hydride generation			Ethylation		
	Mean (ng Sn g ⁻¹)	S.D. (ng g ⁻¹)	R.S.D. (%)	Mean (ng Sn g ⁻¹)	S.D. (ng g ⁻¹)	R.S.D. (%)
BuSn ³⁺	572	35	6	115	15	13
Bu ₂ Sn ²⁺	467	34	7	619	87	14
Bu ₃ Sn ⁺	405	51	13	953	89	9

derivatization occurs and the signal is suppressed by interference from the extract. In this work, 1.0 g of spiked sediment was extracted with 45 ml of solvent, then 0.2 and 0.4 ml of extract were analysed using the hydride generation and ethylation methods, respectively. The concentration detection limits were calculated and are given in Table 4.

Following legislative restrictions on the use of anti-fouling paints containing TBT, butyltin concentrations in some environmental matrices have decreased [6,7]. In this event, the ability to measure low levels of TBT is important in order to develop appropriate monitoring strategies and to monitor the effects of the legislation. It was noted in previous experiments that the ethylation method for determining TBT is less likely to be subject to interference from other compounds that may be present in environmental samples. Also, a larger amount of extract can be added to the reactor, thereby improving the detection limit. To demonstrate this, ca. 1.0 g of unspiked Main River sediment was extracted with 45 ml of methanolic HCl and 16 ml of extraction solution were analysed. The detection limits were calculated and are given in Table 4. The detection

limit of TBT in the sediment was reduced to 0.44 ng Sn g⁻¹ dry mass. This is approximately 100 times lower than that obtained by the hydride generation method.

Conclusions

The *in situ* techniques of hydride generation and ethylation, two rapid, convenient speciation methods, were compared for the determination of butyltin species in river sediment. MBT and DBT can be determined quantitatively by the hydride generation method. For TBT, however, the analysis suffers from critical interference in extraction of the sediment, and therefore it is difficult to achieve accurate quantitative results. With the ethylation method, accurate determination of DBT and TBT in the sediment can be achieved but a lower recovery of MBT is observed, probably because of loss during the centrifugation procedure in which MBT may be coprecipitated with colloidal material. Although sodium tetrahydroborate is easier to handle than sodium tetraethylborate, derivatization using the latter reduces matrix effects during the TBT determination in sediments. Using the ethylation method, no foaming occurs during derivatization,

TABLE 4

Detection limits of butyltin species in sediment

Species	Hydride generation		Ethylation		Ethylation	
	ng	ng Sn g ⁻¹ dry mass ^a	ng	ng Sn g ⁻¹ dry mass ^b	ng	ng Sn g ⁻¹ dry mass ^c
BuSn ³⁺	0.03	6.0	0.07	9	0.07	0.20
Bu ₂ Sn ²⁺	0.03	6.0	0.34	38	0.03	0.10
Bu ₃ Sn ⁺	0.15	33	0.11	12	0.15	0.44

^a 45 ml of extraction solvent, 0.2 ml of which was analysed. ^b 45 ml of extraction solvent, 0.4 ml of which was analysed. ^c 45 ml of extraction solvent, 16 ml of which plus 0.8 ml of NaBEt₄ solution were added to the reaction vessel.

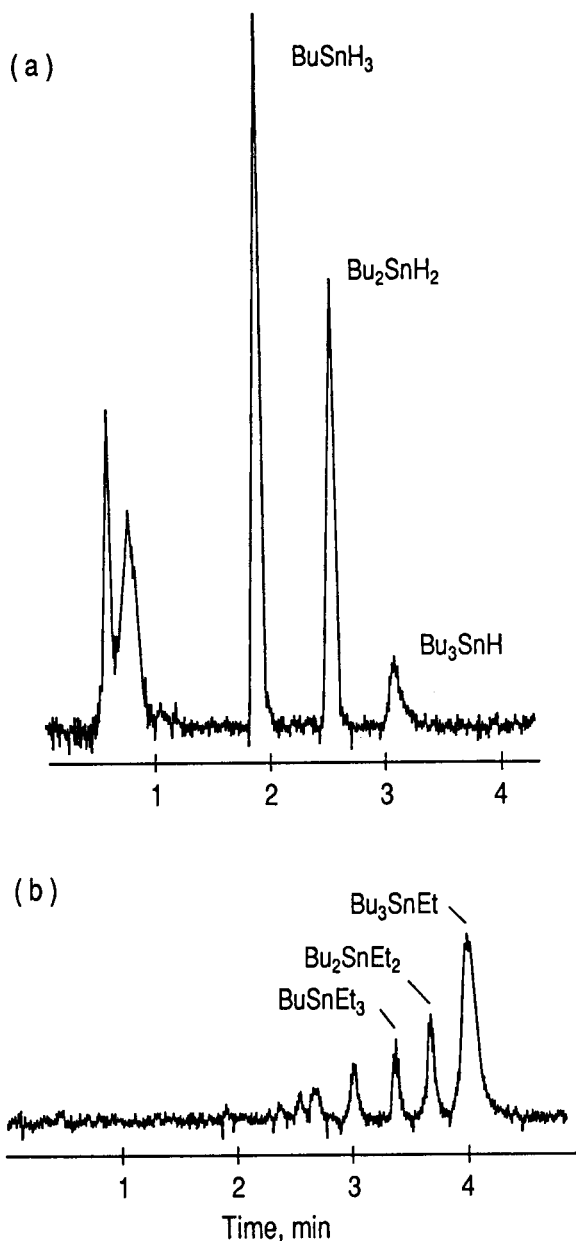


Fig. 5. Chromatograms of analysis of spiked River Main sediment using (a) hydride generation and (b) ethylation.

there is less interference from the extract and there is no high-pressure build-up during analysis. Therefore, a large amount of sediment extract can be used in the procedure and the detection limits of butyltins in sediment can be significantly

improved. The in situ ethylation technique with a variable extraction volume method offers an accurate, sensitive method for the determination of TBT in sediments.

The authors are grateful to C. Harris and T. W. Andreae for assistance with the manuscript. Y.C. thanks the Max Planck Society for generous support.

REFERENCES

- 1 M.A. Champ and W.L. Pugh, in *Ocean's 87*, Proceedings 4, Marine Technology Society and IEEE Ocean Engineering Society, Halifax, Nova Scotia, 1987, p. 1296.
- 2 R.J. Maguire, *Appl. Organomet. Chem.*, 1 (1987) 475.
- 3 R.J. Huggett, M.A. Unger, P.F. Seligman and A.O. Valkirs, *Environ. Sci. Technol.*, 26 (1992) 232.
- 4 C.A. Krone, D.W. Brown, D.G. Burrows, R.G. Bogar, S.L. Chan and U. Varanasi, *Mar. Environ. Res.*, 27 (1989) 1.
- 5 K. Fent, *Mar. Environ. Res.*, 28 (1989) 477.
- 6 A.O. Valkirs, B. Davidson, L.L. Kear, R.L. Fransham, J.G. Grovhoug and P.F. Seligman, *Mar. Environ. Res.*, 32 (1991) 151.
- 7 M.E. Waite, M.J. Waldock, J.E. Thain, D.J. Smith and S.M. Milton, *Mar. Environ. Res.*, 32 (1991) 89.
- 8 H.A. Meinema, T. Burger-Wiersma, G. Versluis-de Han and E.Ch. Gevers, *Environ. Sci. Technol.*, 12 (1978) 288.
- 9 V.F. Hodge, S.L. Seidel and E.D. Goldberg, *Anal. Chem.*, 51 (1979) 1256.
- 10 M.O. Andreae and J.T. Byrd, *Anal. Chim. Acta*, 156 (1984) 147.
- 11 C.L. Matthias, J.M. Bellama, G.J. Olson and F.E. Brinckman, *Environ. Sci. Technol.*, 20 (1986) 609.
- 12 M.D. Müller, *Fresenius' Z. Anal. Chem.*, 317 (1984) 32.
- 13 R.J. Maguire and H. Huneault, *J. Chromatogr.*, 209 (1981) 458.
- 14 O.F.X. Donard, S. Rapsomanikis and J.H. Weber, *Anal. Chem.*, 58 (1986) 772.
- 15 M.D. Stephenson and D.R. Smith, *Anal. Chem.*, 60 (1988) 696.
- 16 C.L. Matthias, J.M. Bellama, G.J. Olson and F.E. Brinckman, *Int. J. Environ. Anal. Chem.*, 35 (1989) 61.
- 17 M.D. Stephenson, D.R. Smith, L.W. Hall, Jr., W.E. Johnson, P. Michel, J. Short, M. Waldock, R.J. Huggett, P. Seligman and S. Kola, in *Ocean's 87*, Proceedings 4, Marine Technology Society and IEEE Ocean Engineering Society, Halifax, Nova Scotia, 1987, p. 1334.
- 18 L. Schebek, M.O. Andreae and H.J. Tobschall, *Int. J. Environ. Anal. Chem.*, 45 (1991) 257.
- 19 N.S. Makkar, A.T. Kronick and J.J. Cooney, *Chemosphere*, 18 (1989) 2043.

- 20 L. Schebek, M.O. Andreae and H.J. Tobschall, *Environ. Sci. Technol.*, 25 (1991) 871.
- 21 P.F. Seligman, A.O. Valkirs and R.F. Lee, in *Ocean's 86, Proceedings 4, Marine Technology Society, Washington, DC, 1986*, p. 1189.
- 22 V. Desauziers, F. Leguille, R. Lavigne, M. Astruc and R. Pinel, *Appl. Organomet. Chem.*, 3 (1989) 469.
- 23 J.R. Ashby and P.J. Craig, *Sci. Total Environ.*, 78 (1989) 219.
- 24 S. Rapsomanikis, O.F.X. Donard and J.H. Weber, *Anal. Chem.*, 58 (1986) 35.
- 25 Y. Cai, S. Rapsomanikis and M.O. Andreae, *J. Anal. At. Spectrom.*, in press.
- 26 S.Z. Zhang, Y.K. Chau, W.C. Li and A.S.Y. Chau, *Appl. Organomet. Chem.*, 5 (1991) 431.
- 27 Y. Cai, S. Rapsomanikis and M.O. Andreae, *Mikrochim. Acta*, 109 (1992) 67.

Determination of fluorine and iodine in biological materials

Marcel Langenauer and Urs Krähenbühl

Laboratorium für Radiochemie, Universität Bern, Freiestrasse 3, CH-3000 Berne 9 (Switzerland)

Armin Wytenbach

Paul Scherrer Institute (PSI), CH-5232 Villigen PSI (Switzerland)

(Received 25th August 1992)

Abstract

Fluorine and iodine were determined in some biological reference materials. Radiochemical neutron activation analysis was used for iodine and ion-selective potentiometry for fluorine. The two elements were separated from the matrix elements by pyrohydrolysis in the presence of vanadium(V) oxide. The volatile compounds were absorbed in sodium hydroxide solution for the determination of fluorine and in acidic silver nitrate solution for the determination of iodine. This method gives low detection limits with small sample sizes.

Keywords: Ion-selective electrodes; Neutron activation methods; Potentiometry; Radiochemical methods; Biological samples; Fluorine; Iodine; Pyrohydrolysis

Usually chlorine and bromine can be easily determined in biological materials by instrumental neutron activation analysis with thermal neutrons (ITNA) via ^{38}Cl and ^{82}Br . The determination of iodine via ^{128}I is more difficult, especially at low concentrations, because the activities from ^{38}Cl , ^{24}Na , ^{42}K and ^{56}Mn are too dominant. Instrumental neutron activation analysis with epithermal neutrons (IENA) improves the situation for iodine [1]; the detection limit was found to be ca. 200 ng g^{-1} , but it depends on the ratio of epithermal to thermal neutrons and on the manganese concentration of the sample. As many plant materials contain very low iodine concentrations ($< 500 \text{ ng g}^{-1}$) in combination with high

manganese concentrations ($> 100 \text{ } \mu\text{g g}^{-1}$), it was felt that a radiochemical separation of iodine would be superior to IENA.

Ion-selective potentiometry for the determination of fluorine is a very selective and sensitive method [2]. The major problem is to avoid contamination and the loss of fluorine during the wet digestion.

In this work, radiochemical neutron activation analysis with thermal neutrons (RTNA) followed by pyrohydrolysis in the presence of vanadium(V) oxide was used to determine iodine in biological reference materials. It is possible to separate iodine selectively from matrix elements, and especially from chlorine, and to measure it with a very low Compton background contribution. Fluorine can also be detected very well with an ion-selective electrode after the same separation. The results obtained for biological reference ma-

Correspondence to: U. Krähenbühl, Laboratorium für Radiochemie, Universität Bern, Freiestrasse 3, CH-3000 Berne 9 (Switzerland).

materials were in good agreement with data in the literature.

EXPERIMENTAL

A procedure to determine halogens in rock samples by radiochemical neutron activation analysis for chlorine, bromine and iodine followed by the determination of fluorine with an ion-selective electrode on the same sample was published by Dreibus et al. [3]. This extraction method was later modified by Langenauer et al. [4], applying higher temperatures for faster completion of the reaction. In this work, this procedure was further modified for the determination of iodine and fluorine in biological samples.

Determination of iodine

Pulverized samples (80 mg) were irradiated at a thermal neutron flux of $2 \times 10^{13} \text{ n cm}^{-2} \text{ s}^{-1}$ for

2 min in the SAPHIR research reactor of the Paul Scherrer Institute. After allowing important short-lived activities (e.g., ^{28}Al) to decay for 5–10 min, the samples were mixed in a nickel crucible with 250 mg of vanadium(V) oxide (V_2O_5) and placed in a quartz tube. Figure 1 shows the apparatus for the extraction of iodine and fluorine. The quartz tube was filled with quartz-wool in the direction of the nitrogen flow after the crucible to retain incompletely oxidized particles. The samples were heated to a temperature of 1000°C by sliding the preheated oven to the position of the crucible and maintained at this temperature for 10 min. During the extraction of the halogens the tube was flushed with nitrogen (80 ml min^{-1}) saturated with water vapour. The volatile compounds were absorbed in 2 ml of acidic silver nitrate solution (8% HNO_3 saturated with silver nitrate) [5]. The final volume at the end of the separation was about 4.0 ml. The γ -ray spectrum of this solution was measured 25 min

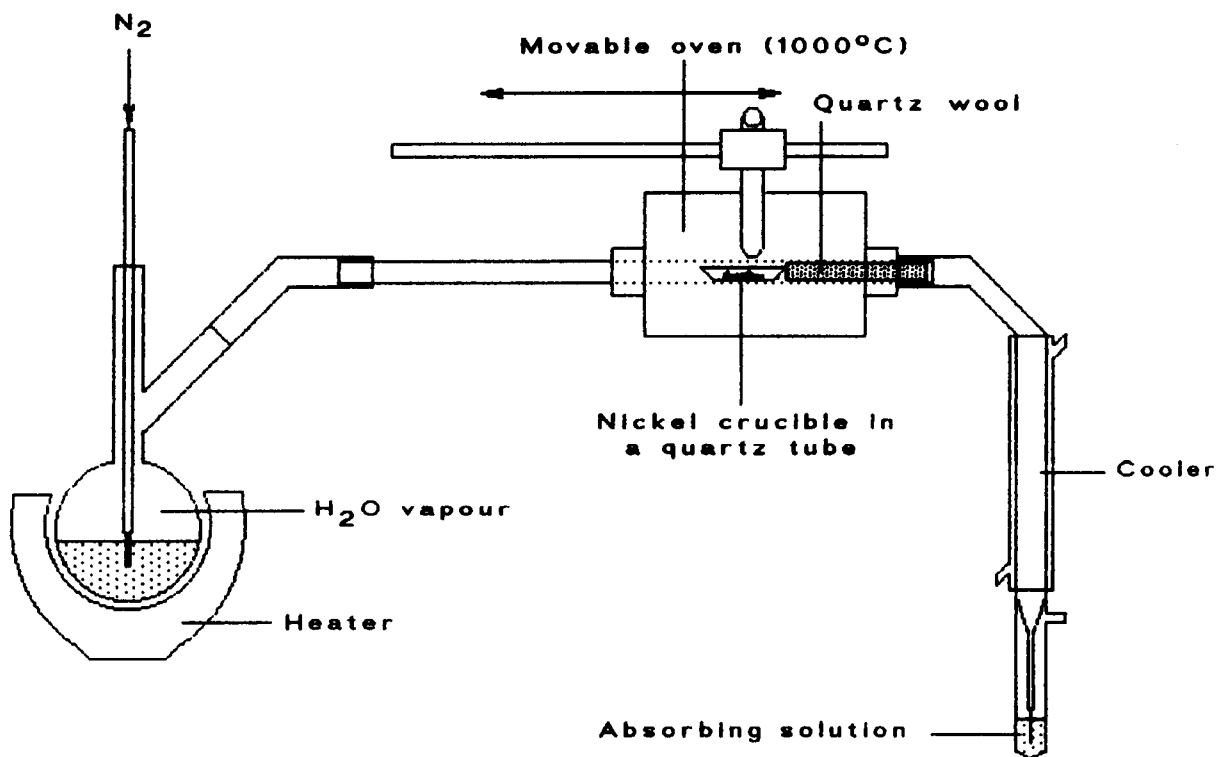


Fig. 1. Apparatus for pyrohydrolysis of biological samples for the determination of fluorine and iodine. Absorbing solution: acidic silver nitrate solution for iodine and sodium hydroxide solution for fluorine.

after the irradiation in counting vials with a well-type Ge(Li) detector for 30 min.

From the ^{128}I activity ($t_{1/2} = 25$ min, γ -line at 443 keV), the mass for iodine was calculated relative to standard samples. Standards were prepared by irradiation of about 100 mg of ammonium carbonate containing known amounts of iodine and also chlorine and bromine. After the irradiation they were dissolved in a sodium hydroxide solution and made up to the same final volume for counting.

Determination of fluorine

For the determination of fluorine the same separation procedure as for iodine was used, but without irradiation of the samples. This time the vanadium(V) oxide contained 1.9 mg of sodium chloride, 3.4 mg of sodium bromide and 5.0 mg of sodium iodide as carriers and, instead of the acidic silver nitrate solution, 0.5 ml of 2.8 M sodium hydroxide solution was used for the absorption of the fluorine species. All manipulations following the separation were made in plastic equipment. Volumes of 0.5 ml of 2.8 M hydrochloric acid and 1.0 ml of 0.47 M phosphate buffer ($\text{Na}_2\text{HPO}_4\text{-KH}_2\text{PO}_4$) were then added to a final volume of 7.0 ml ($\text{pH} = 6.00 \pm 0.05$). The electrochemical potential was measured with a fluoride-selective electrode and compared with the potential of reference solutions.

RESULTS AND DISCUSSION

All results given are means of replicate independent analyses as indicated in the tables. The analytical errors given are one standard deviation (1σ) from the mean. Table 1 gives the results for the fluorine concentrations in biological reference materials. The result for orchard leaves (SRM 1571) is given with one standard deviation (1σ) because only one analysis was accomplished. All results for fluorine are in good agreement with the literature data. The relatively large error for hay (V-10) may be due to some inhomogeneity of the material. The detection limit for fluorine was calculated to be $1 \mu\text{g g}^{-1}$. The extraction of fluorine from the matrix and the absorp-

TABLE 1

Comparison of results obtained by ion-selective potentiometry for fluorine in biological reference materials

Standard	Concentration ($\mu\text{g g}^{-1}$)	
	This work ^a	Literature
Orchard leaves (SRM 1571)	4.3 ± 0.3 (1)	3.9 ± 0.5 ^b
Citrus leaves (SRM 1572)	2.6 ± 0.1 (3)	– ^c
Pine needles (SRM 1575)	3.6 ± 0.3 (9)	3.0 ± 0.6 ^b
Spruce needles (CRM 101)	4.4 ± 0.3 (5)	4.3 ^{d,e}
Hay (V-10)	8.6 ± 0.8 (3)	10.64 ^f

^a Mean \pm standard deviation with number of determinations in parentheses. ^b From Gladney et al. [6]. ^c No value given. ^d From Griepink et al. [7]. ^e Not certified. ^f From International Atomic Energy Agency [8].

tion in the sodium hydroxide solution were quantitative for the biological materials examined.

The result for iodine in orchard leaves (SRM 1571) is in good agreement with the literature data (Table 2). The results for pine needles (SRM 1575) and citrus leaves (SRM 1572) are 62% higher and 21% lower than the concentrations given in the literature, respectively.

To calculate the decontamination factors for chlorine and bromine, the concentrations of these elements were also determined in the solutions via ^{38}Cl ($t_{1/2} = 37.2$ min, γ -line at 1642 keV) and ^{80}Br ($t_{1/2} = 17.4$ min, γ -line at 616 keV). Owing to the use of the quartz-wool in the tubes (see Fig. 1) and the limited retention of chlorine and bromine species in the silver nitrate solution, on average only 2.1% and 13.5% of the total chlorine and bromine were found in the solutions, respectively. Virtually no γ -rays other than those of ^{38}Cl , ^{80}Br and ^{128}I were detected in the meas-

TABLE 2

Comparison of results obtained by radiochemical neutron activation analysis for iodine in biological reference materials

Standard	Concentration ($\mu\text{g g}^{-1}$)	
	This work	Literature
Orchard leaves (SRM 1571)	0.155 ± 0.010 (2) ^a	0.165 ± 0.040 ^b
Citrus leaves (SRM 1572)	1.49 ± 0.03 (5)	1.88 ^c
Pine needles (SRM 1575)	0.235 ± 0.015 (2)	0.145 ^b

^a Mean \pm standard deviation with number of determinations in parentheses. ^b From Gladney et al. [6]. ^c From Wyttenbach et al. [1].

ured solutions. The detection limit for iodine was calculated to be in the range 7–15 ng g⁻¹ following Currie [9].

To establish that all the iodine was absorbed in the acidic solution of silver nitrate, the nitrogen was conducted through a second absorption unit containing 4 ml of silver nitrate solution. Taking into account that no iodine was detected in this solution, the detection limit was calculated to be 2 ng g⁻¹.

From the result for orchard leaves (SRM 1571) it can be stated that the separation from the matrix and other trace elements was excellent and that the absorption of iodine in the acidic silver nitrate solution was quantitative.

Conclusions

Very low iodine concentrations can be determined with high precision with this procedure because the separation from other disturbing radionuclides is excellent, especially for ³⁸Cl. Fluorine can also be determined at low concentrations without any contamination or losses. The good separation from the matrix elements gives excellent results.

This work was supported by the Swiss National Science Foundation.

REFERENCES

- 1 A. Wytttenbach, L. Tobler and V. Furrer, in B. Sansoni (Ed.), *Instrumentelle Multielementanalyse*, VCH, Weinheim, 1985, p. 137.
- 2 G. Cousen and U. Bartels, *CLB Chem. Labor Betrieb*, 1 (1985) 19.
- 3 G. Dreibus, B. Spettel and H. Wänke, in L.H. Ahrens (Ed.), *Origin and Distribution of the Elements*, Pergamon, Oxford, New York, 1979, p. 33.
- 4 M. Langenauer, U. Krähenbühl, V. Furrer and A. Wytttenbach, *Geostand. Newsl.*, 16 (1992) 41.
- 5 J. Oravec, *J. Radioanal. Nucl. Chem. Lett.*, 150 (1991) 287.
- 6 E.S. Gladney, C.E. Burns, D.R. Perrin, I. Roelandts and T.E. Gills, *Natl. Bur. Stand. (U.S.), Spec. Publ.* 260-88 (1984).
- 7 B. Griepink, E.A. Maier and H. Muntau, *Report EUR 12680 EN*, Commission of the European Communities, Brussels, 1990.
- 8 L. Pszonicki and A.N. Hanna, *Report IAEA/RL/123*, International Atomic Energy Agency, Vienna, 1984.
- 9 L.A. Currie, *Anal. Chem.*, 40 (1968) 586.

Determination of platinum in environmental and geological samples by radiochemical neutron activation analysis

D. Wildhagen and V. Krivan

Sektion Analytik und Höchstreinigung, Universität Ulm, Albert-Einstein-Allee 11, W-7900 Ulm (Germany)

(Received 17th August 1992)

Abstract

A radiochemical neutron activation analysis technique was developed for the determination of traces of platinum in environmental and geological samples via the indicator radionuclide ^{199}Au , based on the separation of gold on polyurethane foam from 1 M HCl. In the determination of platinum at the ng g^{-1} level in the presence of antimony at concentrations higher than about $5 \mu\text{g g}^{-1}$, owing to a slight co-retention of antimony, further decontamination of the indicator radionuclide fraction was necessary. The effect of neutron flux and irradiation time on the extent of the second-order interfering reaction $^{197}\text{Au}(n,\gamma)^{198}\text{Au}(n,\gamma)^{199}\text{Au}$ and the effect of the gold content on the limit of detection of platinum are considered in detail. The feasibility of this technique was tested by the analysis of environmental and geological samples, and the results obtained were compared with those of other methods.

Keywords: Neutron activation methods; Radiochemical methods; Environmental samples; Geological materials; Platinum

Since the introduction of catalytic cleaning of automobile exhaust gases, platinum has become a new pollutant of the environment. For the determination of the platinum baseline levels in the environment and of possible health hazards, reliable and efficient analytical methods for the determination of this element in a wide variety of samples are required.

There are a number of methods for the determination of platinum in various environmental samples at concentrations down to 0.1 ng g^{-1} . Several graphite furnace atomic absorption spectrometric (GFAAS) procedures have been reported [1–5], of which that by Eller et al. [4]

seems to be the most powerful, with a limit of detection of 0.4 ng g^{-1} when applied to the analysis of the NIST Standard Reference Materials Orchard Leaves (SRM 1571) and Bovine Liver (SRM 1577). However, this method requires a large-scale preconcentration of platinum prior to its determination. This preconcentration procedure was also applied in the analysis of SRM Orchard Leaves and Bovine Liver by x-ray fluorescence with excitation by total reflectance (TXRF) and a limit of detection comparable to that of GFAAS was achieved [6]. Adsorption voltammetry combined with detection by the catalytic hydrogen wave can achieve limits of detection at the 0.1 ng g^{-1} level [7]. Nevertheless, the performance of this technique requires a high analytical standard in order to recognize and minimize possible interferences due to surfactants and residues from decomposition acids.

Correspondence to: V. Krivan, Sektion Analytik und Höchstreinigung, Universität Ulm, Albert-Einstein-Allee 11, W-7900 Ulm (Germany).

In the application of tandem mass spectrometry to the determination of platinum in rock samples, a detection limit of 10 pg g^{-1} has been reported [8,9]; however, this technique is available in only a few laboratories.

Radiochemical neutron activation analysis (RNAA) based on the production of the indicator radionuclide ^{199}Au and its separation using different procedures has also been used for the determination of low contents of platinum in geological, industrial, environmental and biological materials. Among these, a very powerful method is that developed by Zeisler and co-workers [10–12], which is based on the precipitation of elemental gold at elevated temperatures. The very low limit of detection they achieved at the pg g^{-1} level is mainly due to irradiation of very large sample portions (up to 20 g) with low gold concentrations causing no strong interference from the second-order reaction. Tjioe et al. [13] used the same separation technique and achieved a detection limit of 1 ng g^{-1} . In other RNAA techniques reported, the separation of gold is based on extraction [14], ion exchange [15] and coprecipitation with selenium [16]. However, no detailed data on the selectivity and sometimes the limits of detection were given. Some of the limits of detection reported (up to 30 ng g^{-1} [15]) are insufficient for the present demands.

In this work, a technique for the selective separation of gold based on its adsorption on polyurethane foam from hydrochloric acid medium and, at higher accompanying concentrations of antimony, supplemented by extraction with dithizone, was developed and applied to the analysis of three different kinds of samples. In addition, the extent of the second-order interference reaction from gold and especially its dependence on the thermal neutron flux and irradiation time were evaluated.

EXPERIMENTAL

Reagents and radiotracers

All reagents used for the separation procedure were of analytical-reagent grade and supplied by Merck (Darmstadt, Germany). The original con-

centrations of nitric acid and hydrochloric acid were about 65% and 37%, respectively. The exact concentration of the hydrochloric acid was determined by titrimetry. Polyurethane foam of the polyether type (PUF) was obtained from Gummi-Welz (Ulm, Germany).

Radiotracers of the elements investigated were prepared by irradiation of pure metals or suitable compounds in a nuclear reactor as described below. The radiochemical purity of the radiotracers was checked by high-resolution γ -ray spectrometry.

Samples and standards

The samples investigated were a street dust and corn plant with elevated platinum contents and a geological material, obtained within the scope of the programme "Qualitätssicherung und Qualitätskontrolle der analytischen Daten, Forschungsverbund Edelmetallemissionen" from Dr. W. Wegscheider (Technical University of Graz, Austria). Sample portions of 150–180 mg were sealed into Suprasil quartz ampoules (Heraeus, Hanau, Germany). Standards were prepared in a clean bench by pipetting a known amount of the respective element stock solution into cleaned Suprasil quartz ampoules. The standards were dried in a desiccator over Siccapent (Merck) at reduced pressure and room temperature. After irradiation, the surface of the ampoules containing the standards was etched before counting.

Instrumentation

In the radiotracer experiments, a well-type $3 \times 3 \text{ in. NaI(Tl)}$ detector coupled with a single-channel analyser (Berthold, Wildbad, Germany) was used for counting the γ -rays. A high-resolution γ -ray spectrometer system (EG&G Ortec, Munich, Germany), consisting of an intrinsic germanium detector with an FWHM of 1.72 keV at the 1332-keV γ -ray of ^{60}Co , an efficiency of 44% relative to a $3 \times 3 \text{ in. NaI(Tl)}$ detector and a peak-to-Compton ratio of 78:1, and an ADCAM multi-channel buffer, was used for checking the radiochemical purity of the radiotracers and counting the ^{199}Au γ -rays in activation analysis. The γ -ray spectra were evaluated with a Digital

Equipment Professional 350 computer using the Ortec Geligam program version 1.7.

The irradiated samples were digested in 25-ml PTFE pressure bombs (Berghof, Eningen, Germany).

For elution, an IP4 peristaltic pump (Ismatec, Zürich, Switzerland) was used for operating several columns simultaneously.

Irradiation and decay time

The street dust samples were irradiated for 16 h and the corn plant and the geological samples for 24 h at a thermal neutron flux of $1.3 \times 10^{13} \text{ cm}^{-2} \text{ s}^{-1}$ in the FRM reactor of Munich Technical University (Garching, Germany). Before handling, the irradiated corn plant samples were allowed to decay for 1 day and the other samples for 3 days.

Determination of distribution coefficients

The distribution coefficients for static conditions (batch method) were determined by means of the radiotracer technique. The distribution coefficient D is defined as the ratio of the total amount of the element per gram of dry sorbent to the total amount of the element per millilitre of the solution. Before use, the PUF was washed in sequence with 6 M HCl, distilled water and acetone, then dried and weighed. To 1.5 ml of 0.1–6 M HCl, 10 μl of the radiotracer solution containing 1 μg of inactive carrier were added. The specific activities for ^{198}Au , ^{122}Sb and ^{46}Sc were between 10^5 and $10^6 \text{ Bq } \mu\text{g}^{-1}$ and for ^{113}Sn about $300 \text{ Bq } \mu\text{g}^{-1}$. The average volume/weight ratio of the solute and sorbent was 105 ml g^{-1} . To adjust the equilibrium, the foam was periodically

squeezed at about 30-min intervals during a 6-h period by means of a plastic plunger in order to bring fresh solution into contact with the foam.

Radiochemical separation procedure

The separation columns were made of 2-ml syringes having an active bed of $5 \times 0.8 \text{ cm}$ packed with two PUF cylinders (about 200 mg of foam). Before use, they were pretreated with 10 ml of 1 M HCl. After addition of 10 μg of carrier for Au, Sc and Sn, the irradiated street dust and corn plant samples were digested with a mixture of 3 ml of HNO_3 and 1 ml of HCl and the geological sample with a mixture of 2.5 ml of HNO_3 , 1 ml of HCl and 0.5 ml of HF (all concentrated acids) in 25-ml PTFE pressure bombs at 220°C for 10 h. The sample solution was evaporated nearly to dryness under an infrared lamp. After addition of 1 ml of concentrated HCl and evaporation to dryness, the residue was transferred into 4 ml of 1 M HCl. This solution was squeezed through a $0.45\text{-}\mu\text{m}$ pore size cellulose nitrate membrane filter (*caution*: gold is strongly adsorbed on a cellulose acetate filter) and then passed through the PUF column. The column was eluted with 1 M HCl until 40 ml of eluate had been collected and counted.

Additional procedure for high Sb / Pt ratios

In the case of higher antimony and low platinum concentrations in the sample ($\geq 5 \text{ } \mu\text{g g}^{-1}$ and $< 50 \text{ ng g}^{-1}$, respectively), the column was subsequently eluted with 15 ml of acetone. This solution was evaporated to dryness under an infrared lamp and the residue was dissolved in 400 μl of aqua regia and evaporated nearly to

TABLE 1

Nuclear data [17] for analytically interesting nuclear reactions induced on platinum with reactor neutrons

Nuclear reaction	Isotope abundance (%)	Cross-section (barn)	$t_{1/2}$	Main γ -lines (keV) [intensity, (%)]	Activation yield ($\text{Bq } \mu\text{g}^{-1}$) ^a	Possible interfering reaction
$^{196}\text{Pt}(n,\gamma)^{197}\text{Pt}$	25.3	0.69	18.3 h	191.3 [5.7]	4180	$^{197}\text{Au}(n,p)^{197}\text{Pt}$ ^b
$^{198}\text{Pt}(n,\gamma)^{199}\text{Pt} \xrightarrow{\beta^-} ^{199}\text{Au}$	7.2	3.7	30.8 min 3.14 days	542.7 [16.4] 158.4 [40.0]	2840	

^a Activity at the end of irradiation (1 day) for a neutron flux of $\Phi_{\text{th}} = 1.3 \times 10^{13} \text{ cm}^{-2} \text{ s}^{-1}$ and $\Phi_{\text{ep}} = 4 \times 10^{11} \text{ cm}^{-2} \text{ s}^{-1}$. ^b Due to a cross-section of 2 μbarn , in practice irrelevant.

dryness. Then 100 μl of concentrated HCl were added and the solution was evaporated again nearly to dryness. This step was repeated with 50 μl of concentrated HCl. The residual drop was transferred into 1 ml of 1 M HCl, then the procedure from the stage of addition of aqua regia was repeated once more. The resulting 2 ml of HCl solution was extracted with 2 ml of 0.001 M dithizone in chloroform and the activity of the organic phase was counted.

RESULTS AND DISCUSSION

Activation and interference from gold

Because of the multi-isotope composition of natural platinum, irradiation with reactor neutrons leads to a multitude of nuclear reactions of which only the two considered in Table 1 are of analytical interest. Although the first reaction yields a higher specific activity of ^{197}Pt , in general, the second reaction, producing via subsequent decay of ^{199}Pt the indicator radionuclide ^{199}Au , is more suitable for the determination of platinum in biological, environmental and geological samples. Owing to the seven-fold higher intensity of the 158.4-keV γ -line of ^{199}Au in comparison with the 191.3-keV γ -line of ^{197}Pt , the indicator radionuclide ^{199}Au produced by the breeding process from ^{199}Pt provides higher sensitivity. Further, the longer half-life of ^{199}Au allows highly active samples to decay prior to their radiochemical treatment without an essential loss of sensitivity. This is especially relevant when

extremely low concentrations of platinum are to be determined in samples with major components undergoing strong activation with thermal neutrons.

However, using the analytical reaction yielding ^{199}Au as indicator radionuclide, the second-order interfering reaction from gold $^{197}\text{Au}(n,\gamma)^{198}\text{Au}(n,\gamma)^{199}\text{Au}$ has to be considered. This interfering reaction can strongly affect the detection limit of platinum and the degree of accuracy achievable. In addition to the concentration ratio of platinum and gold, the limit of detection depends on the irradiation conditions. The generation of ^{199}Au by the second-order reaction from gold depends on the square of the thermal neutron flux while its generation by the analytical reaction from platinum is proportional to the thermal neutron flux. Using activation equations modified for this case [18,19], the contribution of the second-order interfering reaction to the total activity of the indicator radionuclide ^{199}Au as a function of the thermal and epithermal neutron flux and the irradiation time can be estimated. From the data in Table 2 obtained in this way for the two different neutron fluxes that were available, it is evident that the contribution of the interference reaction induced on gold to the total activity of ^{199}Au increases with increasing neutron flux and increasing irradiation time. On the other hand, the interference-free limit of detection decreases with increasing neutron flux and irradiation time.

Because of the strong dependence of the effect of these two irradiation parameters on the Pt/Au ratio in the sample, in each instance an optimum

TABLE 2

Activities (A) of ^{199}Au produced from 1 ng of Pt and 1 ng of Au at two different neutron fluxes and different irradiation times at the end of irradiation

Irradiation time (s)	$\Phi_{\text{th}} = 10^{14}$; $\Phi_{\text{ep}} = 2 \times 10^{12} \text{ cm}^{-2} \text{ s}^{-1}$			$\Phi_{\text{th}} = 1.3 \times 10^{13}$; $\Phi_{\text{ep}} = 4 \times 10^{11} \text{ cm}^{-2} \text{ s}^{-1}$		
	A_{Pt} (Bq)	A_{Au} (Bq)	A_{Pt} as % of total	A_{Pt} (Bq)	A_{Au} (Bq)	A_{Pt} as % of total
10^2	4.80×10^{-4}	1.27×10^{-3}	27.37	6.98×10^{-5}	2.43×10^{-5}	74.18
10^3	4.33×10^{-2}	0.127	25.41	6.25×10^{-3}	2.43×10^{-3}	72.00
10^4	0.191	12.4	13.34	0.277	0.239	53.63
10^5	22.5	981	2.24	3.25	20.1	13.94
10^6	94.1	15 590	0.60	14.0	451	2.93
Saturation	102	18 164	0.56	14.8	575	2.50

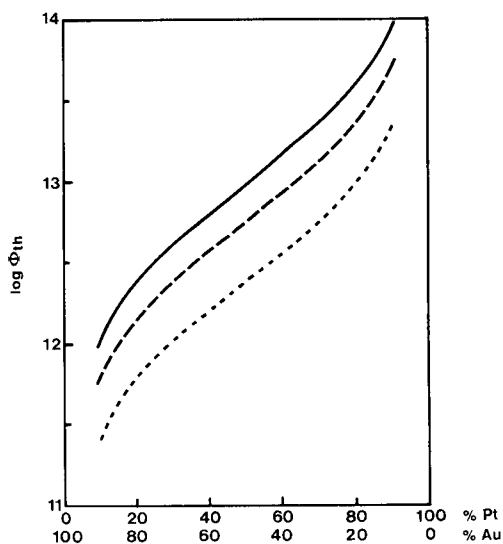


Fig. 1. Optimum thermal neutron flux versus percentage of Pt and Au relative to the total content of both in the sample for three different percentage activity contributions from Pt to the total activity of ^{199}Au : solid line, 20%; dashed line, 30%; dotted line, 50%.

compromise has to be found. A meaningful assumption could be based on the requirement that the contribution of ^{199}Au generated from platinum to the total ^{199}Au activity at the end of the irradiation should not be lower than 20%.

It is considered useful to give a general treatment of the rather complicated mutual coherence between limit of detection, Pt/Au ratio, thermal neutron flux and irradiation time in a more general manner. Using the activation equations for the analytical and the second-order interfering reaction, a computer program was developed by Kratz and Mayer [20]. Assuming a certain Pt/Au ratio and a certain percentage activity contribution from platinum to the total ^{199}Au activity, this program calculates the optimum thermal neutron flux and irradiation time leading to the maximum generable activity. The program (written in BASIC and running on an IBM-compatible PC) is available from the authors. It was used to obtain Figs. 1 and 2, which give the optimum thermal neutron flux (Fig. 1) and the corresponding irradiation time (Fig. 2) for each Pt/Au ratio and for percentage activity contributions of 20, 30 and 50% of platinum to the total ^{199}Au activity. In a

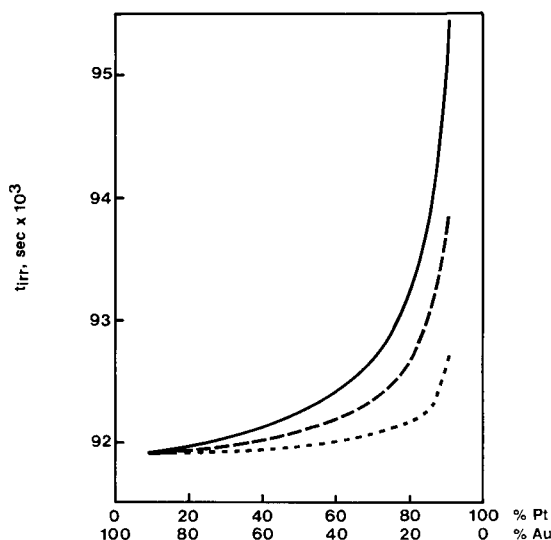


Fig. 2. Optimum irradiation time versus percentage of Pt and Au relative to the total content of both in the sample for three different percentage activity contributions from Pt to the total activity of ^{199}Au : solid line, 20%, dashed line, 30%; dotted line, 50%.

similar way, Fig. 3 was obtained, giving the dependence of the ^{199}Au activity on the Pt/Au ratio, generated at the optimum thermal neutron

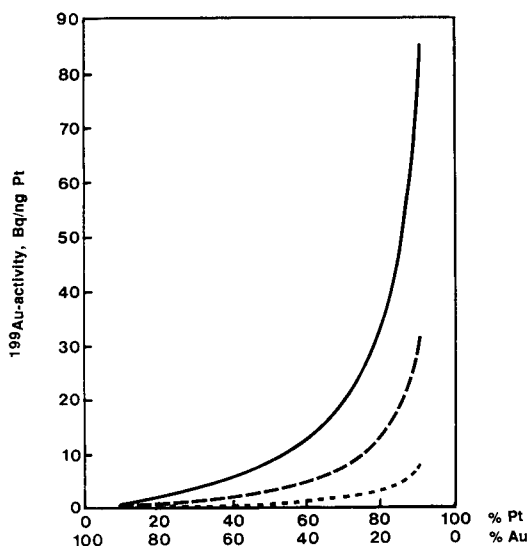


Fig. 3. Dependence of the maximum ^{199}Au activity on the Pt/Au ratio generated at optimum thermal neutron flux and irradiation time at the end of irradiation assuming 1 ng of Pt in the irradiated sample. Activity contribution from Pt: solid line, 20%; dashed line, 30%; dotted line, 50%.

flux and irradiation time and assuming 1 ng of Pt in the irradiated sample. For example, assuming a Pt/Au ratio of 1:1 (1 ng each of Pt and Au), at platinum contributions to the total ^{199}Au activity of 20, 30 and 50%, the total activity would be 7.95, 3.08 and 0.79 Bq, respectively.

Figure 4 shows the dependence of the limit of detection of platinum on the Pt/Au concentration ratio applying the optimum neutron flux and irradiation time obtained from Figs. 1 and 2 and assuming a percentage activity contribution of 20, 30 and 50% to the total ^{199}Au activity from platinum. The limits of detection were obtained by applying the 3σ criterion to the calculated net area of the 158.4-keV peak resulting from the second-order interfering reaction induced on gold, and considering the Compton background originating from the 411.8-keV γ -ray of ^{198}Au . From Fig. 4 it is evident that the interference from gold is the main limiting factor of this method, as with decreasing Pt/Au ratio the detection limit for platinum strongly increases.

For these experiments, two nuclear reactors were available, one providing a thermal neutron flux of $1.3 \times 10^{13} \text{ cm}^{-2} \text{ s}^{-1}$ and the other $10^{14} \text{ cm}^{-2} \text{ s}^{-1}$. With the requirement that at least 20% of the total ^{199}Au activity should be produced from Pt, the above-discussed treatment leads to the decision that at Pt/Au concentration ratios of more than 5:1 the higher thermal neutron flux is more suitable whereas at Pt/Au ra-

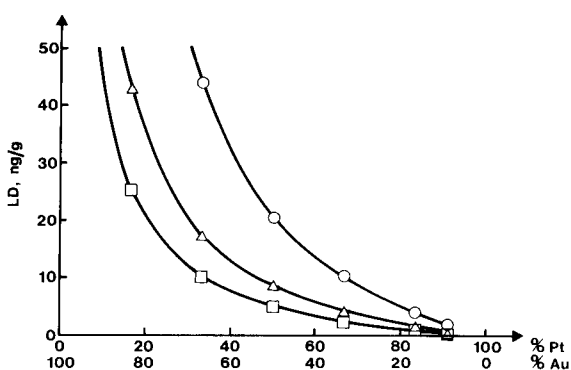


Fig. 4. Dependence of the limit of detection on the Pt/Au concentration ratio in the sample using optimum neutron flux and irradiation time (see Figs. 1 and 2) for percentage activity contributions from Pt to the total ^{199}Au activity of (\square) 20%, (Δ) 30% and (\circ) 50%.

TABLE 3

Possible γ -ray interferences in counting the 158.4- and 208.2-keV γ -rays of ^{199}Au

Interfering γ -ray (keV) [intensity (%)]	Nuclide	$t_{1/2}$ (days)	Mode of production
159.4 [68.0]	^{47}Sc	3.41	$^{46}\text{Ca}(n,\gamma)^{47}\text{Ca}(\beta^-)$, $t_{1/2} = 4.54 \text{ days}$ ^{47}Sc
158.6 [86.3]	$^{117\text{m}}\text{Sn}$	14.0	$^{116}\text{Sn}(n,\gamma)^{117\text{m}}\text{Sn}$
208.3 [11.0]	^{177}Lu	6.71	$^{176}\text{Lu}(n,\gamma)^{177}\text{Lu}$

tios of less than 5:1 the lower neutron flux is more favourable, if an appropriate irradiation time is applied (obtainable from the same kind of plots as shown in Fig. 2).

Instrumental interferences

Possible instrumental interferences due to overlapping of the γ -rays emitted by the indicator radionuclide and by other radionuclides are listed in Table 3. In the analysis of environmental, biological and geological samples, the most serious γ -ray interference originates from ^{47}Sc generated from ^{46}Ca . Therefore, the quantitative removal of calcium and scandium from the final fraction to be counted for ^{199}Au is an important criterion to be considered in the development of a separation procedure for this purpose.

Radiochemical separation

From the above discussion, it is evident that an improvement of the neutron activation analysis of environmental and geological samples can be achieved only by an effective separation of the matrix activity and of the radionuclides ^{47}Ca , ^{47}Sc and $^{117\text{m}}\text{Sn}$ causing instrumental interferences in counting the indicator radionuclide ^{199}Au . The experience gained with the retention behaviour of PUF from different acids under static and dynamic conditions [21–26] suggested that this separation system could be a suitable approach also for the solution of the present task, where the use of HCl medium seemed to be the most advantageous [26]. Therefore, the separation behaviour of Au, Sc and Sn in HCl media was investigated in more detail by using the radio-tracer technique under batch and dynamic condi-

tions. Figure 5 shows the dependence of the distribution coefficients on the concentration of hydrochloric acid in the range 0.1–6 M. Calcium was not included in this investigation series as its retention on PUF from HCl cannot be expected; only anionic complexes are able to undergo retention, depending on the hydrophobic character of the complex [27].

On the basis of the above batch studies and using distribution coefficients for the PUF–HCl system reported previously [26,28] and some preliminary studies under dynamic conditions, a separation procedure based on the use of 1 M HCl as the liquid-phase medium was developed. The flow chart is shown in Fig. 6. By means of the radiotracer technique it was determined that, using this procedure, $99.9 \pm 0.05\%$ of Au(III) is retained on the PUF column whereas Sc(III) and Sn(IV) are eluted with yields of $> 99.995\%$ and 99.6% , respectively.

Taskaev et al. [14] investigated the separation of ^{199}Au on PUF for the determination of platinum in biological samples and reported the problem of not being able to achieve a satisfactory removal of ^{82}Br . In the present procedure, bromine is eliminated by volatilization in the digestion and evaporation step so that only an extremely low ^{82}Br activity is counted.

During the development of the separation procedure, a particular behaviour of antimony was observed. Therefore, this element was investi-

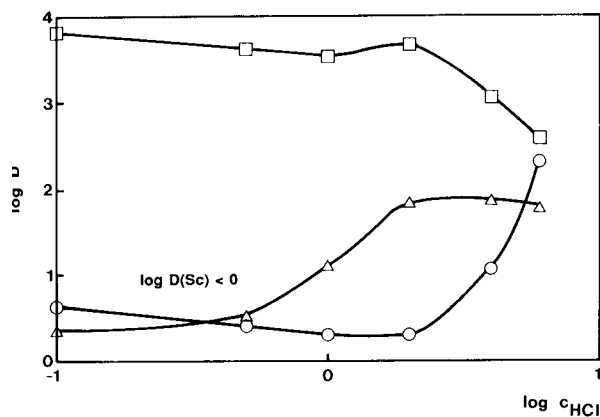


Fig. 5. Distribution of (□) Au, (○) Sb, Sc [$\log D(\text{Sc}) < 0$] and (△) Sn between PUF and HCl.

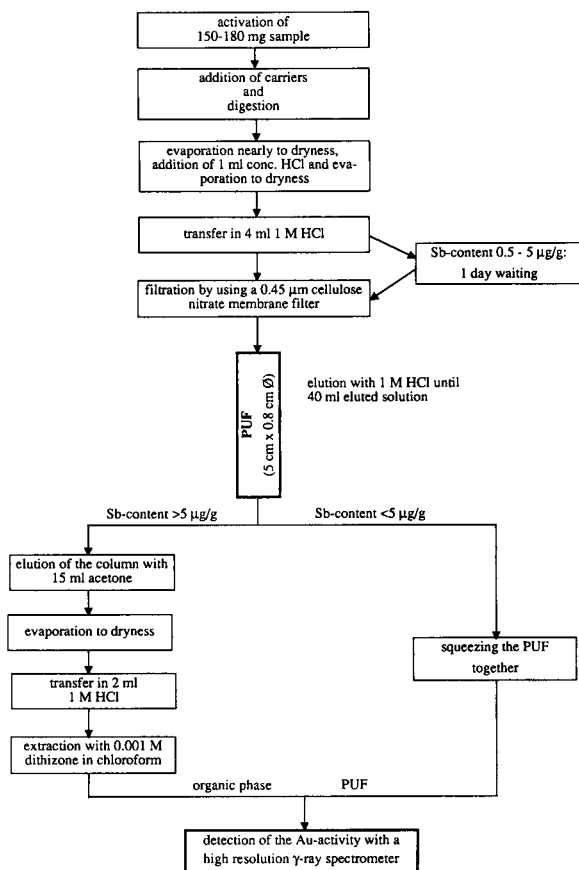


Fig. 6. Flow chart of the radiochemical separation procedure.

gated in more detail. It was found that the percentage of antimony retained on the PUF column depends strongly on the age of the sample solution, i.e., on the time elapsed between the preparation of the 1 M HCl solution and carrying out the separation. If the separation is carried out after 1–2 h, about 10% of the antimony is retained on the column, and with increasing time elapsed the percentage of antimony adsorbed decreases. After keeping the solution for 1 day an adsorption of about 1% and after 2 days about 0.1% were estimated. The decrease in the adsorption of antimony with increasing time can be explained by hydrolysis of the species SbCl_6^- to SbOCl_4^- and $\text{SbO}_2\text{Cl}_2^-$ [29] by which the adsorption process is realized.

Owing to the generation of ^{122}Sb , higher antimony concentrations in the sample ($> 5 \mu\text{g g}^{-1}$)

give rise to a considerable Compton background in the γ -spectrum and, consequently, an increase in the limit of detection of platinum even when the separation is performed after a waiting time of 1 day. A waiting time of 2 days would lower the Compton background sufficiently, but as a result of the decay of ^{199}Au the limit of detection of Pt increases. Therefore, the possibility of a more effective decontamination of ^{199}Au with respect to ^{122}Sb was sought.

Quantitative specific elution of antimony from the column was tried using different approaches including elution with KI-containing 1 M HCl [reduction of Sb(V) to Sb(III), which is not adsorbed on PUF from this medium], elution with H_2SO_4 via complex formation of Sb(V) [30], elution with 1 M NH_4F (the SbF_6^- species are expected to be adsorbed more weakly than SbCl_6^- on PUF) and elution with 20% $(\text{NH}_4)_2\text{S}_x$ solution via the formation of soluble thioantimonate. All these efforts were unsuccessful. A reduction of Sb(V) to Sb(III) prior to the separation is not possible because of reduction of Au(III).

Another possibility for reducing the background contribution from ^{122}Sb could be based on the different distributions of ^{199}Au and ^{122}Sb within the column. For instance, it could be possible that ^{199}Au is retained on the top of the column and the rest of the ^{122}Sb mainly in another zone or uniformly distributed in the col-

umn. In such a case, further miniaturization of the column or counting only the top section of it would essentially reduce the background contribution from ^{122}Sb . However, a detailed investigation of the distribution by means of the radio-tracer technique showed that the main fraction (> 95%) of residual antimony was retained, similarly to gold (> 97%), in the top section of the column. Therefore, for the separation of these two radionuclides, both elements were first eluted from the column with 15 ml of acetone (with a yield of $99.8 \pm 0.1\%$ for Au and $99.0 \pm 0.1\%$ for Sb), and after transfer into 1 M HCl they were separated by extraction with dithizone in chloroform (extraction yield $99.0 \pm 0.1\%$ for Au and $4.3 \pm 1.4\%$ for Sb in the organic phase).

Analysis of environmental and geological samples

The method was applied to the analysis of two environmental samples and one geological sample. The street dust sample was taken from an electrofilter of a tunnel and homogenized. The corn plant sample consisted of freeze-dried corn leaves from a plant grown on platinum-loaded soil. The geological sample was the standard reference material Nickel–Copper–Cobalt Ore SU-1a of the Canada Centre for Mineral and Energy Technology with a certified platinum content of $410 \pm 60 \text{ ng g}^{-1}$.

TABLE 4

Platinum contents in street dust, corn plant and Nickel–Copper–Cobalt Ore SU-1a determined by the proposed method and comparison with the results obtained by independent techniques in other laboratories [31]

Sample	This method (ng g^{-1})			Other methods (ng g^{-1})			
	Pt content	Limit of detection	Au content	AdsVol	ICP-MS	ID-ICP-MS	GFAAS
Street dust ^k	14.5 ± 1.3	3.6	5.6 ± 0.7	11.2 ± 1.1 ^a	12.1 ± 1.1 ^b 8.4 ± 1.2 ^j	13.7 ± 0.9 ^c	9.3 ± 3.2 ^d 670 ± 81 ^e
Corn plant ^l	642 ± 38	13	10.9 ± 2.4	534 ± 28 ^a	427 ± 18 ^b 999 ± 624 ^e 403 ± 22 ^j	703 ± 20 ^c 502 ± 47 ^f	523 ± 21 ^g 630 ± 97 ^h
SU-1a ^m	169 ± 72	20	124 ± 68	228 ± 46 ^a 315 ± 139 ⁱ	421 ± 187 ^b 103 ± 8 ^e 190 ± 41 ^f		

^{a–j} Laboratories participating in the round-robin study. ^j [32]. ^k RNAA: $t_{\text{irr}} = 16 \text{ h}$, $t_{\text{d}} = 3 \text{ days}$. ^l RNAA: $t_{\text{irr}} = 24 \text{ h}$, $t_{\text{d}} = 1 \text{ day}$. ^m RNAA: $t_{\text{irr}} = 24 \text{ h}$, $t_{\text{d}} = 3 \text{ days}$; $\Theta_{\text{th}} = 1.3 \times 10^{13} \text{ cm}^{-2} \text{ s}^{-1}$.

For the determination of platinum in these samples, it was necessary to make corrections for the contribution of gold to the total ^{199}Au activity. The correction was done by comparison of the net areas of the peaks at 411.8 keV of ^{198}Au (generated only from Au) and at 158.4 keV of ^{199}Au (generated from Au and Pt) of irradiated samples and simultaneously irradiated gold standards. The platinum content was obtained by comparison of the corrected peak area at 158.4 keV for the sample and the peak area of a simultaneously irradiated platinum standard.

As discussed before, the limit of detection of platinum achievable depends on the Pt/Au ratio in the sample, which determines the optimum irradiation conditions and, consequently, the minimum detectable ^{199}Au activity from Pt. In addition, the Compton background in counting the 158.4-keV γ -ray of ^{199}Au originating from the 411.8-keV γ -ray of ^{198}Au increases with increasing gold content in the sample. For example, the real, i.e., by the gold content affected limit of detection for the determination of platinum in the street dust sample is 3.6 ng g^{-1} , but assuming a negligible gold content, it would be 0.9 ng g^{-1} .

The determined platinum contents and the respective limits of detection are given in Table 4. The results represent averages of four separate determinations for which the standard deviations are also given. For the determination of platinum in the corn plant and the geological sample, it was sufficient to perform only the first stage of the separation procedure and to count the gold radionuclides adsorbed on the PUF column (see Fig. 6). However, in the analysis of the street dust, owing to the higher antimony content, it was necessary to perform the whole separation procedure including the extraction.

For comparison, the results obtained by several independent analytical methods are also given in Table 4. These methods include GFAAS, inductively coupled plasma mass spectrometry (ICP-MS) without and with isotope dilution (ID-ICP-MS) and adsorptive voltammetry (AdsVol).

The results obtained by the other methods for the street dust sample, taking into account the low platinum content and the relatively difficult matrix, are in good agreement with the results of

this method except that of 670 ng g^{-1} obtained by GFAAS (laboratory e). Excluding this outlying result, the average value of all results of the participating laboratories was $12.01 \pm 2.06 \text{ ng g}^{-1}$.

Considering the relatively high platinum content in the corn plant sample, the range of deviation of the results obtained by the different methods and laboratories ($400\text{--}1000 \text{ ng g}^{-1}$) is unsatisfactory. This is true even if the value of 999 ng g^{-1} is excluded as an outlier.

The agreement of the results is most unsatisfactory for the geological standard reference material SU-1a. Only one result of $421 \pm 187 \text{ ng g}^{-1}$ was near to the certified value of $410 \pm 60 \text{ ng g}^{-1}$. The results of the participating laboratories are in the range of $103\text{--}421 \text{ ng g}^{-1}$ and the present RNAA method gave $169 \pm 72 \text{ ng g}^{-1}$. In addition, the standard deviations of the individual laboratories are, excluding laboratory e, too high (up to 44.4%). This could be an indication of insufficient homogeneity of this geological standard reference material.

The results of this interlaboratory study show that, considering the high requirements dictated by the demand to be able to determine with good accuracy low concentrations of platinum in various environmental and biological samples, there is still a need to improve the analytical methodology for this purpose. In the present state of development of the methodology, RNAA, in spite of its not being well suited for routine analysis, plays an important role. The developed radiochemical procedure proved to be applicable to the analysis of materials of various nature containing platinum at different concentration levels.

We thank W. Kratz and S.R. Mayer (Department of Mathematics V, University of Ulm) for developing and making available the computer programme mentioned above, and Dr. W. Wegscheider for making available the samples and the results of the round robin study. We also thank the GKSS Forschungszentrum (Geesthacht, Germany), and the FRM Reaktorstation Garching, TU München (Garching, Germany), for making available free of charge the irradiation facilities.

REFERENCES

- 1 F. Alt, U. Jerono, J. Messerschmidt and G. Tölg, *Mikrochim. Acta*, III (1988) 299.
- 2 G.E.M. Hall, K.N. de Silva, J.C. Pelchat and J.E. Vaiva, *Geol. Surv. Can. Pap.*, 87-1A (1987) 477.
- 3 C.E. Dunn, *J. Geochem. Explor.*, 25 (1986) 21.
- 4 R. Eller, F. Alt, G. Tölg and H.J. Tobschall, *Fresenius' Z. Anal. Chem.*, 334 (1989) 723.
- 5 V.F. Hodge and M.O. Stallard, *Environ. Sci. Technol.*, 20 (1986) 1058.
- 6 F. Alt, in P. Braetter and P. Schramel (Eds.), *Trace Element Analytical Chemistry in Medicine and Biology*, Vol. 5, de Gruyter, Berlin, New York, 1988, p. 279.
- 7 K. Hoppstock, F. Alt, K. Cammann and G. Weber, *Fresenius' Z. Anal. Chem.*, 335 (1989) 813.
- 8 J.C. Rucklidge, M.P. Gorton, G.C. Wilson, L.R. Kilius, A.E. Litherland, D. Elmore and H.E. Gore, *Can. Mineral.*, 20 (1982) 11.
- 9 E.F. Stumpf and J.C. Rucklidge, *Econ. Geol.*, 77 (1982) 1419.
- 10 R. Zeisler and R.R. Greenberg, *J. Radioanal. Chem.*, 75 (1982) 27.
- 11 R.R. Greenberg, R.F. Fleming, and R. Zeisler, *Environ. Int.*, 10 (1984) 129.
- 12 R. Zeisler and R.R. Greenberg, in P. Braetter and P. Schramel (Eds.), *Trace Element Analytical Chemistry in Medicine and Biology*, de Gruyter, Berlin, New York, 1988, p. 297.
- 13 P.S. Tjioe, K.J. Volkers, J.J. Kroon, J.J.M. deGoeij and S.K. The, *Int. J. Environ. Anal. Chem.*, 17 (1984) 13.
- 14 E. Taskaev, M. Karaivanova and T. Grigorov, *J. Radioanal. Nucl. Chem.*, 120 (1988) 75.
- 15 I.M. Valente, M.J. Minski and P.J. Peterson, *J. Radioanal. Chem.*, 71 (1982) 115.
- 16 J. Kucera and J. Drobnik, *J. Radioanal. Chem.*, 75 (1982) 71.
- 17 G. Erdtmann, *Neutron Activation Tables*, Verlag Chemie, Weinheim, 1976.
- 18 D. DeSoete, R. Gijbels and J. Hoste, *Neutron Activation Analysis*, Wiley, New York, 1972.
- 19 W. Gebauhr, *Fresenius' Z. Anal. Chem.*, 185 (1962) 339.
- 20 W. Kratz and S.R. Mayer, personal communication.
- 21 R. Caletka and V. Krivan, *Fresenius' Z. Anal. Chem.*, 321 (1985) 61.
- 22 R. Caletka, R. Hausbeck and V. Krivan, *Fresenius' Z. Anal. Chem.*, 320 (1985) 665.
- 23 R. Caletka, R. Hausbeck and V. Krivan, *Talanta*, 33 (1986) 219.
- 24 R. Caletka, R. Hausbeck and V. Krivan, *Talanta*, 33 (1986) 315.
- 25 R. Caletka, R. Hausbeck and V. Krivan, *J. Radioanal. Nucl. Chem.*, 131 (1989) 343.
- 26 R. Caletka, R. Hausbeck and V. Krivan, *Anal. Chim. Acta*, 229 (1990) 127.
- 27 R.F. Hamon, A.S. Khan and A. Chow, *Talanta*, 29 (1982) 313.
- 28 H.J.M. Bowen, *J. Chem. Soc. A*, (1970) 1082.
- 29 R.J. Meyer and E.H.E. Pietsch (Eds.), *Gmelin, Handbuch der Anorganischen Chemie, Antimon, Teil B*, Gmelin-Verlag, Clauthal-Zellerfeld, 1949, p. 448.
- 30 S. Bajo and U. Suter, *Anal. Chem.*, 54 (1982) 49.
- 31 W. Wegscheider and M. Zischka, *Fresenius' Z. Anal. Chem.*, (1993) submitted for publication.
- 32 H. Baumann, Central Analytical Department Ciba-Geigy, Basel, personal communication.

Direct determination of benzene in gasoline by flow-injection Fourier transform infrared spectrometry

Máximo Galignani, Salvador Garrigues and Miguel de la Guardia

Departamento de Química Analítica, Universidad de Valencia, C/ Dr. Moliner 50, 46100 Burjassot, Valencia (Spain)

(Received 20th July 1992; revised manuscript received 17th August 1992)

Abstract

A Fourier transform infrared spectrometric procedure for the automated determination of benzene in gasoline was developed, based on the use of flow-injection analysis. The method permits the direct determination of benzene without any pretreatment of samples, with a limit of detection of 0.02% (v/v) and a relative standard deviation of ca. 1% [for five independent analyses of a diluted sample containing a 0.4% (v/v) of benzene]. Results found by direct analysis agreed with those obtained by off-line and on-line standard addition methods. A rapid quality control procedure was developed, based on the on-line injection of gasoline samples (diluted 1 + 9 in hexane) into a carrier stream of a 0.5% (v/v) solution of benzene in hexane; in this instance, the baseline corresponds to the upper limit tolerated by the European Economic Community's law for gasolines. Thus, the injection of diluted samples with an appropriate level of benzene must provide no peaks or negative peaks, whereas those with a benzene concentration higher than that tolerated provide positive peaks. A series of real samples were analysed by the proposed procedure and the results obtained were comparable to those given by gas chromatography.

Keywords: Flow injection; Infrared spectrometry; Benzene; Gasoline

The determination of aromatic hydrocarbons in naphthas and motor gasolines is necessary in several areas of the petroleum, petrochemical and related industries [1]. Detailed information on the aromatic composition of fuel materials, intermediates and commercial products is required for process development and quality control programmes. For this purpose, gas chromatography and other chromatographic techniques have been extensively used [2–10]. In addition, legislation in several countries limits the upper concentration of some hydrocarbons in commercial gasolines. For example, the upper

limit tolerated by the European Economic Community's laws for benzene is 5% (v/v), the normal content of benzene in gasolines being 2.5% (v/v). Thus, in some instances the determination of a compound is required in order to check the quality of the final product.

The fact that infrared (IR) spectrometric techniques provide a rapid means for the direct determination of aromatic compounds [11,12] encouraged the development of an inexpensive, rapid and simple method for the direct determination of benzene in gasolines, based on the use of flow-injection Fourier transform IR (FI-FT-IR) spectrometry. The only precedent found in the literature was a standard method of the American Society for Testing and Materials (ASTM) for the IR batch determination of benzene in motor and aviation gasolines [13].

Correspondence to: M. de la Guardia, Departamento de Química Analítica, Universidad de Valencia, C/ Dr. Moliner 50, 46100 Burjassot, Valencia (Spain).

There are few precedents on the use of flow injection in IR analysis [14–18]. However, a method has recently been developed, based on the use of inexpensive flow cells and appropriate software [19–22], which permits the automated analysis of samples by FT-IR spectrometry using simple FI manifolds.

The advantages of FI–FT-IR can be summarized as follows: simple and rapid sampling and cleaning of the flow cells; low consumption of reagents; continuous monitoring of the spectral baseline; and accurate determination of the location of absorption band maxima.

In this work, different FI strategies such as direct analysis, off-line standard addition and on-line standard addition were compared in order to provide an accurate determination of benzene in gasolines. The applicability of the proposed method was evaluated by comparison of the analysis of real samples by the direct FI–FT-IR procedure and by gas chromatography, and interferences in the determination of benzene by the FT-IR method were studied.

EXPERIMENTAL

Apparatus and reagents

A Perkin-Elmer (Model 1750) Fourier transform infrared spectrometer with a temperature-stabilized DTGS detector and equipped with a Series 7700 data station was employed for the spectral measurements at a nominal resolution of 4 cm^{-1} . In all instances, a Specac (Orpington, UK) micro-flow cell with KBr windows and with a spacer of 0.12 mm was used. With this instrument, the full spectra between 4000 and 400 cm^{-1} of samples and standards can be collected in the time domain with a scanning frequency higher than 1 s^{-1} . However, to carry out complete spectral handling as a function of time, a time measurement of 19 s is required to obtain each FIA peak from ten consecutive spectra of each injection.

The manifold employed was a single-channel assembly (see Fig. 1). A Gilson P-2 Minipuls peristaltic pump and Viton® (Iso-Versinic) 0.15 cm i.d. pump tubing were employed to transport

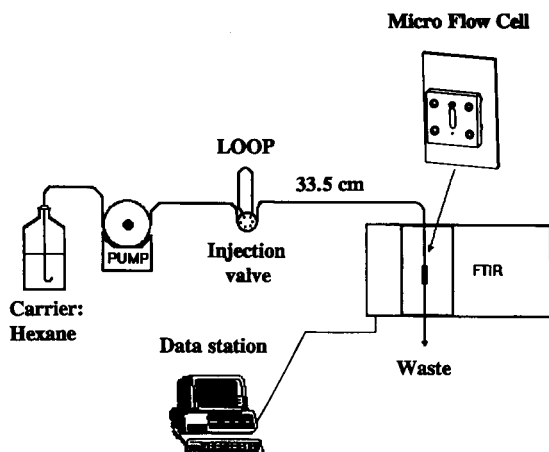


Fig. 1. Manifold employed for the determination of benzene by FI–FT-IR spectrometry.

the carrier and samples. A Rheodyne Type 50 injection valve, with various fixed-volume loops was used for sample introduction. All the connecting tubes (0.8 mm i.d.) were made of PTFE.

The above-mentioned manifold was employed in both the direct and reverse modes. In the former instance, samples were injected into the hexane carrier flow. The reverse mode was performed by an on-line standard addition procedure, in which the sample was continuously fed and the standards were injected into this carrier flow.

Analytical-reagent grade benzene and toluene (Panreac, Barcelona) and hexane (Probus, Barcelona) were used as received.

A series of computer programs were developed in order to carry out continuous absorbance measurements.

Software program

A program was written in OBEY (a Perkin-Elmer computer language) to obtain and store the FT-IR spectra as a function of time. Another program (also written in OBEY) was developed to obtain the corrected peak-height absorbance values, taking into account the selected baseline and the exact position of the absorbance maximum. A third program, written in BASIC, permitted these absorbance values to be recorded as a function of time. All the software employed can be supplied on request at low cost.

Direct analysis

For the direct determination of benzene in gasolines, both samples and standards were injected into the above-indicated manifold. Samples and standards were diluted in hexane. A 1 + 9 dilution was used for samples. Peak-height absorbance measurements were made at 675 cm^{-1} and the baseline established between 712 and 650 cm^{-1} .

Off-line standard addition

Known volumes of a stock solution of benzene in hexane (1%, v/v) were added to the gasoline samples (diluted 1 + 9 in hexane) in order to obtain an added benzene concentration from 0.1 to 0.6% (v/v). These samples were then injected into the manifold and the analysis was carried out under the same conditions as employed for the direct analysis.

On-line standard addition

Gasoline samples, diluted 1 + 9 in hexane, were fed continuously by the carrier stream and the absorbance was adjusted to zero for this baseline value. Subsequently, $100\text{-}\mu\text{l}$ volumes of different standard solutions of benzene in hexane were injected into the system. If the injected concentration of benzene was lower than that of the sample it provided a decrease in the absorbance

value at 675 cm^{-1} but, having previously adjusted the zero value with the carrier stream, it yielded negative peaks; otherwise, positive peaks were obtained. Thus, the interpolation of the experimental data for zero absorbance permits the concentration of benzene in the sample to be obtained.

Reference method

To determine the accuracy of this procedure, a series of five real samples were analysed independently in this laboratory using the FI-FT-IR procedure, and by the laboratory of Petromed (Castellón) using a standard gas chromatographic procedure [23].

RESULTS AND DISCUSSION

FT-IR spectra of benzene in gasoline

Figure 2A shows the transmittance spectra obtained for a capillary film of hexane, a gasoline sample and benzene. As can be seen from the wavenumber range between 850 and 500 cm^{-1} , the hexane spectrum provides a low background for the determination of benzene.

On the other hand, benzene has a well defined band at 675 cm^{-1} that is well resolved in real gasoline samples. This can be seen in Fig. 2B,

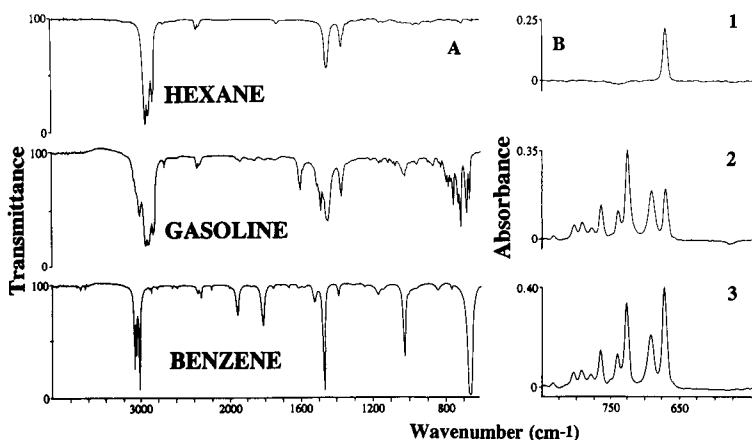


Fig. 2. FT-IR spectra of standards, solvents and samples. (A) Transmittance spectra of hexane (employed as carrier and solvent), an actual gasoline sample and pure benzene standard, all obtained with film. (B) Absorbance spectra of (1) a 0.3% (v/v) solution of benzene in hexane, (2) a 10% (v/v) solution of gasoline in hexane and (3) a 10% (v/v) solution of gasoline plus 0.3% of benzene in hexane.

where the absorbance spectra of benzene, gasoline and benzene plus gasoline are shown. This band was therefore employed in subsequent work for the determination of benzene in gasolines.

Interference of toluene

In the ASTM procedure for the IR spectrometric determination of benzene in gasolines [13] it is indicated that toluene and heavier aromatic compounds interfere in the determination of benzene at 673 cm^{-1} , so it is proposed to calibrate with gasoline stocks containing little or no benzene and to correct the experimental results for the concentration of toluene, established from the IR measurements at 460 cm^{-1} .

It was confirmed experimentally that toluene does not interfere with the benzene band at 675 cm^{-1} , as can be seen by comparing the first-derivative spectra of pure benzene and benzene plus toluene solutions (Fig. 3A). However, an increase in the concentration of toluene causes an increase in the absorbance band at 695 cm^{-1} , which affects the peak-height values at 675 cm^{-1} from 4% (for a toluene:benzene ratio of 5) to 15% (for a toluene:benzene ratio of 15), as can be seen in Fig. 3B. This occurs when the baseline is set at 500 cm^{-1} or between 828 and 575 cm^{-1} .

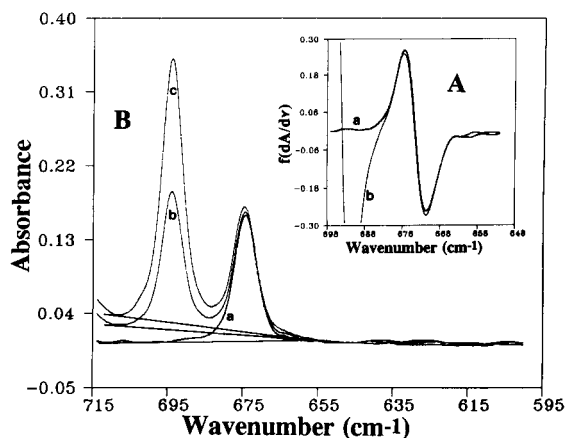


Fig. 3. Effect of toluene on the determination of benzene. (A) First-derivative spectra of (a) 0.2% (v/v) solution of benzene in hexane and (b) a mixture of 0.2% (v/v) benzene plus 3% (v/v) toluene in hexane. (B) Effect of toluene concentration on the absorbance of benzene at 675 cm^{-1} : 0.2% (v/v) solution of benzene in hexane with (a) 0, (b) 1.5 and (c) 3% (v/v) of toluene.

TABLE 1

Study of the interference of toluene on the FT-IR determination of benzene

Toluene concentration (% v/v)	Benzene concentration found (% v/v) ^a		
	A	B	C
0	0.201	0.200	0.200
0.5	0.204	0.203	0.198
1.0	0.207	0.208	0.201
1.5	0.218	0.212	0.199
2.0	0.222	0.218	0.202
3.0	0.229	0.224	0.199

^a (A) For a baseline set at 500 cm^{-1} ; (B) for a baseline established from 828 to 575 cm^{-1} ; (C) for a baseline established from 712 to 650 cm^{-1} .

However, when the baseline is established between 712 and 650 cm^{-1} , the concentration found for a benzene solution in the presence of increasing amounts of toluene remains constant (see Table 1).

Hence it can be concluded that for the analysis of real gasoline samples in which benzene is present at a concentration level between 2 and 5% and toluene at ca. 10% (v/v), benzene can be directly determined by FT-IR spectrometry at 675 cm^{-1} using a baseline defined between 712 and 650 cm^{-1} .

Effect of FIA parameters

The effects of the injected sample volume and carrier flow-rate on the sensitivity and reproducibility of the flow-injection peaks were studied.

For a fixed hexane carrier flow of 0.28 ml min^{-1} , it was found that the sensitivity increases when the sample volume increases; absorbance values similar to those found for the continuous passage of a solution of benzene in hexane were obtained when volumes $\geq 300\text{ }\mu\text{l}$ were injected (see Fig. 4). The peak height decreases as the flow-rate increases, as shown in Fig. 5. This effect was more evident when a small sample volume was employed.

In subsequent studies a carrier flow of 0.28 ml min^{-1} and an injection volume of $300\text{ }\mu\text{l}$ were selected for the direct determination of benzene in gasolines.

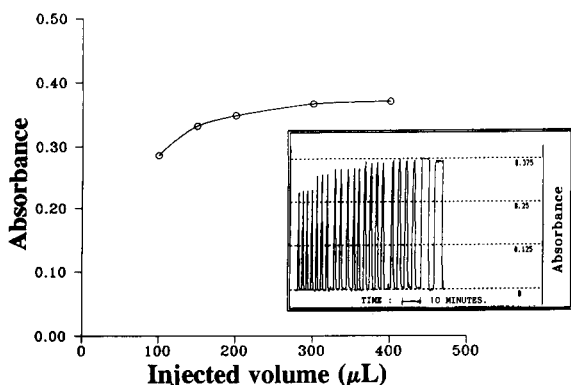


Fig. 4. Effect of the injected sample volume on the absorbance of benzene solutions. Inset: FIA recording obtained for different volumes injected and also for the continuous passage of 0.5% (v/v) benzene solution. Carrier flow-rate, 0.28 ml min⁻¹.

Analytical parameters for the direct determination of benzene

Analytical parameters such as the dynamic range, sensitivity, limit of detection and relative standard deviation (R.S.D.) for five independent measurements of a sample solution containing 0.4% (v/v) of benzene are given in Table 2. From these data, it can be concluded that the procedure is sensitive and reproducible.

Taking into account the dynamic range of the FI-FT-IR measurements and the normal benzene content of gasoline samples, however, it is

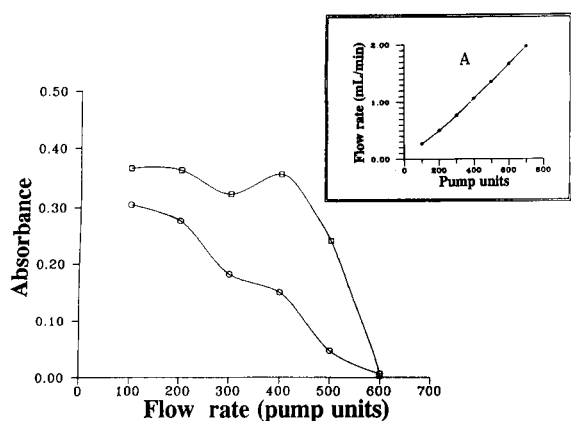


Fig. 5. Effect of the carrier flow-rate on the height of the FIA recording for injection volumes of (○) 100 and (□) 300 μL. (A) Relationship between the potentiometric pump units and the actual carrier flow-rate values.

TABLE 2

Analytical parameters for the direct determination of benzene in gasolines

Parameter	Valve ^a
Dynamic range	0.02–0.80% (v/v)
Calibration equation	$A = 0.001 + 0.769C$ (C in %, v/v); $R^2 = 0.9998$
Sensitivity	$0.769 A C^{-1}$ (C in %, v/v)
Limit of detection for $K = 3$ ^b	0.02% (v/v)
Precision (R.S.D.)	1.0% ($n = 5$) (for a sample containing 0.4%, v/v)

^a A = absorbance; C = concentration; R^2 = regression coefficient. ^b Probability level of 95%.

recommended that gasoline samples are diluted 1 + 9 by volume in hexane.

Analysis using the standard addition method

Results obtained by direct analysis were compared with those given by the standard addition method, in order to establish the effect of the matrix on the determination of benzene by FI-FT-IR spectrometry. Standard additions were made both off- and on-line.

Figure 6 shows that similar calibration lines were obtained by injection of both 300 μl of benzene standards and 300 μl of diluted gasoline samples with added benzene standard, respectively. Typical regression lines obtained in the

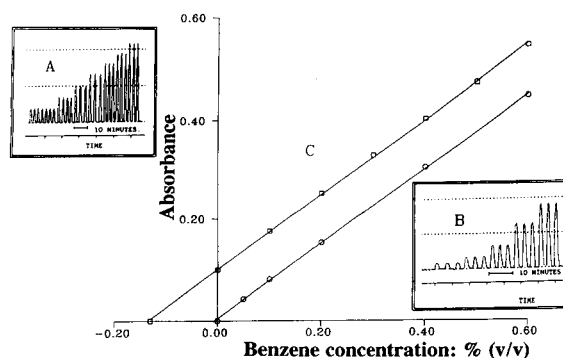


Fig. 6. FI-FT-IR off-line standard addition for the determination of benzene in gasolines. (A) Original FIA recording obtained for the injection of standards in the addition method; (B) original FIA recording obtained for the direct determination; (C) Comparison between the calibration graphs obtained by the two procedures in the same session.

same session were absorbance $A = 0.001 + 0.759C$ and $A = 0.099 + 0.757C$, where C is the benzene concentration (%), respectively. The similarity of the slopes of these two equations indicates the absence of matrix effects in the FT-IR determination of benzene in gasolines.

In order to confirm the absence of interference from toluene and also from other aromatic compounds present in the gasolines, a gasoline was analysed by adding different amounts of sample to a standard benzene solution. In this instance, the regression line $A = 0.153 + 0.761C$ was found for the addition experiment, the slope of which was comparable to that obtained in the same session for a normal calibration of $A = 0.001 + 0.756C$, again indicating the absence of interferences in the determination of benzene at 675 cm^{-1} using the selected baseline.

The injection of standards into the carrier stream of a sample provides an on-line standard addition [24,25]. Therefore, experiments were carried out by injecting $100\text{-}\mu\text{l}$ volumes of benzene standard solutions into a carrier stream of a diluted gasoline sample. The use of an injection volume lower than $300\text{ }\mu\text{l}$ was justified in this instance in order to obtain a homogeneous mixture of the sample and the added standard.

Figure 7 shows, as an example, the original FIA recording corresponding to the on-line standard addition. It can be seen that after adjusting to zero the baseline values obtained for the carrier stream of diluted samples, negative peaks

were found when the concentration of the injected standard was lower than that of the diluted sample, whereas positive peaks were found when the standard concentration was higher than that of the diluted sample. From the experimental values, a regression line between the corrected absorbance values and the concentration of the injected benzene solutions can be found. The actual concentration of the sample can be determined by interpolation in the regression line for an absorbance value of zero.

A typical regression line for the on-line standard addition has the equation $A = -0.173 + 0.543C$, which has a slope of the same order as that obtained by the direct analysis using injection volumes of $100\text{ }\mu\text{l}$. In this instance the sensitivity is 26.5% lower than that found for injection volumes of $300\text{ }\mu\text{l}$.

Determination of benzene in real gasoline samples

Four commercial gasoline samples, two containing lead additives (one regular and another of the premium type) and two unleaded samples, were analysed using the direct, off- and on-line standard addition procedures. The results found in all instances (see Table 3) are comparable, so it can be concluded that the proposed procedures could be applied to the rapid determination of benzene in real samples without any pretreatment.

In order to evaluate the accuracy of the devel-

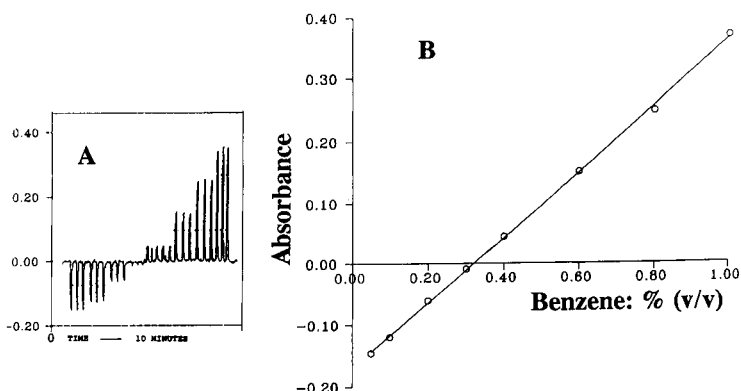


Fig. 7. FI-FT-IR on-line standard addition for the determination of benzene in gasolines. (A) Original FIA recording; (B) standard addition calibration graph obtained for a carrier flow of 0.28 ml min^{-1} of a 10% (v/v) solution of gasoline in hexane, using injection volumes of $100\text{ }\mu\text{l}$.

TABLE 3

Results of determination of benzene in real gasoline samples

Sample	Benzene concentration (% v/v) ^a		
	Direct method	Off-line standard addition	On-line standard addition
Unleaded 1	3.20 ± 0.06	3.05 ± 0.06	3.20 ± 0.10
Unleaded 2	5.05 ± 0.09	5.10 ± 0.10	5.20 ± 0.15
Regular	3.10 ± 0.09	3.00 ± 0.06	3.00 ± 0.08
Premium	3.56 ± 0.08	3.50 ± 0.07	3.46 ± 0.07

^a Mean values ± standard deviation (n = 5).

oped FI-FT-IR method, five commercial gasolines were analysed in this laboratory using the direct procedure and also by a laboratory for petrol analysis using the reference chromatographic procedure [23]. As Table 4 shows, the results obtained by both methods are comparable, so it can be concluded that the accuracy of the FI-FT-IR is comparable to that of the reference method.

Using the direct procedure, eighteen injections per hour could be made, which is a very high value compared with the sample frequency in the gas chromatographic analysis.

Rapid method for the quality control of benzene in gasolines

Gasolines are commercial products produced by well known methodology. Hence, in practical quality control of the finished products, the actual problem is to establish the compliance of the benzene content with the upper limit tolerated by legislation. In this regard, and based on the expe-

TABLE 4

Comparison of the determination of benzene in gasolines by FI-FT-IR spectrometry and gas chromatography (GC)

Sample	Benzene concentration (% v/v)	
	FI-FT-IR ^a	GC
Unleaded 1	3.06 ± 0.04	3.00
Unleaded 2	2.96 ± 0.06	2.86
Unleaded 3	2.82 ± 0.03	2.67
Regular	2.75 ± 0.03	2.79
Premium	3.26 ± 0.04	3.31

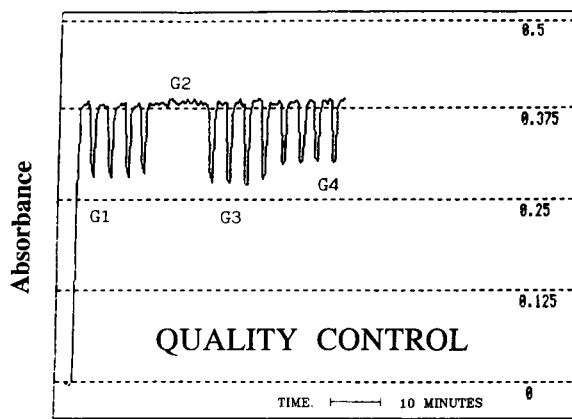
^a Mean values ± standard deviation (n = 5).

Fig. 8. Control chart for the rapid quality control of the benzene content in gasoline samples. The carrier is a 0.5% (v/v) solution of benzene in hexane, which was employed to establish the baseline. The FIA recording corresponds to an injection volume of 100 μ l of a 10% (v/v) solution of gasoline in hexane. Samples that give negative peaks have a benzene content lower than that allowed by law.

rience gained with the on-line standard addition method, a rapid procedure was developed to test the benzene content of gasolines.

A 0.5% (v/v) solution of benzene in hexane was continuously fed as carrier, and gasoline samples (diluted 1 + 9 in hexane) were injected into this carrier flow. In this system, samples with a benzene content higher than the upper limit provided positive peaks, and so the product could be easily rejected. Figure 8 shows the quality control chart for the four samples assayed, where it is evident that sample G2 is at the upper level of acceptability.

Conclusion

These experiments have shown that benzene can be determined accurately and simply in gasoline samples by FI-FT-IR spectrometry. The procedure is free from matrix interferences and only requires dilution of the samples with hexane. The use of the on-line standard addition procedure permits rapid quality control of the benzene content in real gasoline samples in order to verify their compliance with the maximum tolerated level established by legislation.

The method, based on the discrete injection of samples into a carrier flow, is rapid but it does not permit the accumulation of a series of spectra for each sample or standard solution. For the determination of trace compounds, new experiments in the stop-flow mode are in progress that permit spectral averaging and a substantial increase in sensitivity.

M. Galignani acknowledges a grant from the Agencia Española de Cooperación Internacional and S. Garrigues acknowledges a grant from the Conselleria de Cultura, Educació i Ciència de la Generalitat Valenciana, to carry out PhD studies.

REFERENCES

- 1 N. Kosal, A. Bhari and M.A. Ali, *Fuel*, 69 (1990) 1012.
- 2 W.N. Sanders and J.B. Maynard, *Anal. Chem.*, 40 (1968) 531.
- 3 M. Bronder and A. Forse, *Labor Praxis*, 13 (1989) 21.
- 4 Annual Book of ASTM Standards, American Society for Testing and Materials, Philadelphia, 1987, D-3606-87.
- 5 S.K. Poole, K.G. Furton and C.F. Poole, *J. Chromatogr. Sci.*, 26 (1988) 67.
- 6 F.P. Di Sanzo and W.J. Giarroco, *J. Chromatogr. Sci.*, 26 (1988) 258.
- 7 S.V. Egazar'yants, A.V. Kiselev, Yu.S. Nikitin and V.S. Fadeev, *Zh. Anal. Khim.*, 43 (1988) 695.
- 8 R.C. Ludwig and R. Eksteen, *LC·GC*, 6 (1988) 250.
- 9 J.M. Levy and J.P. Guzowski, *Fresenius' Z. Anal. Chem.*, 330 (1988) 207.
- 10 R.M. Campbell, M.M. Djordjevic, K.E. Markides and M.L. Lee, *Anal. Chem.*, 60 (1988) 356.
- 11 V. Ramaswamy, S.S. Sarowha and J.D. Singh, *J. Chem. Technol. Biotechnol.*, 36 (1986) 378.
- 12 V. Ramaswamy, V. Kothiyal, J.D. Singh and R. Kishna, *J. Chem. Technol. Biotechnol.*, 41 (1988) 255.
- 13 Annual Book of ASTM Standards, American Society for Testing and Materials, Philadelphia, 1986, D-4053-86.
- 14 D.K. Morgan, N.D. Danielson and J.E. Katon, *Anal. Lett.*, 18 (1985) 1979.
- 15 B.E. Miller, N.D. Danielson and J.E. Katon, *Appl. Spectrosc.*, 42 (1988) 401.
- 16 S.V. Olesisk, S.V. French and M. Novotny, *Anal. Chem.*, 58 (1986) 2256.
- 17 O.J. Curram and W.G. Collier, *Anal. Chim. Acta*, 177 (1985) 259.
- 18 M. Guzmán, J. Ruzicka, G.D. Christian and P. Shelley, *Vib. Spectrosc.*, 2 (1991) 1.
- 19 M. de la Guardia, S. Garrigues, M. Galignani, J.L. Burguera and M. Burguera, *Anal. Chim. Acta*, 261 (1992) 53.
- 20 M. Galignani, S. Garrigues and M. de la Guardia, paper presented at the XXVII CSI, Bergen, Norway, June 1991, paper B-PO-29.
- 21 S. Garrigues, M. Galignani and M. de la Guardia, *Analyst*, in press.
- 22 S. Garrigues, M. Galignani and M. de la Guardia, *Talanta*, in press.
- 23 Annual Book of ASTM Standards, American Society for Testing and Materials, Philadelphia, 1991, D-3606-91.
- 24 J.F. Tyson and A.B. Idris, *Analyst*, 109 (1984) 23.
- 25 V. Carbonell, A.R. Mauri, A. Salvador and M. de la Guardia, *J. Anal. At. Spectrom.*, 6 (1991) 581.

Entrapped copper(II) carbonate for indirect determination of glycine by flow injection atomic absorption spectrometry

J.V. Garcia Mateo

Departamento de Química, Colegio Universitario CEU, 46113 Moncada, Valencia (Spain)

J. Martínez Calatayud

Departamento de Química Analítica, Universidad de Valencia, C/ Dr. Moliner 50, 46100 Burjassot, Valencia (Spain)

(Received 26th May 1992; revised manuscript received 24th August 1992)

Abstract

Copper(II) carbonate was physically entrapped in a polyester during polymerization. The resulting solid resin was used as a reactor for glycine determination by means of a flow injection manifold and applied to pharmaceutical formulations; the glycine complexed with and thus dissolved some of the immobilized Cu(II), which was monitored by an atomic absorption spectrometer. The calibration graph is linear in the range 1.2–35 $\mu\text{g ml}^{-1}$ glycine, the detection limit is 1.2 $\mu\text{g ml}^{-1}$, the relative standard deviation at 20 $\mu\text{g ml}^{-1}$ is 1.1% ($n = 20$) and the sample throughput is 180 h^{-1} .

Keywords: Atomic absorption spectrometry; Flow injection; Copper carbonate; Glycine

Packed-bed reactors, filled with solid or immobilized reagents, have become one of the most interesting trends in continuous-flow methodologies, including flow injection analysis (FIA) [1–3]. The popularity of this type of FIA assembly can be ascribed to the advantages it offers over dissolved reagents, namely increased sensitivity and injection rate, resulting from the inherently lower sample dispersion. Other advantages are derived from the different on-line applications offered, such as sample [4] or reagent pretreatment, conversion reactions [5–7] and integrated reaction–detection devices [8,9].

The approaches to the preparation of solid-bed

reagents and the physico-chemical mechanisms used to immobilize a given reagent are usually dictated by its nature and the analytical purpose of the immobilization. A first approach is “natural” or existing immobilization, such as with strong insoluble reductants [10], some metals [11] or minerals [12,13] and even immobilized enzymes in their natural biochemical environment [14]. The other broad category of reagent immobilization approaches involves the physical or chemical immobilization of the reagent on a solid support by confinement or retention [15], absorption, electrostatic bonding to an ion-exchange resin [5,6] or covalent bonding [16].

This paper deals with a strategy for reagent immobilization for use in continuous-flow methodologies which was described in a previous paper [19]. Polymerization reactions of linear un-

Correspondence to: J. Martínez Calatayud, Departamento de Química Analítica, Universidad de Valencia, C/ Dr. Moliner 50, 46100 Burjassot, Valencia (Spain).

saturated polyester chains allows reactive beds to be prepared with the desired preselected configuration and dimensions for the column and a suitable particle size. A mixture of a reagent and a commercial polyester solution leads to physical entrapment of the reagent when the polymer has hardened; the product obtained can be mechanically manipulated. Different reagents can be immobilized. In this work, the immobilization of copper carbonate was carried out for the indirect determination of glycine by atomic absorption spectrometry.

EXPERIMENTAL

Reagents

Analytical-reagent grade chemicals were used unless indicated otherwise.

An aqueous solution of glycine (Probus) in deionized water, caffeine (Fluka, pure) acetylsalicylic acid (Panreac, pure), ascorbic acid (Merck), sorbitol (Acofarma, pure), sodium carbonate and sodium hydroxide (Probus) and sodium borate (Panreac) were used. The solid-bed reactor was prepared with $\text{CuCO}_3 \cdot \text{Cu}(\text{OH})_2 \cdot 2\text{H}_2\text{O}$ (Panreac). AL-100-A polyester resin solution (Reposa) containing low-molecular-weight polyester chains, a cobalt compound as activating agent of the reaction and methyl ethyl ketone as catalyst (Akzo) were employed.

Flow injection assembly

A single-channel, continuous-flow manifold was used with the column between the injection valve and detector. A Rheodyne Model 5041 sample injector and a Gilson Minipuls 2 pump were used. Copper(II) was determined using a Perkin-Elmer Model 5000 atomic absorption spectrometer at 324.8 nm. PTFE tube coils in the FI assembly were of 0.8 mm i.d.

Procedures

The bed reactor was prepared as described previously [19]. A 25-g amount of copper carbonate was added to 2 ml of the resin solution; after homogenization by manual stirring, 1 ml of the catalyst was added and the resulting mixture was

stirred before it became solid. The solid obtained was dried at room temperature for 2–3 h, then broken with a hammer and reduced to small particles with the aid of a coffee grinder. The different-sized particles were separated by sieving, washed with distilled water and dried, then the preselected size was sieved again. The resulting solid particles were stored in distilled water until use and introduced by suction into 1.2 mm i.d. PTFE tubing.

The first few assays under continuous-flow conditions were intended to adjust the bed stability at an acidic pH. For the purpose, aqueous HCl solutions of different pH values were passed through a 10-cm column. The reactor had i.d. 0.8 mm, an average particle size of 300–400 μm and a carbonate content of 0.8 g per ml of resin. The detector used was an atomic absorption spectrometer and deionized water was used as a blank. The pH range investigated was 3.01–5.10. The results obtained revealed that the extent of dissolution of the reagent decreased with increasing pH and was virtually zero at $\text{pH} \approx 5$.

Glycine determination in pharmaceutical formulations

Tablets. The required amount of powdered tablets (4.2 g) was dissolved in hot water. If some precipitate remained the solution was filtered and the volume was made up to 1000 ml with distilled water. A 5-ml volume of buffer solution was added to 3.4-ml aliquots and diluted to 100 ml.

Drinking ampoules. The ampoule content was made up to 1000 ml. A 5-ml volume of buffer solution was added to 4-ml aliquots and diluted to 100 ml.

RESULTS AND DISCUSSION

Some preliminary experiments were done in order to study the reaction between the CuCO_3 -resin and glycine. For this purpose, 0.1 g of the resin was brought into contact with 5 ml of 0.01 M glycine in a test-tube and allowed to stand for 3 min, after which the UV-visible spectrum of the supernatant was recorded. This experiment

was repeated by using different concentrations of CuCO_3 in the resin between 0.4 and 1.0 g/ml. The recorded spectrum showed an absorption band at 632 nm corresponding to the Cu(II) -glycine complex and the absorbance was found to increase with increasing concentration of copper in the resin.

The influence of pH was tested by adjusting the pH of the sample solution with HCl or NaOH. The results obtained demonstrated that the complex is formed in a wide pH range; the highest absorbances were obtained from pH 8.5 to 10. Suitable pH and ionic strength were established by testing different basic media, and some of them at different concentrations. The glycine concentration was $22.96 \mu\text{g ml}^{-1}$. Figure 1 shows the absorbances obtained from the different media. NaOH and a buffer solution ($\text{Na}_2\text{B}_4\text{O}_7\text{-HCl-NaOH}$) were the most effective media. The optimum pH range was found to be 9.0–9.50; a pH of 9.30 was finally adopted, adjusted with $\text{Na}_2\text{B}_4\text{O}_7\text{-HCl-NaOH}$ buffer.

A preliminary assay was done to determine whether the resin could be used as a reactive bed under continuous-flow conditions in studying the stability of measurements with time (measurements were made every 1 min over a period of 60 min). The column was subjected to rapid consumption (i.e., to continuously flowing analyte solution instead of discrete sample volumes); the carrier solution, which contained $20.4 \mu\text{g ml}^{-1}$ glycine at pH 9.30, flowed continuously through the column, and no injections were performed. The outputs increased with time up to about 10 min; subsequently the column remained stable (same outputs) with an average absorbance of 0.053 ($n = 45$). The influence on the peak height of the pretreatment based on continuous passage of the buffered analyte solution through the column has been described elsewhere [20] for another packed-bed reactor. The results obtained revealed that any column would be sufficiently stable for the present purposes after being subjected to a 15-min pretreatment.

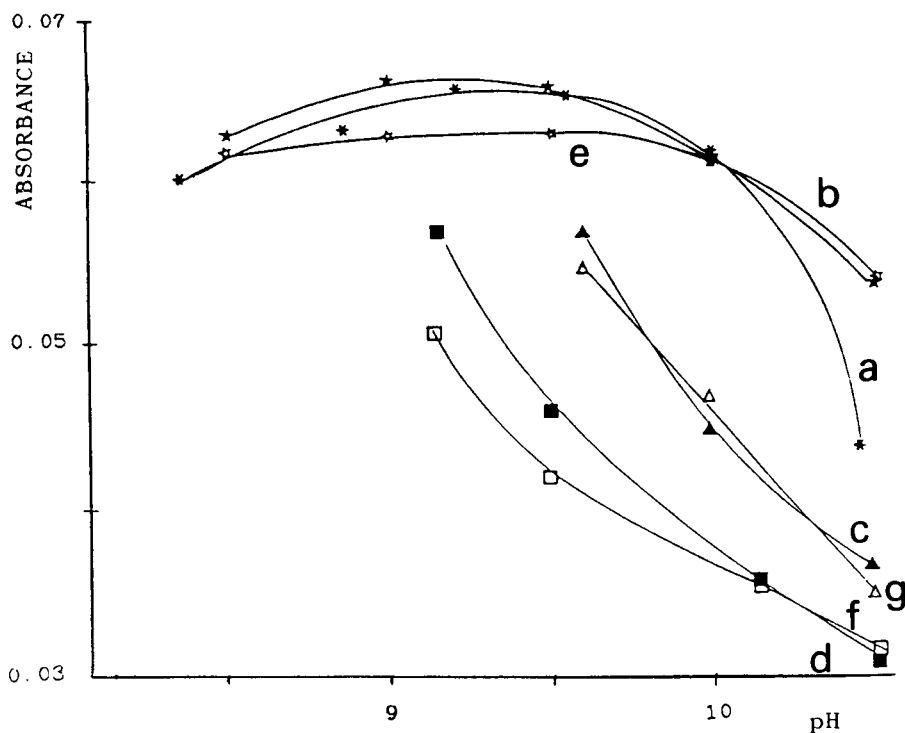


Fig. 1. Influence of different buffer solutions: (a) NaOH; (b) $\text{Na}_2\text{B}_4\text{O}_7 \cdot 10\text{H}_2\text{O-HCl-NaOH}$ (diluted); (c) $\text{NaHCO}_3\text{-NaOH}$ (diluted); (d) $\text{NaHCO}_3\text{-Na}_2\text{CO}_3$ (diluted); (e) $\text{Na}_2\text{B}_4\text{O}_7 \cdot 10\text{H}_2\text{O-HCl-NaOH}$; (f) $\text{NaHCO}_3\text{-Na}_2\text{CO}_3$; (g) $\text{Na}_2\text{CO}_3\text{-NaOH}$.

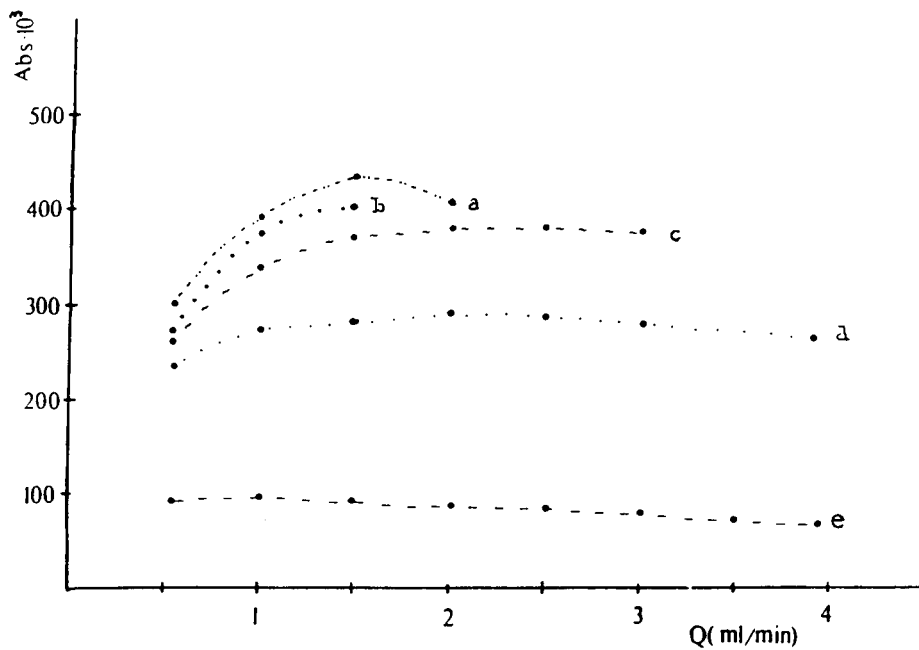


Fig. 2. Influence of particle size: (a) 120–150 μm ; (b) 90–120 μm ; (c) 150–200 μm ; (d) 200–300 μm ; (e) 300–400 μm . Packed-bed reactor: 9.5 cm \times 0.8 mm i.d., 0.8 g/ml reagent–resin.

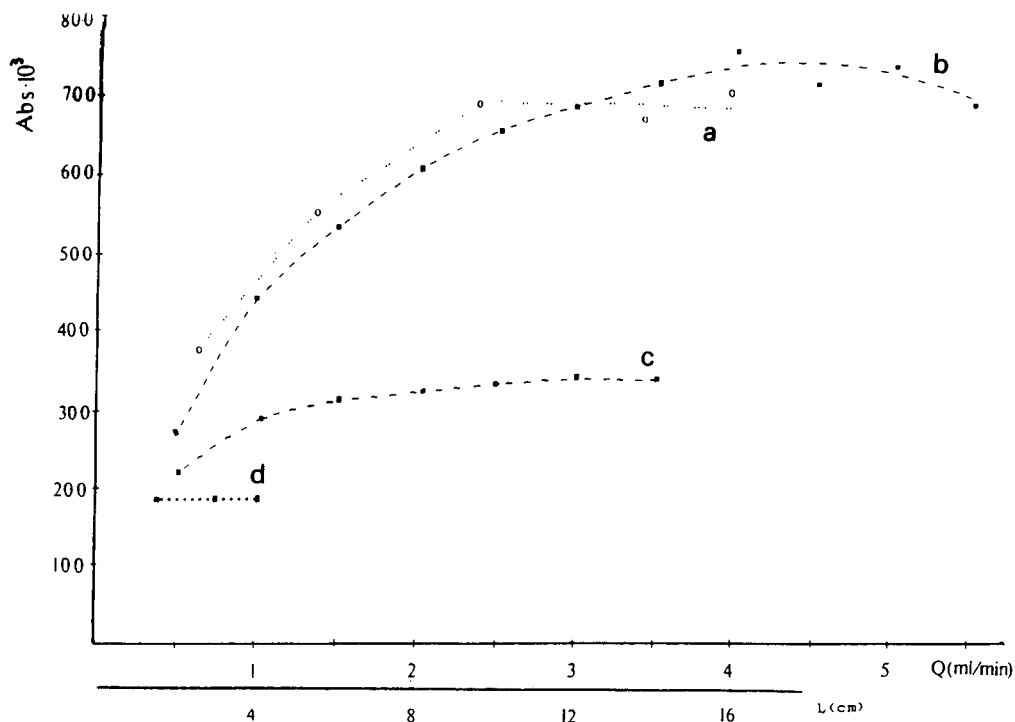


Fig. 3. Influence of reactor length and inside diameter. (a) Reactor length (i.e. = 1.2 mm). Reactor i.d.: (b) 1.5 mm; (c) 0.8 mm; (d) 0.5 mm.

FIA and chemical parameters were optimized by the univariate method in order to achieve a compromise between adequate peak height, sample throughput, reproducibility and column lifetime. FIA parameters were optimized first, particularly those influencing the reactor performance: particle size, amount of reactant immobilized per ml of resin and inner diameter and length of the reactor. In a subsequent step the carrier flow-rate and injected sample volume were optimized, the optimum values being used to re-optimize the chemical variables, pH and buffer concentration of the carrier solution.

The optimum particle size for the single-channel system used, which included a 9.5 cm \times 0.8 mm i.d. reactor containing 0.8 g CuCO_3 /ml resin, was determined by injecting 100- μl aliquots containing 50 $\mu\text{g ml}^{-1}$ glycine at pH 9.30 (the carrier solution was adjusted to the same pH). As can be seen in Fig. 2, the signal decreased with increasing particle diameter throughout the range studied (90–120 to 300–400 μm). As small particle sizes only afforded modest flow-rates, a particle size of 150–200 μm was chosen for subsequent work.

The assembly and optimum particle size described above were used to study the effect of the reagent concentration in the resin, which was varied between 0.4 and 1.6 g/ml. This variable proved to have a large influence on the transient signal. A stable peak-height signal was obtained over the range 0.8–1.2 g/ml; lower concentrations gave smaller signals. A concentration of 1 g/ml was adopted for subsequent experiments.

The inner diameter of the reactor influenced both the transient signal obtained and the maximum allowed flow-rate. Of special note in this respect is the increase in the signal with increase in the reactor diameter (i.e., with increasing amount of reagent, Fig. 3). Obviously, the signal increased with increasing reactor length over the range studied (2.5–15.8 cm) until the sample dispersion offset the effect of the increased amount of resin. The signal stabilized at lengths greater than 9.5 cm, so a reactor length of 13.5 cm was chosen as optimum.

Increasing flow-rate over the range 1–5 ml/min produced an increased signal up to about

3.5 ml/min, above which it levelled off and then decreased at flow-rates higher than 4.5 ml/min. Note that the nebulizer uptake was manually adjusted in order to obtain the best possible transient signal. A flow-rate of 4.2 ml/min was considered to be a sensible choice.

The sample volume injected was optimized by using the assembly described above, into which aliquots containing 20 $\mu\text{g ml}^{-1}$ glycine were injected in order to avoid signal saturation. This parameter was found to have little influence: the signal increased only slightly (with the exception of the first few points). An injection volume of 345 μl provided the best compromise between peak height and injection rate.

The chemical variables previously optimized were reoptimized by using the optimum FIA assembly on account of the significance of the kinetic component of the system. Thus, aliquots of sample and buffer containing 20 $\mu\text{g mol}^{-1}$ glycine in the $\text{Na}_2\text{B}_4\text{O}_7\text{-HCl-NaOH}$ solution at pH values between 8.5 and 10.5 were injected. The results revealed an optimum pH range between 9.0 and 9.5 and the advisability of using a low buffer concentration in order to avoid the effects of too high an ionic concentration on flame phenomena. A pH of 9.25 and a buffer concentration of 0.005 M were selected.

ANALYTICAL APPLICATIONS

The calibration graph was linear between 1 and 35 $\mu\text{g ml}^{-1}$ glycine. According to IUPAC rules [21], the detection and determination limits were 1.2 and 4.4 $\mu\text{g ml}^{-1}$, respectively. The study was carried out by preparing packed-bed reactors (13.5 cm \times 1.5 mm i.d. and concentration 1 g/ml) from independent immobilizations. Different amounts of resin, from 10 g in 10 ml to 30 g in 30 ml, were prepared. The day-to-day stability of the packed-bed reactors was tested by comparing the linear graphs obtained with recently prepared and used columns, which were stored for different time periods up to 15 days, and the calibration graph was measured with or without repeating the continuous-flow pretreatment. Some of the results obtained are given in Table 1. The

TABLE 1

Effect of column pretreatment on sensitivity

No. ^a	Slope ^b (R.S.D., %)	Intercept ^c (R.S.D., %)	Correlation coefficient ^d
1	20.7 (3.4)	18.1 (0.4)	0.999
2	21.0 (3.7)	11.7 (2.9)	0.998
3	15.7 (1.7)	24.5 (3.5)	0.995
4	15.3 (4.4)	20.7 (9.9)	0.994

^a 1, Total amount of prepared resin 30 g in 30 ml; 2, 3 and 4, total amount 10 g in 10 ml. Nos. 1 and 2 were recently prepared columns (only exposed to a 15-min pretreatment); 3 and 4 were stored for 15 days, with or without repeating the continuous-flow pretreatment, respectively. The reported figures are the means of five independent immobilizations. All calibration graphs were measured by injecting eight different glycine solutions (1, 5, 10, 15, 20, 25 and 30 $\mu\text{g ml}^{-1}$) with five replicates. ^b (Absorbance per $\mu\text{g ml}^{-1}$ glycine) $\times 10^3$. ^c Absorbance $\times 10^3$. ^d Of typical calibration graph.

slope of the linear graph decreased after being stored during 15 days; however, good linearity was retained.

The reproducibility of the proposed procedure and the sample throughput were determined by repeatedly injecting a sample containing 20 $\mu\text{g ml}^{-1}$ glycine. Bearing in mind, the influence of the pretreatment of the column, the reproducibility was studied by varying the time during which a buffered solution of glycine (20 $\mu\text{g ml}^{-1}$ and pH 9.30) was continuously flowing through the column; after the pretreatment a series of twenty injections were made in the usual way. The pretreatment times tested were 0, 5, 10, 15 and 20 min. The stability and height of the transient signals were clearly influenced by the pretreatment; 15 min was selected for the optimum use of the columns. The results obtained were as follows [pretreatment (minutes), average absorbance ($n = 20$) and R.S.D. (%]): 0, 0.174, 17.7; 5, 0.309, 1.4; 10, 0.380, 1.9; 15, 0.420, 1.8; and 20, 0.408, 1.1. The samples injection rate was 180 h^{-1} .

The tolerance of the proposed procedure to potential interferents accompanying glycine in pharmaceutical preparations was studied by assaying solutions containing 20 $\mu\text{g ml}^{-1}$ glycine and various amounts of each suspected interferent. The maximum tolerated levels obtained by

comparison with a reference solution containing glycine only were as follows (the pairs of values represent the "maximum" tolerated concentration in $\mu\text{g ml}^{-1}$ and the percentage relative error given by that concentration, respectively): acetylsalicylic acid, 100, 1.5; ascorbic acid, 100, 13.1; sorbitol, 1000, 5.2; caffeine, 1000, 0.7; sodium chloride, 1000, 0.7; sodium fluoride, 526, 2.0; citric acid, 49, 3.3; alanine, 6.0, 12.2; phenylalanine, 5.0, 10.5; leucine, 5.0, 11.9; valine, 5.2, 10.5; potassium iodide, 188, 1.6; nicotinamide, 196, 1.3; thiamine hydrochloride, 50.0, 4.5; L-glutamic acid, 20.0, 6.2; iron(II) sulphate, 495, 2.8; and zinc sulphate, 500, 1.8. The study of interferents such as iron(II) and zinc ions required the pre-separation of the obtained basic salts when the pH of solution was adjusted to 9.25.

The proposed method was applied to the determination of glycine in two commercially available pharmaceutical preparations, namely tablets (Okal) and drinking vials (Actilevol). The results obtained were consistent with those certified on the labels: Okal, certified 100 mg and found 102.7 mg per tablet; Actilevol, certified 500 and found 499.1 mg per vial.

Conclusions

The proposed procedure for the immobilization of reagents for use in continuous-flow systems is straightforward as a result of the substrate being immobilized as the support is being generated. As the immobilization procedure simply involves non-specific physical entrapment at room temperature, it can be applied to a variety of reagents, whether stable or not. In addition, the particle size can be readily controlled and, more important, the concentration of immobilized reagent used can be obtained easily, which allows the preparation of beds with the required degree of reactivity. The beds thus obtained are chemically and mechanically stable enough for use under continuous-flow conditions. The proposed continuous-flow procedure presents some additional advantages for glycine determination over an alternative FI method [20], namely a lower linear application range, a highly increased injection throughput and better selectivity.

REFERENCES

- 1 J. Ruzicka and A. Aindal, *Anal. Chim. Acta*, 216 (1989) 243.
- 2 H.A. Mottola, *Quim. Anal.*, 8 (1989) 119.
- 3 J. Martínez Calatayud and J.V. Garcia Mateo, *Analyst*, 116 (1991) 327.
- 4 E.A. Novikov, L.K. Zolotov and A. Yu, *Anal. Chim. Acta*, 230 (1990) 157.
- 5 J. Martínez Calatayud, C. Gomez Benito and D. Gaspar Gimenez, *J. Pharm. Biomed. Anal.*, 8 (1990) 667.
- 6 J. Martínez Calatayud and C. Gomez Benito, *Anal. Chim. Acta*, 231 (1990) 259.
- 7 G.K.C. Low and R.W. Mathews, *Anal. Chim. Acta*, 231 (1990) 259.
- 8 M.A. Shakir and A.T. Faizullah, *Analyst*, 114 (1989) 951.
- 9 B.F. Band, F. Lazaro, M.D. Luque de Castro and M. Valcarcel, *Anal. Chim. Acta*, 229 (1990) 117.
- 10 Y. Zhang, P. Riby, A.G. Cox, W. Cameron, C.W. McLeod, A.D. Date and Y.Y. Cheng, *Analyst*, 113 (1988) 125.
- 11 S. Devi and A. Townshend, *Anal. Chim. Acta*, 225 (1989) 331.
- 12 A. Kojlo and J. Martínez Calatayud, *J. Pharm. Biomed. Anal.*, 8 (1990) 663.
- 13 S.R. Varma, J. Martínez Calatayud and H.A. Mottola, *Anal. Chim. Acta*, 233 (1990) 235.
- 14 S.L. Belli and G.A. Rechnitz, *Anal. Lett.*, 19 (1986) 403.
- 15 H. Hwang and P.K. Dasgupta, *Anal. Chem.*, 59 (1987) 1356.
- 16 P. Linares, M.D. Luque de Castro and M. Valcarcel, *Anal. Chim. Acta*, 230 (1990) 199.
- 17 M.T. Jeppesen and E.H. Hansen, *Anal. Chim. Acta*, 214 (1988) 147.
- 18 G. Maeder, J.L. Veuthey, M. Pelletier and W. Haerdi, *Anal. Chim. Acta*, 231 (1990) 115.
- 19 J. Martínez Calatayud and J.V. Garcia Mateo, *Analyst*, 265 (1992) 81.
- 20 J. Martínez Calatayud and J.V. Garcia Mateo, *Analyst*, 116 (1991) 327.
- 21 H. Freiser and G.H. Nancollas (Eds.), *IUPAC Compendium of Analytical Nomenclature*, Pergamon, Oxford, 2nd edn., 1987.

Extraction of dicyanoaurate(I) using supported liquid membranes in a flow-injection manifold: evaluation of extractants

D.E. Barnes, M.J.C. Taylor and G.D. Marshall

Process Analytical Science, Analytical Science Division, Mintek, Private Bag X3015, Randburg 2125 (South Africa)

J.F. Van Staden

University of Pretoria, Pretoria (South Africa)

(Received 2nd September 1992; revised manuscript received 16th November 1992)

Abstract

Several potential extractants were considered as the active compound in supported liquid membranes (SLMs) for the selective extraction of dicyanoaurate(I) from alkaline process solutions. SLM systems containing primary, secondary, tertiary, and quaternary amines, in which the extraction and back-extraction is achieved in one step, are proposed. The various SLMs were compared using flow-injection analysis (FIA). They were evaluated on the basis of their stability, selectivity, and respective permeability for gold.

Keywords: Flow-injection; Amines; Dicyanoaurate(I); Gold; Solvent extraction; Supported liquid membranes

Several sensitive methods for the determination of gold are found in the literature [1–4]. These methods either require expensive and sophisticated instrumentation, or lengthy and labour-intensive preconcentration techniques. These characteristics mitigate against automation and the development of process analyzers. We have reported on a simple method for the enrichment of dicyanoaurate(I) followed by measurement by flame atomic absorption spectrophotometry (AAS) [5]. This paper continues that study by evaluating a variety of amine extractants for the selective extraction of gold.

The extraction and enrichment of gold-bearing solutions has received considerable attention on

both the macro scale for the recovery of gold from ores [2,6–9] and on the micro scale for its accurate and sensitive determination [10–13]. In industry gold is recovered from cyanide leach solutions either by reduction with zinc (i.e. precipitation) or by adsorption onto activated carbon or resins. Solvent extraction has been employed by various researchers for the separation and concentration of dicyanoaurate(I) [8,14–19]. Economic considerations have prevented these successful laboratory-scale experiments from being extended to the process scale. Other reasons include limitations arising from the manipulation of large volumes of different phases, the loss of expensive extractants, and growing resistance to the handling of potentially harmful solvents.

Supported liquid membranes (SLMs), which use relatively small volumes of organic solvents, have previously been suggested as a simpler alter-

Correspondence to: D.E. Barnes, Process Analytical Science, Analytical Science Division, Mintek, Private Bag X3015, Randburg 2125 (South Africa).

native to solvent extraction. Such systems have been used for both metallurgical extraction and the removal of contaminants from various process solutions [20–23].

An organic diluent, containing one or more solvent-extraction reagents, is adsorbed as a thin layer on a suitable inert porous support. This organic layer, interposed between two aqueous solutions, is termed SLM. The organic phase is held in the pores of the support by lipophilic and capillary forces. The membranes are stable for extended periods because of the hydrophobicity of the support and the organic phase.

The extraction of the desired species from the aqueous solution into the thin organic layer occurs simultaneously with its back-extraction into the second aqueous solution. This results in the selective transport of the solute, from the feed solution through the SLM to a stripping solution. The effective concentration of solute in the ideal SLM remains well below saturation, since the solute is continuously removed from the SLM by the stripping solution. This ensures very effective use of the extraction reagent, which is often expensive or potentially toxic.

The advantages of using SLMs over conventional solvent extraction include: the use of small amounts of organic reagents, minimum loss of organic reagents, reduced handling of potentially toxic reagents, the simplicity of the system, and ease of automation. Since the organic phase is immobilized on an inert support, large volumes of aqueous solutions can be used to achieve high aqueous-to-organic phase ratios, without phase separation problems. SLMs allow geometries with large ratios of surface area to volume, suited to efficient permeation and a high transport rate of the solute between two aqueous phases.

Leach liquors from gold-bearing ores are typically in an aqueous medium with a pH value between 10 and 12. The gold is usually leached as the dicyanoaurate(I) complex. It was the aim of the present investigation to study SLMs of various extractants that have previously been successfully used for the solvent extraction of gold from alkaline cyanide solutions. The extractants evaluated included primary, secondary, tertiary, and quaternary alkyl amines. A flow-injection method

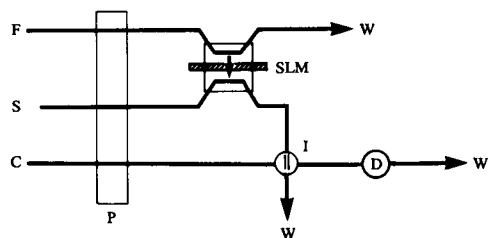


Fig. 1. Flow-injection manifold. C = flow-injection carrier stream, D = detector, F = feed solution, I = injection valve, P = pump, S = stripping solution, SLM = supported liquid membrane unit, W = waste.

that has been described previously [24] was used as a versatile diagnostic tool. Membrane characteristics that were considered include permeability to gold, stability, and specificity.

Although the primary reason for the investigation study was the evaluation of various extractants for their inclusion as SLMs in a simple method of analysis, the findings could benefit plant-scale studies as well.

EXPERIMENTAL

Apparatus

The construction of the SLM unit and the preparation of both the SLM and the manifold (Fig. 1) has been described previously [24]. Control of the various devices was achieved using an IBM-compatible personal computer (PC). The software package FlowTEK [25], designed for computer-aided flow-analysis, provides for the control of the pump, switching of the injection valve, and acquisition of data.

The dicyanoaurate(I) complex was detected spectrophotometrically at 240 nm, using a Jasco UVIDEK spectrophotometer. A linear calibration curve for the gold complex in the concentration range 5–100 mg l⁻¹ was obtained. Thiourea absorbs strongly at 240 nm, and interfered with the spectrophotometric detection of gold.

A Varian Spectra 10/20 atomic absorption spectrophotometer was used for the detection of gold in those tests where thiourea was used as the stripping solution. The instrumental conditions specified by the manufacturer were used. Deu-

terium-arc background correction was applied and the resulting response was directed, via the on-board microprocessor, to a chart recorder.

Reagents

All reagents were of Analytical Reagent grade. Deionised water was used throughout the investigation. A stock solution containing 1000 mg l^{-1} of gold-containing complex and 200 mg l^{-1} sodium cyanide was prepared. Appropriate dilutions were made from this stock solution to prepare the buffered feed solutions. Two buffers were used. A phosphate buffer, with a pH value of 7, was prepared from potassium dihydrogen phosphate (KH_2PO_4) and disodium hydrogen phosphate ($\text{Na}_2\text{HPO}_4 \cdot 2\text{H}_2\text{O}$). A carbonate buffer with a pH value of 10 was prepared from sodium carbonate (Na_2CO_3) and sodium hydrogencarbonate (NaHCO_3). The strength of the buffer in the feed solution was 0.1 M.

The stripping solution for the SLMs containing the tertiary, secondary, and primary amines was 0.1 M sodium hydroxide. For the quaternary amines, the stripping solution was 1 M thiourea in 0.25 M sulphuric acid.

The carrier solution was the same as the stripping solution, 0.1 M sodium hydroxide. The feed, stripping and carrier solution were all pumped at a flow-rate of 1.5 ml min^{-1} .

Procedure

Permeation of SLMs. The feed solution containing a known amount of gold (typically 100 mg l^{-1}) was passed over the SLM, and the amount of gold permeating through the SLM was determined by automatic analysis of the stripping solution every two minutes. The amount of gold that permeated through the SLM was expressed as a percentage of the gold in the feed solution. This ratio was plotted as a function of time, for a freshly prepared SLM. Fig. 2 shows a typical permeation profile. Similar profiles were used to evaluate and compare different SLMs. The maximum permeation rate of the analyte through the SLM is indicated by H_m . This parameter can be used to judge the rate of loading and stripping of a particular SLM. The time required to reach H_m is indicated by t_c . This parameter gives an indica-

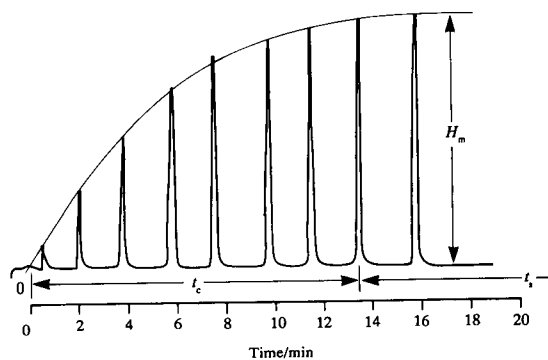


Fig. 2. Typical permeation profile. H_m is the maximum permeation, t_c is the time it takes to reach this permeation, and t_s is the time that this permeation is maintained for.

tion of the time for the specific system to reach equilibrium. The stability of a particular SLM is given by the time, t_s , for which the maximum plateau is maintained.

The values for H_m were used to select the three most promising extractants. In a second suite of experiments these three extractants were evaluated with respect to their stability.

Selectivity. The selectivity of the three extractants (TDA, LA-2, and Aliquat 336) was compared in the final suite of experiments. Organic phases containing the constituents at concentrations levels given in Table 1 were used as SLMs.

The SLMs were evaluated with respect to their enrichment of gold and were tested for two different spiked plant solutions. Gold-bearing plant solutions typically contain between $10 \text{ } \mu\text{g l}^{-1}$ and 20 mg l^{-1} gold complex. The concentrations of the other base-metal cyanide complexes (viz. iron, silver, nickel, copper, and cobalt) vary considerably but are usually below 10 mg l^{-1} . The pH value of these solutions is normally between 10 and 11. The two filtered plant solutions were

TABLE 1

Constituents of the organic phases used in the selectivity tests (%)

	SLM 1 (TDA)	SLM 2 (LA-2)	SLM 3 (Aliquat 336)
Extractant	1 (m/v)	17.5 (v/v)	20 (v/v)
TBP	49.5 (v/v)	41.25 (v/v)	40 (v/v)
Heptane	49.5 (v/v)	41.25 (v/v)	40 (v/v)

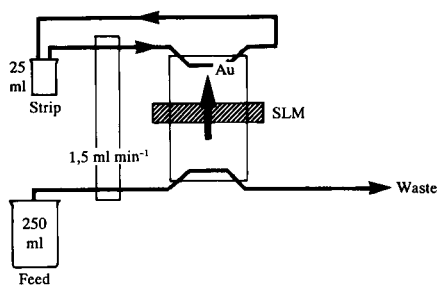


Fig. 3. Manifold for the selectivity tests.

spiked with the respective cyanide complexes so that they contained 10 mg of each metal. In addition 10 mg l⁻¹ of gold was added as the dicyanoaurate(I) complex. The sample solutions were buffered to avoid changes in permeation, due to changes in the pH value of the feed solution while it travels through the SLM. The same buffered sample solution was used for all three SLMs to allow comparison between the systems.

The manifold used for these tests is shown in Fig. 3. A 250 ml portion of each of the adjusted plant solution was passed, in a once-through mode, on one side of the SLM. The gold was collected in 25 ml of a suitable stripping solution, which was circulated on the other side of the SLM. Both solutions were pumped at a flow-rate of 1.5 ml min⁻¹. When TDA and LA-2 SLMs were used, the stripping solution was 0.1 M sodium hydroxide. For the Aliquat 336 SLM, 1 M thiourea in 0.25 M sulphuric acid was used as the stripping solution.

Aliquots of the two spiked sample solutions and the various stripping solutions were analyzed by ICP-MS, with some of the results being cross-checked by AAS. Enrichment was determined from these results and confirmed by ion-interaction chromatography with photometric detection [4].

RESULTS AND DISCUSSION

Protonation of amines

The primary, secondary, and tertiary amines are referred to as weak-base amines, as opposed

to strong-base quaternary amines. The weak-base amines contain a nitrogen atom with an orbital bearing a lone pair of electrons, which allows the amine to accept a proton and become positively charged. Although protonation of the weak-base amines can be achieved by acidification of the aqueous feed solution, this option is undesirable in the present application for at least three reasons. Firstly, at low pH values, the extraction becomes unselective. Secondly, acidification of typical plant cyanide solutions is hazardous because of the formation of free cyanide. Thirdly, the undesirable formation of bubbles occurs at low pH values, due to the presence of the carbonate in the process solutions.

An elegant solution to a similar problem in conventional solvent extraction has been provided by the use of Lewis base modifiers in the organic phase [26]. The pH value at which the modified weak-base amines extract gold can thus be altered, from very acidic solutions to more basic solutions. It has been shown that the apparent change in basicity does not influence the extraction of other metal cyanide anions to the same extent.

Organic modifiers that have been suggested and tested by Mooiman and Miller [15] and Miller et al. [26] include the alkyl phosphorus esters, sulfones, and sulfoxides. Trioctylphosphine oxide (TOPO), tributyl phosphate (TBP) and dibutyl butyl phosphonate (DBBP), when tested in a solvent-extraction system, were found to behave similarly.

The use of modifiers in the weak-base amine SLMs was investigated. Although TOPO gave marginally better extraction efficiencies, TBP was selected as the modifier in the present investigation due to its more favourable solubility characteristics in both aqueous and organic solutions over the chosen pH range. Furthermore it did not interfere in the spectrophotometric determination of gold.

The effect of TBP on permeation is depicted in Fig. 4. Higher TBP concentrations improved the extraction of gold from feed solutions with pH values of 7 and 10, and enhanced the permeation of gold through the SLM. At pH 7 a maximum H_m value of 13% was obtained for a SLM

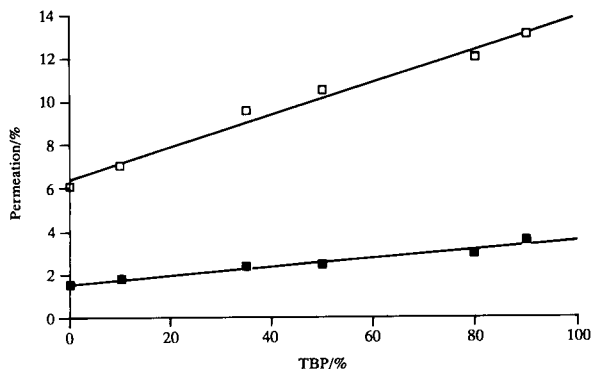


Fig. 4. The effect of the percentage TBP on the permeation of gold through a SLM containing 10% (v/v) LA-2 in heptane. □ = pH 7, ■ = pH 10.

that contained 10% (v/v) LA-2, and 90% (v/v) TBP. It is important to note that the percentage of gold permeating through this SLM was doubled using TBP as the modifier.

Modifiers and solvents

The so-called 'modifiers' are extractants in their own right, for example TBP and TOPO [26]. They are called modifiers here but their potential as extractants should not be ignored. It should be noted though that as extractants they extract gold over the pH range 1 to 13 [27]. Because the extraction is independent of pH value [6,17], a pH gradient across the SLM does not allow back-extraction of the gold from these organic phases. Furthermore, the strong affinity of these extractants for gold makes back-extraction by other complexing reagents difficult. SLMs rely on an extraction and back-extraction reaction. Because of the difficulty in finding a suitable stripping solution, the permeation of gold through SLMs containing only the modifier was expected to be low.

SLMs containing only TBP and TBP-DEB (diethylbenzene) (50:50, v/v) were tested. If an acidified feed solution and a stripping solution containing 0.1 M sodium hydroxide were used, only 1.6% of the gold permeated through the SLM. It is reported that gold could be stripped from the TBP alone at low ionic strength and high temperature in conventional solvent extrac-

tion [26]. When hot distilled water was used as the stripping solution, 2% of the gold permeated through the SLM. The SLM containing only TBP gave marginally better permeations than the SLM containing the TBP-DEB mixture.

Certain oxygen-containing organic solvents, such as diethyl ether, diethylene, di-isobutylketone, and methyl isobutylketone, have an affinity for the gold complex. The solvent replaces the solvating water molecules that usually surrounds the cyanide complex, thereby increasing the solubility of the complex in the organic phase. Mooiman et al. [27] considered the extraction capabilities of some of these organic diluents in solvent extraction. They are, however, significantly soluble in aqueous solutions, which render them unsuitable as the organic phase in SLMs.

Tromp et al. [16] investigated the transport of gold through a SLM containing macro-cyclic ethers. They used two stirred chambers, containing the feed solution on the one side of the SLM and the stripping solution on the other. Macro-cyclic ethers are extremely costly, and therefore were not considered further in the present investigation.

Primary amines

Several weak-base amine SLMs were used, with a suitable modifier, for the extraction and back-extraction of gold from neutral and alkaline solutions. The feed stream was adjusted to a pH value of either 7 or 10, using the appropriate buffers. The gold was extracted from these solutions into the SLMs, and back-extracted using a 0.1 M sodium hydroxide stripping solution (Fig. 5).

The permeabilities of several SLMs containing primary amines with different chain lengths were compared. Those with carbon chain lengths of less than ten were prepared by dissolving 10% (v/v) of the appropriate amine in 40% (v/v) heptane and 50% (v/v) TBP. Tridecyl amine (TDA), pentadecyl amine (PDA) and heptadecyl amine (HDA) are all waxes, and are sparingly soluble in heptane. However, it was possible to dissolve 1% (m/v) TDA in heptane. Saturated solutions of PDA and HDA were prepared in heptane-TBP (50:50, v/v) for the permeability

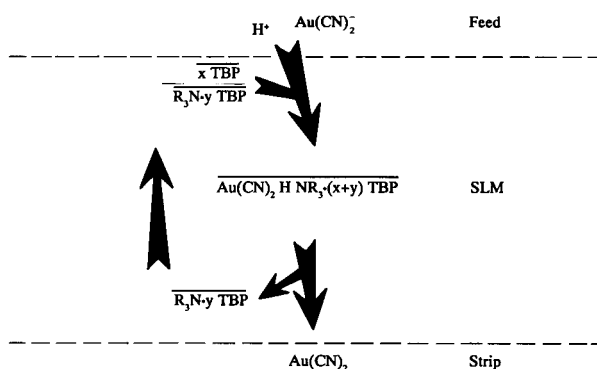


Fig. 5. A schematic illustrating the permeation of gold through SLMs containing primary, secondary, and tertiary amines.

tests. The maximum permeation ratio, H_m , for each of the tested amines is given in Table 2.

The permeation rates increased as the chain length increased up to a chain length of thirteen, where an H_m value of 15% was obtained. The longer the chain length of the extractant, the more hydrophobic the ion-pair formed between the solvent and the dicyanoaurate. This affects the extraction rate of the gold complex into the organic phase, and accounts for the increase in permeation. The amines with shorter chain lengths are also more soluble in the aqueous solutions, which results in less stable SLMs. The decline in the maximum permeation for SLMs that contain amines with more than thirteen carbon atoms might be due to the small amount of extractant in the SLM or to viscosity effects. TDA was chosen for further tests.

Owing to the basicity of the amine in the SLM, it is expected that the extraction of the gold will

TABLE 2

Permeability of SLMs containing primary amines with different chain lengths

Extractant	H_m (%)	
	pH 7	pH 10
Ethyl	5	1.5
Propyl	7	2
Nonyl	11.5	1.7
Tridecyl	15	4
Pentadecyl	12	2
Heptadecyl	10	1

TABLE 3

Permeability of SLMs containing secondary amines with different chain length

Extractant	H_m (%)	
	pH 7	pH 10
Diethyl	2.9	0.3
Dipropyl	3.3	0.3
Dihexyl	3	1
LA-2	10.5	2.4
Adogen 283 (ditridecyl)	9	5.2

be favoured by feed solutions with lower pH values. As expected, the permeation of gold from feed solutions at pH 10 is considerably less than from feed solutions at pH 7.

It should be noted that the manifold used was designed for the quick scanning of various extractants, and the ratio of surface area to volume was not optimized. However, the fact that 15% of the gold could be extracted by an SLM with such a small area ($2.4 \times 10^{-4} \text{ m}^2$) is promising. Membrane designs with large surface areas have been described [22,23], and would be a logical consideration in the design of an optimized SLM manifold.

Secondary amines

The secondary amines followed a similar trend to the primary amines with respect to the permeability of the SLM for gold (Table 3). A commercial extractant LA-2 (a mixture of secondary amines with chain lengths between 12 and 15) gave the best results ($H_m = 10.5\%$). Generally, the secondary amines did not give SLMs with the same high permeation rates as their primary amine equivalents.

Mooiman et al. [27] commented on the effect of different diluents on the extraction of metal cyanide complexes in solvent extraction by amine extractants. They found that the diluent had an insignificant effect on the extraction of gold when primary amines were used. However, the choice of diluent did have an effect on the extraction of gold when secondary, and tertiary amines were used. They also found that organic solutions in which hexane is used can extract gold from solutions with higher pH values than those in which

TABLE 4
The effect of different solvents on permeation

Solvent	H_m (%)	
	pH 7	pH 10
Chloroform	14.4	2
Diethylbenzene (DEB)	14.5	7
Heptane	14.4	2
Tributyl phosphate (TBP)	16	9

xylene is used. This effect was observed only for the extraction of gold, and did not affect the extraction of the other base-metal cyanide complexes [28].

The effect of the diluent on the permeation of a SLM containing LA-2 as extractant was tested. Four different organic solutions were prepared containing 15% (v/v) LA-2, 50% (v/v) TBP and 35% (v/v) diluent (DEB, heptane, chloroform, or TBP). SLMs prepared from these solutions were then evaluated, and the results are summarised in Table 4.

The effect of the different solvents at pH 10 was more pronounced than at pH 7. However, the diluent did have a smaller effect on the performance of SLMs than it had in conventional solvent-extraction systems. A SLM that contained the amine dissolved only in TBP gave slightly better extraction kinetics particularly at pH 10. This can be ascribed to the synergistic effect of TBP and LA-2 described earlier.

The effect of the concentration of the extractant was tested by using different concentrations of LA-2 in 50% (v/v) TBP made up in heptane. The results are shown in Fig. 6. The permeation increased with an increase in the amount of LA-2 in the SLM, up to a maximum ($H_m = 14.8\%$) at a concentration of 17.5% (v/v) LA-2, and then decreased for higher concentrations of LA-2.

Tertiary amines

The permeation of gold through the SLMs was lowest when tertiary amines were used (Table 5). The same trend was observed with respect to the carbon chain length. The highest permeation ($H_m = 9\%$) was obtained with a commercial amine, Alamine 336 (tricaprylyl amine).

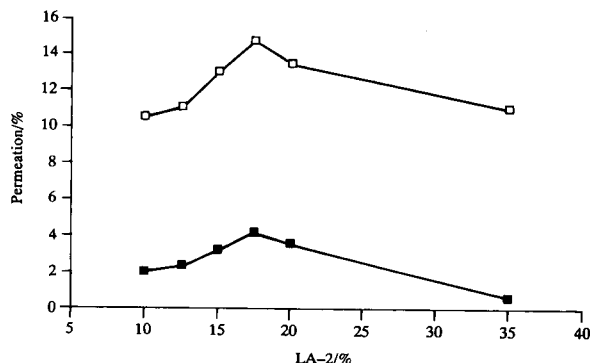


Fig. 6. The effect of the concentration of LA-2 in the organic phase on the SLM's permeability to gold. □ = pH 7, ■ = pH 10.

Quaternary amines

Quaternary amines ($R_4N^+OH^-$) are strong bases that are completely ionized. The mechanism of extraction with strong-base SLMs is quite different to that of the weak-base amines (Fig. 7). The gold complex forms an ion pair with the strong-base amine irrespective of the pH value of the feed solution. As a result, a pH gradient across the SLM cannot be used to back-extract the gold into the stripping solution [16]. In conventional solvent extraction, thiourea has been used for the back-extraction of gold from organic phases containing a quaternary amine such as Aliquat 336 (methyl tricaprylyl ammonium chloride, the alkyl being principally octyl and decyl amine) [18]. Back-extraction is achieved using thiourea (Fig. 8), which competes with the cyanide for the gold. The addition of acid to the stripping solution helped to destabilize the gold complex, and enhanced the stripping of the gold from the

TABLE 5

Permeability of SLMs containing tertiary amines with different chain lengths

Extractant	H_m (%)	
	pH 7	pH 10
Trimethyl	1.8	0.2
Triethyl	2	0.2
Tributyl	3.6	0.2
Triocetyl	5.5	0.4
Alamine 336	9	2

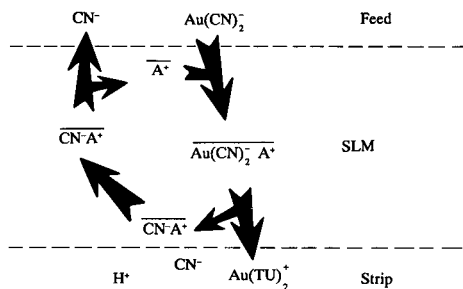


Fig. 7. A schematic illustrating the permeation through a SLM containing quaternary amines, showing the displacement of cyanide from the gold complex by thiourea (TU) in an acidic medium.

organic phase. This approach was tried in the SLM system. The SLM consisted of 20% (v/v) Aliquat 336, in TBP–heptane (50:50, v/v). The feed solution contained 50 mg l^{-1} gold complex buffered at pH 7. The stripping solution consisted of 1 M thiourea in 0.25 M sulphuric acid. Due to the absorbance of thiourea in the UV spectrum, the colorimetric method could not be used for the determination of gold. AAS was therefore chosen as the method of detection.

Two SLMs containing quaternary amines were tested. A high gold permeation (a H_m value of 17.5%) was achieved for the Aliquat 336 SLM. A SLM containing tetrabutylammonium hydroxide (TBAOH) gave a similar H_m value. However, a SLM containing Aliquat 336 displayed better reproducibility and stability than the one containing TBAOH. This is due to the lower solubility of Aliquat 336 in the aqueous phase.

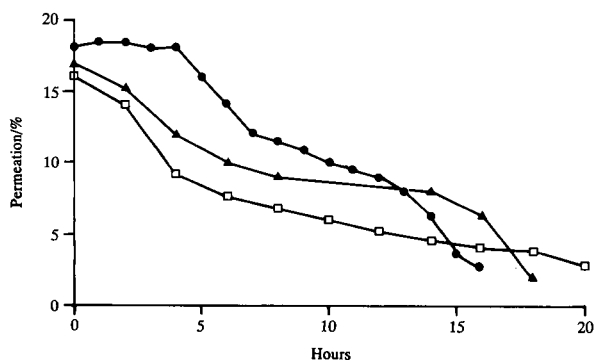


Fig. 8. Stability of SLMs containing amine extractants. ▲ = Tridecylamine, □ = LA-2, ● = Aliquat 336.

It was found that the concentration of Aliquat 336 did not affect the permeation of the gold through the SLM either. A SLM containing 20% (v/v) Aliquat 336 gave the same results as a SLM with 1% (v/v) Aliquat 336. The effect of different diluents on the extraction of gold using SLMs containing Aliquat 336 was also tested. Both heptane and DEB were tested, and performed similarly to feed solutions containing low concentration (below 100 mg l^{-1}) of gold. Aliquat 336 was chosen as the quaternary amine for further tests and the SLM was prepared with 20% Aliquat 336 in heptane–TBP (50:50, v/v).

Stability

The stability of the SLMs containing the three chosen extractants is shown in Fig. 8. The permeation of the SLM containing Aliquat 336 remains stable over approximately 4 h. This is considerably better than the permeation ratio of the other two SLMs. All three SLMs demonstrated a similar gradual decrease in permeation ratio with time.

Selectivity

The selectivity of three SLMs was compared using the experimental conditions as described under experimental.

Samples from two different mines were obtained. Sample A was a concentrate of repulped filter cake, and sample B was a waste solution. Gold plant A uses sodium cyanide in the cyanidation step, while plant B uses calcium cyanide. For all the experiments sample A was buffered at pH 7 without any difficulty. When an attempt was made to buffer sample B, both at pH 7 and pH 10, the calcium precipitated. In the SLM system using Aliquat 336, it is not necessary to buffer the feed solution. However, calcium was found to precipitate in the present system when it came into contact with the sulphuric acid in the stripping solution. To prevent the precipitation of calcium, EDTA was added to sample B which was buffered at pH 10 and used for the selectivity tests. Precipitation still occurred at pH 7, even in the presence of EDTA.

The results of the selectivity study are shown in Fig. 9a and b. The y-axis displays the ratio

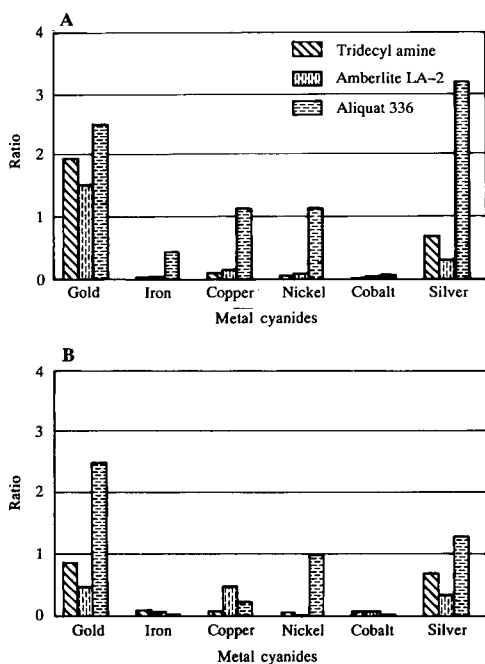


Fig. 9. Selectivity of the various SLMs. The respective concentration of all metals in the feed solutions was 10 mg/l. Sample A: concentrate of a repulped filter cake (pH 7). Sample B: waste solution (pH 10).

between the concentration of the metals in the stripping solution to that in the feed solution.

Although the SLM that contained the Aliquat 336 resulted in the highest enrichment of gold for both samples, it also gave the poorest selectivity. From sample A, considerable enrichment of silver, but also of copper in the stripping solution was evident. Both elements were considerably less extracted from sample B, possibly due to the presence of the EDTA. Nickel was found to co-extract from both solutions, and to a similar extent. A very small amount of iron was extracted from sample A, and even less from sample B. Negligible cobalt was extracted from both samples.

The enrichment of gold by extraction with a SLM containing TDA was considered next. Enrichment factors for sample B were expected to be lower than those for sample A, due to the higher pH value of the feed solution B (pH 10). Compared to the SLM with Aliquat 336, gold was enriched to a lesser extent, but very little of the

base metals were co-extracted. Only silver was co-extracted in significant amounts in both tests.

The SLM containing LA-2 was inferior with respect to enrichment, for both samples tested. It gave the lowest enrichment factor for gold, and although it was more selective than the SLM prepared from Aliquat 336 it was not as selective as the SLM containing TDA. Again, significant co-extraction was experienced with silver. In sample B both silver and copper were co-extracted.

Conclusion

A FIA-SLM system was used to compare various amine extractants on the basis of their selectivity, permeability to gold, and their stability. As was found in a previous investigation [24], FIA proved to be a useful tool for the rapid comparison of the various SLMs.

Two possible mechanisms are postulated for the selective transport of gold from alkaline or neutral cyanide solutions to a second aqueous solution. These mechanisms are based on solvent-extraction processes, and incorporate the simultaneous extraction and back-extraction of gold. The first mechanism was applied to SLMs containing the weak-base amines (primary, secondary, and tertiary amines), and the second to SLMs containing strong-base quaternary amines.

With weak-base amine SLMs, it was found that the presence of a Lewis base modifier (TBP) was necessary to facilitate the extraction of dicyanoaurate(I) from alkaline solutions. Back-extraction was possible with stripping solutions at pH 13. In general the highest permeability for gold was obtained with SLMs containing an amine extractant with an average carbon chain length of between ten and fifteen. Primary amines gave higher permeabilities to gold than the respective secondary amines, which again gave higher permeabilities than tertiary amines.

Strong-base extractants extract gold from feed solutions at almost any pH value. However, the back-extraction is more difficult, and requires an acidified thiourea stripping solution. Of the strong-base extractants tested, Aliquat 336 gave the best results.

Based on the maximum permeation of gold, three of the most promising SLMs were selected

for further testing. These were two weak-base SLMs, TDA and LA-2, and a strong-base SLM, Aliquat 336. The three SLMs displayed similar stabilities. Although the SLM test system was not design to exploit ratios of surface area to volume, it was possible to enrich gold from both neutral and alkaline plant solutions. In the enrichment tests with plant solutions, selective preconcentration of gold were obtained with the TDA SLM. An Aliquat 336 SLM gave higher enrichment, but was less selective.

The simultaneous extraction and back-extraction of gold from plant solutions, using amine SLMs, has potential for automated separation and enrichment of gold before analysis. In addition SLMs offer effective use of small amounts of organic solutions, with high sample-to-organic-phase ratios. The loading and stripping of the organic solution is fast. At dynamic equilibrium, more than 15% of gold permeates through the SLM, during the short contact time (less than 10 s) between the feed solution and the organic phase. In this regard a system that exploits optimum surface-area-to-volume ratios needs investigation.

The investigation was aimed at the analytical applications of this separation technology, but the principles established also apply to the large-scale separation of gold from process solutions. It is therefore possible that the SLM methodology could be scaled up for the recovery or upgrading of gold from solutions such as the eluate from the carbon-in-pulp (CIP) process, or from more complex concentrates such as precious-metal recovery solutions.

This paper is published by permission of Mintek.

REFERENCES

- 1 W.C. Lenahan and R. de L. Murray-Smith, *Assay and Analytical Practice in the South African Mining Industry*, S. Afr. Inst. Min. Metall. Monograph series, No. M6, SAIMM, Johannesburg, 1986.

- 2 G.G. Stanley, *The Extractive Metallurgy of Gold in South Africa*, Vol. 2, National Book Printers, Goodwood, 1987.
- 3 R.V.D. Robert, C. Pohlandt-Watson, H.J. Du Plessis and G.D. Marshall, Report No. M359, Mintek, Randburg, 1985.
- 4 C. Pohlandt, *S. Afr. J. Chem.*, 38 (1985) 110.
- 5 M.J.C. Taylor, D.E. Barnes and G.D. Marshall, *Anal. Chim. Acta.*, 265 (1992) 71.
- 6 M.D. Adams, Mintek, Randburg, personal communication.
- 7 F.J. Algaucil, A. Hernandez and A. Luis, *Hydrometall.*, 24 (1990) 157.
- 8 A. Okuda, *Jap. Pat.*, Jpn. Kokai Tokkyo Koho JP 63,216,930 (1987).
- 9 G.J. McDougal, M.D. Adams and R.D. Hancock, *Hydrometall.*, 18 (1987) 125.
- 10 C.A. Flemming and R.D. Hancock, *J. S. Afr. Inst. Min. Metall.*, 79 (1979) 334.
- 11 C.A. Flemming and G.J.S. Cromberge, *Afr. Inst. Min. Metall.*, 84 (1984) 125.
- 12 N.R. Das and S.N. Bhattacharyya, *Talanta*, 23 (1976) 535.
- 13 T. Groenewalt, *Anal. Chem.*, 6 (1968) 863.
- 14 P.A. Riveros, *Proc. 2nd Int. Conf. Sep. Sci. Technol.*, CIMM, Hamilton, Ontario, October 1–4, 1989, Canadian Society of Chemical Engineering.
- 15 M.B. Mooiman and J.D. Miller, *Hydrometall.*, 16 (1986) 245.
- 16 M. Tromp, M. Buggard and M.J.F. Leroy, *J. Membr. Sci.*, 38 (1988) 295.
- 17 R.Y. Wan and J.D. Miller, *J. Met.*, Dec (1986) 35.
- 18 P.A. Riveros, *Hydrometall.*, 24 (1990) 135.
- 19 A.H. Schwellnus and B.R. Green, *Solv. Extract. Ion Ex.*, 8 (1990) 223.
- 20 S.P. Sandoval and L.E. Schultze, Report RI 9264, Bureau of Mines, Washington, DC, 1989.
- 21 N.N. Li, R.P. Cahn, D. Naden and R.W.M. Lai, *Hydrometall.*, 9 (1983) 277.
- 22 P.R. Danesi and M.B. Mooiman, *Sep. Sci. Technol.*, 19 (1984–85) 857.
- 23 M. Teramoto, H. Matsuyama, H. Takaya and S. Asano, *Sep. Sci. Technol.*, 22 (1987) 229.
- 24 D.E. Barnes and J.F. Van Staden, *Anal. Chim. Acta.*, 261 (1992) 441.
- 25 G.D. Marshall and J.F. Van Staden, *Anal. Instrum.*, 20 (1992) 79.
- 26 J.D. Miller, R.J. Wan, M.B. Mooiman and P.L. Sibrell, *Sep. Sci. Technol.*, 22 (1987) 487.
- 27 M.B. Mooiman, J.D. Miller and M.M. Mena, *Proc. Int. Separation and Extraction Conf. (ISEC'83)*, August 26–September 2, 1983, Denver, CO, The Metallurgical Society of American Inst. of Mining, Metallurgical and Petrochemical Engineers, New York, 1983, p. 530.
- 28 J.D. Miller and M.B. Mooiman, *Sep. Sci. Technol.*, 19 (1984–85) 895.

Preparation of an anion-exchange resin with quaternary phosphonium chloride and its adsorption behaviour for noble metal ions

M. Fujiwara and T. Matsushita

Department of Materials Chemistry, Faculty of Science and Technology, Ryukoku University, Seta, Otsu 520-21 (Japan)

T. Kobayashi, Y. Yamashoji and M. Tanaka

Department of Applied Chemistry, Faculty of Engineering, Osaka University, Yamada-oka, Suita 565 (Japan)

(Received 9th June 1992; revised manuscript received 30th October 1992)

Abstract

An anion-exchange resin was prepared by the reaction of chloromethylated polystyrene with tris(2,6-dimethoxyphenyl)phosphine. It possesses high sorption selectivity for noble metal ions such as gold(III) and platinum(IV). In addition, complete separation between gold(III) and copper(II) was achieved from hydrochloric acid solution with this resin using a column system.

Keywords: Ion exchange; Copper; Extraction; Gold; Heavy metals

The selective separation of heavy metal ions is important in industrial and analytical chemistry. For this purpose, many extractants and chelating resins have been synthesized and some of them have been shown to be practically applicable [1,2]. Triphenylphosphine (Ph_3P) is one of the most popular ligands which can coordinate with noble metal ions [3–5]. It has been applied as an extractant for metal ions such as gold(III), platinum(IV) and palladium(II) from acidic media. In a previous paper [6], it was demonstrated that the extraction abilities of tris(2,6-dimethoxyphenyl)phosphine [(2,6-MeOPh) $_3\text{P}$] and tris(2,4,6-trimethoxyphenyl)phosphine [(2,4,6-MeOPh) $_3\text{P}$] for noble metal ions from hydrochloric acid solutions

are superior to that of Ph_3P , and that the extractions proceed via ion-pair formation between quaternary phosphonium cations and the negatively charged chloro complexes, AuCl_4^- and PtCl_6^{2-} . This means that these methoxy-substituted triarylphosphines have such high basicities that they can readily form phosphonium cations in solutions with low concentrations of hydrochloric acid. These results prompted the development of an anion-exchange resin by the reaction of (2,6-MeOPh) $_3\text{P}$ with chloromethylated polystyrene.

In this paper, the preparation of the anion-exchange resin and its adsorption behaviour towards noble metal ions such as gold(III) and platinum(IV) and other transition metal ions, copper(II) and iron(III), are described. The column separation between gold(III) and copper(II) ions using this resin is also reported.

Correspondence to: M. Fujiwara, Department of Materials Chemistry, Faculty of Science and Technology, Ryukoku University, Seta, Otsu 520-21 (Japan).

EXPERIMENTAL

Materials

Standard solutions of metal ions were prepared by dissolving NaAuCl_4 , $\text{FeNH}_4(\text{SO}_4)_2 \cdot 12\text{H}_2\text{O}$ and CuCl_2 in 0.1 M hydrochloric acid and used after dilution to the required concentration. A standard solution of platinum(IV) was prepared by dissolving $\text{H}_2\text{PtCl}_6 \cdot 6\text{H}_2\text{O}$ in 1.0 M hydrochloric acid. $(2,6\text{-MeOPh})_3\text{P}$ was prepared in a similar manner to that described in the literature [7,8]. Chloromethylated polystyrene (100-mesh beads, divinylbenzene cross-linkage = 3%, chlorine content = 22.87%) was obtained from Mitsubishi Kasei. Other reagents were of analytical-reagent grade.

Measurements

Atomic absorption spectrometric measurements were made on a Nippon Jarrell Ash AA-8500 Mark II spectrometer using an oxygen-acetylene or nitrous oxide-acetylene flame. Infrared spectra were recorded on a Shimadzu IR-470 grating spectrophotometer. UV absorption spectra were recorded on a Hitachi 340 recording spectrophotometer.

Preparation of anion-exchange resin

After chloromethylated polystyrene beads (5.0 g) had been swollen in dioxane (700 cm^3) for 5 h at room temperature, $(2,6\text{-MeOPh})_3\text{P}$ (15.0 g) was added and the mixture was mechanically stirred for 24 h at 70°C . After the dioxane had been decanted, fresh dioxane (300 cm^3) was added to the residue of beads and the mixture was stirred for 4 h at room temperature to remove physically adsorbed $(2,6\text{-MeOPh})_3\text{P}$. The beads were collected on a glass filter, washed with dioxane and then diethyl ether and dried in vacuo. The results of elemental analyses for the anion-exchange resin were C 68.26, H 6.42, Cl 12.22, P 3.19%. The amount of $(2,6\text{-MeOPh})_3\text{P}$ covalently bound to the beads was calculated on the basis of the elemental analyses. The $(2,6\text{-MeOPh})_3\text{P}$ content in the resin was 1.0 mmol g^{-1} . The unreacted $(2,6\text{-MeOPh})_3\text{P}$ was recovered from the decanted solution, filtrates and washings by evaporation. The amount of recovered $(2,6\text{-MeOPh})_3\text{P}$

was 5.0 g. The amount of bound $(2,6\text{-MeOPh})_3\text{P}$ can be calculated by subtracting 5.0 g from the amount of compound added. Its value implies that 1 g of the resin contained 1 mmol of $(2,6\text{-MeOPh})_3\text{P}$, which is in good agreement with that calculated above. These results indicate that 30% of the chlorine was electrostatically bound to the beads as a counter anion to a quaternary phosphonium, and that 70% of chlorine was covalently bound, i.e., unreactive. The scheme for the preparation of the anion-exchange resin is shown in Fig. 1.

Procedure for adsorption of metal ions on the resin in the batch system

Adsorption experiments on metal ions in the batch system were carried out by using a 10-cm^3 test-tube, with a stopper, containing an aqueous solution of metal ion [gold(III), copper(II), iron(III), or platinum(IV)] ($5.0 \times 10^{-4} \text{ M}$, 10 cm^3) and the resin (50 mg). The test-tube was shaken for an appropriate time from 5 to 180 min at room temperature by using a shaker. When the maximum capacity of this resin toward gold(III) ion was measured, an aqueous solution of gold(III) ion ($1.0 \times 10^{-2} \text{ M}$, 25 cm^3) was used and the shaking time was 24 h. After shaking, the resin was separated by filtration, the filtrate was diluted with water and the concentration of the metal ions that remained in it was determined by atomic absorption spectrometry for gold(III), copper(II) and iron(III) and by spectrophotometry for platinum(IV).

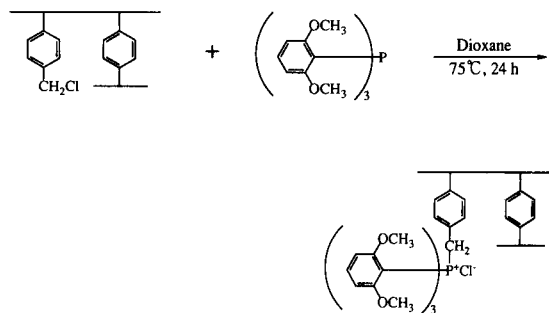


Fig. 1. Scheme for the preparation of the anion-exchange resin.

Procedure for adsorption of metal ions on the resin in the column system

Separation of gold(III) and copper(II) ions in the column system was carried out under the following conditions. A column (i.d. 8 mm) was packed with 3 g of the resin, which was fully swollen in advance with 0.1 M hydrochloric acid. Hydrochloric acid (0.1 M, 250 cm³) containing both copper(II) (5.0×10^{-3} M) and gold(III) (5.0×10^{-4} M) was eluted at a flow-rate of 0.5 cm³ min⁻¹. Eluates were fractionated into 5-cm³ portions, which were then diluted with water to determine the concentrations of the eluted metal ions. For the elution of the adsorbed gold(III) ion on the resin, a buffer solution of 0.5 M NH₃–0.1 M NH₄Cl was used as the eluent.

RESULTS AND DISCUSSION

Characterization of the anion-exchange resin

As described under Experimental, a reasonable amount of (2,6-MeOPh)₃P (30%) could be incorporated into chloromethylated polystyrene beads, which corresponds to an anion-exchange capacity of 1.0 mmol g⁻¹. This was confirmed by the result for the loading capacity (ca. 1 mmol g⁻¹) of the resin towards gold(III) ion: the adsorption experiment was carried out in the presence of gold(III) ion in excess over the resin capacity in the batch system as described under experimental. This ion-exchange capacity is larger than that (ca. 0.08 mmol g⁻¹) of the resin obtained by the reaction of Ph₃P with chloromethylated polystyrene beads under the same conditions for (2,6-MeOPh)₃P. Such a high reactivity of (2,6-MeOPh)₃P toward the chloromethylated polystyrene can be ascribed to its high basicity [9].

Figure 2 shows the IR spectra of the anion exchange resin, (2,6-MeOPh)₃P and the chloromethylated polystyrene beads. The spectrum of the resin exhibits characteristic bands due to (2,6-MeOPh)₃P at slightly higher frequencies and those due to chloromethylated polystyrene at almost the same frequencies. Although the intensities of the latter bands are relatively weaker than those of the former bands, the intensity of the band observed around 680 cm⁻¹ is

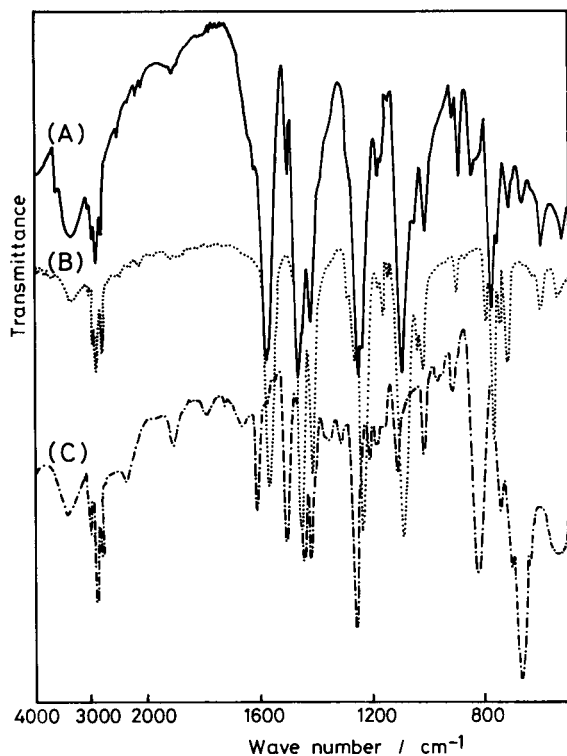


Fig. 2. IR spectra of the (A) the anion-exchange resin, (B) tris(2,6-dimethoxyphenyl)phosphine and (C) chloromethylated polystyrene.

much weaker than that of chloromethylated polystyrene. Because C–Cl stretching vibrations due to chloromethyl groups should be observed in this region[10], the IR spectrum of the resin indicates that (2,6-MeOPh)₃P is incorporated into the chloromethylated polystyrene by the formation of quaternary phosphonium chloride as shown in Fig. 1.

Effect of shaking time on the loading capacity

Figure 3 shows the effect of shaking time on the loading capacity of the resin for metal ions in the batch system. The concentration of hydrochloric acid was 0.1 M for gold(III), copper(II) and iron(III) and 1.0 M for platinum(IV). The loading capacities for gold(III) and platinum(IV) reached 0.080 and 0.075 mmol g⁻¹, respectively, after shaking for 3 h. On the other hand, almost no copper(II) and iron(III) ions were adsorbed on the resin after shaking for 3 h. These results

indicate that this resin possesses a high selectivity for noble metal ions. Hence the selective separation of gold(III) or platinum(IV) from acidic solutions containing the above-mentioned heavy metal ions may be accomplished.

Effect of HCl concentration on adsorption capacity

The capacities of the resin toward gold(III), platinum(IV), copper(II) and iron(III) ions were found to depend on the HCl concentration of the sample solutions. For gold(III) and platinum(IV) ions the capacities gradually decreased with an increase in HCl concentration from 0.1 to 3.2 M. However, the capacity for iron(III) ion increased linearly with increase in HCl concentration. In particular, almost no copper(II) ion was adsorbed on the resin over the range 0.1–5.0 M HCl. For gold(III) and platinum(IV) ions, the main species adsorbed on the anion-exchange resin are $[\text{AuCl}_4]^-$ and $[\text{PtCl}_6]^{2-}$, respectively. These anionic species are formed even at a lower concentration of HCl [11,12]. As the HCl concentration is increased, the relative concentrations of these anionic species should increase but free chloride ions also increase in concentration and act as a competitive adsorbate against the metal ions of interest. Therefore, the capacities for gold(III) and platinum(IV) were gradually lowered with increase in HCl concentration. On the other hand, with copper(II) and iron(III) ions, much higher HCl concentrations are required for the forma-

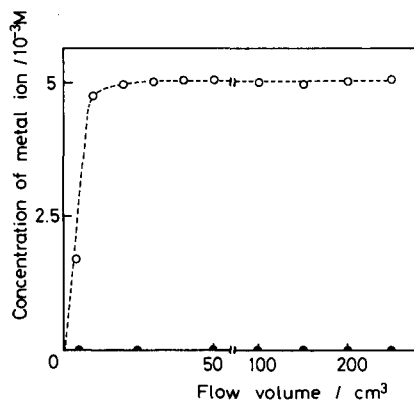


Fig. 4. Breakthrough curves of (●) gold(III) and (○) copper(II) ions in the column system.

tion of $[\text{CuCl}_4]^{2-}$ or $[\text{CuCl}_3]^-$ and $[\text{FeCl}_4]^-$, which are considered to be the adsorbed species on the resin. Hence the capacities towards these ions increased linearly with increase in HCl concentration. The adsorption behavior of the present anion-exchange resin towards the metal ions reflects the relative stabilities of their anionic chloro complexes, just like common basic anion-exchange resins such as Dowex-1 and Amberlite IRA-400(Cl).

Separation between gold(III) and copper(II) in the column system

The anion-exchange resin was applied as an adsorbent for the column separation of gold(III) and copper(II) ions. Figure 4 shows the breakthrough curves of the gold(III) and copper(II) ions, which were obtained under the conditions described under Experimental. The copper(II) ions was quickly eluted and its concentration in the effluents reached a feed concentration of 5×10^{-3} M within an effluent volume of 30 cm^3 . On the other hand, the gold(III) ion was completely adsorbed on the resin and was not eluted even with effluent volumes over 250 cm^3 . This means that the complete separation of two metal ions is achieved by this resin when one ion is anionic and the other is not.

Reflectance spectrum of gold(III) adsorbed on the resin

Figure 5 shows the diffuse reflectance spectrum of the resin with gold(III) ions adsorbed

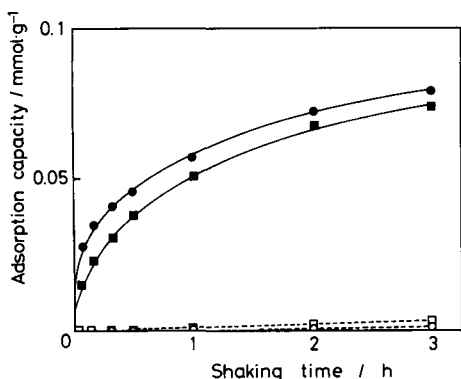


Fig. 3. Effect of shaking time on the loading capacities of the anion-exchange resin towards (●) gold(III), (■) platinum(IV), (○) copper(II) and (□) iron(III) ions.

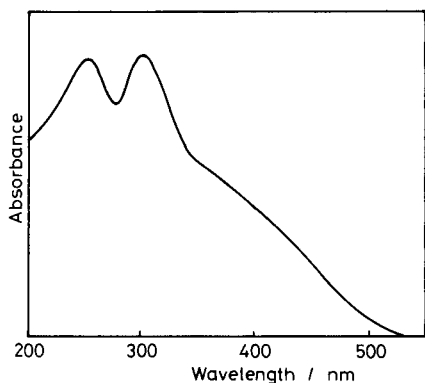


Fig. 5. Reflectance spectrum of the anion-exchange resin with gold(III) ions adsorbed from 0.1 M hydrochloric acid solution.

from 0.1 M hydrochloric acid solution. Two absorption maxima were observed at 255 and 304 nm with a shoulder around 390 nm. The reflectance spectrum of the resin itself shows two absorption maxima at 255 and 295 nm. The solution spectrum of gold(III) in 0.1 M hydrochloric acid where gold(III) ions exist as the anionic chloro complex $[\text{AuCl}_4]^-$ shows an absorption peak at 314 nm with a weak shoulder band around 400 nm [13]. These results indicate that gold(III) ions are adsorbed on the resin as the anionic complex $[\text{AuCl}_4]^-$.

Recovery of gold(III) adsorbed on the resin

In order to recover the adsorbed gold(III) ions on the resin, two processes in the batch system were preliminarily examined. One involved treatment with buffer solutions of 0.1 M CH_3COOH –0.1 M CH_3COONa at different pH values (3–5),

but the recovery of gold(III) was very low. The other involved treatment with a mixed solution of 0.1 M NH_4Cl –0.5 M NH_3 . In this process, a reasonable amount of gold(III) ion could be stripped from the resin. Therefore, this mixed solution was employed as the eluent to recover the adsorbed gold(III) ion in the column system. The gold(III) was quickly eluted within an elution volume of 50 cm^3 with a recovery of 17%.

REFERENCES

- 1 E.B. Sandell and H. Onishi (Eds.), *Photometric Determination of Traces of Metals*, Wiley-Interscience, New York, 1978.
- 2 T. Sekine and Y. Hasegawa (Eds.), *Solvent Extraction Chemistry*, Dekker, New York, 1977.
- 3 P. Senise and F. Levi, *Anal. Chim. Acta*, 30 (1960) 509.
- 4 M. Mojski, *Talanta*, 27 (1980) 7.
- 5 K.R. Koch and J.E. Yates, *Anal. Chim. Acta*, 147 (1983) 235.
- 6 Y. Yamashoji, T. Kawaguchi, T. Matsushita, M. Wada, M. Tanaka and T. Shono, *Anal. Sci.*, 4 (1988) 431.
- 7 M. Wada and S. Higashizaki, *J. Chem. Soc., Chem. Commun.*, (1984) 482.
- 8 M. Wada, S. Higashizaki and A. Tsuboi, *J. Chem. Res. (M)*, (1985) 467.
- 9 Y. Yamashoji, T. Matsushita, M. Wada and T. Shono, *Chem. Lett.*, (1988) 43.
- 10 R.M. Silverstein, G.C. Bassler and T.C. Morrill (Eds.), *Spectrometric Identification of Organic Compounds*, Wiley, New York, 4th edn., 1981.
- 11 F.A. Cotton and G. Wilkinson (Eds.), *Advanced Inorganic Chemistry*, Wiley, New York, 2nd edn., 1966.
- 12 K. Brajter and K. Slonawska, *Anal. Lett.*, 21 (1988) 311.
- 13 F.H. Fry, G.A. Hamilton and J. Turkevich, *Inorg. Chem.*, 5 (1966) 1944.

Determination of urinary fluoride by ion chromatography

Yoshimasa Michigami, Yasuyoshi Kuroda, Kazumasa Ueda and Yoshikazu Yamamoto

*Department of Chemistry and Chemical Engineering, Faculty of Technology, Kanazawa University, 2–40 Kodatsuno,
Kanazawa 920 (Japan)*

(Received 15th July 1992; revised manuscript received 30th October 1992)

Abstract

An ion chromatographic method was developed for the determination of trace amounts of free urinary fluoride, using an ODS column dynamically coated with cetyldimethyl-*n*-butylammonium bromide. The many inorganic and organic anions commonly found in urine had little effect on the determination of fluoride.

Keywords: Ion chromatography; Fluoride; Urine

Fluoride is widely present in biological fluids and tissues, especially in bone and tooth. It is easily absorbed but is excreted slowly from the body, which may result in chronic poisoning. Fluoride has a strong effect on most enzymes and acute poisoning by fluoride is almost always caused by blockage of the enzyme functions. Hence monitoring of fluoride in the body is important.

Many methods, including ion-selective electrodes [1,2], gas chromatography [3,4] and graphite furnace molecular absorption spectrometry [5], have been developed for the determination of fluoride in biological fluids. Some ion chromatographic procedures have been reported for the determination of fluoride [6–10], but few have been applied to the determination of fluoride in biological fluids. Because fluoride has weak retention on anion-exchange resins it tends to co-elute at short retention times with co-existing cations and anions in biological fluids. In this paper, the determination of free fluoride in urine

by ion chromatography using a coated column is described. The necessary sample treatment is simply dilution after removal of co-existing cations.

EXPERIMENTAL

Apparatus and reagents

The ion chromatographic equipment consisted of a pump (CCPD, Tosoh, Japan), a variable-wavelength ultraviolet–visible detector (UV-8000), a column oven (CO-8000) and a flat-bed pen recorder (YEW Type 3066, Yokogawa, Japan).

All chemicals were analytical-reagent grade, and deionized, distilled water, further filtered through a 0.45- μ m membrane filter, was used throughout. Cetyldimethyl-*n*-butylammonium bromide (CDMBuABr) was synthesized from cetyldimethylamine and *n*-butyl bromide and purified with silica gel.

Dynamically coated columns were prepared using columns (150 \times 4.6 mm i.d.) packed with ODS resin (Capcell pack C₁₈, AG-120; Shiseido). The coating procedure was similar to that used in

Correspondence to: Y. Michigami, Department of Chemistry and Chemical Engineering, Faculty of Technology, Kanazawa University, 2–40 Kodatsuno, Kanazawa 920 (Japan).

TABLE 1

Chromatographic conditions

Column	ODS column coated with cetyldimethyl- <i>n</i> -butylammonium bromide
Flow-rate	0.8 ml min ⁻¹
Column temperature	35°C
Sample loop	100 μl
Eluent	0.8 mM nicotinate–0.01 mM urate (pH 9.0)
Cleaning solution	5.0 mM nicotinate–0.1 mM urate (pH 9.0)

previous work [11]. The ion-exchange capacity of the CDMBuABr-coated column was 0.08 meq g⁻¹ for the eluent anion and the theoretical plate number of the column for fluoride was about 4800. Regeneration of the column was carried out by washing with methanol and then coating again with CDMBuABr.

The chromatographic conditions are given in Table 1.

Procedure

A 5-ml urine sample was diluted to 10 ml with deionized, distilled water. The dilute solution was then passed through a cation-exchange resin (Dowex 50W-X8, H⁺ form) column to remove cations in the urine. A further fivefold diluted solution of the sample was injected on to the column. A chromatogram was recorded for 20 min at 245 nm, at which wavelength the maximum response of fluoride was observed. The column was flushed with cleaning solution for 20 min to remove the strongly retained anions and was then conditioned with the eluent until the next injection. The concentration of fluoride was calculated by using calibration graphs that were constructed daily.

RESULTS AND DISCUSSION

Column and eluent

The columns coated with cetyltrimethylammonium bromide and cetylpyridinium chloride gave broad peaks and overlapping peaks of fluoride, hydrogen carbonate and lactate, whereas the col-

umn coated with CDMBuABr gave a satisfactory resolution of fluoride and the other anions.

The effect of the eluent pH on the retention times of acetate, hydrogencarbonate, chloride, fluoride and lactate are shown in Fig. 1. In the low pH range (5.5–8.0) the broad peak of hydrogencarbonate interfered with the peak of fluoride. The ratios of the retention times of the anions to that of fluoride were independent of the eluent pH. The optimum eluent adopted was 0.8 mM nicotinate–0.01 mM urate (pH 9).

Retention times of various anions

The retention times of various inorganic and organic anions are given in Table 2. The retention time of fluoride was 16.1 min and the retention times of all the anions studied were longer than this. Hydrogencarbonate, glutamate and lactate, usually present at significant levels in urine, were eluted near the retention time of fluoride. However, 2 mM hydrogencarbonate, 2 mM glutamate and 0.8 mM lactate, which correspond to

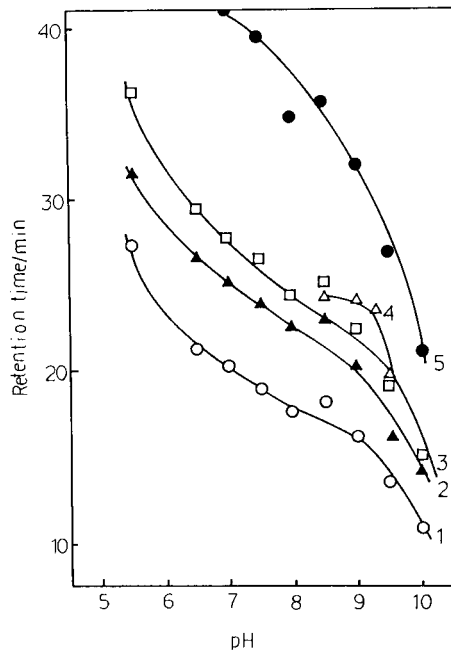


Fig. 1. Effect of eluent pH on the retention times of various anions. 1 = Fluoride; 2 = acetate; 3 = lactate; 4 = hydrogencarbonate; 5 = chloride. Other conditions as in Table 1.

TABLE 2
Retention times of various anions

Anion	Retention time (min)	Anion	Retention time (min)
Acetate	19.2	D-Glucuronate	> 35
Hydrogen-carbonate	25.9	Guanidoacetate	> 35
Chloride	30.0	Hippurate	> 35
Fluoride	16.1	Nitrate	> 35
Glutamate	25.9	α -Ketoglutarate	> 35
Lactate	20.6	Pyruvate	> 35
Urate	26.4	Sulphate	> 35
Oxaloacetate	35.0		

about 40 times the concentrations in urine [12], were tolerated. Anions such as D-glucuronate, guanidoacetate hippuric acid, nitrate, α -keto-glutarate and sulphate, usually present in urine, were strongly retained on the column so it was difficult to elute them with the eluent. However, these anions could be removed from the column with 5.0 mM nicotinate–0.2 mM urate cleaning solution within 15 min. The column was then flushed for 20 min with the above cleaning solution.

Calibration

The calibration graph was linear up to 50.0 $\mu\text{g ml}^{-1}$ fluoride. The detection limit was 0.06 μg

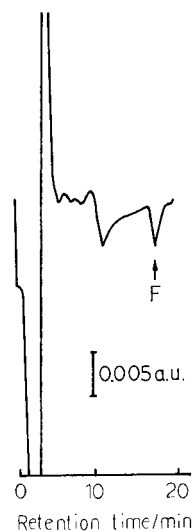


Fig. 2. Chromatogram of a urine sample. Conditions as in Table 1.

TABLE 3
Results of determination of fluoride in urine samples

Sample No.	Fluoride concentration ($\mu\text{g ml}^{-1}$)	
	Proposed method	La-ALC method ^a
1	0.90	0.89
2	1.95	1.51
3	ND ^b	ND
4	3.33	3.44
5	ND	ND
6–15	2.97 \pm 0.89 ^c	–

^a Lanthanum–alizarin complexone method [13] using the standard addition method. ^b Not detected. ^c Mean \pm standard deviation.

ml^{-1} . The relative standard deviation ($n = 5$) was 4.92% for a 1 $\mu\text{g ml}^{-1}$ concentration.

Chromatogram of a urine sample

A typical chromatogram of urine is shown in Fig. 2. The fluoride peak (retention time 16 min) was found to be free from interferences from the usual co-existing anions.

Recovery of fluoride in urine

The recoveries of fluoride determined by adding known concentrations (5 and 10 $\mu\text{g ml}^{-1}$) of fluoride to urine were 98.3–101.3% and the relative standard deviation of was 2.95% ($n = 5$).

Determination of fluoride in urine

Fluoride was determined in 15 urine samples from male subjects. The results obtained are given in Table 3. The values determined by the proposed method agreed well with those obtained by the lanthanum–alizarin complexone spectrophotometric method [13].

REFERENCES

- 1 M. Nedeljković, B. Antonijević and V. Malović, *Analyst*, 116 (1991) 477.
- 2 J.F. van Staden and S.D.J. van Rensburg, *Analyst*, 116 (1991) 807.
- 3 R. Ikenishi and T. Kitagawa, *Chem. Pharm. Bull.*, 36 (1988) 810.
- 4 R. Ikenishi, T. Kitagawa, M. Nishiuchi, K. Takehara, H. Yamada, I. Nishino, T. Umeda, K. Iwatani, Y. Nakagawa, M. Sawai and T. Yamashita, *Chem. Pharm. Bull.* 36 (1988) 662.

- 5 M. Gómez, I. Rodríguez, C. Càmara and M.P. Palacios, *Analyst*, 115 (1990) 553.
- 6 C. Saigne, S. Krchner and M. Legrand, *Anal. Chim. Acta*, 203 (1987) 11.
- 7 M. Ichikuni and T. Tsurumi, *Anal. Sci.*, 6 (1990) 111.
- 8 V.B. Conrad and W.D. Brownlee, *Anal. Chem.*, 60 (1988) 365.
- 9 W. Kroth and J. Ellis, *Talanta*, 31 (1984) 467.
- 10 R.T. Talasek, *J. Chromatogr.*, 465 (1989) 1.
- 11 Y. Michigami, Y. Yamamoto and K. Ueda, *Analyst*, 114 (1989) 1201.
- 12 Japan Society of Biological Chemistry, *Biological Chemistry Databook (I)*, Tokyo Kagaku Dohjin, Tokyo, 1979, p. 1597.
- 13 H. Hashitani, H. Yoshida and H. Muto, *Bunseki Kagaku*, 16 (1967) 44.

Structure–activity relationship study on paraffin inhibitors for crude oils (INIPAR model II)

M. Cristante and J.-L. Selves

Groupe de Recherche Instrumentation et Mesure, Département Mesures Physiques, IUT, 115 Route de Narbonne, 31077 Toulouse Cedex (France)

G. Grassy

Groupe de Recherche en Modélisation, 31 Allées Jules Guesdes, 31400 Toulouse (France)

J.P. Colin

DRD.P, Service Analyses Pétrolières, ELF Aquitaine, Etablissement de Boussens, 31360 Saint Martory (France)

(Received 23rd March 1992; revised manuscript received 28th September 1992)

Abstract

Principal component analysis was applied in an attempt to predict the activity of paraffin inhibitors on crude oils. Using a data matrix consisting of activity and physico-chemical parameters it was possible to classify crude oils and chemical inhibitors into different families. From the relationships between these families, a method (INIPAR model) which permits the choice of the best paraffin inhibitor was proposed.

Keywords: Principal component analysis; Crude oils; Oil additives; Paraffin inhibitors; Structure–activity relationships

The extraction of crude oil from an oilfield is a production process facing several difficulties which depend on the nature of the field, the climate, the crude oil, etc. [1–3]. These difficulties must be overcome in order to maintain a high level of crude oil production. Every production delay or pause causes large financial losses. The possibility of paraffin deposition on the production equipment is a very important constraint which must be correctly evaluated so as to avoid frequent production stoppages. The risk of paraffin deposition is attributed first, and most impor-

tant, to the nature of the crude oil, and second to the climate (exploitation temperatures).

At present there is no set solution to resolve the problem of paraffin deposition. Although several methods are available to reduce the problem, it is still necessary to choose the most effective solution based on the exploitation conditions. The method usually adopted consists in adding small amounts of chemical additives to the crude oil in order to suppress paraffin deposition. The essential role of these additives is to act on either the crystallization of the paraffin [4,5] or on the crude oil viscosity [6–9]. When this method is ineffective, other possibilities exist, but these are less economical and, unlike the use of additives, are not preventative. The suppression of deposition

Correspondence to: J.-L. Selves, Groupe de Recherche Instrumentation et Mesure, Département Mesures Physiques, IUT, 115 Route de Narbonne, 31077 Toulouse Cedex (France).

can be done thermally (hot oil, heaters, etc.) [10], mechanically (scrapers) [1] or chemically (with solvents) [12,13].

Despite the advantages of using additives over other methods, there still remains the task of selecting the appropriate additive. This task is complicated by the absence of a reliable, inexpensive method for matching the most effective additive to a crude oil [14–16].

In a previous paper [17], additives and crude oils were classified based on their physico-chemical properties. Also, the additives' capacity to diminish the crystallization temperature (T_c) of the paraffin contained in a crude oil was measured. In this work, the crude oil classification was improved and the additives' effectiveness to reduce the deposition of paraffin and to lower the crude oil viscosity were measured. The aim of this study was to develop a system capable of

assisting in the selection of an additive. The selection of the additive depends on the type of crude oil and on the effect sought (crystallization temperature, paraffin deposition or viscosity) [18].

EXPERIMENTAL

Crude oils

Sixty-seven crude oils were investigated. In order to classify each crude oil, the following analytical characteristics were determined: the weight percentage of paraffin (variable *Par*); the weight percentage of paraffin having a carbon atom number greater than 29 (variable *C30*); the weight percentage of asphaltene (variable *As*); and the crystallization temperature (variable *TCCB*). The experimental methods for measuring these characteristics have been described previously [17,18].

TABLE 1

IR frequencies (cm^{-1}) used to identify petroleum samples involved in oil spills

[19]	[20]	[21]	[22]	[23]	[24]	This work
1695			1630			
1600		1600	1605 1520	1600	1600	1604
1460		1460	1460			
1375		1375	1375		1375	
1305			1305	1305		
1165	1160		1165 1155	1160	1160	1168
	1145			1145		1155
	1070			1070		1076
1035	1020	1025	1030	1020	1030	1032
	955		960	955		
	915		918	918		
	890		890	890		890
875	870	870	870	870	870	870
	845		845	849		846
	820					833
815	810	810	810	810	810	810
	805					
	790		795	790		790
	780		780	780		783
	770					
	765		765	765		767
745	740		740	745	740	743
725	725					724
	720	720	720	720	720	
	695		695			
			675			

TABLE 2

IR bands (cm^{-1}) with correlation coefficient $R > 0.90$

	1604	1168	1155	1076	1032	890	870	846	833	810	790	783	767
1168	0.91												
1155	0.91	0.99											
1076		0.96	0.96										
1032				0.95									
890	0.92	0.91	0.91										
870	0.96	0.93	0.93			0.96							
846	0.91	0.92	0.93										
833							0.95						
810							0.94	0.94	0.92				
790										0.96			
783										0.92	0.97		
767												0.92	
743													0.92

In addition to these characteristics, new physico-chemical parameters were determined from infrared and proton NMR spectrometry, as follows.

Infrared spectrometry. The large number of oil spills that have occurred during the past decade have led to increased efforts to find suitable analytical techniques to characterize petroleum products. Several groups of workers [19–24] have found that with the appropriate data analyses, infrared spectrometry can be used to identify a large proportion of the petroleum samples involved in these oil spills. A list of frequencies, used with success by these groups of workers, are given in Table 1.

We recorded infrared spectra (Bruker IFS-88 spectrometer) of the crude oil samples; the maximum absorbance of the fifteen principal bands between 720 and 1600 cm^{-1} were used to characterize the samples. The wavenumbers of these bands were as follows: 1064 ± 4 , 1168 ± 2 , 1155 ± 2 , 1076 ± 1 , 1032 ± 2 , 890 ± 2 , 870 ± 6 , 846 ± 2 , 833 ± 1 , 810 ± 5 , 790 ± 1 , 783 ± 2 , 767 ± 2 , 743 ± 2 and $724 \pm 4 \text{ cm}^{-1}$. Owing to their large analytical errors, the strong hydrocarbon peaks at 1375 and 1460 cm^{-1} were not used in the analysis, in accordance with previous results [20,22]. Because no sample exhibited an absorption in the vicinity of 1980 cm^{-1} , this value was chosen to define the horizontal baseline.

The measurement of all fifteen bands may not be necessary for identifying the crude oils. There is undoubtedly redundant information present in each infrared spectrum.

To reveal any high degree of correlation between two peaks and to justify the selection of only one of them, the correlation coefficient for all 122 pairs of absorption bands for each crude oil was computed. Table 2 lists those correlation coefficients (R) which exceed 0.90.

An examination of Table 2 results in the elimination of the peaks at 1168, 1155, 890, 870 and 846 cm^{-1} in favour of the peak at 1604 cm^{-1} , which designates an aromatic absorption. The 1076 cm^{-1} peak which is highly correlated with the 1032 cm^{-1} peak ($R = 0.95$) is eliminated. The deletion of the peaks at 833, 790 and 783 cm^{-1} leaves the 810 cm^{-1} peak. The peak at 767 cm^{-1} is suppressed in favour of the peak at 743 cm^{-1} ($R = 0.92$). Finally, of those studied, only five bands are independent; these frequencies, at

TABLE 3

IR bands (cm^{-1}) with correlation coefficients $R < 0.90$

	1604	1032	810	743
1032	0.84			
810	0.9	0.88		
743	0.58	0.7	0.73	
724	-0.33	-0.2	-0.24	0.3

TABLE 4
¹H NMR assignments

Parameter	Chemical shift range (ppm from Me ₄ Si)	Aromatic hydrogen type	Aliphatic hydrogen type
<i>Har</i>	8.5–6.0	Aromatic hydrogen	
<i>Hal</i>	3.8–1.9	Hydrogen in CH, CH ₂ and CH ₃ groups α to an aromatic ring	
<i>Hbe</i>	1.9–1.0	Hydrogen in CH and CH ₂ groups β or further from an aromatic ring; hydrogen in CH ₃ groups δ to an aromatic ring	Hydrogen in CH and CH ₂ groups; hydrogen in saturated rings of C ₃ or more
<i>Hga</i>	1.0–0.5	Hydrogen in CH ₃ groups or further from an aromatic ring	Hydrogen in CH ₃ aliphatic groups

1604, 1032, 810, 743 and 721 cm⁻¹, are stronger and better defined than the bands eliminated.

No correlation coefficient among the possible pairs is greater than 0.90. Table 3 lists the correlation coefficients for these final five absorption bands.

In order to conduct more objective comparisons and as the exact thickness of the samples analysed is not known, the ratio of absorbances was calculated. These ratios are $I_1 = A_{1604}/A_{724}$, $I_2 = A_{1032}/A_{724}$, $I_3 = A_{810}/A_{724}$, $I_4 = A_{743}/A_{724}$, $I_5 = A_{1604}/A_{743}$, $I_6 = A_{1032}/A_{743}$, $I_7 = A_{810}/A_{743}$,

TABLE 5

Activity on the viscosity of seven crude oils

Additive	V ₁	V ₂	V ₃	V ₄	V ₅	V ₁₀	V ₁₁
1	1.55	1.60	46.25	140.00	13.15	10.00	1.40
2	3.50	1.95	7.40	93.30	3.55	4.45	1.15
3	1.25	1.00	18.50	140.00	1.30	0.20	1.00
4	2.35	0.80	92.50	140.00	18.40	0.05	2.35
5	2.35	1.15	92.50	140.00	15.35	0.10	2.35
6	2.80	1.35	23.10	140.00	3.70	8.00	1.40
7	3.50	1.65	12.30	70.00	3.05	8.00	1.15
8	2.80	0.75	185.00	140.00	5.40	0.05	2.35
9	1.15	1.20	2.20	1.20	0.70	0.80	0.40
10	1.15	1.25	1.50	2.80	1.00	1.60	0.90
11	1.25	1.20	2.10	1.10	1.15	0.20	0.80
12	2.80	1.25	92.50	140.00	3.55	6.65	1.40
13	1.25	0.75	61.70	280.00	4.85	0.10	2.35
14	1.55	1.20	3.40	16.20	1.05	0.65	1.00
15	2.35	0.75	61.70	280.00	9.20	0.30	2.35
16	1.75	0.70	61.70	140.00	2.55	0.05	2.35
17	1.15	1.10	2.20	0.95	1.15	0.20	0.90
18	1.40	1.20	4.10	140.00	1.90	8.00	1.00
19	2.35	0.75	92.50	280.00	18.40	0.10	2.35
20	2.80	1.40	92.50	140.00	7.10	10.00	1.75
21	2.35	1.40	4.10	140.00	1.25	6.65	1.00
22	1.15	1.15	2.30	0.90	0.95	1.60	0.90
23	3.50	0.85	92.50	140.00	11.50	5.00	1.75
24	0.70	0.80	61.70	280.00	1.60	4.00	1.75

$I_8 = A_{1604}/A_{1032}$, $I_9 = A_{810}/A_{1032}$ and $I_{10} = A_{810}/A_{1604}$. These parameters represent the different proportions of the hydrocarbon families (aromatics, saturated compounds, etc.) constituting the crude oil.

NMR spectrometry. Four parameters were obtained from ^1H NMR spectrometry. A spectrum of a typical sample is shown in Fig. 1. The ^1H NMR spectra are divided into the four sections [25,26] listed in Table 4 and their integrated intensities were computed.

Measurement of activity

Viscosity. Crude oil viscosity was measured with a Rheomat 30 viscometer. A sample of crude oil was mixed with 200 mg kg^{-1} of additive. The sample was heated at 70°C for 4 h and kept at 45°C for 6 days to remove the thermal history of the crude oil. The measuring cell, which contained 100 ml of sample, was introduced into a thermostated bath. The bath temperature programme was 45°C for 20 min, decreased at 15°C h^{-1} to 0°C . The shear rate applied during the analysis was 2.64 s^{-1} . The viscosity value (V_x) was measured at the temperature T_v defined as $T_v =$

TABLE 6

Activity on the paraffin deposition (weight of deposit) of five crude oils

Additive	D_1	D_2	D_5	D_6	D_7
1	2.00	1.45	2.30	1.45	1.60
2	2.15	1.75	1.40	1.25	2.70
3	0.95	0.75	0.95	1.10	1.15
4	0.75	1.25	0.90	0.85	1.50
5	1.45	0.90	0.80	0.75	1.10
6	2.20	1.95	1.15	1.45	2.00
7	2.15	1.85	1.05	1.15	1.20
8	1.55	1.60	0.85	0.75	1.25
9	1.10	1.20	1.00	0.95	0.85
10	0.95	1.10	1.10	0.65	1.25
11	0.95	1.35	1.05	1.00	1.00
12	2.00	1.65	1.20	1.05	1.50
13	0.90	0.80	0.75	0.95	1.85
14	0.70	1.90	1.20	1.05	1.10
15	0.65	0.90	0.85	1.00	1.85
16	0.70	0.75	0.75	1.15	1.85
17	1.00	1.20	1.00	0.85	1.00
18	1.90	2.15	1.95	1.65	2.20
19	1.10	1.70	0.90	1.00	1.85
20	1.95	1.60	1.30	1.45	1.50
21	2.10	1.50	1.65	1.85	2.70
22	0.85	1.30	1.00	0.95	1.10
23	1.60	1.25	1.25	1.20	1.40
24	0.95	2.15	0.75	1.10	2.00

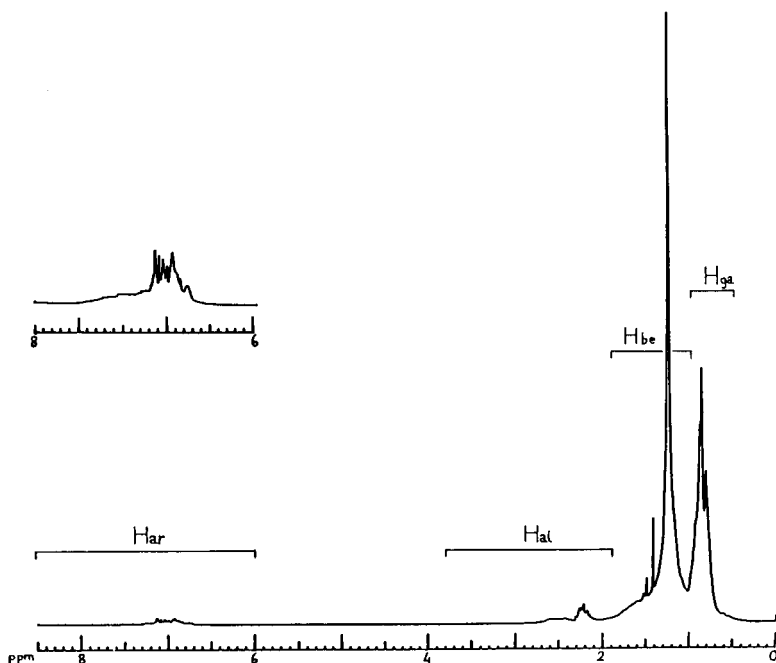


Fig. 1. ^1H NMR spectrum of a typical sample of crude oil.

TCCB – 25°C. If the temperature *TCCB* was < 25°C, the viscosity was measured at 0°C.

Paraffin deposition test. This experiment consisted in inducing paraffin deposition on two copper plates maintained at a constant temperature. A sample of crude oil was mixed with 200 mg kg⁻¹ of additive, heated at 70°C for 4 h and kept at 40°C for 6 days. The sample (1 l) was circulated, in a closed circuit, tangentially to the plates which had a total surface area of 80 cm². The flow-rate was 50 l h⁻¹ (shear rate 200 s⁻¹) and the temperature was maintained at 40°C for 17 h. The copper plate temperature was maintained 10°C below the *TCCB* of the pure crude oil.

From this experiment two types of information were obtained: the weight of the paraffin deposition and the deposit hardness, which corresponds to the amount of heavy paraffins (total number of carbon atoms greater than 29) contained in the

deposit. This measurement was obtained by gas chromatography [17].

In order to preserve homogeneous variables, the activity (ability of the additive to lower the viscosity, the deposit weight and hardness) is expressed as value measured in the absence of the additive/value measured in the presence of the additive.

The experimental results are given in Tables 5–7.

MULTIVARIATE STATISTICAL ANALYSIS

The extraction of information from the results of a chemical experiment most often involves the analysis of a considerable number of variables, and not infrequently a small number of these may contain most of the chemical information. The problems faced by the chemist are: how can all *n* variables be analysed simultaneously in order to reveal correlations between them?; and how can the dimensionality of the problem be objectively reduced in order to interpret and visualize these correlations?

Multivariate statistical techniques [27–31], such as principal component analysis (PCA) [32–36] are suitable for these purposes. These techniques have been developed and extensively applied in the social sciences and their applications to chemical problems are increasing [37–42].

PCA is one of the most commonly applied methods. Its mathematical principles are readily available [43–45] and will not be repeated here. PCA is a completely objective mathematical technique for identifying important axes of variation of data in a multi-dimensional data space. PCA searches for correlations among all variables simultaneously, extracting linear combinations of highly correlated variables that describe, in turn, the greatest amount of sample variance, the second greatest, and so on. Its main use, therefore, lies in dimensionality reduction. It also affords two useful graphical tools: the principal plane which allows one to see if each object (crude oil or additive) brings up any original information – if two objects of the same kind are very close to each other in this plane, their informative con-

TABLE 7

Activity on the paraffin deposition (deposit hardness) of five crude oils

Additive	1C +	2C +	5C +	6C +	7C +
1	0.30	1.00	0.80	0.70	0.70
2	0.20	0.95	0.85	0.70	0.60
3	0.90	1.10	0.90	0.90	0.90
4	1.25	1.00	0.95	1.30	0.60
5	0.40	1.00	0.95	1.35	1.20
6	0.20	0.85	0.90	0.65	0.60
7	0.25	0.95	0.95	0.85	0.90
8	0.35	1.00	1.00	1.20	1.20
9	0.85	1.00	1.00	1.00	1.10
10	0.75	1.00	1.00	1.45	1.00
11	1.00	1.00	1.00	1.15	1.00
12	0.25	1.00	0.90	0.95	0.70
13	0.90	1.05	1.10	1.30	0.70
14	1.25	0.95	0.95	0.95	1.00
15	1.25	1.00	1.05	1.00	0.70
16	1.25	1.05	1.05	0.90	0.80
17	0.85	1.00	1.00	1.00	0.90
18	0.25	0.90	0.85	0.45	0.50
19	0.50	0.95	1.00	0.95	0.80
20	0.25	1.00	0.90	0.75	0.80
21	0.25	0.95	0.90	0.45	0.50
22	1.25	1.05	1.00	1.10	1.00
23	0.35	1.05	0.90	0.95	0.90
24	0.70	0.90	1.10	1.20	1.00

tents are similar according to the descriptors used [46]; and the correlation circle, which allows the study of the correlations between each variable and the correlations between variables and principal components (PC) [47,48].

This method affords the chemist an excellent means of visually representing the main characteristics of the data distribution in an objective way. The program used comes from the software package MOLDESIGN [49], kept at the ANADO library, RI, CNUSC, in Montpellier (France). This software was developed by the Modeling Research Group in the Paul Sabatier University at Toulouse (France) in liaison with the southern national computer center (CNUSC) at Montpellier.

Selection of the physico-chemical parameters of crude oils

Among the 18 parameters that describe the 67 crude oils, there are undoubtedly some redun-

TABLE 8

Groups of parameters containing information

Group	Variables possessing similar information				
	With the same sign			With opposite sign	
1	<i>C30</i>	<i>TCCB</i>			<i>Har</i>
2	<i>I₁</i>	<i>I₇</i>	<i>I₆</i>		<i>Hga</i>
3	<i>Hal</i>	<i>I₂</i>	<i>I₃</i>	<i>As</i>	<i>Par</i>
4		<i>I₄</i>			<i>Hbe</i>

dant descriptors. In order to limit the set of experimental parameters for further practical studies, selection of the most pertinent physico-chemical parameters was performed. The 18 parameters in the correlation circle (Fig. 2) were analysed. It should be noted that the coordinate of a variable is a function of the correlation coefficient between this variable and the PC considered [50], and that the longer the vector length, the better the variable is described.

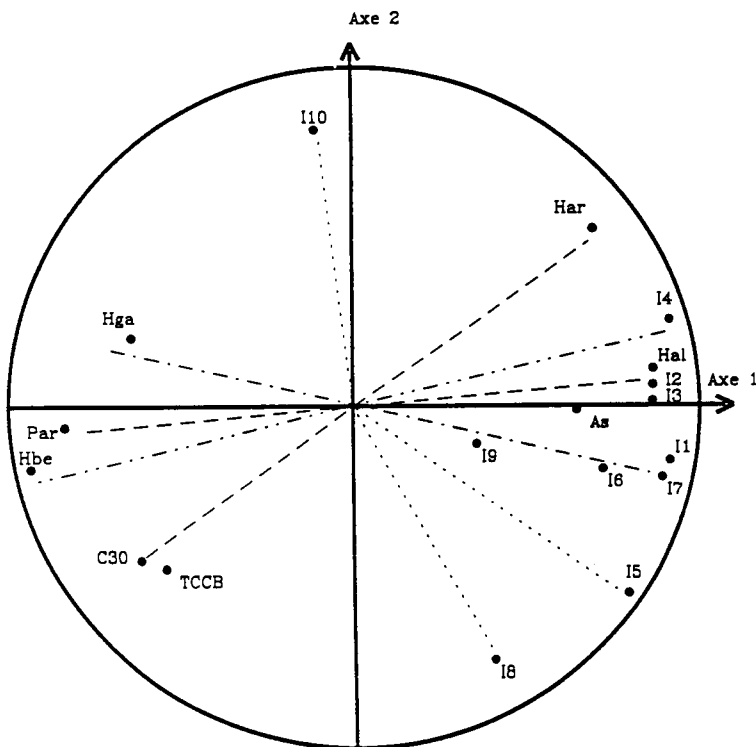


Fig. 2. Correlation circle.

TABLE 9
PCA of crude oils

No.	Eigenvalue	%	Total %	Eigenvector	Axis 1	Axis 2	Axis 3
1	4.06	58.05	58.05	<i>Par</i>	-0.438	0.208	0.250
2	1.61	22.97	81.02	<i>C30</i>	-0.325	0.430	0.541
3	0.55	9.43	90.45	<i>I₁</i>	0.470	-0.005	0.258
4	0.37	5.28	95.72	<i>I₄</i>	0.420	-0.308	0.330
5	0.17	2.39	98.11	<i>I₅</i>	0.436	0.270	0.054
6	0.12	1.70	99.82	<i>I₈</i>	0.294	0.475	0.348
7	0.01	0.18	100.00	<i>I₁₀</i>	-0.171	-0.615	0.588

The analysis of this correlation circle reveals several features: parameters *I₅*, *I₈* and *I₁₀* are well described and independent of the other variables: parameter *I₉* has little effect on the system and can be eliminated; and there are four groups

of parameters containing similar information, which are listed in Table 8.

From group 1, variable *C30* was selected because the heavy paraffins have a great influence on the deposit hardness. Variable *I₁* was retained

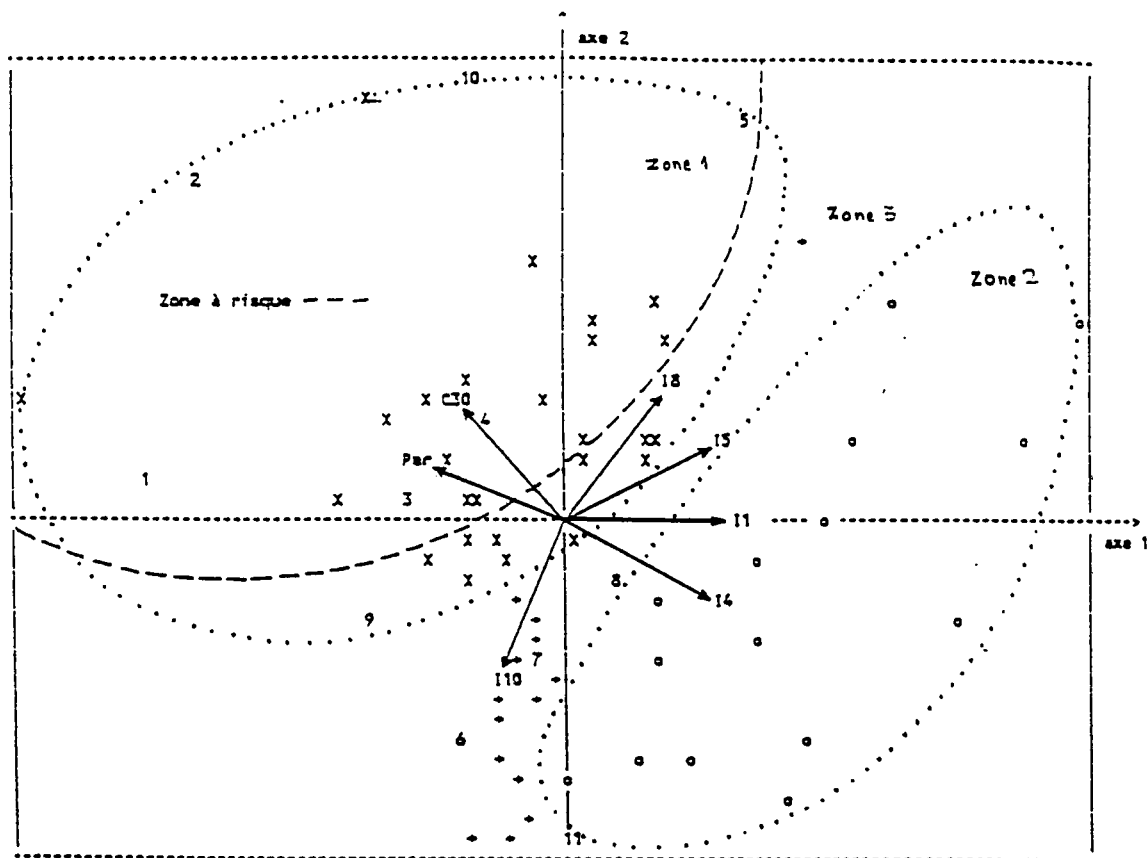


Fig. 3. PCA of the physico-chemical properties of the crude oils. Principal plane. \times = Paraffinic oils; \circ = aromatic and asphaltenic oils; $+$ = intermediate oils.

TABLE 10

PCA of the activities on the viscosity

No.	Eigenvalue	%	Total %	Eigenvector	Axis 1	Axis 2	Axis 3
1	3.44	49.10	49.10	V_1	0.164	-0.591	0.414
2	1.85	26.39	75.49	V_2	-0.362	-0.485	0.083
3	0.71	10.15	85.65	V_3	0.468	-0.106	0.168
4	0.47	6.71	92.36	V_4	0.416	-0.065	-0.678
5	0.30	4.32	96.67	V_5	0.403	-0.195	0.262
6	0.15	2.09	98.76	V_{10}	-0.138	-0.601	-0.515
7	0.09	1.24	100.00	V_{11}	0.518	-0.013	-0.022

from group 2 because it is the best described. In group 3, the information contained by the variable As (percentage of asphaltenes) and by the variables Har , I_2 and I_3 (aromatic compounds) is similar but of opposite sign to the information contained by the variable Par (paraffinic compounds). This result suggests that paraffinic crude oils contain little asphaltene and aromatic compounds. Owing to its intrinsic role in paraffin deposition, the variable Par is retained. The variable Hbe is suppressed in favour of I_4 because this parameter is more isolated.

In all, seven parameters were retained for this study: Par , $C30$, I_1 , I_4 , I_5 , I_8 and I_{10} .

Classification of crude oils

The results obtained by PCA for the physico-chemical properties of the crude oils (Table 9) are represented by the eigenvalues and the eigenvector coordinates in the variable space. The first two eigenvectors, which hold more than 81% of the information, define the principal plane on

which the projection of every object is represented by a symbol and every variable by a vector (Fig. 3).

Classification of additives based on their activity on viscosity

Table 10 gives the results of the PCA method applied to a set of 24 additives defined by their activity on the viscosity of seven crude oils (variables V_1 , V_2 , V_3 , V_4 , V_5 , V_{10} and V_{11}). The principal plane of this PCA represents more than 75% of the information content in the multi-dimensional data space.

Classification of additives based on their activity on paraffin deposition

The results of this PCA can be used to differentiate between the additives according to their action on the weight of paraffin deposited (variables D_1 , D_2 , D_5 , D_6 and D_7) and the deposit hardness (variables $1C+$, $2C+$, $5C+$, $6C+$ and $7C+$). The principal plane of this PCA

TABLE 11

PCA of the activities on the paraffin deposition

No.	Eigenvalue	%	Total %	Eigenvector	Axis 1	Axis 2	Axis 3
1	5.70	56.99	56.99	D_1	0.357	-0.171	-0.281
2	1.39	13.95	70.94	D_2	0.268	-0.541	0.178
3	1.33	13.33	84.26	D_5	0.333	0.178	-0.271
4	0.65	6.52	90.78	D_6	0.369	0.225	0.102
5	0.36	3.56	94.35	D_7	0.278	0.178	0.501
6	0.21	2.10	96.45	$1C+$	-0.313	0.291	0.287
7	0.13	1.34	97.79	$2C+$	-0.251	0.506	-0.378
8	0.12	1.21	99.01	$5C+$	-0.317	-0.132	0.457
9	0.06	0.61	99.62	$6C+$	-0.366	-0.201	-0.020
10	0.04	0.38	100.00	$7C+$	-0.286	-0.407	-0.351

represents 71% of the total inertia of the data (Table 11).

RESULTS AND DISCUSSION

Classification of crude oils

Figure 3 shows the relationship between the objects (crude oils), the variables (analytical features) and the first two principal axes to which the following meanings can be given. Axis 1 separates the crude oils which possess a great amount of paraffins (variable *Par*) from aromatic crude oils (variable I_1). Axis 2 essentially distinguishes the crude oils according to the two variables I_8 and I_{10} . These parameters represent different proportions of aromatic compounds constituting

the crude oil. The complexity of crude oils is such that it is impossible to relate precisely the infrared spectral bands to specific compounds, but in our experience I_{10} is a parameter inversely proportional to the presence of monosubstituted aromatic rings and I_8 is directly proportional to the polyaromatic content.

An investigation of the principal plane allows the definition of three zones for crude oils according to their chemical composition. Zone 1 (objects denoted by \times) groups the crude oils which have a paraffinic feature. Zone 2 (objects denoted by \circ) is constituted by crude oils which possess an aromatic feature; asphaltenic crude oils are included in this zone. Zone 3 (objects denoted by \square) contains crude oils with a chemical composition intermediate between those of

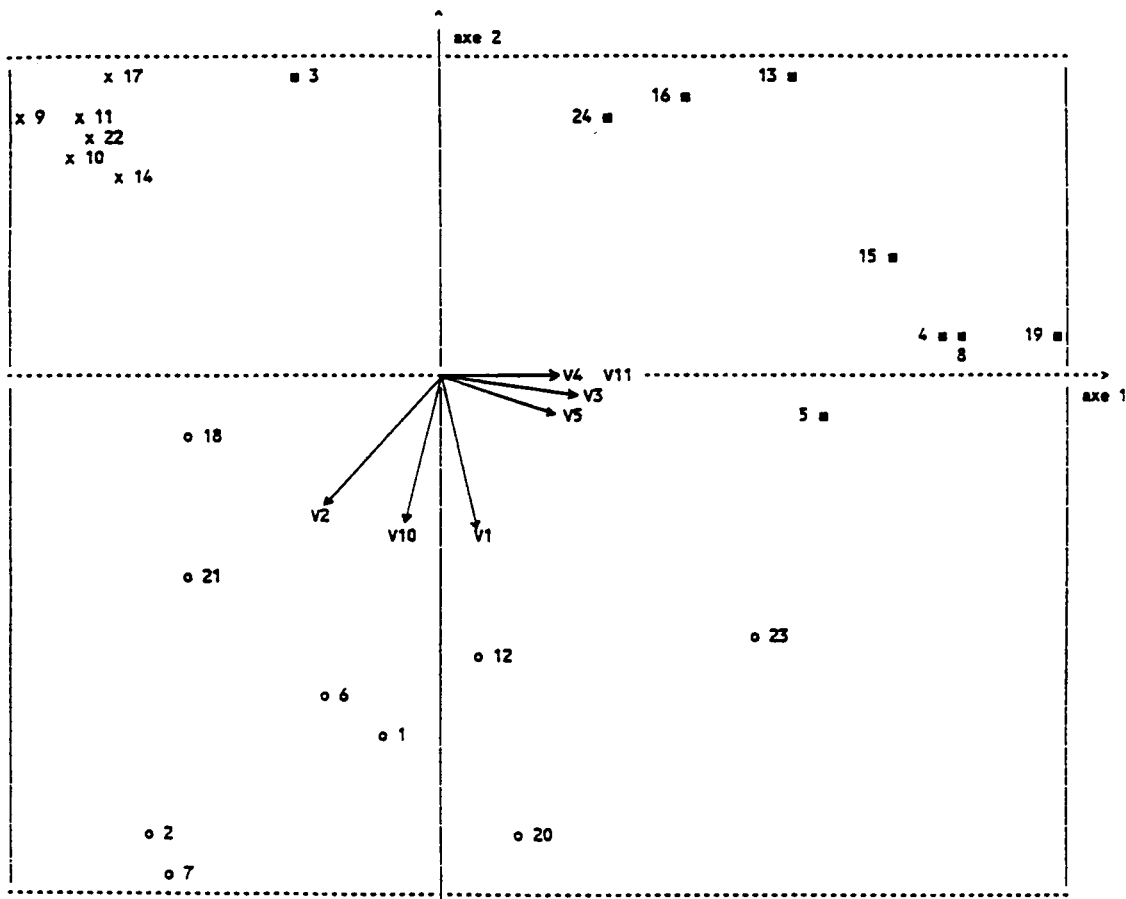


Fig. 4. PCA of activities on the viscosity. Principal plane.

zones 1 and 2. In addition, it was observed that crude oils known to give paraffin deposits are all included in zone 1. They are located in the risk zone of Fig. 3.

Based on the physico-chemical properties of a new crude oil and its location on the factorial plane (Fig. 3), its tendency to form paraffin deposits is revealed. This tendency must be evaluated in the context of the exploitation conditions, in particular the temperature.

With the aim of measuring the activity of the 24 additives on a set of crude oils susceptible to creating paraffin deposits, eleven crude oils were selected. They were chosen to be representative of the entire paraffinic crude oil population and are denoted by the numbers 1–11 in Fig. 3. Six of these crude oils appear in the risk zone, with

samples 1, 2 and 10 in extreme positions; the other five crude oils have a less marked paraffinic character, especially sample 11, which is rather aromatic.

Classification of additives based on their activity on viscosity

Before analysing the results of this PCA, it should be noted that the viscosities of the crude oils 6, 7, 8 and 9 were not measured because of too low a viscosity in the temperature range investigated.

Figure 4 represents the principal plane of the analysis. The following meaning can be attributed to the principal axes. Axis 1 is an activity axis on crude oils 3, 4, 5 and 11. Axis 2 classifies the additives according to their efficiency relative to

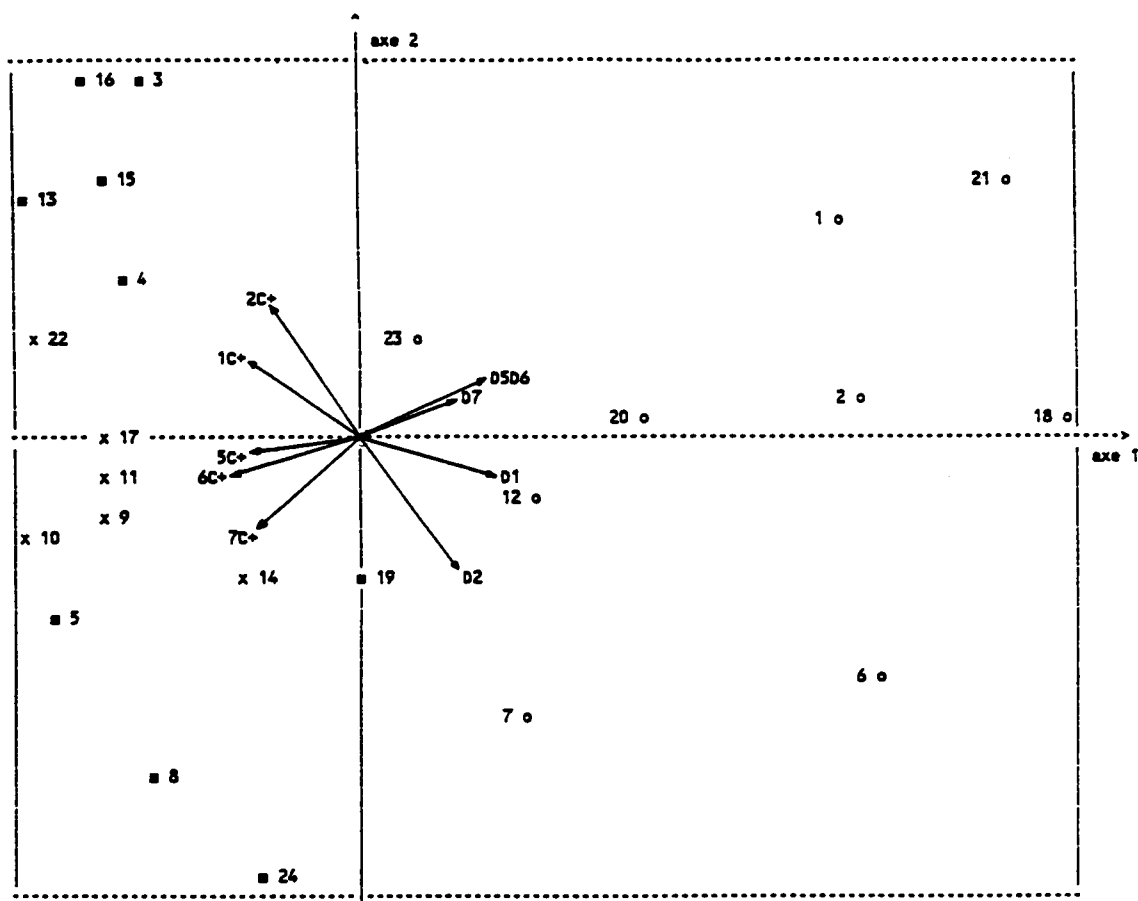


Fig. 5. PCA of activities on paraffin deposition. Principal plane.

the crude oils 1, 2 and 10. Two groups of variables and two groups of crude oils (1, 2, 10 and 3, 4, 5, 11) emerged from this analysis. Also, for these two groups, the crude oils 1, 2 and 10 are located deeply inside the risk zone (Fig. 3) and the crude oils 3, 4 and 5 are located near the limit of the risk zone whereas sample 11 is located well away from this zone.

Based on an investigation of the principal plane of the PCA of activities on the viscosity (Fig. 4), three families of additives can be distinguished. Family A (objects denoted by ■) contains the additives which have a specific activity on crude oils of type 3, 4, 5 and 11. Among them, the most effective additives are 19, 4, 8, 15 and 5 and to a lesser extent 13, 16 and 24. Additive 3 possesses the lowest activity. Family B (objects denoted by ○) corresponds to the compounds which are effective on crude oils 1, 2 and 10. Additives from family C (objects denoted by ×) have little or no activity. It can be noted that these three families are identical with those defined previously [17], obtained from a PCA on the additives' physico-chemical properties.

This result clearly confirms that there is a strong relationship between the selected physico-chemical parameters of the different families of additives and their activity [18].

Classification of additives based on their activity on paraffin deposition

Figure 5 represents the relationships between the objects, the variables and the two first PCs. The following meaning can be attributed to these two axes. Axis 1 shows the opposing behaviour of the variables representing the weight of deposits (on the right) and the variables representing the hardness of these deposits (on the left). Axis 2 separates the additives having a strong activity on the variable D_2 from the additives lowering the hardness of the paraffin deposits of this same crude oil.

A global analysis of the directions of the different vectors shows that the variables representing the weight of deposit are inversely correlated with the variables representing the deposit hardness. For the same crude oil the average correlation coefficient between these two types of vari-

ables is $R = -0.85$. This value signifies that the more the paraffin deposition is inhibited by an additive, the more the deposit contains heavy paraffins. This phenomenon, which had not been clearly demonstrated until now, can be explained by the additives' inactivity toward the heavy paraffins.

The study of the objects represented on the principal plane permits the three families of additives to be distinguished in the following way: additives of family A (objects denoted ■) possess the property of lowering the deposit hardness. Their efficiency depends on the nature of the crude oil. The additives 3, 4, 13, 15 and 16 are very active on the deposit hardness originating from the crude oil samples 1 and 2, whereas the additives 5, 8, 19 and 24 are essentially active on the crude oil samples 5, 6 and 7. Family B (objects denoted by ○) contains the additives which possess the best activity on the weight of the deposits. The most effective are inhibitors 18, 21, 6, 2 and 1 and to a lesser extent additives 20, 12, 7 and 23. Family C (objects denoted by ×) contains inhibitors which have activities similar to those of family A. However, the compounds of family C, being grouped near axis 1, have far less dependence on the nature of the crude oil.

A general activity efficiency rating of the weight of deposit, based on its coordinate on the principal axis, can be attributed to each inhibitor. The five best additives of family B have an activity efficiency rating approaching 80%.

As in the viscosity studies, the inhibitors constituting the three families A, B and C are identical with those constituting the three families defined previously [17].

Conclusion

PCA of physico-chemical and activity parameters can be effectively applied to the investigation of structure–activity relationships. Based on PCA projections, it has been shown that crude oils can be located in three zones and a “risk zone” points out the crude oils most susceptible to creating paraffin deposits; the additives are divided into three families distinguished by their physico-chemical properties [17,18]; a total of seven crude oil physico-chemical parameters are

sufficient to evaluate and additive efficiency toward viscosity, paraffin deposition and crystallization temperature; and the physico-chemical characteristics of the additives [17,18] are strongly linked to their activity efficiencies.

From these results, it is possible to develop a systematic process for choosing the best inhibitors. For example, PCA can be used to position a new crude oil on the principal plane after having determined its seven physico-chemical parameters. When the crude oil's position from the risk zone is known, the use of Fig. 3 and the PCA principal planes of activities on T_c [17,18], viscosity and paraffin deposition allow the choice of the best additives. The same process can be carried out with new additives. Every new object (crude oil or inhibitor) can be introduced into the INIPAR model so as to increase its database.

The authors thank ELF Aquitaine for its contribution to the development of this work by means of scholarships and Mr. J.-N Gorce for technical assistance.

REFERENCES

- 1 D. Shock, J.D. Sudbury and J.J. Crocket, *J. Pet. Technol.*, 7 (1955) 23.
- 2 J.M. McCall and R.L. Johnson, Proceedings of the 31st Annual South Western Petroleum Short Course, Texas Tech University, Lubbock, TX, 1984, p. 457.
- 3 M.E. Newberry, *Soc. Pet. Eng. AIME Pap.*, No. 11561 (Feb.) (1983).
- 4 M.E. Newberry and K.M. Barker, *Soc. Pet. Eng. AIME Pap.*, No. 13796 (1985) 53.
- 5 J.C. Petinelli, *Rev. Inst. Fr. Pet.*, 34 (1979) 771.
- 6 R.C. Price, *J. Inst. Pet. London*, 57 (1971) 106.
- 7 G.E. Addison, *Soc. Pet. Eng. AIME Pap.*, No. 13391 (1984) 203.
- 8 J. Briant, *Rev. Inst. Fr. Pet.*, 18 (1963) 1.
- 9 W.J. Maltlach and M.E. Newberry, *Soc. Pet. Eng. AIME Pap.*, No. 11851 (May) (1983).
- 10 G.T. Woo, S.J. Garbis and T.C. Gray, *Soc. Pet. Eng. AIME Pap.*, No. 13126 (1984) 1.
- 11 K.M. Fagin, *Pet. Eng.*, 1 (1945) 105.
- 12 J. Svetgoff, *Oil Gas J.*, 82 (1984) 79.
- 13 G.G. McClafflin and D.L. Whitfill, *Soc. Pet. Eng. AIME Pap.*, No. 12204 (1983) 1.
- 14 S.M. Bucaram, *J. Pet. Technol.*, 36 (1984) 779.
- 15 F. Bosselet, J.M. Letoffe, P. Claudy, B. Damin and P. Maldonado, *Thermochim. Acta*, 70 (1983) 49.
- 16 J.-L. Mendell and F.W. Jessen, *Soc. Pet. Eng. AIME Pap.*, No. 2868 (1970) 171.
- 17 M. Cristante, J.-L. Selves, G. Grassy, J. Orrit and E. Garland, *Anal. Chim. Acta*, 229 (1990) 267.
- 18 M. Cristante, Thèse, Université Paul Sabatier, Toulouse, 1989, TOU3 0157.
- 19 J.S. Mattson, *Anal. Chem.*, 43 (1971) 1872.
- 20 P.F. Lynch and C.W. Brown, *Environ. Sci. Technol.*, 7 (1973) 1123.
- 21 F.K. Kawahara, J.F. Santner and E.C. Julian, *Anal. Chem.*, 46 (1974) 266.
- 22 J.S. Mattson, C.S. Mattson, M.J. Spencer and S.A. Starks, *Anal. Chem.*, 49 (1977) 297.
- 23 C.P. Anderson, T.J. Killeen, J.B. Taft and A.P. Bentz, *Environ. Sci. Technol.*, 14 (1980) 1230.
- 24 C.J. Chaumery, Rapport d'Etude No. 006/86 296 EPS-HOM/E/OC/NP, Service Hydrographique et Oceanique de la Marine, Brest, 1986.
- 25 D.T. Allen, D.W. Grandy, K.M. Jeong and L. Petrakis, *Ind. Eng. Chem., Process Des. Dev.*, 24 (1985) 737.
- 26 D.R. Clutter, L. Petrakis, R.L. Stenger and R.K. Jensen, *Anal. Chem.*, 44 (1972) 1395.
- 27 S. Wold and O.H.J. Christie, *Anal. Chim. Acta*, 165 (1984) 51.
- 28 M. Feinberg, *Anal. Chim. Acta*, 191 (1986) 75.
- 29 P.H. Weiner and D.G. Howery, *Anal. Chem.*, 44 (1972) 1189.
- 30 D.L. Massart and L. Kaufman, *The Interpretation of Analytical Chemical Data by the Use of Cluster Analysis*, Wiley, New York, 1983.
- 31 G.N. Lance and W.J. Williams, *Comput. J.*, 9 (1967) 71.
- 32 S. Wold, K. Esbensen and P. Geladi, *Chemom. Intell. Lab. Syst.*, 2 (1987) 37.
- 33 P.J. Lewi, in B.R. Kowalski (ed.), *Chemometrics, Mathematics and Statistics in Chemistry*, Reidel, Dordrecht, 1984, pp. 351–376.
- 34 H.T. Eastment and W.J. Krzanowski, *Technometrics*, 24 (1982) 73.
- 35 G. Grassy, Y. Rival, J.-C. Teulade, J.-P. Chapat, M. Simeon de Buochberg and M. Attisso, *Eur. J. Med. Chem., Chim. Ther.*, 20 (1985) 199.
- 36 S. Wold, *Technometrics*, 20 (1978) 397.
- 37 B. Walczak, J.R. Chretien, M. Dreux, L. Morin-Allory, M. Lafosse, K. Szymoniak and F. Membrey, *J. Chromatogr.*, 252 (1986) 123.
- 38 R.W. Rozett and L.E. Petersen, *Anal. Chem.*, 47 (1975) 1301.
- 39 C. Maubert, C. Guerin, F. Mabon and G.J. Martin, *Anal. Chem.*, 16 (1988) 434.
- 40 G. Grassy, R. Escale, J.-P. Chapat, J.-C. Rossi and J.P. Girard, *Eur. J. Med. Chem., Chim. Ther.*, 14 (1979) 493.
- 41 G. Grassy, J.-C. Teulade, J.-P. Chapat, M. Simeon de Buochberg and M. Attisso, *Eur. J. Med. Chem., Chim. Ther.*, 17 (1982) 109.
- 42 I.E. Frank and B.R. Kowalski, *Anal. Chem.*, 54 (1982) 232R.

- 43 M.L. Weiner and P.H. Weiner, *J. Med. Chem.*, 16 (1973) 655.
- 44 G.K. Menon and A. Cammarata, *J. Pharm. Sci.*, 66 (1977) 304.
- 45 O.M. Kvalheim, *Chemom. Intell. Lab. Syst.*, 2 (1987) 127.
- 46 P. Broto, G. Moreau and C. Vandycke, *Eur. J. Med. Chem., Chim. Ther.*, 19 (1984) 79.
- 47 G. Milhaud, J.N. Talbot and G. Coutris, *Thérapie*, 29 (1974) 611.
- 48 O.M. Kvalheim, D.W. Aksnes, T. Brekke, M.O. Eide, E. Sletten and N. Telnaes, *Anal. Chem.*, 57 (1985) 2858.
- 49 G. Grassy and M. Bonnafous, *Chemom. Intell. Lab. Syst.*, 5 (1989) 221.
- 50 E. Diday, J. Lemaire, J. Pouget and F. Testu, *Traitement des Données Statistiques*, Dunod, Paris, 1982, p. 190.

Determination of sub-ng g⁻¹ concentrations of thorium and uranium in microelectronic materials by radiochemical neutron activation analysis

M. Franek and V. Krivan

Sektion Analytik und Höchstreinigung, Universität Ulm, Albert-Einstein-Allee 11, W-7900 Ulm (Germany)

(Received 7th August 1992; revised manuscript received 26th October 1992)

Abstract

A radiochemical neutron activation analysis technique for the determination of thorium and uranium in various high-purity microelectronic materials was developed. It is based on the production of ²³³Pa and ²³⁹Np as indicator radionuclides for Th and U, respectively, and their simultaneous separation by anion exchange from 12 M hydrochloric acid followed by elution with 1 M ammonium fluoride. Using the radiotracer technique, separation yields of Np and Pa and 32 other elements were determined. The method was applied to the determination of Th and U at ng g⁻¹ and sub-ng g⁻¹ levels in high-purity quartz, silicon nitride, polyimide and aluminium oxide. Depending on the kind and purity grade of the sample, limits of detection of 10–100 pg g⁻¹ were achieved. Comparison of the results obtained by this method with those obtained by instrumental neutron activation analysis and inductively coupled plasma mass spectrometry showed satisfactory agreement and illustrates the advantages of this technique when ultra-low concentrations of Th and U are to be determined.

Keywords: Neutron activation methods; Radiochemical methods; Microelectronic materials; Thorium; Uranium

Naturally occurring α -emitters are known to be responsible for changes in the potential of memory cell units by single-event phenomena causing the so-called “soft error effect” [1,2]. Considering the natural abundance and the half-lives of the α -emitting radioactive isotopes, thorium and uranium are the only elements of practical significance. With rapidly increasing integration densities in very-large-scale integration (VLSI) technology for various materials used in this field, the maximum tolerable α -particle fluxes are less than 0.001 cm⁻² h⁻¹, corresponding to thorium and uranium concentrations lower than 6 and 1 ng g⁻¹, respectively [3]. The required purity

of wafer silicon and package materials used for integrated circuits (ICs) is even higher and this demand challenges the efficiency of analytical chemistry as in no other application field.

Considering the importance of irradiation-induced damage of ICs by radioactive isotopes and the limitations put on the direct measurements of such low α -particle fluxes [4,5], a number of attempts have been made to achieve the sensitivity necessary for the detection of extremely low contents of thorium and uranium. The methods developed for the determination of thorium and uranium in silicon- and aluminium-based microelectronic materials include inductively coupled plasma (ICP) atomic emission spectrometry [6,7], total reflection x-ray fluorescence spectrometry [3,8], laser fluorimetry [9] and direct current polarography [7]. However, the most powerful tech-

Correspondence to: V. Krivan, Sektion Analytik und Höchstreinigung, Universität Ulm, Albert-Einstein-Allee 11, W-7900 Ulm (Germany).

niques are mass spectrometry (MS) and activation analysis. ICP–MS [3,10–12] provides excellent detection sensitivities for both elements. However, it requires the decomposition of the sample and, usually, matrix–trace analyte separation and further sample solution handling prior to the actual measurement. Neutron activation analysis (NAA) has proved to be a very suitable method for the determination of ultra-low concentrations of thorium and uranium in silicon-based and organic polymer materials and, with certain restrictions, also in aluminium and aluminium-based materials. Among the different possible methods based on nuclear activation, including delayed neutrons [4,13], fission track counting [4,14], detection of the daughter nuclide ^{140}La of ^{140}Ba produced by the ^{235}U fission [15], the determination of thorium and uranium via the indicator radionuclides (IRNs) ^{233}Pa and ^{239}Np , respectively, has proved to be of great practical importance.

Instrumental NAA (INAA) has been applied to analysis of silicon for Th and U at concentration levels down to sub-ng g^{-1} [9,13,16–19]. However, when applied to the analysis of some other materials for microelectronics, such as quartz, organic polymers and silicon- and aluminium-based ceramics, usually the dominating activities of the medium-lived radionuclides ^{82}Br and ^{24}Na give rise to a Compton background that considerably increases the detection limit especially of the IRN of uranium ^{239}Np ($t_{1/2} = 2.36$ h). Other radionuclides produced from various trace impurities can cause a similar limiting effect on the determination of both elements. Therefore, the extremely low limits of detection required can be achieved only by using radiochemical separations. Radiochemical NAA (RNAA) based on different techniques for the separation of ^{233}Pa and ^{239}Np has been applied to the determination of Th and U at ng g^{-1} and sub-ng g^{-1} levels in aluminium [13,20–24], quartz [20] and a mixture of quartz and potting plastics [25]. However, the applicability of almost all of these procedures is more or less strongly matrix dependent.

In this work, a more universal and extremely sensitive technique for the determination of thorium and uranium was developed and applied to

the analysis of silicon nitride and aluminium oxide ceramic powders, high-purity quartz and polyimide materials.

EXPERIMENTAL

Reagents and radiotracers

All reagents were of analytical-reagent grade from Merck (Darmstadt). Stock standard solutions were prepared by dissolution of thorium and uranium salts [$\text{Th}(\text{NO}_3)_4 \cdot 5\text{H}_2\text{O}$ and $\text{UO}_2(\text{NO}_3) \cdot 6\text{H}_2\text{O}$, respectively]. The original concentrations of the hydrofluoric acid, nitric acid and hydrochloric acid were 40%, 65% and 37% (w/v), respectively. The ion-exchange resin Dowex 1-X8 (100–200 mesh, Cl^- form) was supplied by Fluka (Buchs, Switzerland). Radiotracers were produced by irradiation of evaporated stock standard solutions in the nuclear reactor described below and monitored for radiochemical purity by γ -ray spectrometry.

Samples and standards

The sample SiO_2 -1 and the polyimide materials were analysed within an intercomparison campaign of Ciba-Geigy (Basle), the ultra-pure silicon wafers and the sample SiO_2 -2 were obtained from the National Institute of Standards and Technology (Gaithersburg, MD), joining the silicon intercomparison of ASTM TG 10.05.12. The ceramic powders Si_3N_4 -1, Si_3N_4 -3 and Al_2O_3 -1 were commercially available materials supplied by Toyo Soda (Tokyo), H.C. Starck (Goslar, Germany) and Sumitomo Chemical (Osaka), respectively, and the sample Si_3N_4 -2 was produced on a small scale by Elektroschmelzwerk ESK (Kempton, Germany). For checking the accuracy, the quartz material SiO_2 -3 (BCS-CRM 313/1) from the Bureau of Analysed Samples, (Middlesbrough, UK) was used as a standard reference material that has been well characterized earlier by an interlaboratory comparison [3]. Standards were prepared from element solutions in ampoules made of Suprasil quartz tubes (Heraeus Quarzschmelze, Hanau, Germany), cleaned by surface etching with dilute hydrofluoric acid.

Irradiation

For the irradiation, 100–200 mg of silicon nitride and quartz, 100–150 mg of aluminium oxide and 500 mg of silicon wafer were sealed in Suprasil quartz ampoules of 6 mm i.d. The polyimide samples (200–250-mg portions) were enclosed in ampoules of 8 mm i.d. under a nitrogen atmosphere in order to avoid the exothermic reaction between oxygen and hydrogen released by radiolysis from the polyimide sample during irradiation. The inorganic samples were irradiated simultaneously with standards in the FRG-2 reactor of the GKSS Research Centre (Geesthacht, Germany) at a thermal neutron flux of $1 \times 10^{14} \text{ cm}^{-2} \text{ s}^{-1}$ for 7 days (ceramic powders, SiO₂-1) and 10 days (Si, SiO₂-2), respectively, whereas the organic samples were irradiated for 5 days in the FRG-1 reactor of GKSS at a thermal neutron flux of $5 \times 10^{13} \text{ cm}^{-2} \text{ s}^{-1}$. Cooling times including the necessary transport of approximately 4 days were applied. The sample-containing ampoules were etched outside again and opened carefully with a low-speed diamond saw.

Instrumentation

The high-resolution γ -ray spectrometer system used consisted of an intrinsic Ge detector with an efficiency of 44% [3 \times 3 in. NaI(Tl)], an energy resolution of 1.72 keV (⁶⁰Co, 1.332 MeV), and a peak-to-Compton ratio of 78:1. The detector was connected with an ADCAM (analogue-to-digital converter and multi-channel analyser) of 919 type (16K) and an AT-286 computer for monitoring, processing and storing the spectra using the MS-DOS-based Omnigam software package (Vs 3.5), all obtained from EG & G Ortec (Munich). Depending on the material and concentration of Th and U, counting times between 7×10^4 and 2×10^5 s were applied. For the determination of distribution coefficients and elution curves, a well-type 3 \times 3 in. NaI(Tl) detector coupled with a single-channel analyser from Berthold (Wildbad, Germany) was used.

Radiotracer experiments

The procedures described below were developed by using the radiotracer technique for

checking the yields. Distribution coefficients of ²³⁹Np and ²³³Pa from HCl media on Dowex 1-X8 were determined under batch conditions and elution curves from the influent and the different eluent media were obtained by counting 1-ml portions using a single-channel analyser. Quantitative yields for the complete separation procedure were determined by using the γ -ray spectrometer described above.

Radiochemical procedure

Prior to counting for INAA, the surface of silicon wafer samples was etched with 2 ml of HF by slow addition of three times 50 μ l of HNO₃. For the radiochemical procedure, the ceramic powders and polyimide samples were transferred into 25-ml PTFE liners (50-ml liners for aluminium oxide) of a pressure digestion system II from Berghof (Eningen, Germany) and decomposed under the following conditions with respect to digestion reagents and heating times for each material: silicon nitride powders with 3 ml of HF and 2 ml of HNO₃ at 180°C for 8 h, aluminium oxide powders with 7 ml of HCl and 230°C for 10 h and polyimide with 4 ml of HNO₃ and 1 ml of HF at 220°C for 8 h. The quartz samples were decomposed in a similar manner to the silicon nitride powders.

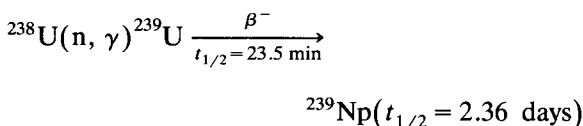
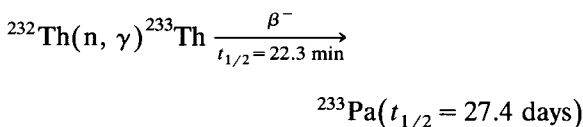
Separation procedure

Solutions resulting from the decomposition of all samples excluding aluminium oxide were evaporated in TPX beakers under an IR lamp nearly to dryness and the residue was taken up with three times 3-ml portions of 12 M HCl. Columns of 33 mm \times 9 mm i.d. with an active bed of 2 ml made of polyethylene syringes were filled with Dowex 1-X8 and pretreated with 10 ml of 12 M HCl. The sample solution was passed through the column using a peristaltic pump at a flow-rate of 0.5 ml min⁻¹ and the column was then eluted with 12 M HCl until a volume of 40 ml was obtained (fraction 1). The column was then eluted with 10 M HNO₃ up to a volume of 10 ml for co-adsorbed nuclides (fraction 2) followed by a 20-ml portion of 1 M NH₄F solution for the quantitative elution of ²³⁹Np and ²³³Pa (fraction 3).

RESULTS AND DISCUSSION

INAA

The determination of both elements is based on their activation via an (n, γ) reaction followed by β^- decay of the activation products to the indicator radionuclides ^{233}Pa and ^{239}Np :



The most important nuclear data are given in Table 1. Owing to the high cross-section of the analytical reactions, the activity yields achievable for the breded indicator radionuclides ^{233}Pa and ^{239}Np lead to extremely low limits of detection. Another advantageous feature of this activation method is the freedom from any nuclear interference reactions.

The nuclear reactions induced by reactor neutrons on silicon-based materials and on organic polymers produce no radionuclides that affect the counting of ^{239}Np and ^{233}Pa . In irradiation of aluminium-based materials, the only relevant nuclide, ^{24}Na ($t_{1/2} = 15.0$ h), is formed by an (n, α) reaction induced by fast neutrons of the fission

spectrum. The high Compton background resulting from its 1368.6- and 2754.1-keV γ -rays increase the detection limits of indicator radionuclides with half-lives up to several days, including ^{239}Np . However, by the choice of a suitable irradiation facility providing a high $\Phi_{\text{th}} : \Phi_{\text{f}}$ ratio and by applying appropriate cooling times, the interference from ^{24}Na can be significantly minimized. Thus, INAA provides a high detection sensitivity for a large number of elements to be determined in microelectronic materials of this kind. However, owing to the high cross-sections for activation with thermal neutrons, some trace impurities even when present at low concentrations can produce radionuclides of dominating activities in the irradiated sample giving rise to a high Compton background in counting ^{239}Np and ^{233}Pa by γ -ray spectrometry. In almost all the materials investigated, this background is to a considerable extent caused by the medium-lived radionuclides ^{82}Br ($t_{1/2} = 1.47$ days) and ^{24}Na which, in some quartz and ceramic samples, is further increased by the contribution from ^{140}La ($t_{1/2} = 1.68$ days). When longer cooling times are applied ($t_{\text{d}} > 20$ days) the main contributors to the Compton background are the radionuclides ^{60}Co , ^{51}Cr , ^{59}Fe , ^{181}Hf , ^{124}Sb , ^{46}Sc and, in the case of aluminium oxide powders, also the radionuclides of the lanthanoids such as ^{141}Ce and ^{160}Tb .

Instrumental γ -ray interferences in counting the most intensive γ -rays of ^{239}Np and ^{233}Pa (see

TABLE 1

Main nuclear data for the production and properties of the indicator radionuclides ^{233}Pa (for Th) and ^{239}Np (for U) [26,27]

Element/isotopic abundance (%)	Cross-section σ_{th} (barns)	Half-life, $t_{1/2}$	Main γ -rays (keV) and intensities (%)	Activity produced (Bq) ^a	
				$t_{\text{ir}} = 1$ day	$t_{\text{ir}} = 20$ days
Th/ ^{232}Th (100)	7.04	^{233}Th 22.3 min			
		$\downarrow \beta^-$			
		^{233}Pa 27.4 days	311.90 (33.7), 300.11 (5.8), 340.47 (3.88), 98.44 (15.5)	5.7×10^4	9.2×10^5
U/ ^{238}U (99.27)	2.70	^{239}U 23.5 min			
		$\downarrow \beta^-$			
		^{239}Np 2.355 days	277.60 (14.1), 228.19 (10.7), 106.13 (22.7), 209.75 (3.2)	5.2×10^5	2.1×10^6

^a Activity produced for $\Phi_{\text{th}} = 10^{14} \text{ cm}^{-2} \text{ s}^{-1}$ and $\Phi_{\text{th}} : \Phi_{\text{f}} = 10 : 1$.

Table 1) are possible from the radionuclides ^{51}Cr (320.07 keV), ^{192}Ir (316.49 keV), ^{182}Ta (229.32 keV), ^{183}Ta (313.01/313.28 keV) and ^{75}Se (279.53 keV), having their γ -rays near to the main γ -rays of ^{239}Np and ^{233}Pa . For the above reasons, optimum detection sensitivities can be achieved by selective separation of ^{239}Np and ^{233}Pa with special respect to the removal of the above-discussed radionuclides responsible for the Compton background.

RNAA

For all the materials analysed, decomposition conditions were optimized considering the handling of active samples, freedom from possible losses and suitability of the sample solution for further processing. For the complete digestion of the polyimide materials and of the refractory ceramic powders, the autoclave system proved to be the most suitable. The medium resulting from the decomposition of the silicon nitride and silicon dioxide powders and of the polyimide materials had to be changed for separation by evaporation followed by taking up the residue with 12 M HCl. The recoveries for this stage of the procedure were > 99% for Np and Pa, and they were quantitative for a large number of elements including Co, Cr, Cs, Fe, Ga, Hf, K, Mo, Na, Rb, Sb, Se, Zn and Zr also. Losses caused mainly by adsorption occurred up to 10% for Au, Ce, Sc, Sn, Ta and W and up to 30% for Ba and Eu.

For aluminium oxide and aluminium nitride powders, the solution resulting from the decomposition with hydrochloric acid could be used directly for the separation.

Based on a comprehensive review of the ion-exchange behaviour of Np and Pa from different media [28] and earlier work on the separation on Dowex 1-X8 resin from 8 M HNO_3 [13], concentrated HF–HCl [22,23] and 9 M HCl [20,24], ion exchange was chosen as the separation principle for this purpose. Investigations under batch and dynamic conditions showed that the anion exchange on Dowex 1-X8 from 12 M HCl was the most suitable separation method with respect to the criteria discussed above.

The strong adsorption of Np and Pa on anion-exchange resins from concentrated HCl solutions results from the formation of chloro complexes having the highest stable oxidizing state +V: $\text{M}(\text{OH})_2\text{Cl}_4^-$ (4–6 M HCl), MCl_6^- (6–9 M HCl) and MCl_7^{2-} (9–12 M HCl) [29,30]. In 12 M HCl, no hydrolysis or formation of polymeric species takes place and the highest adsorption on the resin is achieved. For dynamic separation conditions from 12 M HCl, the retention of ^{239}Np and ^{233}Pa on the column was found to be > 99.98% and > 99.8%, respectively. The behaviour of 32 other elements in this separation procedure is summarized in Table 2, showing the yields obtained in the individual separation steps. From 12 M HCl, Au, Fe, Ga, Mo, Sb, Se, Sn and Ta are

TABLE 2

Percentage yields of Np and Pa and 32 other elements obtained for the individual separation steps of the RNAA procedure ^a

Fraction 1 (40 ml of 12 M HCl)	Fraction 2 (10 ml of 10 M HNO_3)	Fraction 3 (20 ml of 1 M NH_4F)
(A) Np > 99.98%	(A) Np > 99.95%	(B) Np > 99.9%
(A) Pa > 99.8%	(A) Pa ~ 99.5%	(B) Pa > 99%
(B) Ag, Ba, Ca, Cd, Ce, Cr, Cs, Eu, In, K, La, Mn, Na, Rb, Sc, Sr	(B) Co, Hf, Re, W, Zn, Zr	(B) Fe, Ga, Mo
(C) As, Hf, Ir	(C) As, Fe, Ir, Mo, Se, Ta	(C) As, Ir, Se, Sn, Ta
(A) Au, Co, Fe, Ga, Mo, Re, Sb, Se, Sn, Ta, W, Zn, Zr	(A) Au, Ga, Sb, Sn	(A) Au, Sb

^a Retention in the respective separation steps: (A) quantitative adsorption (> 95%); (B) quantitative elution (> 97%); (C) non-quantitative distribution.

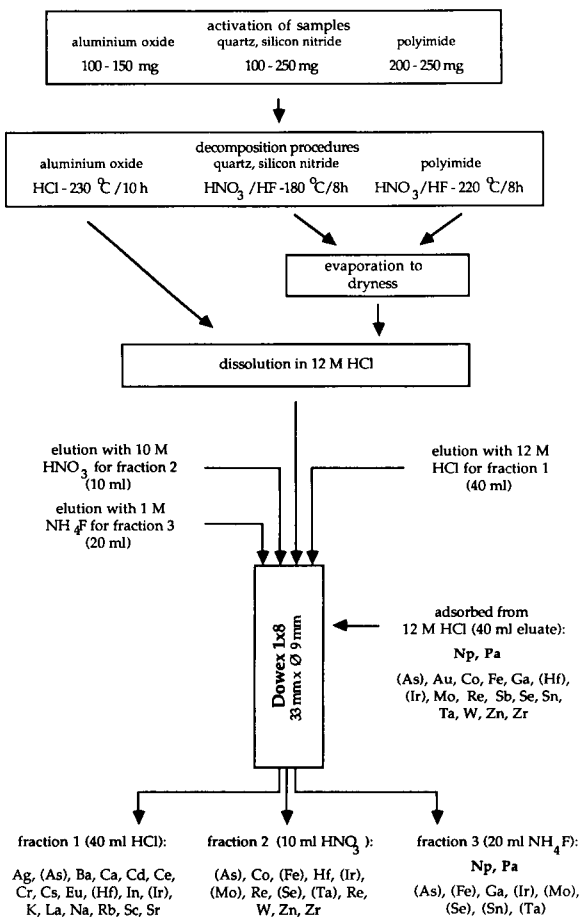


Fig. 1. Flow chart of the radiochemical separation procedure for the determination of thorium and uranium via the indicator radionuclides ²³³Pa and ²³⁹Np, respectively, in different microelectronic materials by RNAA.

co-adsorbed with yields > 99% and Co, Re, W, Zn, and Zr with yields ≥ 95%. As, Hf and Ir are adsorbed on the resin with non-quantitative yields and poor reproducibility. Sixteen elements are eluted quantitatively into fraction 1.

A flow chart of the developed separation procedure is given in Fig. 1, indicating the distribution of Np, Pa and 32 other elements. The elution with 10 M HNO₃ was aimed at the removal of the co-adsorbed elements from Np and Pa remaining on the column with yields > 99.95% and ca. 99.5%, respectively. By using concentrations of HNO₃ lower than 10 M, a more favourable distribution can be achieved especially for Fe; how-

ever, Pa starts to be co-eluted also (2 M HNO₃, 65%; 6 M HNO₃, 6%; 10 M HNO₃, 0.5%), whereas Np is retained quantitatively in the range from 6 to 10 M HNO₃. An eluent volume of 10 ml was found to be sufficient for the complete removal of Co, Hf, Re, W, Zn and Zr from the column into fraction 2. The elution yield for Fe and Mo can be considerably improved (from 35% to 80% and from 20% to 95%, respectively) by using an eluent volume of 20 ml while the elution yield of the other four elements with a non-quantitative distribution (As, Ir, Se and Ta) increases only slightly on doubling the eluent volume. However, under these conditions, 4% of Pa is also co-eluted.

The quantitative elution of Np (> 99.9%) and Pa (> 99%) with 1 M NH₄F is caused by the formation of the MF₇²⁻ species which are retained only weakly on the column and, therefore, are eluted into fraction 3. Only the following elements are co-eluted into fraction 3: Ta (5%), As (10%), Se (15%), Ir (20%), Sn (30%), Fe (65%; 20% by using 20 ml of 10 M HNO₃ eluent), Mo (80%; 5% as for Fe) and Ga (100%; 70% as for Fe); the percentage data are relative to 100% before the separation. Practical consequences of this possible co-elution are discussed below.

Analysis of microelectronic materials

The developed RNAA method was applied to the determination of low contents of thorium and uranium in the microelectronic materials silicon nitride, quartz, aluminium oxide and polyimide. Depending on the trace composition of the sample, the limits of detection obtained for different materials applying this separation procedure were in the range 10–30 pg g⁻¹ for thorium and 10–200 pg g⁻¹ for uranium. In Table 3, limits of detection of RNAA estimated experimentally on the basis of 3σ are compared with limits of detection of INAA. As can be seen, the limits of detection are lower with RNAA than with INAA by factors between 2 and 100 for thorium, and between 5 and 330 for uranium.

In ceramic materials, the limits of detection of INAA are normally determined by one or some few impurities leading to a dominant activity in the irradiated sample. Therefore, depending on

TABLE 3

Limits of detection (3σ) of thorium and uranium for the RNAA method as applied to analysis of different microelectronic materials and comparison with those of INAA

Material	Element	Limit of detection (pg g^{-1})	
		RNAA	INAA
Silicon wafer	Th	–	2
	U	–	3
SiO ₂ -1	Th	10	300
	U	20	1700
SiO ₂ -2	Th	7	15
	U	10	50
Si ₃ N ₄ -1	Th	30	500
	U	100	500
Si ₃ N ₄ -2	Th	10	1000
	U	30	10000
Si ₃ N ₄ -3	Th	1000	5000
	U	200	35000
Al ₂ O ₃ -1	Th	35	500
	U	300	50000
Polyimide	Th	10	500
	U	20	1000

the impurities and their concentrations, RNAA leads to different improvement factors of the limits of detection as compared with INAA. For example, in the material Si₃N₄-2 the content of lanthanum of $17.5 \mu\text{g g}^{-1}$ is responsible for the poor limit of detection for uranium of 10 ng g^{-1} whereas with a ¹⁴⁰La-selective group separation a limit of detection of 0.2 ng g^{-1} could be achieved [31]. However, using the almost analyte-selective separation procedure described here, the limit of detection could further be reduced to 0.03 ng g^{-1} . In addition to causing a considerable increase in the detection limits as a result of the high Compton background, the radionuclides ¹⁸²Ta and ¹⁸³Ta, e.g., as produced from a tantalum content of $0.3 \mu\text{g g}^{-1}$ in the material Si₃N₄-3, caused heavy instrumental spectral interferences. These could be avoided by using a suitable separation procedure [31].

Among a large number of samples analysed, only the determination of uranium in the sample

TABLE 4

Contents of thorium and uranium determined by the RNAA method and comparison with results obtained by INAA and ICP-MS for different high-purity microelectronic materials

Material	Element	Content (ng g^{-1})		
		RNAA ^a	INAA	ICP-MS ^b
SiO ₂ -1	Th	0.23	< 0.3	0.19
	U	0.19	< 1.7	0.15
SiO ₂ -2	Th	< 0.007	< 0.015	–
	U	< 0.01	< 0.05	–
Si ₃ N ₄ -1	Th	4.4 ± 0.2	$(2.8 \pm 0.4)^c$	< 2
	U	2.2 ± 0.2	2.6 ± 0.6	2.5
Si ₃ N ₄ -2	Th	0.19 ± 0.02	< 1	< 1
	U	0.06 ± 0.01	< 10	< 1
Si ₃ N ₄ -3	Th	< 1 ^d	< 5	< 2
	U	1.0 ± 0.3	< 35	< 2
Al ₂ O ₃ -1	Th	69 ± 2	–	–
	U	46 ± 2	< 50	–
Polyimide-1	Th	< 0.04	< 0.5	0.06
	U	0.34 ± 0.05	< 1	0.23
Polyimide-2	Th	< 0.04	< 0.5	< 0.05
	U	0.18	< 1	0.16
Reference material (SiO ₂ -3)	Th	$0.18 \pm 0.02 \mu\text{g g}^{-1}$	$0.19 \pm 0.01 \mu\text{g g}^{-1}$	$0.19 \mu\text{g g}^{-1}$
	U	$0.11 \pm 0.01 \mu\text{g g}^{-1}$	$0.11 \pm 0.01 \mu\text{g g}^{-1}$	$0.11 \mu\text{g g}^{-1}$

^a $n = 3$, except for SiO₂-1 and polyimide-2 ($n = 2$) and reference material SiO₂-3 ($n = 10$). ^b Personal communication from J. Pavel, Central Analytical Department, Ciba-Geigy (Basle). ^c Instrumental interference by the 320.07-keV γ -ray of ⁵¹Cr. ^d Counting at the 300.11-keV γ -ray.

SiO₂-1 by counting the 277.60-keV γ -ray and the determination of thorium in the sample Si₃N₄-3 using the 311.90-keV γ -ray was interfered with by ⁷⁵Se and ¹⁸³Ta, respectively. In the determination of thorium, the interference caused an increase of the limit of detection by a factor of about 100, whereas in the determination of uranium the interference did not lead to such a far-reaching consequence as another γ -ray with comparable intensity at 228.19 keV could be used.

The results obtained for thorium and uranium in various microelectronic materials are summarized in Table 4. Comparison with the INAA data demonstrates the necessity to use an efficient radiochemical separation to achieve the required detection sensitivity. Different samples were analysed also by ICP-MS as a suitable independent method, which provided results in good accordance with the RNAA procedure even at very low concentration. For ceramic materials with refractory character such as silicon nitride powder the wet chemical decomposition leads to media which, for analysis by ICP-MS, require further handling, usually dilution, reducing the detection power of this method for Th and U to the low-ng g⁻¹ level. The RNAA procedure, on the other hand, proved to be rather independent of the chemical character of the materials analysed.

The contents of thorium and uranium determined by this method in the material SiO₂-1 (230 and 190 pg g⁻¹, respectively) were, considering the extremely low concentration level, in excellent accord (within 20%) with the results obtained by ICP-MS. In the polyimide materials 1 and 2, uranium contents at the same concentration level determined by RNAA and ICP-MS agreed within 30% and 10%, respectively, whereas the thorium contents were found by both methods to be close to or below the limit of detection.

Concentrations of both elements ranging over several orders of magnitude were also detected in other ceramic powders. In most instances, the detection limits of INAA were not sufficient and only the RNAA method could detect very low concentrations. The results obtained for both elements in the quartz powder material SiO₂-3 by this method and by INAA and ICP-MS show good agreement (see Table 4).

From the results of the analysis of various microelectronic materials for thorium and uranium at different concentration levels, it can be concluded that the developed RNAA method is a very sensitive, reliable and universal technique capable of satisfying the analytical requirements in this field.

The authors gratefully acknowledge financial support of this work by Deutsche Forschungsgemeinschaft (Bonn) and providing irradiation facilities free of charge by the GKSS (Geesthacht, Germany).

REFERENCES

- 1 T.C. May and H.M. Woods, *IEEE Trans. Electron Devices* ED-26 (1979) 2.
- 2 P.M. Carter and B.R. Wilkins, *IEEE Proc. Pt. I: Solid-State Electron Devices*, 134 (1987) 32.
- 3 H. Baumann and J. Pavel, *Microchim. Acta*, III (1989) 413.
- 4 C.A. Handwerker, P.A. Morris, R.L. Cobla and D.R. Gabbe, *IEEE Proc. 34th Elect. Comp. Conf.*, New York, 1984, p. 453.
- 5 K. Kudo, T. Shigematsu, H. Yonezawa and K. Kobayashi, *J. Radioanal. Chem.*, 63 (1981) 345.
- 6 A. Okada and N. Hirate, *Bunseki Kagaku*, 37 (1988) T205.
- 7 G. Kudermann and K.-H. Blaufuss, *Microchim. Acta*, II (1985) 85.
- 8 U. Reus, *Spectrochim. Acta, Part B* 44, (1989) 533.
- 9 K. Ishibashi, S. Sakamaki, T. Imasaka and N. Ishibashi, *Anal. Chim. Acta*, 219 (1989) 181.
- 10 H. Matsunaga, N. Hirate and K. Nishikida, *Bunseki Kagaku*, 38 (1989) T21.
- 11 H. Baumann, *Chimia*, 44 (1990) 236.
- 12 K. Takeda, T. Yamagushi, H. Akiyama and T. Masuda, *Analyst*, 116 (1991) 501.
- 13 F.F. Dyer, J.F. Emery, K.J. Northcutt and R.M. Scott, *J. Radioanal. Chem.*, 72 (1982) 53.
- 14 T. Nakanishi, *Fresenius' Z. Anal. Chem.*, 327 (1987) 491.
- 15 W.D. James and C.E. Thompson, *J. Radioanal. Chem.*, 72 (1982) 79.
- 16 P. Ila and F.A. Frey, *J. Radioanal. Nucl. Chem.*, 131 (1989) 37.
- 17 M.L. Verheijke, H.J.J. Jaspers and J.M.G. Hanssen, *J. Radioanal. Nucl. Chem.*, 131 (1989) 197.
- 18 R.M. Lindstrom, in L.A. Casper (Ed.), *Microelectronic Processing: Inorganic Materials Characterization*, American Chemical Society, Washington, DC, 1986.
- 19 G. Revel, N. Deschamps, C. Dardenne, J.L. Pastol, B. Hania and H. Nguyen Dinh, *J. Radioanal. Nucl. Chem. Lett.*, 85 (1984) 137.

- 20 T. Mitsugashira, Y. Koma, S. Hirai, I. Okada, N. Kurashima and H. Sakurai, *J. Radioanal. Nucl. Chem.*, 147 (1991) 69.
- 21 C. Yonezawa, M. Hoshi, E. Tachikawa and H. Kamioki, *Bunseki Kagaku*, 37 (1988) 7.
- 22 K.P. Egger and V. Krivan, *Fresenius' Z. Anal. Chem.*, 331 (1988) 394.
- 23 K.P. Egger and V. Krivan, *Fresenius' Z. Anal. Chem.*, 327 (1987) 119.
- 24 S. Hirai and Y. Hayakawa, *Bunseki Kagaku*, 36 (1987) 284.
- 25 F.F. Dyer, J.E. Emery and L.C. Bate, *J. Radioanal. Nucl. Chem.*, 110 (1987) 221.
- 26 G. Erdtmann and W. Soyka, *The Gamma Rays of the Radionuclides*, Verlag Chemie, Weinheim, 1979.
- 27 G. Erdtmann, *Neutron Activation Tables*, Verlag Chemie, Weinheim, 1976.
- 28 J. Korkisch, *Handbook of Ion Exchange Resins, Part II*, CRC, Boca Raton, FL, 1989.
- 29 Y. Marcus, *Coord. Chem. Rev.*, 2 (1967) 195.
- 30 Y. Marcus, *Coord. Chem. Rev.*, 2 (1967) 257.
- 31 M. Franek and V. Krivan, *Anal. Chim. Acta*, 264 (1992) 345.

Influence of operating parameters on ion intensity in glow discharge mass spectrometry

Morimasa Saito

Materials Characterization Division, National Research Institute for Metals, 3–12, 2-chome, Nakameguro, Meguroku, Tokyo (Japan)

(Received 16th June 1992; revised manuscript received 23rd October 1992)

Abstract

Using a VG 9000 glow discharge mass spectrometer, the influence of sample size, sample position, sample shape, discharge current and discharge voltage was studied in detail. The ion intensity signals of elements were not influenced by the sample shape, but were influenced significantly by the sample position, the sample size, the discharge current and the discharge voltage. The maximum ion intensity signals of elements were obtained when the sample was 8–9 mm from the ion exit slit.

Keywords: Mass spectrometry; Glow discharge; Ion intensity; Steels

Spark-source mass spectrometry (SSMS) is widely used for the simultaneous determination of ultra-trace elements in solid samples, semiconductor materials, high-purity materials, etc. [1–3]. This method gives good accuracy (about 15%) by using the relative sensitivity factor obtained from physical parameters without reference standards [4]. However, the ion yield of this method had a wide energy spread and often gives poor precision [2,3].

Glow discharge mass spectrometry (GDMS) has been developed as a more stable, low-energy alternative ion source. It is very sensitive for direct solid elemental analysis, exhibits a broad dynamic range and is relatively free from matrix effects [5–7]. However, this method suffers from the usual problems accompanying direct solid sample analysis, namely suitability and availability of reference materials, homogeneity concerns and sample configuration requirements.

The parameters affecting GDMS ion signals were studied by Harrison et al. [8] using a low-resolution quadrupole mass analyser. They reported that the critical factors were the electrode position within the source, plasma conditions and composition and the degree of sputtering. Jakubowski et al. [9] also reported on the effects of the power and pressure within the discharge cell on the ion intensity of elements in steels using a low-resolution mass analyser. The quadrupole mass analyser makes it possible to design a simple, inexpensive instrument with high ion transmission, particularly in the low-mass range. However, a limitation to the use of this technique is the low resolution, which makes it impossible to separate molecular ion interferences from elemental ions of the same nominal mass.

Recently, a VG 9000 instrument, based on a high-resolution mass analyser to minimize the molecular ion interferences on elemental ions, has been used for the determination of ultra-trace amounts of elements in high-purity materials containing the metals. However, no detailed study on the influence of parameters such as discharge

Correspondence to: Morimasa Saito, Materials Characterization Division, National Research Institute for Metals, 3–12, 2-chome, Nakameguro, Meguroku, Tokyo (Japan).

voltage, discharge current, sample size, sample shape and sample position on the ion intensity signals of elements using a high-resolution mass analyser has been reported. The object of this study was to determine the optimum conditions for the use of the VG 9000 high-resolution mass analyser for the accurate and precise determination of elements in steels, etc.

EXPERIMENTAL

Instrument and specimens

The instrument used was a VG 9000 glow discharge mass spectrometer (VG Microtrace). The plasma cell is a so-called "simple cell" consisting of a quartz tube and tantalum plate. The volume of the plasma cell is 15.4 cm³ and the discharge gas used is super high-purity argon (> 99.999%).

The standard reference materials NBS SRM 1261, 1262, 1263 and 1264 and JEARI R9 (Hastelloy X heat-resistant alloy) were used (Table 1). The samples were cut with a jeweller's saw and machined into cylinders and squares in the range 5–20 mm in length and 1–2.5 mm in diameter with a cutter and lathe. The samples to be analysed were abraded in acids, followed by washing in ethanol with an ultrasonic cleaner and drying with a hot-air blower, and finally plasma etched for 30 min in the GD source prior to analysis. The pre-etching was carried out using a discharge voltage of 1.0 kV and a discharge current of 2.0 mA. The main instrumental conditions are given in Table 2.

The data presented are average values of three determinations.

RESULTS AND DISCUSSION

Sample size

When the discharge was maintained for long periods, the analytical results were often erratic. This was considered to be due to the variation of the pin sample size. Therefore, the relationship between the pin sample size and the ion intensity signals of elements was examined by using the

TABLE 1

Compositions of the standard samples used ($\mu\text{g g}^{-1}$)^a

Element	NBS	NBS	NBS	NBS	JAERI R9
	SRM 1261	SRM 1262	SRM 1263	SRM 1264	
B	5	25	9.1	110	5
Al	210	950	2400		2600
Si	2230	3900	7400	670	3400
P	150	420	290	180	130
S	170	380	80	280	20
Ti	200	840	500	2400	40
V	110	410	310	1050	400
Cr	6900	3000	13100	650	21500
Mn	6600	10400	1500	2550	3300
Fe					176000
Co	300	3000	480	1500	11800
Ni	19900	5900	3200	1420	
Cu	420	5000	980	2490	430
As	170	920	100	520	
Se	40	[10]	[1]	[3]	
Zr	90	1900	490	680	
Nb	290	2900	490	1570	
Mo	1900	6800	300	4900	
Sn	110	160	(950)	(50)	
Sb	42	120	16	(350)	
La	4	4	6	0.7	
Pr	(1.4)	(1.2)	(1.8)	(0.3)	
Hf	[2]	[60]	[15]	[50]	
W	150	2100	450	1000	(5500)
Pb	0.2	4.3	22	240	
Bi	4	(20)	(8)	(9)	

^a Values in parentheses are not certified, based on a single analytical method and values in square brackets are not certified, approximate values.

standard steel and heat-resistant alloy samples. The discharge current was 1.8 mA, the discharge voltage was 0.9 kV and the sample was ca. 9 mm from the ion exit slit.

TABLE 2

Instrumental operating conditions

Instrument	VG 9000
Discharge gas	Ar
Multiplier system	Ion counting system
Software	VG 9000 issue 3.10
Discharge cell	Simple cell
Discharge current	0.8–2.0 mA
Discharge voltage	0.5–1.2 kV
Pressure (analyser)	$< 1 \times 10^{-6}$ Pa
Resolution	< 4000
Transmittance	90%

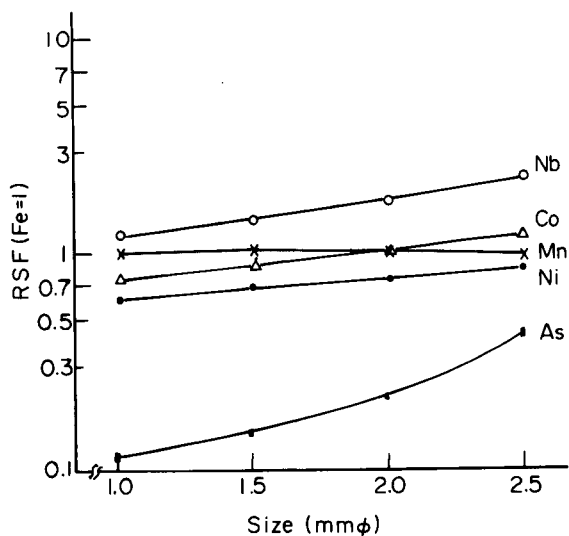


Fig. 1. RSF ($Fe=1$) of elements as a function of sample diameter (mm).

The relative sensitivity factors (RSF) were calculated by using the equation

$$RSF = \frac{\text{ion intensity ratio (ppm)}}{\text{certified value (ppm)}} \quad (1)$$

The ion intensity ratio (I_x/I_{Fe}) was measured as the ratio of the ion intensity corresponding to an element x to that of matrix Fe. Figures 1–3 show the relationship between the RSF values obtained for several elements and the pin sample size (mm diameter). The RSF values shown are average values calculated from those obtained by using the standard samples.

The RSF values for Si, S, P, Co, Ni, As, Zr and Sb increased with increase in the diameter of the pin samples. On the other hand, the values for Sn and Pb decreased with increase in the diameter of the pin samples, and those for Al, Ti, V, Mn, Cr, Cu, Ta, W and Bi did not vary. The RSF values for Zn and Mo varied according to the kind of sample. This seems to be due to sample inhomogeneities. From these results, in order to obtain good accuracy and precision for the determination of elements in metals, the size of the samples to be analysed should be the same as that used in the measurement of the RSF values.

When the discharge current was kept constant at 1.8 mA and the discharge voltage was changed

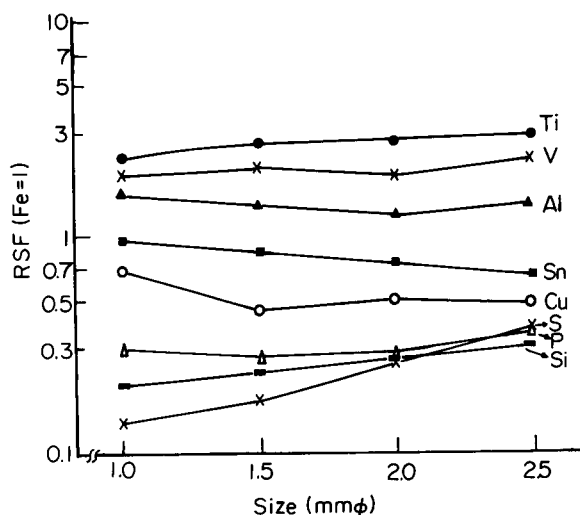


Fig. 2. RSF ($Fe=1$) of elements as a function of sample diameter (mm).

from 0.9 to 0.6 kV, the influence of the sample size on the RSF values for Sn and As was examined. The results are shown in Fig. 4. Sn and As were selected because they were greatly affected by the pin sample size. The RSF value for Sn at a discharge voltage of 0.9 kV increased with increase in the pin sample size. On the other hand, the value obtained at a discharge voltage of 0.6

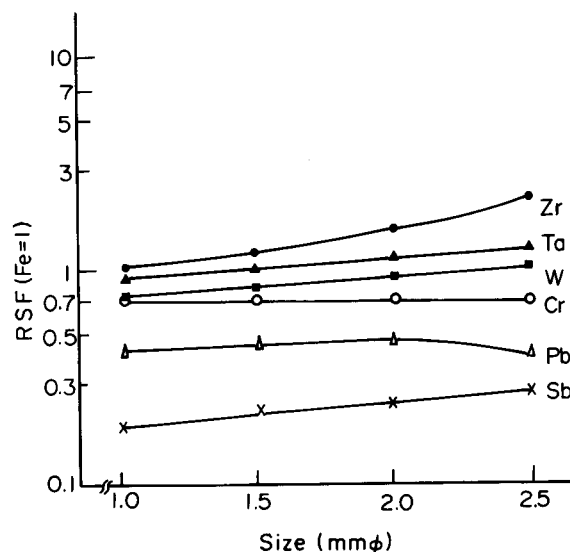


Fig. 3. RSF ($Fe=1$) of elements as a function of sample diameter size (mm).

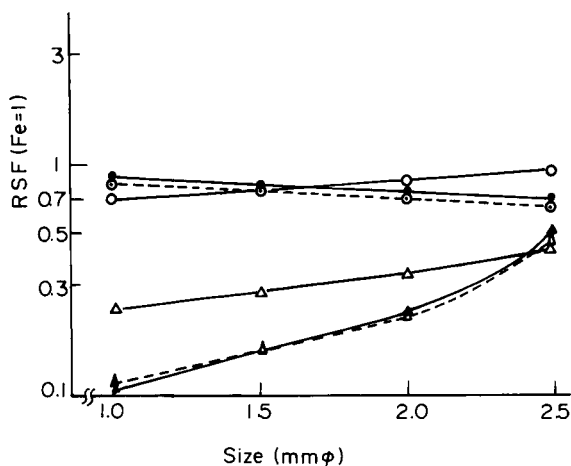


Fig. 4. Influence of discharge voltage and sample shape on $RSF (Fe=1)$ of Sn and As. Discharge current, 1.8 mA. ● = Sn, discharge voltage 0.9 kV, sample in lot form; ▲ = As, discharge voltage 0.9 kV, sample in lot form; ○ = Sn, discharge voltage, 0.6 kV, sample in lot form; △ — △ = As, discharge voltage 0.6 kV, sample in lot form; ○ = Sn, discharge voltage 0.9 kV, sample in square form; △ - - - △ = As, discharge voltage 0.9 kV, sample in square form.

kV decreased with increased in the pin sample size. The RSF value for As increased with increase in the pin sample size at discharge voltages of both 0.9 and 0.6 kV. However, The RSF value obtained for As at a discharge voltage of 0.9 kV was different from that obtained at 0.6 kV. Therefore, the discharge current and voltage should be kept constant. This will be discussed later.

The influence of the sample shapes on the RSF values for Sn and As was also investigated. The samples used in this study were of a lot form and a square form. Figure 4 shows the results obtained when the surface area of the sample exposed to the discharge was the same as that of the sample of a square form. The results show that the sample shape did not affect the accurate determination in elements in metals.

Sample position

It is known that the ion intensity signals of elements vary according to the pin sample electrode position within the discharge cell. The influence of the pin sample electrode position in the plasma cell on the ion intensity signals of

elements was therefore studied using NBS SRM 1261. The pin sample electrode position was varied by changing of the length of the pin samples. The distance between the tip of the pin sample electrode and the ion exit slit was determined by measuring both the length of the pin sample electrode exposed to the discharge and with a helium-neon laser (0.05 W). The other measurement conditions were discharge current 1.6 mA, discharge voltage 0.9 kV and sample diameter 2 mm.

Figures 5-7 show the results. The ion intensity signals for $^{31}P^+$, $^{56}Fe^{2+}$, $^{48}Ti^+$, $^{52}Cr^+$, $^{55}Mn^+$, $^{56}Fe^+$, $^{59}Co^+$, $^{60}Ni^+$, $^{90}Zr^+$ and $^{118}Sn^+$ were maximum at a sample electrode-slit distance of about 8 mm, and the values for $^{11}B^+$, $^{27}Al^+$, $^{28}Si^+$, $^{75}As^+$, $^{77}Se^+$, $^{121}Sb^+$, $^{204}W^+$, $^{208}Pb^+$ and $^{209}Bi^+$ were maximum at a distance of about 9 mm.

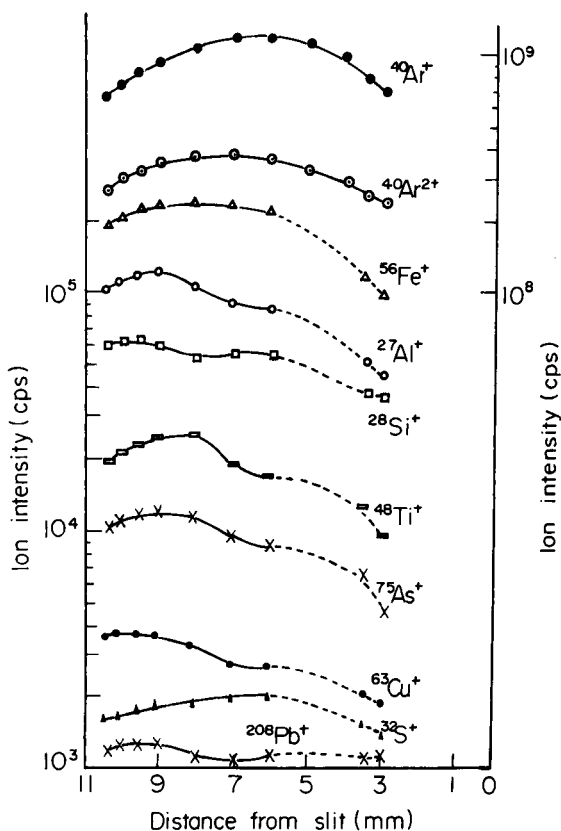


Fig. 5. Ion intensity (cps) of elements as a function of distance (mm) between the tip of the sample and the ion exit slit. Sample, NBS 1261.

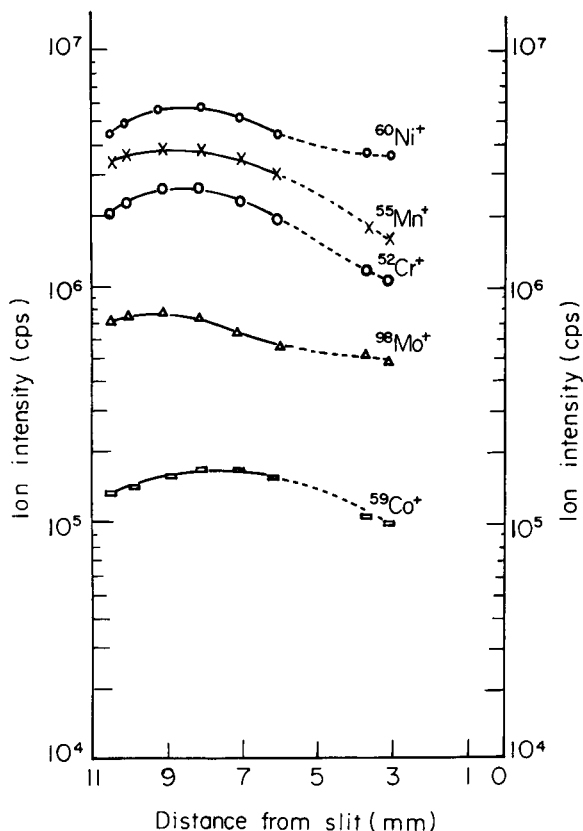


Fig. 6. Ion intensity (cps) of elements as a function of distance (mm) between the tip of the sample and the ion exit slit. Sample, NBS 1261.

However, the ion intensity signals for $^{32}\text{S}^+$ were maximum at a distance of 6–7 mm. The reason for the large differences in the last instance seems to be due to the different ionization mechanism of sulphur from that of other elements (except Ar), but this has not been clarified. When the tip of the pin electrode samples was less than 6 mm from the ion exit slit, the ion intensity signals of elements decreased and were erratic. This seems to be due not only to the phase boundary of the negative glow region, which has an abundance of reactive species, but also to the approach to the cathode dark space, in which the discharge voltage decreases.

From the above results, the pin sample electrode position–slit distance should be set at 8–9 mm, which gives the maximum ion intensity signals for most elements.

Discharge current and discharge voltage

Colby and Evans [10] studied for influence of the discharge current and voltage on the ion intensity by using a hollow-cathode ion source. In this work, the relationship between the discharge current and voltage and the ion intensity of elements using the VG 9000 instrument with a direct current discharge cell was examined with the standard samples and $^{56}\text{Fe}^+$ as the internal standard. Figures 8 and 9 show the results obtained using NBS SRM 1262. The sample diameter was 2 mm, the pin sample electrode was about 9 mm from the ion exit slit and the discharge voltage was kept constant at 0.8 kV. For $^{28}\text{Si}^+$, $^{31}\text{P}^+$, $^{32}\text{S}^+$, $^{48}\text{Ti}^+$, $^{60}\text{Ni}^+$, $^{66}\text{Zn}^+$, $^{75}\text{As}^+$, $^{121}\text{Sb}^+$, $^{141}\text{Pr}^+$ and $^{178}\text{Hf}^+$ the ion intensity ratios (I_x/I_{Fe}) decreased with increase in the discharge current, but for $^{51}\text{V}^+$, $^{52}\text{Cr}^+$, $^{55}\text{Mn}^+$, $^{93}\text{Nb}^+$, $^{98}\text{Mo}^+$, $^{181}\text{Ta}^+$, $^{184}\text{W}^+$ and $^{209}\text{Bi}^+$ the values were almost constant in the range 0.8–2.0 mA. Similar results were obtained using the other standard samples, i.e., NBS SRM 1261, 1263 and 1264 and JEARI R9.

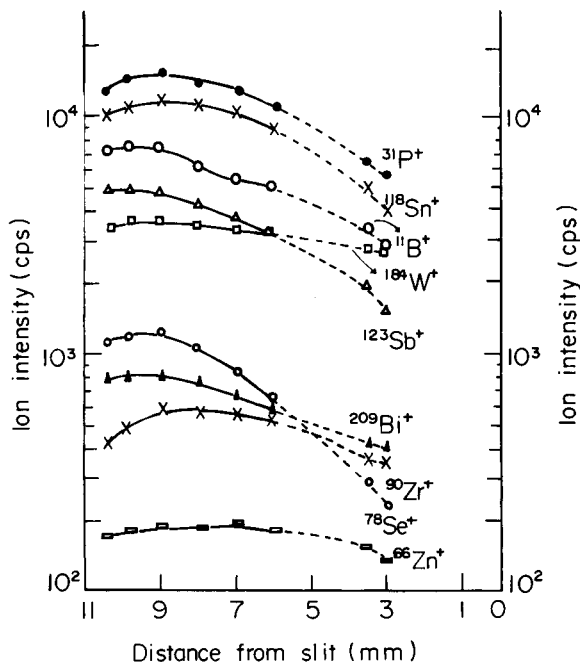


Fig. 7. Ion intensity (cps) of elements as a function of distance (mm) between the tip of the sample and the ion exit slit. Sample, NBS 1261.

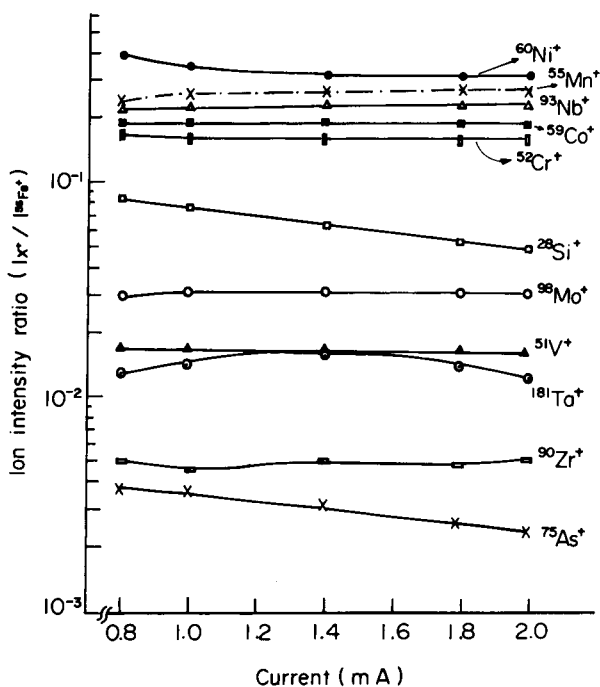


Fig. 8. Ion intensity ratios (I_x/I_{Fe}) of elements as a function of discharge current (mA). Sample, NBS 1262.

Next, the relationship between the discharge voltage and the ion intensity ratios (I_x/I_{Fe}) was examined. Figures 10 and 11 show the results obtained using NBS SRM 1262. The discharge current was kept constant at 1.8 mA and the other measurement conditions were the same as above, except for the discharge voltage. The ion intensity ratios (I_x/I_{Fe}) for $^{11}B^+$, $^{32}S^+$, $^{28}Si^+$, $^{27}Al^+$, $^{63}Cu^+$, $^{75}As^+$, $^{121}Sb^+$, $^{139}La^+$, $^{130}Te^+$ and $^{184}W^+$ increased increasing discharge voltage, whereas those for $^{31}P^+$, $^{51}V^+$, $^{52}Cr^+$, $^{55}Mn^+$, $^{60}Ni^+$, $^{93}Nb^+$, $^{98}Mo^+$, $^{118}Sn^+$, $^{208}Pb^+$ and $^{209}Bi^+$ remained constant in the range 0.6–1.15 kV. Similar results were obtained using the other standard samples, i.e., NBS SRM 1261, 1263 and 1264 and JEARI R9.

The ion intensity ratios, depending on the discharge current and voltage, showed different values according to the elements, as shown in Figs. 8–11. From these results, the discharge current and voltage could not be optimized for each element. However, for the precise determination of the elements in metals, it was found that the

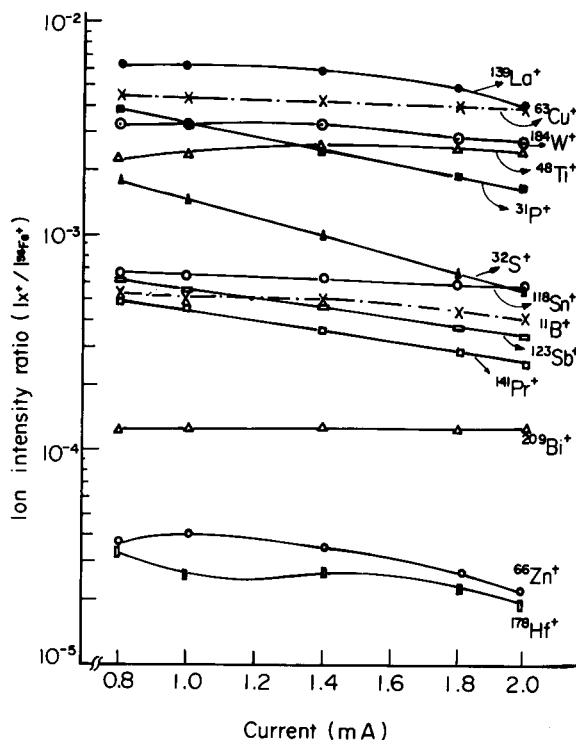


Fig. 9. Ion intensity ratios (I_x/I_{Fe}) of elements as a function of discharge current (mA). Sample, NBS 1262.

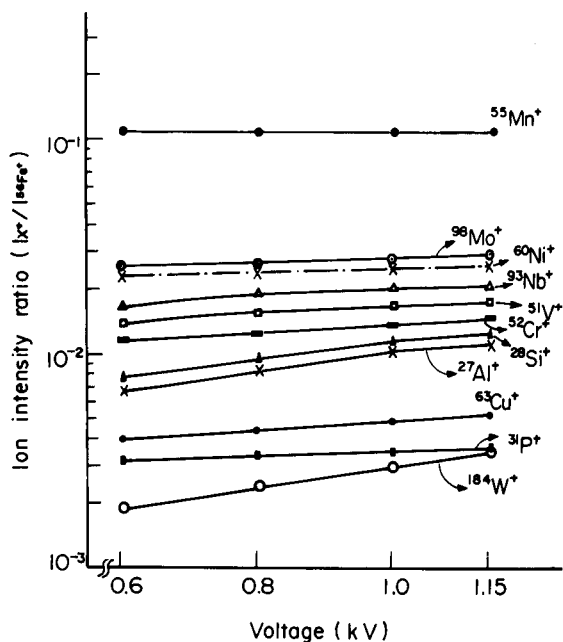


Fig. 10. Ion intensity ratios (I_x/I_{Fe}) of elements as a function of discharge voltage (kV). Sample, NBS 1262.

measurements had to be made under constant conditions of discharge current and voltage.

Reproducibility

The reproducibility using the VG 9000 instrument was examined. Table 3 shows the internal reproducibility (i.e., measurements on the same sample electrode) obtained using the standard steel samples NBS SRM 1261, 1262, 1263 and 1264. The fixed operating conditions were pin sample diameter 2 mm, sample 9 mm from the ion exit slit, discharge voltage 0.9 kV, discharge current 18 mA and integration time 20 s. The average relative standard deviations (R.S.D.s) obtained from six analyses of each standard are given in Table 3. Table 3 also shows the external reproducibility (i.e., measurements on several different sample electrodes) and the reproducibility obtained under different measurement conditions

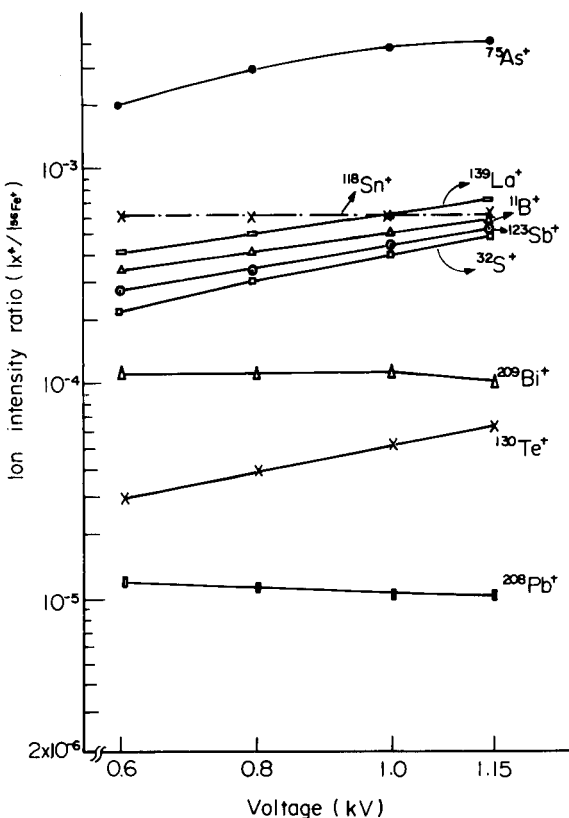


Fig. 11. Ion intensity ratios (I_x/I_{Fe}) of elements as a function of discharge voltage (kV). Sample, NBS 1262.

TABLE 3

Reproducibility of determination of elements in steel samples by GDMS^a

Element	R.S.D. (%)		
	Internal reproducibility ^b	External reproducibility ^c	Measurement reproducibility ^d
B	1.5	3.7	9.6
Al	1.1	1.2	6.4
Si	1.4	1.8	10.5
S	2.3	4.0	12.9
P	1.4	2.4	6.8
Ti	1.8	1.8	7.7
V	0.72	0.71	3.6
Mn	0.63	0.90	2.2
Ni	0.98	1.9	3.6
Cu	1.2	2.6	7.5
Zn	2.2	2.6	9.1
As	1.5	1.4	7.9
Zr	1.0	1.0	2.8
Sn	1.1	1.7	6.6
Pb	1.9	3.6	7.7

^a Samples used: NBS SRM 1261, 1262, 1263 and 1264.

^b Values obtained with same sample electrode. ^c Values obtained with different sample electrodes. ^d Values obtained under different measurement conditions.

(random reproducibility). The R.S.D.s for the internal reproducibility were in the range 0.63–2.2% for steel samples at concentrations ranging from 0.2 $\mu\text{g g}^{-1}$ to 1.99%, and were the same as or slightly better than those for external reproducibility. On the other hand, the R.S.D.s for the reproducibility obtained under different measurement conditions were in the range 2.2–12.9% i.e., poor compared with those for internal and external reproducibility.

Conclusion

These studies with the VG 9000 instrument show that for the precise determination of elements in metals by GDMS, sample size, sample position, discharge current and discharge voltage must be kept constant.

REFERENCES

- 1 A.J. Ahearn (Ed.), Trace Analysis by Mass Spectrometry, Academic, New York, 1972.

- 2 J.R. Bacom and M.U. Allen, *Analyst*, 109 (1984) 1229.
- 3 G.L. Gray, in F. Adams, R. Gijbels and R. Van Grieken (Eds.), *Inorganic Mass Spectrometry*, Wiley, New York, 1990, p. 17.
- 4 M. Saito, *Anal. Chim. Acta*, 236 (1990) 351.
- 5 W.W. Harrison, *J. Anal. At. Spectrom.*, 3 (1988) 867.
- 6 N.E. Sanderson, E. Hall, J. Clark, P. Charalambous and D. Hall, *Mikrochim. Acta*, 1 (1987) 275.
- 7 W.W. Harrison, K.R. Hess, R.K. Marcus and F.L. King, *Anal. Chem.*, 58 (1985) 341A.
- 8 W.W. Harrison, F.L. King, S.L. Tong and C.M. Barshick, in A. Benninghoven, A.M. Huber and H.W. Werner (Eds.), *Secondary Ion Mass Spectrometry, SIMS, Proceedings of the 6th International Conference on Secondary Ion Mass Spectrometry*, Wiley, New York, 1988, p. 825.
- 9 N. Jakubowski, D. Stuewer and W. Vieth, *Anal. Chem.*, 59 (1987) 1825.
- 10 B.N. Colby and C.A. Evans, Jr., *Anal. Chem.*, 46 (1974) 1236.

3,5,6-Trisubstituted 1,2,4-triazines as analytical reagents

Part I. Compounds containing the ferriin functional group or iron(II)–methine chromophore

W.I. Stephen

School of Chemistry, University of Birmingham, Edgbaston, Birmingham B15 2TT (UK)

M.A. Islam

Department of Chemistry, University of Dhaka, Dhaka 1000 (Bangladesh)

(Received 14th September 1992)

Abstract

Fourteen *as*-triazines with different suitable substituents at 3-, 5- and 6-positions have been synthesised. Chelating and chromogenic properties of these new ferriin compounds in reaction with iron(II) have been investigated spectrophotometrically together with a few closely related triazines for comparison. Spectral data, solution conditions favourable for chelate formation and other data are reported. An interesting feature of the absorption spectrum of the iron(II) chelate of the *as*-triazine bearing a substituent on either 3-(2-py)- or 5- and 6-phenyl rings or all is that it exhibits a pair of absorption maxima. The results demonstrate that the chromophoric enhancement of the ferriin functional group due to different 5- and 6-substituents is according to the following order: *p*-methoxyphenyl > 2-furyl > 4-biphenyl > *p*-methylphenyl > 6-methyl-2-pyridyl > phenyl > 2-pyridyl > methyl > hydrogen. Three outstanding chromogens have been found from among the new triazine derivatives which are superior in sensitivity to all ferriin-type chromogens previously reported.

Keywords: Spectrophotometry; Chromogens; Ferriin compounds; Triazines

Among the plethora of organic compounds employed for the colorimetric determination of trace concentrations of metals, the heterocyclic bases containing the α,α -diimine structure



commonly known as the ferriin functional group or the iron(II)–methine chromophore are among the most extensively studied class of reagents.

Correspondence to: W.I. Stephen, School of Chemistry, University of Birmingham, Edgbaston, Birmingham B15 2TT (UK).

The first and best known examples are 1,10-phenanthroline and 2,2'-bipyridine. The ability of these compounds to form stable and intensely coloured iron(II) and copper(I) chelates has prompted extensive investigations, particularly with respect to finding improved colorimetric reagents for iron, copper and certain other elements. The significant contributions in this regard have been made by Smith and Richter [1], Case [2] and Diehl et al. [3]. From their joint programme of research, Smith and Case have also provided important guidelines for the design of special purpose reagents. The contributions of other workers, particularly Schilt [4], a pupil of

Smith are also notable. An important example is the discovery that phenyl substituents *para* to the ferriin nitrogen atoms greatly enhance the molar absorptivities of the metal chelates. Since then, some representative ferriin-yielding chromogens have found general acceptance for the spectrophotometric determination of iron(II); examples are 4,7-diphenyl-1,10-phenanthroline [5], 2,4,6-tris(2-pyridyl)-1,3,5-triazine (TPTZ) [6], 2,6-bis(4-phenyl-2-pyridyl)-4-phenyl-2-pyridine (Terrosite) [7].

Continuing the search for superior chromogenic reagents from among the different possible compounds that contain the ferriin reactive group, Case and co-workers [8–17] have synthesised many compounds and supplied these to Schilt for evaluation as chromogenic reagents. Among this extensive array of ferriin-type compounds, certain *as*-triazine derivatives proved particularly interesting from the standpoint of both sensitivity and usefulness as iron chromogens. Some of the most widely used iron chromogens found to date belong to this *as*-triazine series. It includes: 3-(2-py)-5,6-diphenyl-*as*-triazine (PDT) [18], 3-(4-phenyl-2-py)-5,6-diphenyl-*as*-triazine (PPDT) [18], 2,4-bis(5,6-diphenyl-1,2,4-triazine-3-yl)pyridine (2,4-BDTP) [19], 3-(4-phenyl-2-py)-5-phenyl-*as*-triazine [20] and the water soluble derivatives Ferrozine [21], PPDT-DAS [22], and Ferene[®], the disodium salt of 3-(2-py)-5,6-bis[2-(5-furylsulphonic acid)]-1,2,4-triazine [23].

The joint work of Case and Schilt showed that the incorporation of different groups at the 3-position of 1,2,4-triazine did not produce a chromogen which was superior to the 2-pyridyl group [24]. It has been confirmed [25] that there is little point in designing new methine chromophores by extending the ferriin grouping beyond that of the tridentate functionality. However, it has been shown that if the methine chromophoric group is incorporated in an aromatic system, the resulting chelate tends to be more stable and more intensely coloured. Schilt [18] has reported the trends which accompany changes in substituents of a heterocyclic ring that constitute one half of the ferriin functionality. For example, the replacement of the hydrogen atom *para* to the

imine nitrogen with a methyl, ethyl or phenyl group enhances the chromophoricity of the ligand with respect to metal ion chelation. The order of enhancement is $C_6H_5 > C_2H_5 > CH_3 > H$. In later studies, the effects of substituents at the 5- and 6-positions of 1,2,4-triazine have been demonstrated; i.e., phenyl groups at these positions [18] possess greater sensitivity than those with corresponding hydrogens and methyl groups [19]. However, no attempt has so far been made to introduce more suitable substituents on these positions of 1,2,4-triazine, with the hope of further chromophoric enhancement, although sulphonic groups have of course been added to increase the solubility of the compounds, e.g., Ferrozine [21].

In this laboratory [26,27] work has continued to be directed towards the discovery of more sensitive colour-forming reagents for the spectrophotometric determination of metals by simple synthetic routes. In the present study, it was considered of interest to prepare some *as*-triazines with suitably substituted phenyl (which enhances the electron delocalisation process) and biphenyl groups at 5- and 6-positions, which might lead to further chromophoric enhancement. Fourteen new 3,5,6-trisubstituted-1,2,4-triazines containing the ferriin-functional group have been prepared simply by condensing pyridyl- or a 4-substituted pyridyl-2-hydrazidine with different 1,2-dicarbonyl compounds under mild refluxing conditions. The absorptiometric characteristics of these new *as*-triazines have been studied together with some closely related triazines for comparison. Spectral data, solution conditions favourable for chelating and other data are reported.

The compounds, listed below by name, will be referred to by the following abbreviations: 3-(2-py)-5,6-diphenyl-*as*-triazine (PDT); 3-(4-methyl-2-py)-5,6-diphenyl-*as*-triazine (MPDT); 3-(4-phenyl-2-py)-5,6-diphenyl-*as*-triazine (PPDT); 3-(2-py)-5,6-bis(*p*-methylphenyl)-*as*-triazine (PDMPT); 3-(4-methyl-2-py)-5,6-bis(*p*-methylphenyl)-*as*-triazine (MPDMPT); 3-(4-phenyl-2-py)-5,6-bis(*p*-methylphenyl)-*as*-triazine (PPDMPT); 3-(2-py)-5,6-bis(4-biphenyl)-*as*-triazine (PBBT); 3-(4-methyl-2-py)-5,6-bis(4-biphenyl)-*as*-triazine (MPBBT); 3-(4-phenyl-2-py)-5,6-bis(4-biphenyl)-

as-triazine (PPBBT); 3-(2-py)-5,6-bis(*p*-methoxyphenyl)-*as*-triazine (PBMPT); 3-(4-methyl-2-py)-5,6-bis(*p*-methoxyphenyl)-*as*-triazine (MPBMPT); 3-(4-phenyl-2-py)-5,6-bis(*p*-methoxyphenyl)-*as*-triazine (PPBMPT); 3-(2-py)-5,6-bis(2-furyl)-*as*-triazine (PBFT); 3-(4-methyl-2-py)-5,6-bis(2-furyl)-*as*-triazine (MPBFT); 3-(4-phenyl-2-py)-5,6-bis(2-furyl)-*as*-triazine (PPBFT); 3-(2-py)-5,6-bis(6-methyl-2-py)-*as*-triazine (PBSPT) 3-(4-methyl-2-py)-5,6-bis(6-methyl-2-py)-*as*-triazine (MPBSPT); 3-(4-phenyl-2-py)-5,6-bis(6-methyl-2-py)-*as*-triazine (PPBSPT).

EXPERIMENTAL

Preparation of 1,2-diketones

4,4'-Biphenylbenzil or 1,2-bis(biphenyl)-1,2-dioxoethane

In a 500-ml flask 18 g (0.1 mol) of 4-biphenyl-carboxaldehyde and 100 ml of ethanol were taken. A reflux condenser was attached to the flask, which was heated gently to dissolve the carboxaldehyde. Then a solution of 3.5 g of potassium cyanide in 10 ml of distilled water was added dropwise to the hot solution of carboxaldehyde and the mixture was allowed to reflux. Within 4–5 min of refluxing, it became a solid mass. Then the contents of the flask were cooled, filtered by suction, washed several times with water to remove potassium cyanide and dried in the oven at 100°C. An almost quantitative yield of the product, 4,4'-biphenylbenzoin as a pale yellow material was obtained. A small portion of this material upon recrystallisation from hot toluene gave a white crystalline material, m.p. 152–54°C. Calculated for $C_{26}H_{20}O_2$: C 85.69%; H 5.53%. Found: C 85.9%; H 5.5%.

Attempted oxidation of the above benzoin to 4,4'-biphenylbenzil by nitric acid was not very successful. In this case, the oxidation of benzoin to benzil resulted in a compound or mixture of compounds containing a very low percentage of carbon, which might be due to the decomposition of the benzoin. Oxidation with copper(II) acetate resulted in excellent yields of the benzil. In a 500-ml flask fitted with a reflux condenser, 9.1 g

of crude 4,4'-biphenylbenzil, 0.5 g of copper(II) acetate, 5 g of ammonium nitrate and 250 ml of an 80% (v/v) acetic acid–water solution were taken. The mixture was refluxed for 1 h. On cooling, bright yellow needle-shaped crystals of 4,4'-biphenylbenzil appeared. These were filtered at the pump, washed well with distilled water and dried. The resulting benzil (7.25 g, 80% yield) melted at 140–42°C. Calculated for $C_{26}H_{18}O_2$: C 86.16%, H 5.0%. Found: C 85.9%; H 5.3%.

6,6-Dimethyl-2,2'-pyridil or 1,2-bis(6-methyl-2-pyridyl)-1,2-dioxoethane

Stephen and Uden [27] have already reported the preparation of this compound. In this work, the attempted oxidation of 6,6'-dimethyl-2,2'-pyridoin to the corresponding pyridil by copper(II) acetate and ammonium nitrate was unsuccessful; it resulted in a tar. Air oxidation of this compound led to a higher yield of 6,6'-dimethyl-2,2'-pyridil. In a conical flask 4.0 g of 6,6'-dimethyl-2,2'-pyridoin and 150 ml of ethanol were taken and warmed to make a homogeneous solution. Oxygen was then passed through the solution for about an hour to complete the oxidation, during which the solution was kept warm enough with occasional heating to prevent the crystallisation of the pyridoin. Within the passage of oxygen, the pyridoin did not reappear on lowering the temperature of the solution, the colour of which turned completely from orange to yellow. On cooling and shaking the flask, yellow crystals of 6,6'-dimethyl-2,2'-pyridil started to appear. After reduction of the volume to one third under reduced pressure, 3.5 g (88.2% yield) of material were collected by suction filtration m.p. 176–78°C. Calculated for $C_{14}H_{12}N_2O_2$: C 69.98%; H 5.03%; N 11.60%. Found: C 69.8%; H 5.0%; N 11.7%. The compound, 6,6'-dimethyl-2,2'-pyridil, is very light sensitive. The light yellow crystals turn greenish on exposure to light.

Preparation of hydrazidines related to 2-cyano-4-substituted pyridines

Pyridyl-2-hydrazidine and 4-methylpyridyl-2-hydrazidine were prepared following the method of Case [8] with minor modifications. To avoid

using ether and benzene, dichloromethane and toluene were used as extracting and crystallising solvents respectively and similar yields of hydrazidines were obtained. 4-Phenylpyridyl-2-hydrazidine was prepared according to the method of Kiss [22] incorporating the following modifications. Dichloromethane was used as extracting solvent and the dichloromethane extract was dried over anhydrous sodium sulphate. After complete removal of the solvent under reduced pressure, a light yellow product was obtained. The attempted recrystallisation from toluene or dichloromethane was unsuccessful. Kiss [22] reported that if the recrystallisation of this hydrazidine from benzene was delayed, the impurities catalysed its degradation. The failure to recrystallise from toluene or dichloromethane may be due to slower evaporation of toluene and high solubility of the material in dichloromethane during which it is being degraded by the impurities. Recrystallisation from acetone resulted in very fine needle-shaped white crystalline material in even higher yield than that obtained by Kiss.

Preparation of 3,5,6-trisubstituted 1,2,4-triazines

A series of *as*-triazines (structural formula and the abbreviated names of compounds used throughout this paper are given in Fig. 1) has been prepared simply by condensing a hydrazidine with a suitable 1,2-diketone. It has been observed that if the condensation reaction is carried out by warming or by allowing a 12-h reaction time following the method of Case [8], condensation occurs at one carbonyl group only. The condensation at the other carbonyl group, i.e., ring closure to the *as*-triazine, takes place during recrystallisation from boiling ethanol. However, if the condensation reaction is carried out under mild refluxing conditions rather than warming or allowing just 12 h reaction time, the reduction of the volume under reduced pressure followed by the addition of hexane results in a higher yield of the triazine. This method of preparation has the advantage of obtaining *as*-triazines in one step with high purity. Recrystallisation is not usually required since the melting point and elemental data remain unchanged. In some cases, it has also

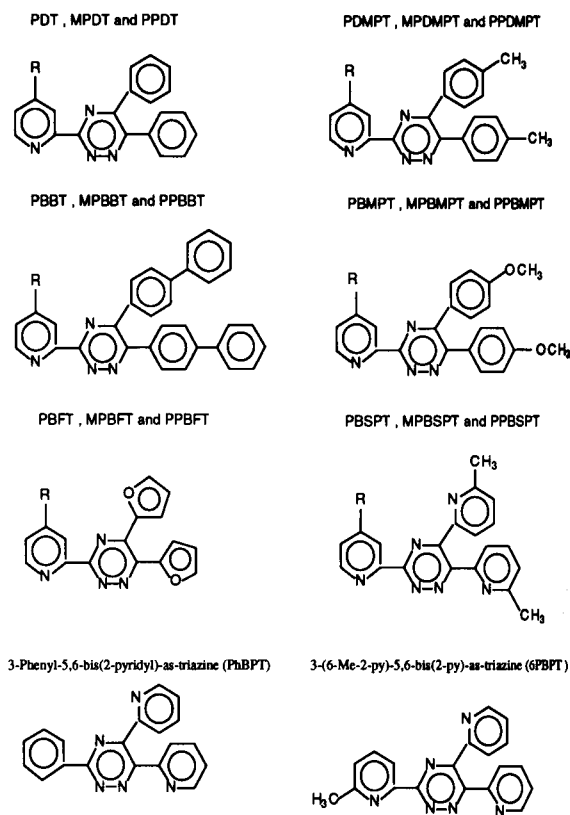


Fig. 1. Abbreviated names of the *as*-triazines and their structural formulae.

been observed that if the refluxing is extended or if vigorous refluxing conditions are used, product isolation is hampered due to the formation of a viscous mass. As the number of phenyl groups in the system increases, product isolation becomes simpler. The yield of the triazines containing the biphenyl groups was almost quantitative. The quantitative nature of this reaction has already been mentioned by Kiss [22] during the preparation of PPDT. It seems that provided the high purity of the reactants is maintained, careful isolation of the product is capable of producing almost quantitative yields of different *as*-triazines. Preparation of *as*-triazines containing the 2-furyl group under different conditions (namely, at room temperature, by heating on a water bath and even under vigorous refluxing conditions) results in the same product. Elemental analysis of this product corresponds to the condensation at

only one carbonyl group. In this case, mild acid hydrolysis is required to yield the triazine. General methods of preparation of the triazines are given below and their characterisation is shown in Table 1.

PDT, MPDT and PPDT

These compounds were prepared according to the method of Case [8] with minor modifications. Equimolar mixtures (0.005 mol) of benzil and pyridyl/4-substituted pyridyl-2-hydrazidine in 15–20 ml of ethanol were warmed gently under reflux for 10–15 min to dissolve the reactants completely. Each solution was allowed to stand for 24 h. The yellow crystalline material was filtered off, washed with a little hexane and air dried.

PDMPT, PBSPT, MPBSPT and PPBSPT

Mixtures of equimolar amounts (0.005 mol) of pyridyl/4-substituted pyridyl-2-hydrazidine and 4,4'-dimethylbenzil/6,6'-dimethyl-2,2'-pyridil in 50 ml of ethanol were heated under reflux for 15 min. The volume of the solution was reduced to one third under reduced pressure in a rotary

evaporator at boiling water bath temperature. The residue, on treatment with 75–100 ml of hot hexane, became homogeneous. Each solution was allowed to stand until the yellow product crystallises and it was then filtered off and air dried.

PBMPT, MPBMPT, MPDMPT and PPDMPT

Equimolar mixtures of pyridyl/4-substituted pyridyl-2-hydrazidine and 4,4'-substituted benzil were reacted as above. The residue on treatment with hexane gave a solid product. In the case of MPDMPT, an additional amount of highly crystalline yellow product was obtained from the mother liquor (hexane). These compounds could be recrystallised from ethanol.

PBBT, MPBBT, PPBBT and PPBMPT

Mixtures of equimolar amounts (0.005 mol) of pyridyl/substituted pyridyl-2-hydrazidine and 4,4'-disubstituted benzil in 150 ml of ethanol were heated under reflux for 15–30 min to dissolve the reactants completely. The reaction mixture was allowed to stand for 48 h. The crystalline yellow material was filtered off, washed with a little hexane and air dried. A further amount of very

TABLE 1

Characterisation of the 3,5,6-trisubstituted 1,2,4-triazines studied

Compound	Yield (%)	m.p. (°C)	Molecular formula	Expected (%)			Found (%)		
				C	H	N	C	H	N
PDT	–	188–190	C ₂₀ H ₁₄ N ₄	–	–	–	–	–	–
PDMPT	68	130–132	C ₂₂ H ₁₈ N ₄	78.08	5.36	16.55	78.1	5.2	16.8
PBBT	95	198–200	C ₃₂ H ₂₂ N ₄	83.09	4.79	12.11	82.9	4.6	11.9
PBMPT	–	143–155	C ₂₂ H ₁₈ N ₄ O ₂	71.34	4.89	15.12	71.2	4.9	15.2
PBSPT	89	158–160	C ₂₀ H ₁₆ N ₆	70.56	4.74	24.68	70.8	4.5	24.8
MPDT	–	167–169	C ₂₁ H ₁₆ N ₄	–	–	–	–	–	–
MPDMPT	86	132–134	C ₂₃ H ₂₀ N ₄	78.38	5.72	15.89	78.4	5.5	15.8
MPBBT	98	169–171	C ₃₃ H ₂₄ N ₄	83.16	5.07	11.75	83.0	5.0	11.5
MPBMPT	87	156–158	C ₂₃ H ₂₀ N ₄ O ₄	71.85	5.24	14.57	71.7	5.3	14.4
MPBSPT	70	156–158	C ₂₁ H ₁₈ N ₆	71.16	5.11	23.71	70.7	5.2	23.9
MPBFT	54	172–174	C ₁₇ H ₁₂ N ₄ O ₂	67.09	3.97	18.40	66.8	4.0	18.0
PPDT	89	191–193	C ₂₆ H ₁₈ N ₄	–	–	–	–	–	–
PPDMPT	64	204–206	C ₂₈ H ₂₂ N ₄	81.13	5.34	13.51	80.9	5.5	13.3
PPBBT	^a	234–236	C ₃₈ H ₂₆ N ₄	84.73	4.86	10.40	84.9	5.2	10.6
PPBMPT	88	200–202	C ₂₈ H ₂₂ N ₄ O ₂	75.32	4.96	12.55	75.2	4.9	12.2
PPBFT	–	163–165	C ₂₂ H ₁₄ N ₄ O ₂	72.12	3.85	15.29	72.2	3.7	15.2
PPBAPT	60	145–147	C ₂₆ H ₂₀ N ₆	74.98	4.84	20.17	74.5	5.2	19.8

^a Almost quantitative.

fine light yellow product was obtained from the mother liquor on reduction of the volume and adding hexane.

MPBFT and PPBFT

Equimolar mixtures (0.005 mol) of 2,2'-furyl and 4-substituted pyridyl-2-hydrazidine were heated under reflux for 15 min. After a few minutes of refluxing, a clear solution was formed and then precipitation of the compound occurred a short time later. After cooling to room temperature and filtering, the isolated material was dissolved in ethanol with the help of a few drops of concentrated hydrochloric acid. The volume of the solution was reduced and after adding hexane, a yellow product appeared during stirring. It was collected by suction filtration and washed with hexane.

Solutions

A stock standard iron solution (1 mg ml⁻¹) was prepared by dissolving 0.510 g of electrolytic iron in sufficient concentrated hydrochloric acid and diluting to 500 ml with distilled water. Suitable aliquots were taken to prepare the working concentration by further dilution. A standard aqueous solution of copper(II) (1 mg ml⁻¹) was prepared by dissolving accurately weighed amounts of AR copper(II) chloride dihydrate.

A range of conventional buffer solutions, formally 1 M in strength was prepared containing, where appropriate, one or more of the following analytical grade chemicals: hydrochloric acid, acetic acid, potassium chloride, sodium acetate, ammonium acetate, ammonium chloride and aqueous ammonia solution. Solutions at unit pH intervals in the range 1–11 were thus obtained. A 10% (w/v) aqueous solution of pure hydroxylammonium chloride was used as reducing agent. A 50% (w/v) aqueous solution of AR grade sodium perchlorate was used in the extraction studies.

A stock solution (0.005 M) of the organic reagents was usually prepared by dissolving the requisite amount in a small volume of absolute ethanol. In some cases, a drop or more of concentrated hydrochloric acid was added to dissolve the reagent. The solution was then diluted to

volume with ethanol. Dilution of the stock solution was made for the determination of the composition of the complexes.

Analytical procedures

Complex formation studies

To each of a series of 25 ml volumetric flasks were added in turn, 5 ml of iron solution (5.1–10.2 μg ml⁻¹), 2 ml of 10% hydroxylammonium chloride solution, 2 ml of the organic reagent solution and 5 ml of buffer solution (different in each flask and covering the range pH 1–11) and then diluted to volume with absolute ethanol. The pH range over which complexation occurred, as indicated by colour formation was noted, and so was the pH range for which colour formation was maximal.

Absorption characteristics

Solutions of the various complexes were prepared for spectrophotometric examination by the following general procedure. An exact amount of metal ion solution was transferred to a 25-ml volumetric flask, 2 ml of 10% hydroxylammonium chloride solution and 5 ml of the organic reagent solution were added, followed by 5 ml of buffer solution of pH 4.76. The contents of the flask were diluted to volume with ethanol. The absorption spectrum of the solution was recorded with a Shimadzu UV–visible recording spectrophotometer (UV-240) using 1-cm glass cells in the visible region and silica cells in the ultraviolet region. In the case of the organic reagent containing biphenyl groups, 50-ml volumetric flasks were used. In all cases at least five different solutions of each complex were prepared and the molar absorptivity (ϵ) of the complex at the wavelength of maximum absorbance (λ_{\max}) was calculated from the linear regression coefficient.

Where measurements were done on chloroformic solutions, the following procedure was used. The metal ion solution was placed in a 50-ml separating funnel followed by other reagents as above and 2 ml of 50% sodium perchlorate solution; 7–8 ml of chloroform were then added and the contents were mixed well. The chloroform layer was collected in a 25-ml

volumetric flask and the extraction was repeated with a further 7–8 ml of chloroform.

Spectra of all solutions were recorded against the similarly prepared reagent blank solution in the appropriate solvents.

Metal to ligand ratios of the chelates were determined spectrophotometrically by the mole-ratio method; once by varying the amount of complexing agent and keeping the amount of iron constant and again by varying the amount of iron and keeping the amount of complexing agent constant. The results are summarised in Table 5.

To evaluate the colour stability of the complex solution, the absorbance of the solution was measured just after making up the solution to volume with the appropriate solvent and again measured after allowing sufficient time.

The interference of copper ion on the determination of iron with most of the triazines, and the masking of this effect, have been observed by the following procedure. Exactly the same amount of standard iron solution was transferred to a series of volumetric flasks followed by standard copper(II) solution containing up to five times the amount of iron present. The colours of the metal complexes with different triazines were developed by the analytical procedure. Absorbances of the solutions were recorded against similarly prepared reagent blanks at the wavelength of maximum absorbance (λ_{\max}). Absorbances of the solution were again measured after masking the copper complex by the addition of 10–15 mg of thiourea. Typical examples are given in Table 3 and 4.

RESULTS AND DISCUSSION

The series of *as*-triazines studied in this investigation react immediately and very sensitively with iron(II) to give highly coloured complexes which are soluble in aqueous–ethanol medium. The apparent slightly slower rate of complexation of the compounds bearing substituents adjacent to the imine nitrogen (i.e., PBSPT series and 6PBPT) may be due to the competition among the possible sterically free and hindered ferriin functionalities. Iron(II) complexes of the triazines

TABLE 2

Formation conditions and properties of the iron(II) complexes (Working pH = 4.76)

Organic reagent	Colour of complex	Time of development	pH ranges for ^a	
			Colour formation	Max. colour formation
PDT	Magenta	Immediate	(1–8)	(3–8)
MPDT	Magenta	Immediate	(2–11)	(3–8)
PPDT	Magenta	Immediate	(2–11)	(3–8)
PDMPT	Violet	Immediate	1–11	2–9
MPDMPT	Violet	Immediate	1–11	1–9
PPDMPT	Violet	Immediate	1–11	1–10
PBBT	Violet	Immediate	1–11	1–10
MPBBT	Violet	Immediate	1–11	1–10
PPBBT	Violet	Immediate	1–11	1–10
PBMPT	Violet	Immediate	1–11	2–8
MPBMPT	Violet	Immediate	1–11	1–9
PPBMPT	Violet	Immediate	1–11	1–9
PBFT	Intense violet	Immediate	–	–
MPBFT	Intense violet	Immediate	1–11	2–8
PPFBT	Blue	Immediate	1–11	1–9
PBSPT	Deep violet	ca. 5 min	1–11	1–10
MPBSPT	Deep violet	ca. 5 min	1–11	1–10
PPBSPT	Deep violet	ca. 5 min	1–11	1–10
PhBPT ^b	Green	ca. 5 min	–	–
6PBPT	Greenish blue	ca. 10 min	–	–

^a The reported values are quoted in parentheses. ^b Prepared and supplied by Dr. W.I. Stephen.

containing the biphenyl groups are relatively less soluble and require an aqueous–ethanol (1:3) mixture. All these triazines are readily accessible by simple synthetic routes. The pH ranges for maximum colour production of the new compounds are generally broad (Table 2). Absorption characteristics of the iron(II) complexes are compiled in Table 5. The wavelengths given are for maximum absorbances, and the molar absorptivity values (ϵ) correspond to the wavelength cited. This type of ferriin-yielding chromogen reacts selectively and very sensitively with iron(II) and only very weakly with other cations [21,23]. It has been observed in this study, that the interference of copper(I) can be entirely and instantaneously eliminated in the visible region by the addition of thiourea (typical examples are given in Tables 3

TABLE 3

Effect of copper(I) on the absorbance of PPBBT-iron(II) complex and its masking $0.51 \text{ mg Fe l}^{-1}$)

Copper added (mg l^{-1})	Absorbance at		Absorbance after masking with thiourea at	
	575 nm	386 nm	575 nm	386 nm
0.000	0.33	0.44	0.330	0.440
0.504	0.35	0.56	0.320	0.440
1.008	0.38	0.68	0.320	0.450
1.512	0.40	0.82	0.320	0.455
2.016	0.43	0.92	0.320	0.460 (0.44) ^a
2.520	0.46	1.06	0.325	0.480 (0.45) ^a
5.040	0.61	1.61	0.330	0.520 (0.46) ^a

^a After approximately 18 h.

and 4). The absorbance of the iron(II) complex of PPBBT at shorter wavelength remains 2–18% higher after masking with thiourea with respect to zero copper depending on the amount of copper present. However, after approximately 18 h the absorbance at this wavelength also becomes equivalent to zero copper within experimental error (Table 4).

Interestingly, the absorption spectrum of the iron(II) complexes of the *as*-triazine bearing a substituent on either 3-(2-py)- or 5- and 6-phenyl or all groups exhibits a pair of absorption maxima (Fig. 2). All complexes appear to obey Beer's law over the selected experimental concentration range (up to 2 mg Fe l^{-1}) at both the wavelengths of maximum absorbance. The substituent on these groups probably favours metal to ligand ($M \rightarrow L$) charge transfer transition. Transitions of this type

TABLE 4

Effect of copper(I) on the absorbance of PPBMPT-iron(II) complex and its masking ($1.02 \text{ mg Fe l}^{-1}$)

Copper added (mg l^{-1})	Corresponding absorbance at 570 nm1	Absorbance after masking with thiourea
0.000	0.68	0.68
1.008	0.74	0.68
2.016	0.80	0.68
3.024	0.87	0.68
4.032	0.94	0.70
5.040	1.00	0.68
7.056	1.15	0.69

can be expected only when the ligand possesses low-lying empty orbitals and the metal ion has filled orbitals lying higher than the highest filled ligand orbitals [28]. The appearance of the second peak in the shorter wavelength region has not been mentioned by either Schilt [18] for MPDT and PPDT or Kiss [22] for PPDT. However, for the first time Kiss [29] has reported that the absorption spectra of iron(II) and copper(I) chelates of the similar type of *as*-triazines, IQDT, IQDT-TAs and TSBT-TAs exhibit two absorption maxima. The absorption spectra of the iron(II) complexes of PBFT, MPBFT, PPBFT, PBSPT, MPBSPT and PPBSPT exhibit a single absorption peak in the visible region. These may give an additional peak in the ultraviolet region. The preparations of PBFT and its sulphonated derivative, Ferene, have been described by Hennesy et al. [23]. They have reported the spectral characteristics of the iron(II) complex of Ferene only. The molar absorptivity of the iron(II) complex of PBFT has been reported here only for comparison with the newly-prepared analogous compounds.

Among the new *as*-triazines, the series with 6-methyl-2-pyridyl substituents at the 5- and 6-positions of 1,2,4-triazine (i.e., PBSPT, MPBSPT and PPBSPT) is the least useful of the iron(II) chromogens prepared in this investigation, although they are more sensitive than that of the reported series bearing phenyl groups at the same positions i.e., PDT, MPDT and PPDT. All other series are more sensitive towards iron(II) than this. The highest sensitivity is shown by the compounds with *p*-methoxyphenyl groups. Schilt et al. [18,19] have reported the molar absorptivities of the iron(II) complexes of 3-(2-py)-*as*-triazine ($\epsilon = 11\,300 \text{ l mol}^{-1} \text{ cm}^{-1}$), 3-(2-py)-5,6-dimethyl-*as*-triazine ($\epsilon = 14\,500 \text{ l mol}^{-1} \text{ cm}^{-1}$) and of 3-(2-py)-5,6-diphenyl-*as*-triazine (PDT, $\epsilon = 24\,000 \text{ l mol}^{-1} \text{ cm}^{-1}$). In this study, it has been observed that the molar absorptivities of the iron(II) complexes of 3-(2-py)-5,6-diphenyl-*as*-triazine (PDT), 3-(2-py)-5,6-bis(*p*-methylphenyl)-*as*-triazine (PDMPT) and 3-(2-py)-5,6-bis(4-biphenyl)-*as*-triazine (PBBT) are $\epsilon_{555} = 24\,400$, $\epsilon_{562} = 27\,500$ and $\epsilon_{570} = 30\,700 \text{ l mol}^{-1} \text{ cm}^{-1}$, respectively. These observations demonstrate clearly the effect of

substituents at the 5- and 6-positions of 1,2,4-triazine. The chromophoric enhancement of the ferrioin functionality is according to the order biphenyl > *p*-methylphenyl > phenyl > methyl > hydrogen. This is because of enhanced electron delocalisation in the molecule. However, the molar absorptivities of the iron(II) complexes of 3-(2-py)-5,6-bis(2-furyl)-*as*-triazine (PBFT) and 3-(2-py)-5,6-bis(*p*-methoxyphenyl)-*as*-triazine

(PBMPT) are found to be $\epsilon_{567} = 31\,300$ and $\epsilon_{562} = 32\,500 \text{ l mol}^{-1} \text{ cm}^{-1}$, respectively. It illustrates that the 2-furyl group is comparable to and the *p*-methoxyphenyl group is better as chromophoric enhancer of the ferrioin-functionality than the biphenyl group. This contradicts the general observations that the involvement of more phenyl rings in the system gives rise to enhanced molar absorptivities. This may be because of some loss

TABLE 5
Absorption characteristics of the iron(II) complexes

Organic reagent	Solution medium	λ_{max} (nm)	ϵ ($\text{l mol}^{-1} \text{ cm}^{-1}$)	Composition M:L	Colour stability
PDT	Ethanol-water	555 (553)	24 400 (24 000)	1:3	> 12 h
MPDT	Ethanol-water	562 (562)	25 460 (24 600)	-	-
		357	22 450		
PPDT	Ethanol-water	566 (561)	29 100 (28 700)	-	-
		358	35 000		
PDMPT	Ethanol-water	561	27 500	1:3	> 2 h
		376	18 300		
MPDMPT	Ethanol-water	566	28 500	1:3	> 4 h
		376	17 750		
PPDMPT	Ethanol-water	565	31 800	-	> 2 h
		384	34 000		
PBBT	Ethanol-water	570	30 700	1:3	> 12 h
		385	37 400		
MPBBT	Ethanol-water	574	31 400	1:3	> 2 h
		391	36 300		
PPBBT	Ethanol-water	575	36 200	1:3	> 12 h
		388	48 200		
PPBBT	Chloroform	574	35 700	-	> 4 h
		384	49 000		
PBMPT	Ethanol-water	562	32 500	1:3	> 2 h
		405	20 200		
MPBMPT	Ethanol-water	568	32 600	1:3	> 2 h
		397	23 400		
PPBMPT	Ethanol-water	570	37 250	1:3	> 6 h
		400	27 700		
PPBMPT	Chloroform	570	37 500	-	-
		404	26 600		
PBFT	Ethanol-water	576	31 300	-	-
MPBFT	Ethanol-water	585	32 100	-	> 1 h
PPBFT	Ethanol-water	589	35 700	1:3	> 2 h
PPBFT	Chloroform	585	35 700	-	> 2 h
PBSPT	Ethanol-water	566	25 100	1:3	> 4 h
MPBSPT	Ethanol-water	570	25 600	-	> 2 h
PPBSPT	Ethanol-water	570	28 800	-	> 2 h
PhBPT	Ethanol-water	660	8 650	-	-
6PBPT	Ethanol-water	575	10 500	-	-
		(600) ^a	7 800		
		(396) ^a	13 900	-	-

^a After approximately 18 h. The reported values are quoted in parentheses.

of coplanarity essential for π -electron delocalisation due to adjacent bulky biphenyl groups. This also demonstrates how simply incorporating methoxy groups on the phenyl rings (PBMPT), results in the sensitivity being increased to a considerable extent, and certainly greater than the iron(II)–methine chromophore derived from 4-arylpiperidine i.e., PPDT [18] and terrosite [7].

Schilt [18] has demonstrated that the replacement of the hydrogen atom *para* to the imine nitrogen of the 3-(2-py)-group with a methyl, ethyl or phenyl group enhances the visible region chromophoricity of the ligand with respect to metal ion chelation. A similar trend has been observed in this study with different sets of compounds. Apparently it seems that the methyl and phenyl substituents enhance the molar absorptivity of the iron(II) complex in the visible region by factors of approximately 1000 and 5000, compared with the hydrogen atom.

The intensity of the second peak also depends on the nature of the substituents on the 5- and 6-phenyl groups in the order phenyl > CH₃ > OCH₃, and on the 2-py-group in the order phenyl > CH₃. This order would be expected on the basis of the availability of the low lying empty orbitals in the ligand. The combined contributions of all these substituents in any combinations are always additive to enhance the chromo-

phoricity of the ferriin functionality at longer wavelength. However, this is not true at the shorter wavelength region, where an antagonistic effect is observed; an explanation of this has yet to be found. An exception is the phenyl and phenyl combination (PPBBT) when a synergistic effect is observed. The presence of the larger number of phenyl rings in the chelate may make M → L charge transfer transitions more probable.

The additive contributions of different substituents on 3-(2-py)-, and 5- and 6-phenyl rings of 1,2,4-triazine to enhance the chromophoricity with respect to metal ion chelation in the visible region make the compounds PPBBT, PPMPT and PPBFT the most sensitive iron(II)–methine chromophores so far reported. The most sensitive iron(II) chromogen so far reported to date is 3-(4-phenyl-2-py)-5-phenyl-1,2,4-triazine [19]. Its iron(II) chelate has a molar absorptivity of 34 800 l mol⁻¹ cm⁻¹ at 560 nm. The molar absorptivities of the iron(II) complexes of PPBBT, PPMPT and PPBFT are $\epsilon_{575} = 36\,200$, $\epsilon_{570} = 37\,250$ and $\epsilon_{589} = 35\,700$ l mol⁻¹ cm⁻¹, respectively, which are significantly greater than that of the above compound. At shorter wavelength it is even greater for the PPBBT complex ($\epsilon_{388} = 48\,200$ l mol⁻¹ cm⁻¹). These two very sensitive absorption maxima of the iron(II) chelate of PPBBT may be utilised to provide a broader dynamic range espe-

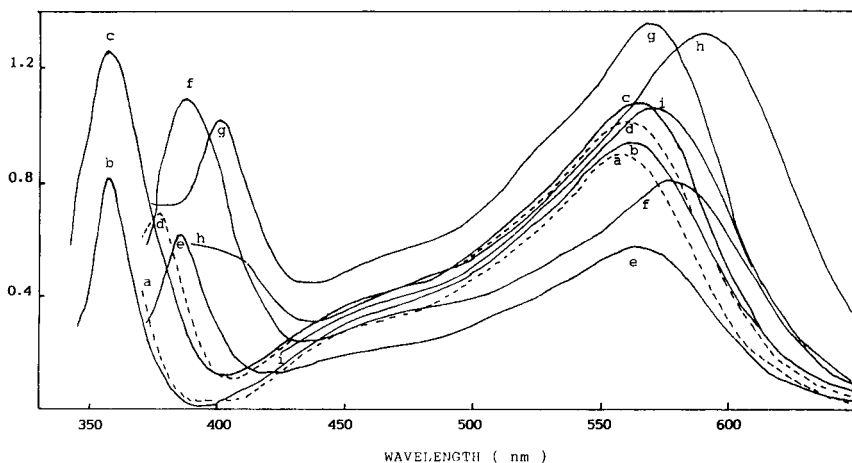


Fig. 2. Absorption spectra of iron(II) complexes of (a) PDT, (b) MPDT, (c) PPDT, (d) PDMPT, (e) PPMPT, (f) PPBBT, (g) PPMPT, (h) PPBFT and (i) PPBSPT in aqueous ethanol medium recorded against reagent blanks in 1-cm cells at a metal concentration of 2.04 mg l⁻¹, except (e) 1.02 mg l⁻¹ and (f) 1.22 mg l⁻¹.

cially for the development of analytical procedures involving microamounts of analyte. The PPBBT complex is comparatively less soluble in aqueous ethanol medium. However, it is easily extracted by chloroform with only a slight loss in sensitivity at the longer wavelength ($\epsilon_{574} = 35\,700 \text{ l mol}^{-1} \text{ cm}^{-1}$) and a slight improvement at the shorter wavelength ($\epsilon_{384} = 49\,000 \text{ l mol}^{-1} \text{ cm}^{-1}$). PPBMPT is the most sensitive ferroin-yielding chromogen found in this study. The presence of the methoxy groups makes it and its metal chelate more soluble in aqueous ethanol medium than any other system. The PPBMPT complex is easily extracted by chloroform over the pH range 2–9. The spectrum of the chloroform solution is very similar to that of the aqueous and ethanolic solutions. There is a slight sensitivity enhancement at the longer wavelength ($\epsilon_{570} = 37\,500 \text{ l mol}^{-1} \text{ cm}^{-1}$) but a loss at the shorter wavelength ($\epsilon_{404} = 26\,600 \text{ l mol}^{-1} \text{ cm}^{-1}$). The PPBFT complex is also easily extracted by chloroform. The spectrum of the chloroform solution shows a small hypsochromic shift with the same molar absorptivity ($\epsilon_{585} = 35\,700 \text{ l mol}^{-1} \text{ cm}^{-1}$). The higher molar absorptivities and colour stability of the complex in the solvent systems studied make the compounds PPBMPT, PPBBT and PPBFT most effective chromogens for the determination of trace amounts of iron. Kiss [22] has demonstrated the relative accessibility of arylpyridine, since the most intense colour formation with iron(II) has been observed in compounds containing the methine chromophoric group derived from arylpyridine. 4,4'-Biphenylbenzil can be prepared almost quantitatively from the commercially-available 4-biphenylcarboxaldehyde. The ease of preparation and very high yield especially of PPBBT and PPBMPT are added advantages. We are studying these further to prepare water soluble sulphonated derivatives for greater convenience. The high sensitivity of PBMPT also offers great promise as a new chromogen, since it is derived from readily available 2-cyanopyridine and anisil.

Schilt et al. [30] have also described the spectral characteristics of the iron(II) chelate of 6PBPT ($\epsilon_{612} = 8400 \text{ l mol}^{-1} \text{ cm}^{-1}$). During the course of this study a series of compounds with the 3-(6-methyl-2-pyridyl)group was also pre-

pared for examination of the chemical behaviour of 3-(2-py)-5,6-disubstituted *as*-triazines in which the imine nitrogen was blocked by incorporating a methyl substituent adjacent to it [31]. It has been observed that after addition of the reagent to an iron(II) solution, the initially developed light green colour of the solution gradually changes to purple. When the solution was buffered (pH 4.76) it led to the formation of a deep violet solution. This is evidence for the possible existence of an intermediate species. The absorption spectrum of this solution shows a single absorption peak at 575 nm with a molar absorptivity of 10 500. An interesting feature of the aqueous and ethanolic solutions of this violet chelate is that after around 18 h, the absorption maximum shifts from 575 to 600 nm. A second absorption maximum at 396 nm with molar absorptivities of $\epsilon_{600} = 7800$ and $\epsilon_{396} = 13\,900 \text{ l mol}^{-1} \text{ cm}^{-1}$, respectively also appear. The reported very low molar absorptivity compared to 10 500 or 7800 $\text{l mol}^{-1} \text{ cm}^{-1}$ may be due to incomplete complexation. However, these values are well comparable with the iron(II) complex of PhBPT ($\epsilon_{660} = 8650 \text{ l mol}^{-1} \text{ cm}^{-1}$). This comparable value would be expected given the structural formula of PhBPT and 6PBPT, where the possible ferroin functionality is derived from exactly the same groups. The molar absorptivities of the iron(II) complexes of 3-(2-py)-5,6-bis(2-py)-*as*-triazine ($\epsilon_{562} = 21\,800 \text{ l mol}^{-1} \text{ cm}^{-1}$) [18] and of 3-(2-py)-5,6-bis(6-methyl-2-py)-*as*-triazine (PBSPT, $\epsilon_{566} = 25\,100 \text{ l mol}^{-1} \text{ cm}^{-1}$) clearly demonstrate that the methyl substituents on the 5- and 6-(2-pyridyl) groups are also capable of enhancing the sensitivity. From the above observations, two important facts emerge. Firstly, it is evident that the 3-(2-py)-nitrogen is highly preferred for forming the ferroin-functionality; secondly, the nitrogens of the 5- and 6-(2-pyridyl) groups are also capable of forming the reactive group in conjunction with the 4- or 1-nitrogen of the triazine nucleus, albeit with much less sensitivity.

The overall chromophoric enhancement with respect to metal ion chelation of the ferroin-functional group of *as*-triazine due to different 5- and 6-substituents is according to the following order:

p-methoxyphenyl > 2-furyl > 4-biphenyl > *p*-methylphenyl > 6-methyl-2-pyridyl > phenyl > 2-pyridyl > methyl > hydrogen.

M.A. Islam thanks the Association of Commonwealth Universities for the award of a scholarship and the University of Dhaka, Bangladesh for granting leave of absence. He also gratefully acknowledges the help, encouragement and keen interest of Dr. Colin L. Graham in the final year of study.

REFERENCES

- G.F. Smith and P. Richter, Phenanthroline and Substituted Phenanthroline Indicators, G.F. Smith Chemical Co., Columbus, OH, 1944.
- F.H. Case, A Review of Synthesis of Organic Compounds Containing the Ferroin Group, G.F. Smith Chemical Co., Columbus, OH, 1960.
- H. Diehl, G.F. Smith, L. McBride and R. Cryberg, The Iron Reagents; Bathophenanthroline, Bathophenanthroline disulphonic acid, 2,4,6-Tripyridyl-*s*-Triazine and Phenyl-2-pyridyl ketoxime, G.F. Smith Chemical Co., Columbus, OH 2nd edn., 1965.
- A.A. Schilt, Analytical Applications of 1,10-Phenanthroline and Related Compounds, Pergamon, New York, 1969.
- G.F. Smith, W.H. McCurdy, Jr. and H. Diehl, *Analyst*, 77 (1952) 418.
- P. Collins, H. Diehl and G.F. Smith, *Anal. Chem.*, 31 (1959) 1862.
- A.A. Schilt and G.F. Smith, *Anal. Chim. Acta*, 15 (1965) 567.
- F.H. Case, *J. Org. Chem.*, 30 (1965) 931.
- F.H. Case, *J. Org. Chem.*, 31 (1966) 2398.
- F.H. Case and L. Kenon, *J. Heterocycl. Chem.*, 4 (1967) 483.
- F.H. Case, *J. Heterocycl. Chem.*, 5 (1968) 223, 413 and 431.
- F.H. Case, *J. Heterocycl. Chem.*, 7 (1970) 1001.
- F.H. Case, *J. Heterocycl. Chem.*, 8 (1971) 1043.
- F.H. Case, *J. Heterocycl. Chem.*, 9 (1972) 457.
- F.H. Case, *J. Heterocycl. Chem.*, 10 (1973) 353.
- F.H. Case, A.A. Schilt and N. Mohammed, *Talanta*, 26 (1979) 85.
- F.H. Case and A.A. Schilt, *Talanta*, 27 (1980) 55.
- A.A. Schilt, *Talanta*, 13 (1966) 896.
- A.A. Schilt, C.D. Chriswell and T.A. Yang, *Talanta*, 21 (1974) 831.
- A.A. Schilt, T.A. Yang, J.F. Wu and D.M. Nitzki, *Talanta*, 24 (1977) 685.
- L.L. Stookey, *Anal. Chem.*, 42 (1970) 779.
- E. Kiss, *Anal. Chim. Acta*, 72 (1974) 127.
- D.J. Hennessy and G.R. Reid, F.E. Smith and S.L. Thompson, *Can. J. Chem.*, 62 (1984) 721.
- A.A. Schilt and W.E. Dunbar, *Talanta*, 16 (1969) 519.
- A.A. Schilt and K.R. Kluge, *Talanta*, 15 (1968) 475.
- W.I. Stephen, *Talanta*, 16 (1969) 939.
- W.I. Stephen and P.C. Uden, *Anal. Chim. Acta*, 39 (1967) 357.
- F.A. Cotton and G. Wilkinson, *Advanced Inorganic Chemistry*, Wiley Interscience, New York, 4th edn., 1980, p. 666.
- E. Kiss, *Anal. Chim. Acta*, 161 (1984) 231.
- A.A. Schilt, W.E. Dunbar, B.W. Grandrud and S.E. Warren, *Talanta*, 17 (1970) 649.
- M.A. Islam, PhD Thesis, University of Birmingham, 1990.

3,5,6-Trisubstituted 1,2,4-triazines as analytical reagents

Part II. Compounds containing the cuproine functional group

W.I. Stephen

School of Chemistry, University of Birmingham, Edgbaston, Birmingham B15 2TT (UK)

M.A. Islam

Department of Chemistry, University of Dhaka, Dhaka 1000 (Bangladesh)

(Received 14th September 1992)

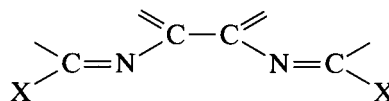
Abstract

A series of *as*-triazines containing the cuproine functional group is achieved by incorporating a methyl substituent adjacent to the imine nitrogen of highly sensitive ferroin-yielding *as*-triazines. These are much more readily prepared than most cuproine reagents. The chelation and chromogenic properties of these cuproine compounds in reaction with copper(I) have been investigated spectrophotometrically. Spectral data, conditions favourable for chelate formation and other data are reported. The results demonstrate that the effect of different substituents at the 5- and 6-positions of 3,5,6-trisubstituted 1,2,4-triazines towards the enhancement of chromophoricity of the cuproine functional group is almost identical except for the 2-furyl substituents. The compound 3-(6-methyl-2-py)-5,6-bis(2-furyl)-*as*-triazine (PFT) is superior in sensitivity to all cuproine-type chromogens previously reported. The copper(I) complex of PFT is extractable by chloroform and *n*-hexanol as a perchlorate ion association complex with appreciable enhancement in sensitivity.

Keywords: Spectrophotometry; Chromogens; Cuproine compounds; Triazines

The sensitivity and selectivity of an organic reagent towards metal ions can be modified to a great extent by incorporating different substituents in the molecule. An example is the development of the ferroin- and cuproine-type of compounds as highly sensitive and selective reagents for the spectrophotometric determination of iron(II) and copper(I) [1–3]. Chromophores of the cuproine-type are distinguished

by the presence of the bidentate chelate functional group



commonly known as the cuproine functional group and have found wide application as highly selective reagents for the spectrophotometric determination of copper(I). Examples are 2,2'-biquinoline ($\epsilon = 6220 \text{ l mol}^{-1} \text{ cm}^{-1}$ at 546 nm) [4,5], 2,9-dimethyl-1,10-phenanthroline (neocuproine, $\epsilon = 7950 \text{ l mol}^{-1} \text{ cm}^{-1}$) at 545 nm [6,7], 2,9-dimethyl-4,7-diphenyl-1,10-phenanthro-

Correspondence to: W.I. Stephen, School of Chemistry, University of Birmingham, Edgbaston, Birmingham B15 2TT (UK).

line (bathocuproine, $\epsilon = 13\,900\text{ l mol}^{-1}\text{ cm}^{-1}$ at 479 nm) [8,9] and the sulphonated derivative of bathocuproine ($\epsilon = 12\,500\text{ l mol}^{-1}\text{ cm}^{-1}$ at 483 nm) [10]. Their excellent selectivity makes them both valuable and practically useful. However, their complicated synthesis tends to make them expensive and limits their accessibility. Stephen and Uden [11,12] proposed alternative and simpler routes for preparing derivatives with comparable sensitivity containing the cuproine-functional group.

The studies reported previously in this series [13] described the preparation and analytical evaluation of certain 3,5,6-trisubstituted-1,2,4-triazines as chromogenic reagents for the spectrophotometric determination of iron(II). All the ferroin-yielding *as*-triazines are very sensitive iron(II) chromogens and some of them are more sensitive than the most sensitive chromogen of the class so far reported. In the present study, with the aim of achieving more sensitive and easily accessible cuproine-type reagents, a series of compounds with the general structural formula shown in Fig. 1, VI was synthesised. This is achieved simply by converting the highly sensitive

ferroin-yielding chromogens to cuproine-yielding ones by incorporating a methyl substituent adjacent to the imine nitrogen. The compounds listed will be referred to by the abbreviated names: 3-(6-methyl-2-py)-5,6-bis(2-py)-*as*-triazine (6PBPT); 3-(6-methyl-2-py)-5,6-bis(6-methyl-2-py)-*as*-triazine (TMPT); 3-(6-methyl-2-py)-5,6-bis(2-py)-*as*-triazine (6PDT); 3-(6-methyl-2-py)-5,6-bis(*p*-methylphenyl)-*as*-triazine (6PDMPT); 3-(6-methyl-2-py)-5,6-bis(4-biphenyl)-*as*-triazine (6PBPT); 3-(6-methyl-2-py)-5,6-bis(*p*-methoxyphenyl)-*as*-triazine (6PBMPT); 3-(6-methyl-2-py)-5,6-bis(2-furyl)-*as* triazine (PFT).

All these *as*-triazines have been prepared by condensing 6-methylpyridyl-2-hydrazidine with different 1,2-diketones under mild refluxing conditions. A literature search revealed that Schilt et al. [14] have reported the spectral characteristics of the copper(I) complexes of 6PBPT and 6PDT, although in the present work these compounds were prepared independently. The other compounds do not appear to have been previously reported. The present study is directed to show the practical accessibility of 6-methylpyridyl-2-hydrazidine and hence this series of compounds by an integrated total synthesis. It also reports the results of our evaluation of these compounds as copper chromogens.

EXPERIMENTAL

The integrated scheme for the total synthesis of this series of compounds is illustrated in fig. 1.

2-Cyano-6-methylpyridine (IV)

This compound was prepared according to the reaction scheme (Fig. 1) by the methods of Ochiai [15] and Feely and Beavers [16] with some modifications. 28 g (0.3 mol) of 2-picoline I (commercial 2-picoline was distilled and the fraction boiling at 128–129°C was used) was converted to the corresponding *N*-oxide II by the method of Ochiai with hydrogen peroxide and glacial acetic acid. This was used directly without purification to prepare the intermediate quaternary salt, 1-methoxy-6-methylpyridiniummethylsulphate III by treating the *N*-oxide with equimolar amounts

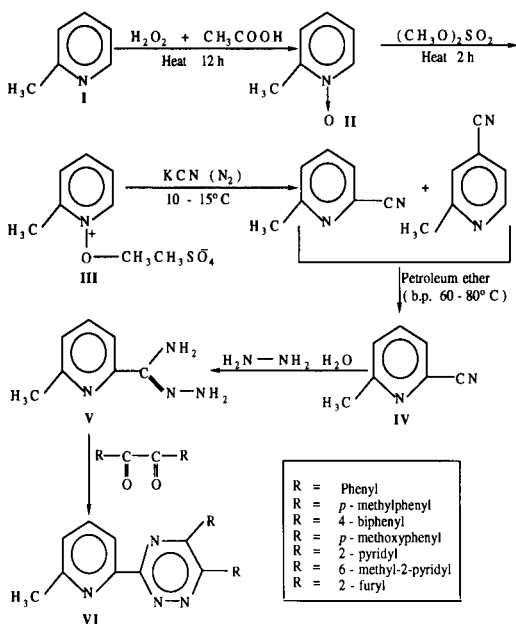


Fig. 1. Integrated scheme for the total synthesis of *as*-triazines containing the cuproine functional group.

of dimethyl sulphate for 2 h at boiling water bath temperature.

The aqueous solution of this crude quaternary salt (75 ml) was added slowly over a period of 1 h to a three-fold molar amount of potassium cyanide solution (175 ml) held around 10°C in an ice bath, whilst purified nitrogen was bubbled through the reaction mixture. The reaction vessel was closed after the addition. It was then kept for another 2 h at the similar temperature (10–15°C), after which it was magnetically stirred for 3 h and kept overnight, maintaining the temperature in a similar range throughout by means of an ice bath. The material deposited at the bottom of the container was filtered at the pump and washed well with distilled water. The product is a mixture of 2-cyano-6-methylpyridine and 4-cyano-6-methylpyridine. It was dissolved in hot light petroleum spirit (b.p. 60–80°C) and the solution decanted from the residue. On cooling and standing for a few hours, 15 g (42.3% yield with respect to 2-picoline) of 2-cyano-6-methylpyridine, m.p. 71–72°C were obtained. The residue may contain 4-cyano-6-methylpyridine. Calculated for $C_7H_6N_2$: C 71.16%; H 5.11%; N 23.71%. Found: C 70.9%; H 4.9%; N 23.4%.

Attempts to prepare 2-cyano-6-methylpyridine from 2-picoline *N*-oxide following the recommended general procedure of Feely and Beavers [16] were unsuccessful because of excessive tar formation. Although they have claimed to be able to isolate the product in the presence of air, repeated attempts during this study were unsuccessful. Even after careful exclusion of the air using purified nitrogen, if the recommended stirring is carried out at room temperature without cooling, the temperature of the reaction mixture goes up resulting in the same excessive tar formation. With the careful exclusion of air and maintaining a low temperature throughout, product isolation was successful. Although there was some tar formation, recrystallisation from hot petroleum spirit resulted in a good yield of pure product.

6-Methylpyridyl-2-hydrazidine (V)

5.9 g (0.05 mol) of 2-cyano-6-methylpyridine, 10 ml of ethanol and 22 ml of 99–100% hydrazine

hydrate were taken in a conical flask and warmed to form a homogeneous solution. It was then magnetically stirred for 2 h to complete the reaction during which the reaction mixture was kept warm enough to prevent crystallisation. On cooling, the reaction mixture solidified; 30 ml of distilled water were added to this mass which was stirred and filtered. The filtrate was extracted with dichloromethane and dried over anhydrous sodium sulphate. After complete removal of the solvent in a rotary evaporator, the residue and the solid product isolated by suction filtration were recrystallised from hot toluene. The yield was 5.5 g (73%) of pure white crystalline hydrazidine, the m.p. of which was 110–112°C. Calculated for $C_7H_{10}N_4$: C 55.98%; H 6.71%; N 37.3%. Found: C 56.2%; H 6.7%; N 37.6%.

3-(6-Methyl-2-pyridyl)-5,6-disubstituted-1,2,4-triazines (VI)

3-(6-Methyl-2-py)-5,6-diphenyl-as-triazine (6PDT)

Mixtures of equimolar (0.005 mol) amounts of 6-methylpyridyl-2-hydrazidine and benzil in 30 ml of ethanol were heated gently under reflux for 15 min. The volume of the solution was reduced to one third in a rotary evaporator. The residue was dissolved in hot hexane and upon cooling and standing for a few hours, a highly crystalline yellow material was filtered off and air dried, (1.2 g, 79.5% yield), m.p. 152–54°C. Calculated for $C_{21}H_{16}N_4$: C 77.75%; H 4.98%; N 17.27%. Found: C 77.9%; H 4.8%; N 17.3%.

3-(6-Methyl-2-py)-5,6-bis(*p*-methylphenyl)-as-triazine (6PDMPT)

Mixtures of equimolar (0.005 mol) amounts of 6-methylpyridyl-2-hydrazidine and 4,4'-dimethylbenzil in 30 ml of ethanol were heated under reflux for half an hour. The volume of the solution was reduced to one quarter under reduced pressure. The residue solidified on treatment with hexane and stirring. The resulting material was collected by filtration and recrystallised from ethanol to give yellow crystals (1.05 g, 59.6% yield), m.p. 129–31°C. Calculated for $C_{23}H_{20}N_4$: C 78.38%; H 5.72%; N 15.89%. Found: C 78.4%; H 5.4%; N 16.2%.

3-(6-Methyl-2-py)-5,6-bis(4-biphenyl)-as-triazine (6PBBT)

Mixtures of equimolar (0.005 mol) amounts of 6-methylpyridyl-2-hydrazidine and 4,4'-biphenylbenzil in 150 ml of ethanol were heated under reflux for half an hour to dissolve the reactants completely and then left to stand for 48 h. The bright yellow crystalline material was filtered off, washed with a little hexane and air dried (2.18 g, 91.6% yield), m.p. 172–74°C. Calculated for $C_{33}H_{24}N_4$: C 83.16%; H 5.07%; N 11.75%. Found: C 83.2%; H 4.8%; N 11.8%.

3-(6-Methyl-2-py)-5,6-bis(p-methoxyphenyl)-as-triazine (6PBMPPT)

Mixtures of equimolar (0.005 mol) amounts of 6-methylpyridyl-2-hydrazidine and 4,4'-dimethoxybenzil in 50 ml of ethanol were heated gently under reflux for 15 min. The volume of the solution was reduced to one third and the residue was dissolved in hot hexane and kept for crystallisation. After filtration, 1.32 g (68.6% yield) of yellow crystalline material were collected and air dried, the m.p. was 169–71°C. Calculated for $C_{23}H_{20}N_4O_2$: C 71.85%; H 5.24%; N 14.57%. Found: C 71.6%; H 5.0%; N 14.3%.

3-(6-Methyl-2-py)-5,6-bis(2-pyridyl)-as-triazine (6PBPT)

Mixtures of equimolar (0.005 mol) amounts of 6-methylpyridyl-2-hydrazidine and 2,2'-pyridil in 30 ml of ethanol were warmed to form a homogeneous solution and allowed to stand overnight. Very fine white crystals (1.6 g) were collected by filtration. Elemental analysis of this product exactly corresponds to the condensation at one carbonyl group of the pyridil. This material and the material isolated from the mother liquor were recrystallised from ethanol to give yellow crystalline material (1.2 g, 74% yield), m.p. 138–40°C. Calculated for $C_{19}H_{14}N_6$: C 69.92%; H 4.32%; N 25.75%. Found: C 69.8%; H 4.0%; N 26.0%.

3,5,6-Tris(6-methyl-2-pyridyl)-as-triazine (TMPT)

Equimolar (0.01 mol) mixtures of 6-methylpyridyl-2-hydrazidine and 6,6'-dimethyl-2,2'-pyridil in 50 ml of ethanol were warmed under reflux

for half an hour. The volume of the solution was reduced to one quarter under reduced pressure. The residue, on treatment with 100 ml of hot hexane and stirring, gave a solid product which was collected by filtration (2.45 g). On standing for a few hours, an additional 0.99 g of highly crystalline yellow material was collected from the mother liquor (hexane). The total yield was 97%. The melting point of the compound was found to be 117–19°C. Calculated for $C_{21}H_{18}N_6$: C 71.16%; H 5.12%; N 23.71%. Found: C 70.9%; H 4.8%; N 24.0%.

3-(6-Methyl-2-py)-5,6-bis(2-furyl)-as-triazine (PFT)

To a stirred suspension of 1.37 g (0.007 mol) of 2,2'-furyl in 10 ml of 2-propanol heated to around 60°C, an equimolar amount of 6-methylpyridyl-2-hydrazidine was added. The stirring at the same temperature was continued for half an hour. On cooling to room temperature and filtering, the isolated solid material was suspended in 15 ml of 0.06 M hydrochloric acid solution. After stirring for two and a half hours, the slurry was suction filtered, washed well with distilled water and then with hexane. After air drying 1.5 g (68.5% yield) of yellow crystalline triazine, m.p. 159–61°C were obtained. Calculated for $C_{17}H_{12}N_4O_2$: C 67.09%; H 3.97%; N 18.40%. Found: C 66.8%; H 3.8%; N 18.7%.

Solutions

A stock aqueous standard solution of copper(II) (1 mg ml⁻¹) was prepared by dissolving accurately weighed amounts of copper (II) chloride dihydrate. A range of conventional buffer solutions, formally 1 M in strength was prepared containing, where appropriate, one or more of the following analytical grade chemicals: hydrochloric acid, acetic acid, potassium chloride, sodium acetate, ammonium acetate, ammonium chloride and aqueous ammonia solution. Solutions at unit pH intervals over the range 1–11 were thus obtained. A 10% (w/v) aqueous solution of pure hydroxylammonium chloride was used as reducing agent. A 50% (w/v) aqueous solution of AR grade sodium perchlorate was used in the extraction studies described below.

Solutions (0.005 M) of the organic reagents were prepared by dissolving the requisite amounts in small volumes of absolute ethanol; in some cases a few drops of concentrated hydrochloric acid were added to dissolve the reagent. The solutions were then diluted to volume with ethanol. For the determination of the composition of the complexes, the stock solution was diluted.

Analytical procedure

Complex formation studies

To each of a series of 25-ml volumetric flasks were added in turn 5 ml of copper(II) solution ($50.4 \mu\text{g ml}^{-1}$), 2 ml of 10% (w/v) hydroxylammonium chloride solution, 2 ml of the particular organic reagent solution and 5 ml buffer solution (a different buffer was used in each flask to cover the range pH 1–11) and then diluted to volume with absolute ethanol. The pH range over which complexation occurred, as indicated by colour formation was noted, and so too was the pH range over which colour formation was maximal. The effect of pH on the extraction of the copper(I)–PFT complex in chloroform as a perchlorate ion association complex at a final concentration of $2.0 \mu\text{g ml}^{-1}$ was determined.

Absorption characteristics

Solutions of the various complexes were prepared for spectrophotometric examination by the following procedures. An exact amount of copper(II) solution was transferred to a 25-ml volumetric flask, 2 ml of 10% hydroxylammonium chloride solution and 5 ml of the organic reagent solution were added, followed by 5 ml of buffer solution of pH 4.76. The contents were diluted to volume with absolute ethanol and the absorption spectrum of the solution was recorded with a Shimadzu UV–visible recording spectrophotometer (UV-240) using 1-cm glass cells in the visible region and silica cells in the ultraviolet region. In the case of the organic reagent containing biphenyl groups, 50-ml volumetric flasks were used. In all cases at least five different solutions of each complex were prepared and the molar absorptivity (ϵ) at the wavelength of maximum ab-

sorbance was calculated from the linear regression coefficient.

Where measurements were done on solutions in solvents other than aqueous ethanol, the following procedure was used. The metal ion solution was placed in a 50-ml separating funnel followed by other reagents as above; 2 ml of 50% (w/v) sodium perchlorate solution and 7–8 ml of the extracting solvent were then added. After shaking, the organic layer was collected in a 25-ml volumetric flask and the extraction was repeated with a further 7–8 ml of the extracting solvent. In the case of the chloroform extracts, 1–2 ml of ethanol were added before dilution to volume with chloroform.

Spectra of all solutions were recorded against the similarly prepared reagent blank solutions in the appropriate solvents.

The absorbance of the solution was measured just after making up the solution to volume with the appropriate solvent. It was again measured after allowing sufficient time to evaluate the solution stability of the complex. The results are given in Table 3.

Metal to ligand ratios of the chelates were determined spectrophotometrically by the mole-ratio method by varying the amount of ligand whilst the concentration of copper was kept constant. All compounds formed bis-complexes with copper(I).

RESULTS AND DISCUSSION

The formation conditions of copper(I) complexes and the effect of variation of pH on the extraction of PFT–copper(I) complex in chloroform as a perchlorate ion association complex are given in Tables 1 and 2 respectively. Of this series of compounds, only 3-(6-methyl-2-py)-5,6-bis(2-py)-*as*-triazine (6PBPT) gave a colour reaction with iron(II). However, all of them do react immediately, sensitively and highly selectively with copper(I) to give highly coloured complexes soluble in aqueous ethanol media. These reactions occurred as predicted. The incorporation of a methyl substituent adjacent to the imine nitrogen results as expected in the complete inhibition of

TABLE 1

Formation conditions of copper(I) complexes
(Working pH = 4.76)

Organic reagent	Colour of complex	Time of development	pH ranges for	
			Colour formation	Max. colour formation
6PDT	Brown	Immediate	1-11	4- 8
6PDMPT	Brown	Immediate	1-11	3- 9
6PBBT	Brown	Immediate	1-11	1-10
6PBMPT	Brown	Immediate	2-11	4-10
6PBPT	Intense brown	Immediate	1-11	3- 8
TMPT	Intense brown	Immediate	1-11	2- 9
PFT	Intense brown	Immediate	1-11	3- 9

TABLE 2

Effect of variation of pH on the extraction of PFT-copper(I) complex in chloroform as a perchlorate ion association complex (2.00 $\mu\text{g Cu ml}^{-1}$)

pH of the buffer solution	Corresponding absorbance at 518 nm (1-cm cell) ^a
2	0.43
3	0.50
4	0.52
5	0.51
6	0.52
7	0.53
8	0.52

^a Colour is stable for > 16 h.

the ferriox reaction and forms the cuproine-reactive group. The ferriox reaction of 6PBPT would be expected given its structural formula. The ferriox functionality must presumably be derived from either nitrogen of 5- or 6-(2-pyridyl) group in conjunction with the 4- or 1-nitrogen of the triazine nucleus.

The results of the spectrophotometric measurements are summarised in Table 3 in which the reported values of two compounds are also given. The wavelengths given are for maximum absorbances and the molar absorptivity values correspond to the wavelength cited.

The absorption spectra of the copper(I) complexes of 6PBPT, TMPT and 6PDT show a single absorption maximum in the visible region with molar absorptivities of $\epsilon_{510} = 7600$, $\epsilon_{505} = 7900$ and $\epsilon_{492} = 7000 \text{ l mol}^{-1} \text{ cm}^{-1}$, respectively. These may give an additional peak in the ultraviolet region. All the systems conform to Beer's law over the experimental concentration range viz. up to $10 \mu\text{g ml}^{-1}$. The present work confirms the findings of Schilt et al. [14] on the analytical utility of 6PBPT and 6PDT. Molar absorptivities of the copper(I) complexes of 6PBPT and TMPT

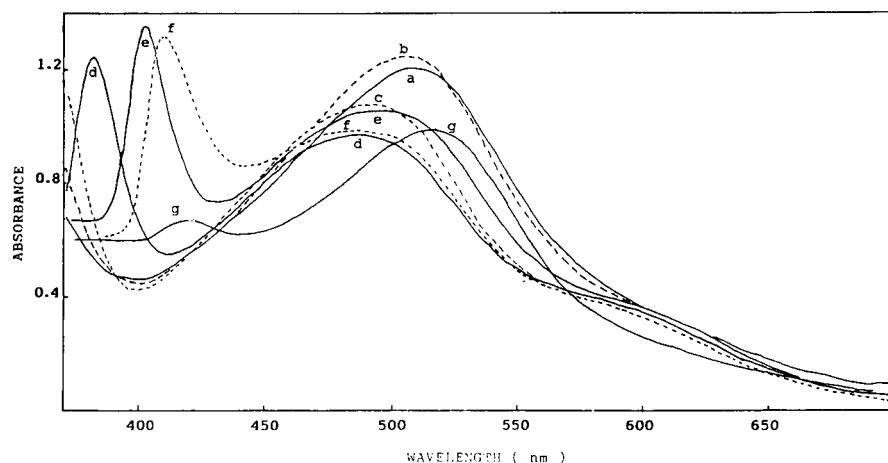


Fig. 2. Absorption spectra of copper(I) complexes of (a) 6PBPT, (b) TMPT, (c) 6PDT, (d) 6PDMPT, (e) 6PBBT, (f) 6PBMPT and (g) PFT in aqueous ethanol medium recorded against reagent blanks in 1-cm cells at a metal concentration of (a), (b), (c) and (d) 10.08 mg l^{-1} ; (e) and (f) 8.06 mg l^{-1} ; and (g) 4.00 mg l^{-1} (1-cm cells throughout).

TABLE 3

Absorption characteristics of the 1:2 copper(I) to ligand complexes

Organic reagent	Solution medium	λ_{\max} (nm)	ϵ ($\text{l mol}^{-1} \text{cm}^{-1}$)	Colour stability
6PDT	Ethanol–water	492 (492) ^a	7000 (7000) ^a	> 2 h
6PDMPT	Ethanol–water	485 380	6100 7800	> 2 h
6PBBT	Ethanol–water	495 402	8450 10 500	> 16 h
6PBMPT	Ethanol–water	485 409	7400 10 000	> 4 h
6PBPT	Ethanol–water	510 (510) ^a	7600 (7000) ^a	–
TMPT	Ethanol–water	505	7900	> 16 h
PFT	Ethanol–water	516	15 440	> 4 h
	Chloroform	518	16 600	> 16 h
	<i>n</i> -Hexanol	520	16 600	

^a Ref. 14.

indicate that two extra methyl substituents on the 5- and 6-(2-pyridyl) groups have very little or no effect on the chromophoricity of the cuproine functional group. On the other hand the positive contribution of these substituents on the ferrioin functional group is a significant one [13]. However, these molar absorptivity values compare favourably with those of the copper(I) complexes of 2,2'-biquinoline ($\epsilon = 6100 \text{ l mol}^{-1} \text{ cm}^{-1}$) [5] and 2,9-dimethyl-1,10-phenanthroline ($\epsilon = 7900 \text{ l mol}^{-1} \text{ cm}^{-1}$) [7], to the latter of which the above compounds are closely related.

The absorption spectra of the copper(I) complexes of 6PDMPT, 6PBBT and 6PBMPT exhibit two absorption maxima (Fig. 2). A similar phenomenon has been observed in case of the iron(II) complexes of analogous *as*-triazines with the ferrioin functional group [13]. All complexes appear to obey Beer's law within the concentration range (0–10 $\mu\text{g ml}^{-1}$) at both wavelengths of maximum absorbance. The introduction of methyl, phenyl or methoxy groups into the *para* positions of 5- and 6-phenyl rings of PDT increases the molar absorptivity of the iron(II) derivative from 24 000 to 26 000, 30 700 and 32 500 $\text{l mol}^{-1} \text{ cm}^{-1}$, respectively. Moreover a second peak appears in the shorter wavelength region, where the molar absorptivity value is less than those in the longer

wavelength value except for phenyl substituents [13]. The molar absorptivities of the copper(I) complexes of 6PDMPT, 6PBBT and 6PBMPT at both the wavelengths of maximum absorbance are $\epsilon_{485} = 6100$ and $\epsilon_{380} = 7800$, $\epsilon_{495} = 8450$ and $\epsilon_{402} = 10 500$ and $\epsilon_{485} = 7400$ and $\epsilon_{409} = 10 000 \text{ l mol}^{-1} \text{ cm}^{-1}$, respectively. These observations demonstrate that the expected order of chromophoric enhancement of the cuproine function group due to methyl, phenyl or methoxy substituents has not occurred similarly to the ferrioin functional group. The effect of these substituents on the cuproine functional group is more or less similar. However, the molar absorptivity values at longer wavelength compare favourably with neocuproine and are higher at the shorter wavelength for 6PBBT and 6PBMPT.

Although the molar absorptivity values of $\epsilon_{402} = 10 500 \text{ l mol}^{-1} \text{ cm}^{-1}$ for 6PBBT complex and of $\epsilon_{409} = 10 000 \text{ l mol}^{-1} \text{ cm}^{-1}$ for 6PBMPT complex are less than that of the most sensitive bathocuproine [9], the relatively easy synthesis of these compounds must represent a significant advantage.

Of the compounds examined, the most promising chromogen for copper is 3-(6-methyl-2-py)-5,6-bis(2-furyl)-*as*-triazine (PFT). Without exception the intensely brown copper(I) chelate of PFT has a greater molar absorptivity in the visible region than any other cuproine-type complex yet reported. It appears to be superior to the exceptionally useful bathocuproine complex [copper(I) complex of 2,9-dimethyl-4,7-diphenyl-1,10-phenanthroline] which has a molar absorptivity of $13 900 \text{ l mol}^{-1} \text{ cm}^{-1}$ at 479 nm and serves for the very selective and sensitive determination of copper in a variety of substances [2]. PFT gives a colour reaction over the pH range 1–10 with maximum colour over pH 2–9. The colour system conforms to Beer's law over the range 0.0–5.0 $\mu\text{g ml}^{-1}$ of copper. The complex is highly soluble in aqueous ethanol mixture, *n*-hexanol and chloroform. The spectrum of the copper(I) chelate has a maximum at 516 nm with a molar absorptivity of $15 440 \text{ l mol}^{-1} \text{ cm}^{-1}$ in an ethanol–water mixture (3:1). The sensitivity of PFT is approximately twice that of other compounds investigated in this study. It has been observed that the

chromophoricity of the ferrioxal functionality of an *as*-triazine is enhanced to a great extent by the 2-furyl groups compared to 2-pyridyl or phenyl groups [13]. Molar absorptivities of the iron(II) complexes of 3-(2-py)-5,6-bis(2-py)-*as*-triazine [17], 3-(2-py)-5,6-diphenyl-*as*-triazine and 3-(2-py)-5,6-bis(2-furyl)-*as*-triazine are $\epsilon_{562} = 21\,800$, $\epsilon_{555} = 24\,000$ and $\epsilon_{575} = 31\,000 \text{ l mol}^{-1} \text{ cm}^{-1}$, respectively. The very high molar absorptivity of the copper(I) complex of PFT compared to 6PBPT and 6PDT complexes demonstrates that the 2-furyl group is also very effective in increasing the chromophoricity of the cuproine functionality. It has been observed in this cuproine-yielding *as*-triazine series that when a substituent is present on the 5- and 6-phenyl rings, an extra peak appears in the shorter wavelength region. This peak moves towards longer wavelengths depending on the nature of the substituent, i.e., methyl (380 nm), phenyl (402 nm) and methoxy (409 nm). It is also tempting to suggest that the very high molar absorptivity of the PFT complex compared to 6PDMPT, 6PBBT and 6PBMPT might be due to merging of the two peaks resulting in a doubling of the sensitivity of the complex.

The complex was extracted by chloroform and *n*-hexanol. The PFT complex is quantitatively extractable by chloroform over the pH range 3–8. The spectrum of the chloroform and *n*-hexanol solutions is very similar to that of the aqueous and ethanolic solutions with a slight bathochromic shift of the λ_{max} but also an appreciable increase in sensitivity. The λ_{max} of the complex in chloroform solution is 518 nm and in *n*-hexanol solution is 520 nm. However, the molar absorptivity in both the media is $16\,600 \text{ l mol}^{-1} \text{ cm}^{-1}$. Like all other compounds of this series, PFT also forms a bis-complex of excellent colour stability in all the solvent systems studied. The cuproine reagents, 2,2'-biquinoline, neocuproine and bathocuproine, are not easy to synthesise and their prices are comparatively high. The higher sensitivity of this new reagent than that of the popularly used most

sensitive bathocuproine, the quantitative extractability in immiscible organic solvents, the excellent colour stability and the easy synthesis of PFT are reasons why this compound may prove to be a better alternative to bathocuproine. A sulphonated derivative would have further advantages.

M.A. Islam thanks the Association of Commonwealth Universities for the award of a scholarship and the University of Dhaka, Bangladesh for granting leave of absence. He also gratefully acknowledges the help, encouragement and keen interest of Dr. C.L. Graham.

REFERENCES

- 1 H. Diehl, G.F. Smith, L. McBride and R. Cryberg, The Iron Reagents; Bathophenanthroline, Bathophenanthroline disulphonic acid, 2,4,6-Tripyridyl-*s*-triazine and Phenyl-2-pyridyl ketoxime, G.F. Smith Chemical Co., Columbus, OH, 2nd edn., 1965.
- 2 H. Diehl, G.F. Smith, A.A. Schilt and L. McBride, The Copper Reagents; Cuproine, Neocuproine, Bathocuproine, G.F. Smith Chemical Co., Columbus, OH, 2nd edn., 1972.
- 3 F.H. Case, A Review of Synthesis of Organic Compounds Containing the Ferrioxal Group, G.F. Smith Chemical Co. Columbus, OH, 1960.
- 4 J.G. Breckenridge, R.W.J. Lewis and L.A. Quick, Can. J. Res. 17 (1939) 258.
- 5 J. Hoste, Anal. Chim. Acta, 4 (1950) 23.
- 6 F.H. Case, J. Am. Chem. Soc., 70 (1948) 3994.
- 7 G.F. Smith and W.H. McCurdy, Jr., Anal. Chem., 24 (1952) 371.
- 8 F.H. Case and J.A. Brennan, J. Org. Chem., 19 (1954) 919.
- 9 G.F. Smith and D.H. Wilkins, Anal. Chem., 25 (1953) 510.
- 10 D. Blair and H. Diehl, Talanta, 7 (1961) 163.
- 11 W.I. Stephen and P.C. Uden, Anal. Chim. Acta, 39 (1967) 357.
- 12 W.I. Stephen, Talanta, 16 (1969) 939.
- 13 M.A. Islam and W.I. Stephen, Anal. Chim. Acta, 274 (1993) 335.
- 14 A.A. Schilt, W.E. Dunbar, B.W. Grandrud and S.E. Warren, Talanta, 17 (1970) 649.
- 15 E. Ochiai, J. Org. Chem., 18 (1953) 534.
- 16 W.E. Feely, and E.M. Beavers, J. Am. Chem. Soc., 81 (1959) 4004.
- 17 A.A. Schilt, Talanta, 13 (1966) 895.

Membrane inlet manometry for the measurement of water activity in aqueous and organic solutions

H. Degn and N.-U. Frigaard

Institute of Biochemistry, Odense University, DK-5230 Odense (Denmark)

(Received 17th September 1992)

Abstract

An apparatus for continuous measurement of water activity is described where a water permeable membrane is used to separate the sample from the vacuum of a continuously pumped chamber. When the sample contains no other component than water which permeates through the membrane at a significant rate the steady state pressure in the vacuum chamber is a function of the water activity of the sample. A polypropylene terephthalate membrane was used which is highly permeable to water and virtually impermeable to atmospheric gases and volatile organic liquids. The vacuum chamber is pumped by a turbomolecular pump and the pressure is measured by a Penning gauge. The apparatus is calibrated by the help of aqueous salt solutions of known water activity. Examples of measurements of water activity in binary alcohol–water mixtures are presented and compared with data from the literature.

Keywords: Alcohols; Membranes; Water activity

Water activity is an important parameter in many systems such as enzyme catalyzed reactions in organic media [1], the growth of microorganisms [2] and the seasoning and storage of food [3]. A simple and reliable method for continuous measurement of water activity is therefore needed. Classical methods for water activity measurement are discontinuous in principle and very time consuming. The water activity in a binary salt solution can be determined directly by measurement of the vapour pressure above the solution because only the water component has a measurable vapour pressure [4]. This cannot be done with mixtures of water and another volatile compound as both components will contribute to the total vapour pressure above the mixture. In order to determine the activities of the components of binary mixtures of volatile liquids the

total vapour pressure and the molar ratio of a condensate of the gas phase are measured [5,6]. Different methods for the determination of water activity in food have been compared [7]. We have previously reported the use of membrane inlet mass spectrometry (MIMS) for the continuous measurement of water activity in solution [8,9]. In this technique a hydrophilic polypropylene terephthalate membrane is used to separate the sample from the vacuum of the mass spectrometer. Water diffuses through the membrane into the mass spectrometer at a rate proportional to the water activity in the sample. As the water signal of the mass spectrometer is proportional to the rate of entry of water the measurement is linear with respect to water activity. In the course of applying this technique to different samples we have found that atmospheric gases and a large class of volatile organic liquids such as hexane, toluene, propanol, diisopropyl ether, dioxane etc. do not penetrate the polypropylene terephthalate

Correspondence to: H. Degn, Institute of Biochemistry, Odense University DK-5230 Odense (Denmark).

membrane at a significant rate compared to water. When water activity measurements are done on samples containing, besides water, only components that do not permeate through the membrane, the total pressure in the instrument is governed only by the water activity in the sample and, therefore, the water activity can be determined with the help of a pressure gauge without the use of a mass spectrometer. In the present paper we describe a simple instrument based on this principle that can be used to measure the water activity in aqueous salt solutions and mixtures of water and organic liquids with an error of less than 1% and a 10–90% response time of 100 s at 25°C.

A membrane sensor for on-line measurement of water activity in fermentors has previously been published [10]. It consists of a capacitive humidity probe enclosed in a small volume of air which is separated from the sample by a microporous hydrophobic membrane. Although the chamber can be purged with dry air the measurement essentially depends on equilibration of the internal gas volume and the polymer dielectric of the humidity probe with water from the sample. The response time of the device depends on the time required for equilibration of the polymer dielectric which is reported to depend strongly on the water activity. The 90% response time increases from 1 to 17 min as the water activity increases from 0 to 1. In our method the response time is expected to depend on the rate of diffusion of water through the membrane, the pumping rate and the water adsorption to the internal surfaces. It was found that in our instrument with a high pumping rate the response time is determined mainly by the adsorption and desorption of water at the internal surfaces of the vacuum chamber.

EXPERIMENTAL

The instrument consists of a turbomolecular pump (TPH 050, Balzers, Liechtenstein) which is fitted with a Penning pressure gauge (IKR 020, TPG 300, Balzers) and a membrane inlet for flow sampling of a similar construction as we have

previously used for on-line monitoring of volatile organic compounds by membrane inlet mass spectrometry [11]. The membrane is a 12 μm film made of polyethylene terephthalate (Melinex 800 from ICI Plastics Division, Welwyn Garden City, UK). The membrane inlet is thermostated by water circulation and the vacuum chamber, including the upper part of the turbomolecular pump, is heated to 120°C by an electric heating tape. The analog signal from the pressure gauge circuit is connected through an A/D converter to a personal computer. There is an approximate logarithmic relationship between the analog signal, E , from the pressure gauge and the pressure, P , in the vacuum chamber. From a diagram in the instruction manual for the pressure gauge we estimate the equation $\log P = 0.5E - 8$ to be a reasonably good approximation. The computer is programmed to collect the analog signal from the pressure gauge repeatedly and convert the signal to pressure according to the above equation with a cycle time of less than 2 s. Water or an aqueous salt solution of known water activity is injected into the sample port and the pressure is read after it has stabilized. A fifth degree polynomial is fitted to the set of points in the P, a_w plane where a_w is the water activity of the sample known from the literature. The polynomial is then used to calculate the activity of unknown samples from the measured signal from the pressure gauge.

RESULTS AND DISCUSSION

Figure 1 shows a calibration curve obtained by measuring the pressure in the vacuum chamber with different solutions of calcium chloride and saturated lithium chloride whose activities are known from the literature [4]. The solid curve is produced by a fifth degree polynomial fitted to the data points. The correlation coefficient is 0.9999. In other similar experiments we have used solutions of a variety of other salts for which the water activity is known. When a variety of salts was used the fit to the polynomial was as good as in the example presented here. From this we conclude that the nature of the salt has no effect

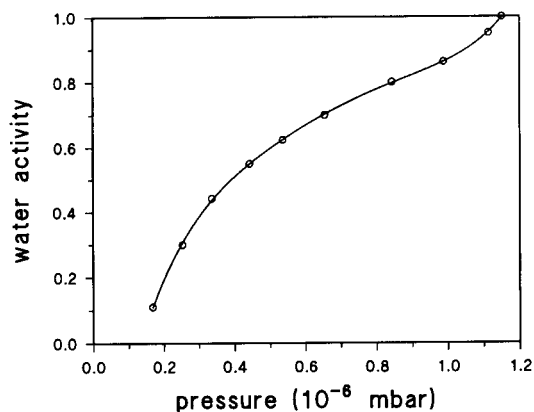


Fig. 1. Calibration curve for water activity measurements. Water activities of different aqueous salt solution known from the literature plotted against the pressures measured with samples of the solutions. The sample of lowest water activity was a saturated solution of lithium chloride. The other samples were calcium chloride solutions of different concentrations. The solid line is produced by a fifth degree polynomial fitted to the points.

on the water activity measurement with our method. Theoretically the calibration curve in Fig. 1 would be expected to be linear. The observed deviation from linearity is probably due to imperfect calibration of the pressure gauge. This imperfection is immaterial for our purpose.

The fifth degree polynomial was installed in the computer program and used to repeatedly convert the recorded pressure to water activity in measurements on samples of unknown water activity. In order to determine the response time the water activity was traced on the computer screen as a function of time. Figure 2 shows the recorded transient when the sample was exchanged by the injection of a new one of different water activity. From this transient we determine the 10–90% response time as 100 s at 25°C. The small peak occurring immediately after the injection of a new sample is due to temperature equilibration of the sample. A positive peak occurs when the injected sample has a higher temperature than the sample cell and a negative peak occurs when the sample is colder. This effect was used to determine the temperature of the sample cell which turned out to be a few degrees higher than that of the thermostat water because of heat

conduction from the hot vacuum chamber. In all measurements represented in Figs. 1 and 3 we have awaited the stabilization of the signal for a few minutes after the injection of the sample before making the reading.

In Fig. 3 is shown the result of applying the technique to binary mixtures of ethanol, 1-propanol, 2-propanol or tertiary butanol with water at different mole fractions. For comparison our measurements with ethanol and 1-propanol are plotted together with data from the literature [6]. We found that there is an excellent agreement between our measurements and the literature values. We have not found any published data on water activities in mixtures of 2-propanol or tertiary butanol and water.

The transients in water activity recorded after changes of sample are qualitatively similar to transients under similar circumstances in measurements of volatile organic compounds by membrane inlet mass spectrometry. These transients have been found to be due to adsorption and desorption of analyte at the internal surfaces of the vacuum chamber [11]. In analogy we conclude that the response time in the apparatus described here is largely determined by the rates of adsorption and desorption of water at the internal surfaces. The shorter response time in the present apparatus compared to that of the mass spectrometer is probably due to the much smaller

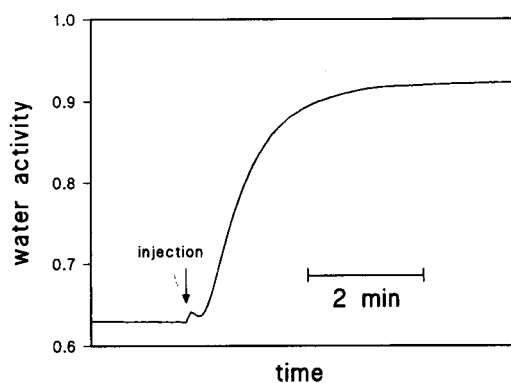


Fig. 2. Continuous recording of water activity in calcium chloride solutions showing the transient after a rapid change of sample. The small initial peak is due to the temperature difference between the injected sample and the measuring cell.

area of the internal surfaces in the former apparatus compared to the latter. Further reduction of the dimensions of the instrument would probably result in further reduction of the response time. However, the response time as it is in our instrument is adequate for on-line measurements on systems such as fermentors where very rapid changes in water activity are not encountered.

In the present work we have shown that membrane inlet manometry is useful for the measurement of water activity in the range from 0.1 to 1. We have not covered the range below 0.1 because

of a lack of standard solutions with such low water activities. We have no reason to believe that the method cannot be used at low water activities. We here present only measurements on liquid samples. In our previous work with membrane inlet mass spectrometry we found that water activity can just as well be measured in a gas phase equilibrated with the liquid sample. It follows that membrane inlet manometry may also be useful for measuring water activity of solid samples through measurement of the gas phase in equilibrium with the solid sample.

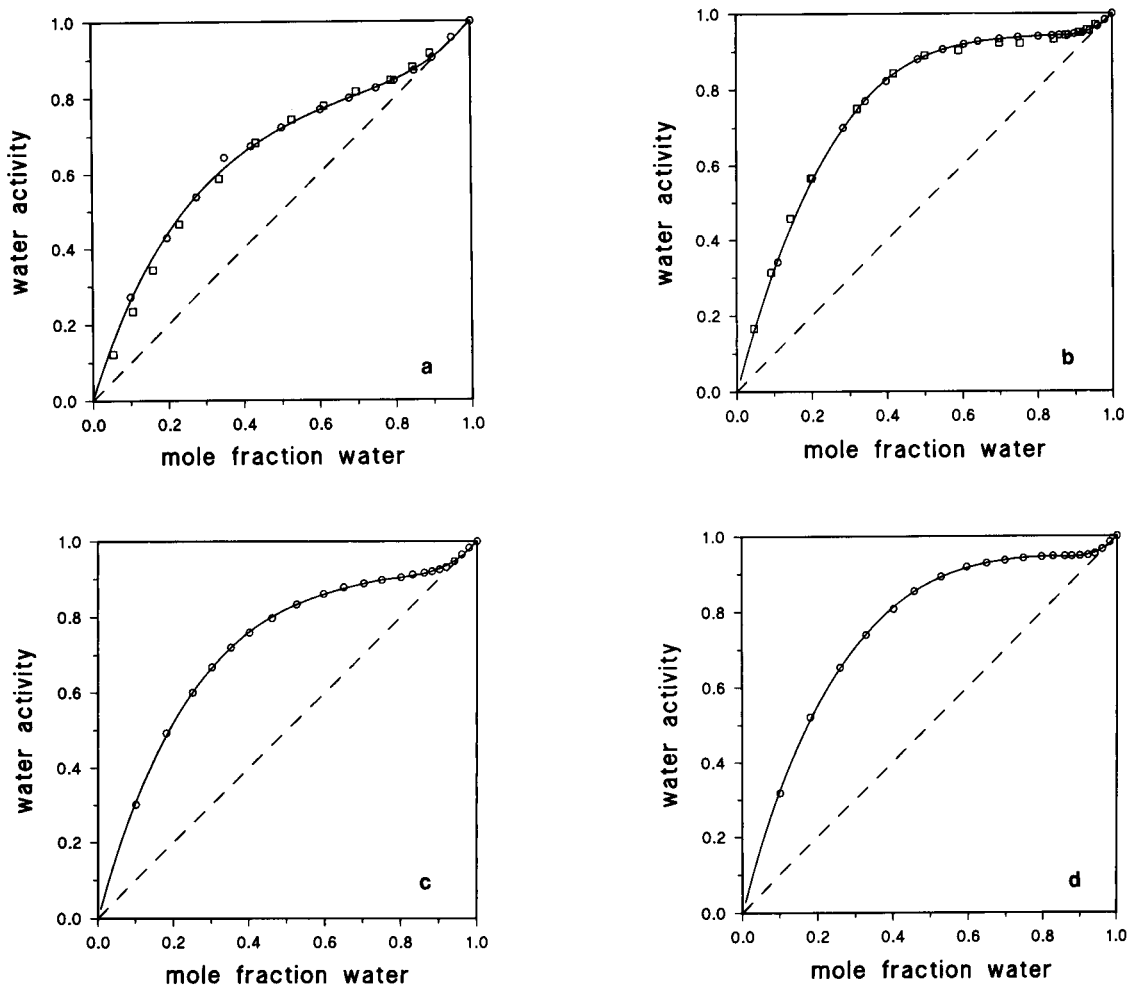


Fig. 3. Water activity measured in binary mixtures of (a) ethanol, (b) 1-propanol, (c) 2-propanol or (d) tertiary butanol and water at different mole fractions at 25°C. The broken line is the Raoult's law reference line. Circles are our measurements. Squares are data recalculated from Ref. 6.

REFERENCES

- 1 M. Goldberg, F. Parvaresh, D. Thomas and M.-D. Legoy, *Biochim. Biophys. Acta*, 957 (1988) 359.
- 2 B. Hahn-Hägerdal, *Enzyme Microb. Technol.*, 8 (1986) 322.
- 3 L.B. Rockland and L.R. Beuchat (Eds.), *Water Activity: Theory and Applications to Food*, Marcel Dekker, New York, 1987.
- 4 R.A. Robinson and R.H. Stokes, *Electrolyte Solutions*, Butterworths, London, 1970.
- 5 M. Randall and H.P. Weber, *J. Phys. Chem.*, 44 (1940) 917.
- 6 R.S. Hansen and F.A. Miller, *J. Phys. Chem.*, 58 (1954) 193.
- 7 M.A. Esteban, M. Alcalá, A. Marcos and J. Fernández-Salguero, *Food Chem.*, 35 (1990) 159.
- 8 S. Bohatka and H. Degn, *Rapid. Commun. Mass Spectrom.*, 5 (1991) 433.
- 9 H. Degn, S. Bohatka and D. Lloyd, *Biotechnology Techniques*, 6 (1992) 161.
- 10 P. Gervais, *Biotechnol. Bioeng.*, 33 (1989) 266.
- 11 F.R. Lauritsen, *Int. J. Mass Spectrom. Ion Processes*, 95 (1990) 259.

A study of the effect of chain length on nearest neighbour interactions of immobilized species

Judy L. Alves

Department of Chemistry, Clark University, Worcester, MA 01610 (USA)

Mauri A. Ditzler

Department of Chemistry, College of the Holy Cross, Worcester, MA 01610 (USA)

(Received 12th June 1992; revised manuscript received 19th October 1992)

Abstract

The effect of varying the length and hydrophobicity of the molecular tether that binds an indicator to a substrate was studied. The length or hydrophobicity of the tether may affect the characteristics of the immobilized indicator in several ways. Of primary interest in this study was the extent to which the tether characteristics control interactions between adjacent immobilized species. We investigated two straight-chain tethers of variable length and two branched-chained tethers of different hydrophobicities. For each of these systems, we investigated nearest neighbour interactions as a function of surface coverage. The extent of this interaction was determined by measuring the degree of coupling between adjacent immobilized aromatic diazonium ions. Our results suggest that nearest neighbour interactions between immobilized species in an aqueous environment are controlled primarily by the hydrophobicity of the tether.

Keywords: Chain length effects; Indicators

An immobilized indicator is central to many modern optical probes (optrodes). The primary goal of the immobilization process is to ensure that the indicator remains at the interface between the optical wave carrier and the analytical solution. A secondary and often inadvertent effect of immobilization is that the analytical characteristics may be altered since the immobilization chain places the indicators in unusual and inhomogeneous environments. The loss of mobility may affect the nature of the analyte–indicator reaction either by restricting allowed alignments and geometries or by altering the entropy driven processes relative to the totally mobile species.

Correspondence to: M.A. Ditzler, Department of Chemistry, College of the Holy Cross, Worcester, MA 01610 (USA).

The possibility that these considerations might alter the mole ratio of the indicator–analyte complex has long been recognized [1,2]. The isolation of species at remote sites on the substrate will favor low stoichiometry complexes. On the other hand, clustering of the immobilized species may lead to complexes with unusually high stoichiometries.

The uncertainty that accompanies the nonuniform distribution of surface-bound species complicates the design and production of a predictable and reproducible system for use in optical probes. However, if these factors can be controlled, it should then be possible to exploit the contrasting effects of immobilization to select the type of reaction exhibited by the indicator. In previous work we utilized restrictive immobiliza-

tion techniques (multiple attachments or short tethers) to improve the selectivity [3] or pH range [4] of an indicator. In both cases the improvement was credited to an inhibition of a potentially interfering complex involving multiple indicator molecules interacting with a single analyte.

In this report we investigate the effect of varying length and hydrophobicity of the molecular chain or tether that attaches the indicator to the substrate. It is reasonable to expect that tether length and hydrophobicity may affect the characteristics of the immobilized reagent molecules in several ways, all of which are relevant to analytical applications. The length and hydrophobicity of the tether may affect the extent to which adjacent immobilized species interact. The interaction between the immobilized species and the substrate surface may also be influenced by a change in tether length or hydrophobicity. Finally, variations in tether length or hydrophobicity may affect the extent to which the immobilized molecules becomes solvated. This study focuses on the effect of chain length and hydrophobicity on the ability of adjacent species to interact.

A previously described method based on an immobilized diazonium ion probe is used to determine the extent of nearest neighbour interactions [5]. Forced interaction between adjacent probes is indicated by their chemical reaction with each other to produce a colored azo product. Isolation of adjacent sites by the tether inhibits this reaction; the reactive diazonium probe eventually reacts with solvent to form the colorless phenol.

EXPERIMENTAL

Synthetic procedures

4-Nitrophenylacetic acid, 4-(4-nitrophenyl)butyric acid, 4-nitrobenzoic acid, and 4-nitrophenylsuccinic acid were obtained from Pfaltz and Bauer. The 2-(4-nitrophenyl)butyric acid was synthesized according to the procedure of Wilds and Biggerstaff [6] from 5 g of 2-phenylbutyric acid (Eastman Organic Chemicals) dissolved in 18.0 ml H_2SO_4 at 0–10°C. Over 1 h 1.6 ml of

HNO_3 was added, and the mixture was allowed to react for 1 additional hour. The mixture was poured over crushed ice to yield approximately 50% of the 2-(4-nitrophenyl)butyric acid. Recrystallization from a toluene–petroleum ether (35–60°C boiling range) mixture produced pale yellow, fluffy crystals of the product m.p. 118–120° (literature 118–121°C). The NMR was consistent with the product being 2-(4-nitrophenyl)butyric acid.

The aminated silica gel substrate was prepared by reacting 85.0 g of dried silica gel (Sigma, Type H, 10–40 μm) in 430 ml toluene with 53 ml of 3-aminopropyltriethoxysilane for 3 h. The gel was washed with toluene, placed in an oven (110°C) overnight, and washed with acetone and ethanol.

Immobilization of the probe system on variable-length chains

4-Nitrophenylacetic acid was bound to the aminated silica gel by reacting with 1.0 g aminated silica gel in 50 ml of methylene chloride for 30 min. One milliliter of the coupling agent 1,3-diisopropylcarbodiimide (DIC) was added. Various amounts of 4-nitrophenylacetic acid (in the range of 0.002–3.0 g) were used to obtain increasing probe coverages. Several polar and non-polar solvents were used to wash all samples (methylene chloride, acetone, distilled water, and ethanol). Removal of trace amounts of solvents was done by placing each sample in an oven (110°C) for 10 min. The nitro moiety was then reduced to the amine with 50 ml of a boiling 5% aqueous solution of sodium dithionite [7].

The other probe precursors were prepared in an analogous fashion from 4-(4-nitrophenyl)butyric acid, 2-(4-nitrophenyl)butyric acid, 4-nitrophenylsuccinic acid, and 4-nitrobenzoic acid.

Coupling vs. hydrolysis competition

The coupling–hydrolysis competition process [5] consisted of taking a 20-mg portion of the immobilized aromatic amine product and adding it to 1 ml of a cold (ice bath) solution of 0.020 g $NaNO_2$ in 1 ml of 1 M HCl in a test tube wrapped so as to exclude light. The reaction continued for 30 min in an ice bath at the end of which unreacted NO_2^- was quenched with an

excess of sulfamic acid in 1 ml of cold water. This produces the diazonium ion which can either couple or hydrolyze. An additional 3 ml of cold water was then added and the reaction mixture was allowed to warm to room temperature. After 3 h, 2 ml of the reaction mixture were transferred to a quartz spectrophotometric cell and a spectrum was taken.

Characterization and instrumentation

Verification of the immobilization of the bound species was accomplished by diffuse reflectance UV–Vis spectroscopy and diffuse reflectance FTIR spectroscopy. Reduction of the nitro moiety to the amine was confirmed by the disappearance of the nitro peaks (6.6 and 7.5 μm) in the FTIR spectrum.

To determine relative coverage of the probe molecule, UV–Vis spectra of the immobilized system were obtained with a Perkin Elmer Lambda 4C spectrometer. The diffuse reflectance spectra were recorded as sample vs. silica gel and subsequently converted to absolute reflectance values by referencing the silica gel to BaSO_4 which is treated as an absolute reflector. The absolute reflectance values were converted to $F(R)$, the Kubelka–Munk function of reflectance. This function of absolute reflectance is proportional to the concentration of the absorber in the sample. Samples were diluted 10:1 with silica gel and ground in a mortar and pestle to minimize the error from regular reflection and ensure that the $\%R$ values were within the range that minimizes error in $F(R)$ [8]. To determine degree of chemical coupling of the probes (azo formation) UV–Vis spectra were recorded on suspensions of the reaction mixture in 1-cm quartz cells. An integrating sphere accessory was used to reduce the effects of scattering. The solid sample was kept suspended by a mechanical Spectrocell stirrer.

RESULTS AND DISCUSSION

We have investigated the effect of four different tethers on the interaction of adjacent probe molecules. The nature of the tether and the probe

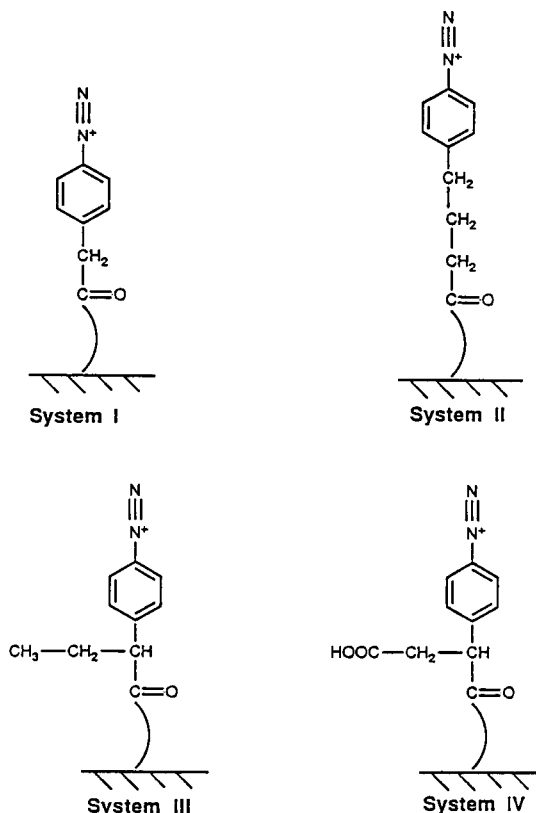


Fig. 1. The four systems studied differ in their tether characteristics. (I) short tether; (II) long tether; (III) short tether with hydrophobic side chain; (IV) short tether with polar side chain.

is shown in Fig. 1. The probe is an aromatic diazonium ion. The fate of the diazonium probe ion (coupling vs. hydrolysis) has been shown to provide a measure of the extent to which adjacent immobilized species interact [5]. In cases where the substrate and tether promote interaction an easily detectable colored azo compound forms as a result of coupling. In cases where the adjacent species do not interact a colorless phenol is produced. The tethers are all based on an initial modification of a silica gel substrate by 3-aminopropyltriethoxysilane. The tether is then extended by an amide linkage formed between the surface bound alkyl amine and an aliphatic carboxylic acid to which the probe is attached. It is this final portion of the tether that we have varied. System I has a single methylene group

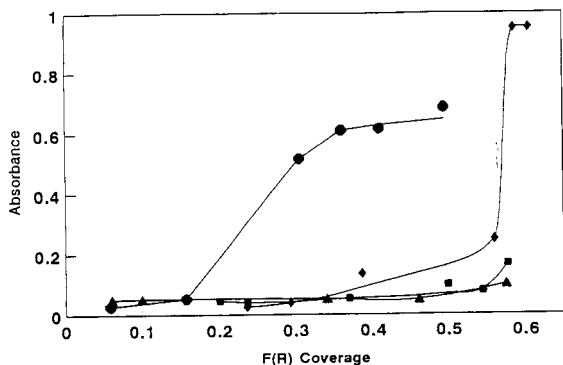


Fig. 2. The absorbance provides a measure of the extent of adjacent probe coupling as a function of surface coverage of probe molecules. Suspensions of 20 mg of substrate in 2 ml of reaction solution were used. Absorbance for System I (\blacklozenge), System II (\blacksquare), System III (\blacktriangle), and System IV (\bullet) were obtained at approximately 450 nm. The marker size approximates the percent error of the $F(R)$ measurements.

between the amide linkage and the probe reagent. In System II this portion of the tether is increased to a three-carbon chain. System II then places the probe at the end of a tether which is both longer and more hydrophobic than that used in System I. System III uses a tether similar to System II, except that the probe is not at the terminal end of the chain. This results in a tether length similar to System I but a degree of hydrophobicity more like System II. System IV is similar to System III in that it uses a four-carbon tether with the probe attached at one of the central positions. It is unique in that the side chain contains a carboxylic acid to decrease its hydrophobicity.

Probe interaction as a function of surface coverage was studied for each of the four systems. The results are shown in Fig. 2. The extent of interaction of neighbouring probes is related to the absorbance of the azo product which forms when adjacent probe molecules react with each other. The surface coverage is proportional to the measured value of the Kubelka–Munk function of reflectance, $F(R)$, of the nitro precursor to the activated probe.

Comparison of the highest attainable values for $F(R)$ suggests that the saturation coverage of

System I–III is similar. This is as expected since the same substrate is used and the method of attaching the probe is similar. For System IV, the maximum value of $F(R)$, and thus its saturation surface coverage, is about 15% less. This is likely attributable to the fact that the tether for this system has the potential to occupy two surface sites. The chain that attaches the probe to the surface has a carboxylic acid at both ends. Initial attachment may be at either end or at both ends. The presence of 15% fewer total probes at saturation coverage suggests that for this particular sample the number of singly attached probes is about 70% of that of System I–III.

None of the systems show significant coupling at low coverage. System I begins to exhibit coupling at intermediate probe coverage with a dramatic increase occurring as coverage approaches saturation levels. System II shows significantly less coupling at both intermediate and saturation coverage. This is contrary to what might be anticipated from the view that the immobilization chain is simply a flexible attachment between the indicator and substrate. The experimental results suggest that the longer chain decreases the nearest neighbour interactions. If the effect of the longer chain was to allow more extensive interaction with neighbours System II would have exhibited greater coupling than System I. In fact, the short tether system coupled better than the long tether system. There are two possible explanations for this unexpected effect.

With the longer chain it may be that System II has greater access to the bulk solvent. If the chains extend fully the probe will interact more extensively with the solvent and thus less with the adjacent surface species (Fig. 3a). With the probes extended in this fashion interactions with the nearest surface bound species could be diminished. The increase in translational freedom may eliminate nearest neighbour interaction imposed by surface alignments. So the longer chain length of System II may allow the probe molecules to better separate from each other than if they were held closer to the substrate as in System I. According to this model, the short chain holds the probe molecules closer to one another forcing an increase in interaction between neighbours, thus

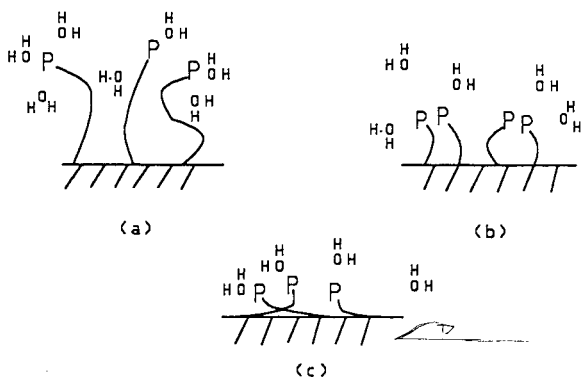


Fig. 3. Possible representations of the probe molecules on variable length tethers are shown: (a) System II extended with access to the bulk aqueous solution, (b) System I held closer to the surface and each other with less access to the bulk aqueous solution, (c) System II displaying hydrophobic tendencies with the apparent avoidance of the aqueous bulk solution.

creating a more favorable coupling environment (Fig. 3b).

On the other hand, it is possible that the longer alkyl tether serves as a hydrophobic anchor. The long tether exhibits greater hydrophobicity than the short tether and is therefore more attracted to the surface of the organosilane-modified silica gel and, thus, it may serve as a restraint to restrict contact between neighbours (Fig. 3c). This model would suggest that the absolute length of the chain is not as important as its "effective" length where its effective length is measured by its ability to extend into the bulk solvent.

System III was designed to distinguish between these two models for explaining the effect of chain length. System III has the chain length of System I; therefore, if the coupling characteristics are indeed controlled by chain length System III should mimic System I. On the other hand, System III (the branched system) is similar to System II in terms of hydrophobicity since they both have the same number of alkyl carbons in their chains. If the characteristics of System II are controlled by its hydrophobic tendencies, System III should mimic the response of System II for it would resemble System II folded up on the surface of the substrate. The results of the chemical cou-

pling vs. hydrolysis competition trials with System III are also shown in Fig. 2. As can be seen the coupling characteristics of System III resemble, quite closely, those of System II. This supports the hypothesis that it is the inability of the longer tether to fully extend into the aqueous solvent that dominates its properties. The probe does not interact with its neighbours because its freedom of motion is inhibited by the collapse of the tether to minimize unfavorable solvent interactions.

On the other hand, significant coupling occurred when a hydrophilic side chain was used. System IV (shown in Fig. 1) contains a four-carbon chain with a carboxylic acid on the side chain. Apparently the resulting increase in hydrophilic character of the tether permits better solvation of the system thereby allowing the probe to lift off the surface of the substrate and into the reactive environment. The degree of coupling is markedly higher for System IV even at intermediate coverage. As stated above it is not possible to attain coverages as high with System IV as with Systems I–III since some of the probes occupy two surface sites. In spite of this complicating factor, the relevant point is clearly that increasing the hydrophobicity of the four carbon tether results in a dramatic increase in the interaction between nearest sites.

The preceding discussions focus on the steric restrictions imposed by the tethers. It is relevant to consider the extent to which these changes in the tether will affect the probe through electronic interactions. Each chain contains an amide linkage which has the potential of withdrawing electron density from the probe. The variation in position of the amide relative to the probe will affect the probe to some extent as will the presence or absence of the alkyl side chain on the tether. In an attempt to minimize these electronic effects and thus emphasize the steric effects, at least one alkyl link was included next to the probe to insulate it from the rest of the chain. The presence of even one methylene spacer will significantly decrease the electronic effects between a ring and a side chain [9]. The effect of whatever leakage there is through the insulating link on the extent of the self-coupling process is

not readily predictable. The self-coupling process involves electrophilic attack of the diazonium group of one probe on the ring of the adjacent probe [5]. The electronic effect from the various groups in the chain will impact the electrophile and the site of attack in an opposing fashion. Chain modifications that make the diazonium ion more electrophilic will make the adjacent probe less susceptible to electrophilic attack. To experimentally determine which effect dominates, we prepared a system that is analogous to System I except the insulating methylene spacer was removed. This places the electron withdrawing amide linkage immediately adjacent to the probe. If the electronic effect plays a significant role in Systems I–IV then it would be reflected in a dramatic way in the system without the insulating link. For the system without the methylene insulator no coupling was observed, even at the highest levels of probe coverage. Thus, if an electronic effect is a major factor in the other systems they should reflect deactivation where electron withdrawing effects exist. In fact, the trend is contrary to this prediction. For example, System I couples more than System II and III, System IV couples more than System III. Consequently, the steric consideration discussed above seem to provide a better explanation of the data than the electronic effects which appear to be contrary to the observed trend.

We conclude that the nature of the tether has a significant impact on the magnitude of the

steric restrictions imposed on an immobilized reagent. Data from the four systems studied suggest that the extent to which an immobilized tether extends into the solvent rather than its absolute length controls the nearest neighbour interactions. Thus, a longer hydrophobic alkyl tether may inhibit nearest neighbour interactions more effectively than an analogous short tether. Further studies concerning the effects of additional side chains, both hydrophobic and hydrophilic are being performed.

This material is based on work supported by the National Science Foundation under Grant CHE 8611588.

REFERENCES

- 1 D.E. Leyden, L.W. Burggraf, D.S. Kendall and F.J. Pern, *Anal. Chim. Acta*, 129 (1981) 19.
- 2 T.J. Pinnavaia, J.G. Lee and M. Abedeni, in D.E. Leyden and W. Collins (Eds.), *Silylated Surfaces*, Gordon and Breach, New York, 1980, p. 333.
- 3 M.A. Ditzler, H. Pierre-Jacques and S.A. Harrington, *Anal. Chem.*, 58 (1986) 195.
- 4 M.A. Ditzler and K.A. Mills, *Anal. Lett.*, 22 (1989) 403.
- 5 M.A. Ditzler, N.T. Spellman and J.M. Dulac, *Anal. Chim. Acta*, 243 (1991) 103.
- 6 A.L. Wilds and W.R. Biggerstaff, *J. Am. Chem. Soc.*, 67 (1945) 789.
- 7 J.M. Hill, *J. Chromatogr.*, 76 (1973) 455.
- 8 G. Kortum, *Reflectance Spectroscopy*, Springer-Verlag, New York, 1969.
- 9 C.D. Johnson, *The Hammett Equation*, Cambridge University Press, New York, 1973, p. 18.

Numerical treatment of titrations with the formation of a reasonably stable complex: titration of thiocyanate with Hg(II)

Víctor Rodríguez Martín

Institute for Professional Formation of Béjar, Béjar, Salamanca (Spain)

Oroncio Jiménez de Blas

Department of Analytical Chemistry, Nutrition and Food Science, Faculty of Chemical Sciences, University of Salamanca, 37008 Salamanca (Spain)

(Received 23rd June 1992; revised manuscript received 20th October 1992)

Abstract

A numerical procedure is described for tracing the curves obtained in the titration of thiocyanate with Hg(II) using Fe(III) as an indicator. The procedure permits the monitoring of the evolution of the concentration of all the species participating in the titration and the determination of the end-point and hence the expected error in the titration. A study was made of the error obtained as a function of the concentration of thiocyanate to be titrated and of the amount of indicator employed. The error decreases on increasing the concentration of the species to be titrated and the amount of Fe(III). Throughout the treatment the effect of dilution is taken into account.

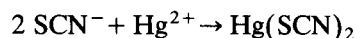
Keywords: Titrimetry; Numerical analysis; Thiocyanate

The numerical treatment of titration curves has been addressed in many works, generally involving acid–base volumetric studies [1–5] or redox titrations [6,7]. However, titrations by complex formation have received little attention.

The determination of a ligand via the formation of a moderately stable complex is a common technique [8,9]. An example of this is the titration of Hg(II) with thiocyanate, or the reverse, that of thiocyanate through the formation of Hg(II) complexes. Both titrations are sufficiently well known from the practical point of view [10]. However, titration curves are not easy to obtain by manual

methods as it is necessary to do the calculation point by point. This becomes more complicated as the number of simplifications becomes smaller. Thus, for example, the end-point should be determined as a function of the concentration of the different species constituting the indicator system. Without this evaluation it is not possible to determine the expected error in the titration.

In this work an algorithm of the curves obtained in the titration of thiocyanate by Hg(II) at pH 0 was developed based on the following reaction:



During the titration four complexes are formed, the formation constants of which are given in Table 1 [11]. Additionally, a precipitate of

Correspondence to: O. Jiménez de Blas, Department of Analytical Chemistry, Faculty of Sciences, University of Salamanca, 37008 Salamanca (Spain).

TABLE 1

Formation constants of complexes

Complex	Log β_i	Complex	Log β_i
HgSCN ⁺	9.1	Fe(SCN) ₃	5.0
Hg(SCN) ₂	17.2	Fe(SCN) ₄ ⁻	6.3
Hg(SCN) ₃ ⁻	20.0	Fe(SCN) ₅ ²⁻	6.2
Hg(SCN) ₄ ²⁻	21.8	Fe(SCN) ₆ ³⁻	6.1
FeSCN ²⁺	2.2	pK _s ^a of	
Fe(SCN) ₂ ⁺	3.6	Hg(SCN) ₂ precipitate	19.6

^a Solubility product.

Hg(SCN)₂ may appear, the solubility product of which is pK_s = 19.6 [11].

The indicator generally employed is Fe(III), which forms six complexes (Table 1). The hydroxylated species of Fe(III) are not considered, as they are not predominant at the pH of the titration.

This kind of situation is necessarily complicated and demands a treatment based on computer-aided calculations. The procedure developed allows one to take into account factors such as the increase in volume, which is often ignored.

COMPUTER STRATEGY

This is based on the solution of the system formed from the equilibrium constants (ten equations), the mass balances (three equations) and the precipitation of Hg(SCN)₂ (one equation).

If a precipitate is not formed, the equation to be solved is

$$\begin{aligned}
 [\text{SCN}]_{\text{added}} = [\text{SCN}^-] &+ \sum_{i=1}^4 \left\{ \frac{i\beta_i[\text{Hg}]_{\text{added}}[\text{SCN}^-]^i}{1 + \sum_{j=1}^4 (\beta_j[\text{SCN}^-]^j)} \right\} \\
 &+ \sum_{i=1}^6 \left\{ \frac{i\beta_i[\text{Fe}]_{\text{added}}[\text{SCN}^-]^i}{1 + \sum_{j=1}^6 (\beta_j[\text{SCN}^-]^j)} \right\}
 \end{aligned} \quad (1)$$

If a precipitate is formed, Eqn. 1 can be simplified to

$$\begin{aligned}
 [\text{SCN}]_{\text{added}} = [\text{SCN}^-] &+ \sum_{i=1}^4 (i\beta_i K_s [\text{SCN}^-]^{i-2}) \\
 &+ \sum_{i=1}^6 \left\{ \frac{i\beta_i [\text{Fe}]_{\text{added}} [\text{SCN}^-]^i}{1 + \sum_{j=1}^6 (\beta_j [\text{SCN}^-]^j)} \right\} \\
 &+ 2C_{\text{pp}} \quad (2)
 \end{aligned}$$

where C_{pp} is the "pseudo-concentration of precipitate" (ratio of the number of moles of precipitate to the total volume).

The overall process begins by assuming that no precipitate is formed, that is, solving Eqn. 1. Once the value of [SCN⁻] and [Hg²⁺] are known, one has to see if a precipitate is formed, by comparison with the solubility product. In the event of a precipitate being formed, Eqn. 2 is solved.

In order to solve both Eqns. 1 and 2, a variant of the bisection method is used, where the intermediate point is taken according to $L = (L_{\text{high}} L_{\text{low}})^{1/2}$.

RESULTS AND DISCUSSION

General shape of the curves

Figure 1 shows the evolution of the different species that are formed in the titration.

The criterion for the detection of the end-point is the disappearance of the red colour from the complexes formed between Fe(III) and thiocyanate. The lowest concentration of Fe(III) detectable by the formation of these complexes is ca. 10⁻⁵ M [11]. The end-point corresponds to the value at which the sum of the concentrations of the Fe(III)-SCN⁻ complexes is this value of 10⁻⁵ M. The interval in which, presumably, the end-point is detected is 10^{-4.5} and 10^{-5.5} M, as shown in Fig. 2.

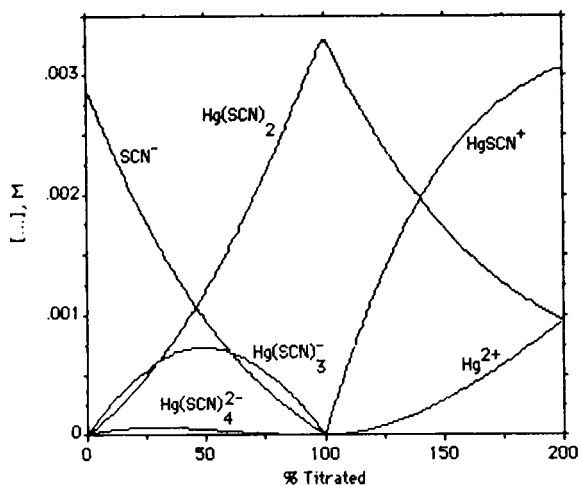


Fig. 1. Evolution of all the species, excluding those of the indicator. Titration of 25 ml of thiocyanate at a concentration of 0.01 M with Hg(II) at the same concentration, using 0.5 ml of a 1 M solution of Fe(III) as the indicator.

Effect of the concentration of thiocyanate to be evaluated

Different simulations of titrations of different concentrations of thiocyanate with the same concentration of Hg(II) were carried out using 0.5 mmol of Fe(III) in 0.5 ml as indicator; these simulations are shown in Figs. 3 and 4.

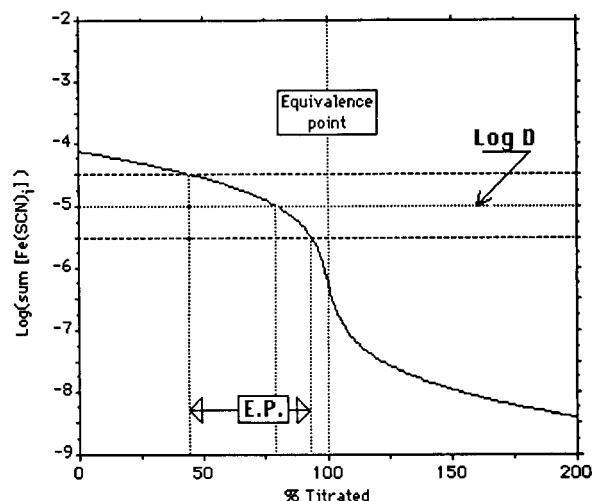


Fig. 2. Determination of the end-point of the titration. The curve corresponds to the simulation of the titration of 25 ml of thiocyanate at a concentration of 1×10^{-4} M with Hg(II) at the same concentration, using 0.5 ml of a 1 M solution of Fe(III) as indicator.

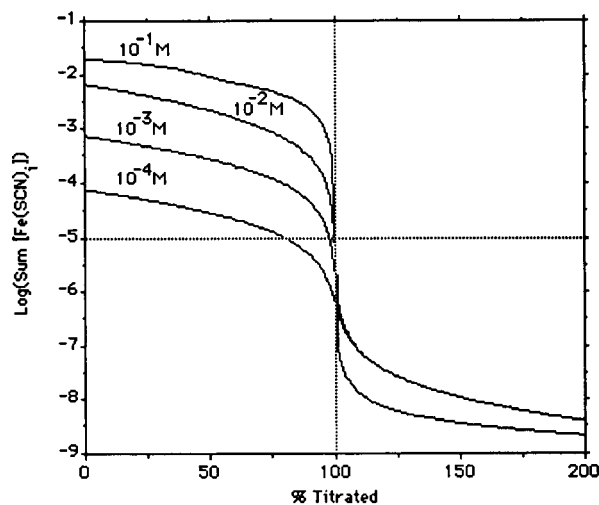


Fig. 3. Plot of the evolution of the Fe(III)-SCN complexes during titration for different concentrations of thiocyanate to be evaluated. The vertical axis represents the logarithm of the sum of concentrations of all the Fe(III)-SCN complexes.

As can be seen, amounts lower than $10^{-2.5}$ M cannot be determined owing to the error involved.

Effect of the amount of indicator

The amount of indicator strongly affects the error arising in the titration. The use of a saturated solution of Fe(III) as an indicator to be

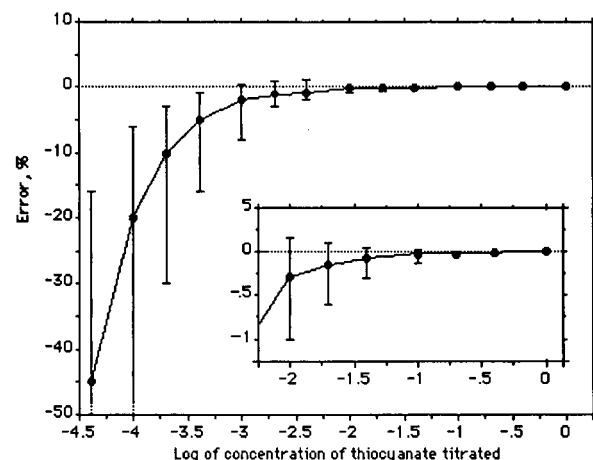


Fig. 4. Plot of estimated error (difference between the end-point and the equivalence point) as a function of the concentration of thiocyanate titrated with the same concentration of Hg(II) using Fe(III) as indicator.

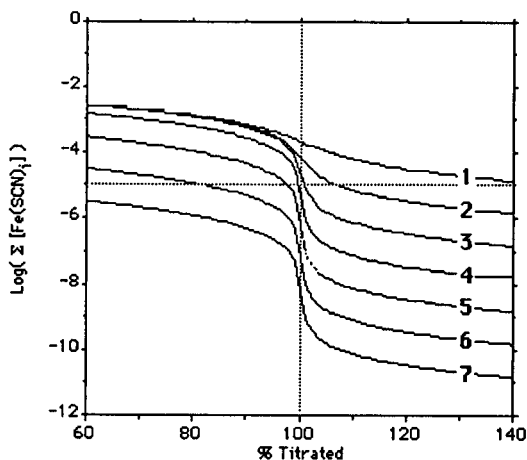


Fig. 5. Titration curves for 25 ml of a solution of 0.02 M thiocyanate with Hg(II) at the same concentration, using different amounts of Fe(III) as indicator [(1) 500; (2) 50; (3) 5; (4) 0.5; (5) 0.05; (6) 0.005; (7) 0.0005 mmol], from a solution of concentration 1 M.

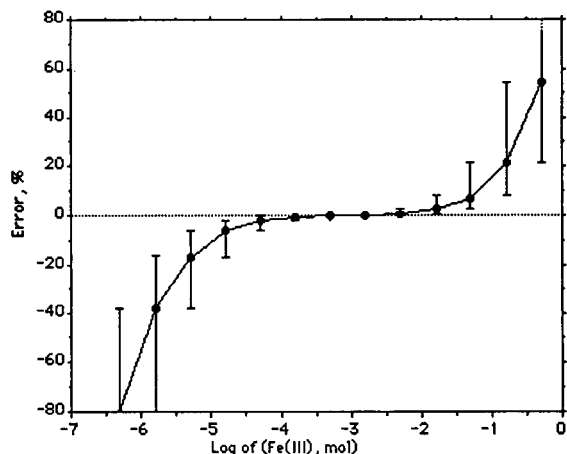


Fig. 6. Expected error intervals for the titration of 25 ml of 2×10^{-2} M thiocyanate with the same concentration of Hg(II) as a function of different amounts of Fe(III) used as indicator, from a solution of concentration 1 M.

added in the titration has been reported [10]. The curve of greatest interest is that corresponding to the sum of the concentrations of the Fe(III)–SCN⁻ complexes. Figure 5 shows these curves for different concentrations of indicator. As can be seen, they are identical, but displaced vertically. These has important repercussions on the error because, as has been stated, the end-point can be taken as the point where the curves intercept the concentration value of 10^{-5} M.

As shown in Fig. 6, the optimum amount of indicator is between 0.1 and 10 mmol; for larger and smaller amounts unacceptable, errors are obtained. One must take into account that 10 mmol corresponds to the use of 10 ml of a solution of indicator of concentration 1 M, an amount that will never be used in practice.

REFERENCES

- 1 G. Gran, *Acta Chem. Scand.*, 4 (1950) 559.
- 2 G. Gran, *Analyst*, 77 (1952) 661.
- 3 A. Johansson, *Analyst*, 95 (1970) 535.
- 4 M.C. Ortiz, J. López Palacios and L.A. Sarabia, *Quím. Anal.*, 7 (1988) 33.
- 5 J. Stur, M. Bos and E. van der Linden, *Anal. Chim. Acta*, 158 (1984) 93.
- 6 A.A.B. Wu and H.V. Malmstad, *Anal. Chem.*, 50 (1976) 2090.
- 7 L.M. Doane, J.T. Stock and J.D. Stuart, *Anal. Chem.*, 50 (1979) 2166.
- 8 W.F. Pickering, *Química Analítica Moderna*, Reverté, Barcelona, 1984, p. 404.
- 9 G.H. Ayres, *Análisis Químico Cuantitativo*, Del Castillo, Madrid, 1970, p. 351.
- 10 I.M. Kolthoff and V.A. Stenger, *Volumetric Analysis: Vol. II: Titration Methods*, Interscience, New York, 1947, p. 330.
- 11 F. Burriel Martí, F. Lucena Conde, S. Arribas Jimeno and

ANALYTICA CHIMICA ACTA, VOL. 274 (1993)

AUTHOR INDEX

- Abe, S.
—, Sone, T., Fujii, K. and Endo, M.
Liquid-liquid extraction of transition metal ions with macrocyclic Schiff bases containing phenol or thiophene subunits 141
- Alder, J.F., see Thomas, C.L.P. 171, 179
- Allegri, G., see Sturaro, A. 163
- Alves, J.L.
— and Ditzler, M.A.
A study of the effect of chain length on nearest neighbour interactions of immobilized species 361
- Andreae, M.O., see Cai, Y. 243
- Barnes, D.E.
—, Taylor, M.J.C., Marshall, G.D. and Van Staden, J.F.
Extraction of dicyanoaurate(I) using supported liquid membranes in a flow-injection manifold: evaluation of extractants 283
- Battiston, G., see Sturaro, A. 163
- Bergveld, P., see Luo, J. 7
- Bier, F.F., see Jockers, R. 185
- Boelens, H.F.M., see Van den Bogaert, B. 71, 87
- Borzitsky, J.A.
—, Dvinin, A.V., Petrukhin, O.M. and Urusov, Yu.I.
Segmental flow injection with ion-selective electrodes for the determination of fluoride in water 125
- Bos, M., see Luo, J. 7
- Bosch, E., see Rosés, M. 147
- Brown, R.B., see Liu, D. 37
- Cai, Y.
—, Rapsomanikis, S. and Andreae, M.O.
Determination of butyltin compounds in sediment using gas chromatography-atomic absorption spectrometry: comparison of sodium tetrahydroborate and sodium tetraethylborate derivatization methods 243
- Carlsen, M.
—, Christensen, L.H. and Nielsen, J.
Flow-injection analysis for the measurement of penicillin V in fermentation media 117
- Christensen, L.H., see Carlsen, M. 117
- Christie, I.M.
—, Vadgama, P. and Lloyd, S.
Modification of electrode surfaces with oxidised phenols to confer selectivity to amperometric biosensors for glucose determination 191
- Colin, J.P., see Cristante, M. 303
- Cristante, M.
—, Selves, J.-L., Grassy, G. and Colin, J.P.
Structure-activity relationship study on paraffin inhibitors for crude oils (INIPAR model II) 303
- Degn, H.
— and Frigaard, N.-U.
Membrane inlet manometry for the measurement of water activity in aqueous and organic solutions 355
- De la Guardia, M., see Gallignani, M. 267
- Ditzler, M.A., see Alves, J.L. 361
- Doretto, L., see Sturaro, A. 163
- Dvinin, A.V., see Borzitsky, J.A. 125
- Endo, M., see Abe, S. 141
- Fernández-Romero, J.M.
—, Luque de Castro, M.D. and Valcárcel, M.
Approaches to the development of spectrophotometric reaction-rate methods by use of immobilized enzymes in continuous-flow systems 99
- Fielden, P.R., see Thomas, C.L.P. 179
- Förster, E.
—, Silva, M., Otto, M. and Pérez-Bendito, D.
Enzymatic determination of alcohol mixtures at the nanogram level by the stopped-flow technique 109
- Franek, M.
— and Krivan, V.
Determination of sub-ng g⁻¹ concentrations of thorium and uranium in microelectronic materials by radiochemical neutron activation analysis 317
- Frigaard, N.-U., see Degn, H. 355
- Fujii, K., see Abe, S. 141
- Fujiwara, M.
—, Matsushita, T., Kobayashi, T., Yamashoji, Y. and Tanaka, M.
Preparation of an anion-exchange resin with quaternary phosphonium chloride and its adsorption behaviour for noble metal ions 293
- Gabor, G., see Walt, D.R. 47
- Gallignani, M.
—, Garrigues, S. and De la Guardia, M.
Direct determination of benzene in gasoline by flow-injection Fourier transform infrared spectrometry 267

- Garcia Mateo, J.V.
— and Martínez Calatayud, J.
Entrapped copper(II) carbonate for indirect determination of glycine by flow injection atomic absorption spectrometry 275
- Garrigues, S., see Gallignani, M. 267
- Goldberg, H.D., see Liu, D. 37
- Goyet, C., see Walt, D.R. 47
- Grassy, G., see Cristante, M. 303
- Guan, J.S., see Yang, X.J. 237
- Islam, M.A., see Stephen, W.I. 335, 347
- Iwamoto, E.
—, Shimazu, H., Yokota, K. and Kumamaru, T.
Atomization of tin in saline water media in graphite furnace atomic absorption spectrometry with a tungsten-coated tube using palladium as a chemical modifier 231
- Jiménez de Blas, O., see Rodríguez Martín, V. 367
- Jin, W., see Qu, L. 65
- Jockers, R.
—, Bier, F.F., Schmid, R.D., Wachtveitl, J. and Oesterhelt, D.
Herbicide biosensor based on photobleaching of the reaction centre of *Rhodobacter sphaeroides* 185
- Johansson, K.
—, Örnemark, U. and Olin, Å.
Solid-phase extraction procedure for the determination of selenium by capillary gas chromatography 129
- Kamo, N., see Kurosawa, S. 209
- Katsu, T., see Watanabe, K. 59
- Katsura, T., see Mizutani, F. 201
- Kitajima, H., see Kurosawa, S. 209
- Kobayashi, T., see Fujiwara, M. 293
- Krähenbühl, U., see Langenauer, M. 253
- Krivan, V., see Franek, M. 317
- Krivan, V., see Wildhagen, D. 257
- Kulys, J.
—, Wang, L. and Maksimoviene, A.
L-Lactate oxidase electrode based on methylene green and carbon paste 53
- Kumamaru, T., see Iwamoto, E. 231
- Kuroda, Y., see Michigami, Y. 299
- Kurosawa, S.
—, Kitajima, H., Ogawa, Y., Muratsugu, M., Nemoto, E. and Kamo, N.
Resonant frequency of a piezoelectric quartz crystal in contact with solutions 209
- Langenauer, M.
—, Krähenbühl, U. and Wyttenbach, A.
Determination of fluorine and iodine in biological materials 253
- Leech, D.
— and Rechnitz, G.A.
Crayfish walking leg neuronal biosensor for the detection of pyrazinamide and selected local anesthetics 25
- Liu, D.
—, Meyerhoff, M.E., Goldberg, H.D. and Brown, R.B.
Potentiometric ion- and bioselective electrodes based on asymmetric polyurethane membranes 37
- Lloyd, S., see Christie, I.M. 191
- Lu, J., see Wang, J. 219
- Luo, J.
—, Olthuis, W., Bergveld, P., Bos, M. and Van der Linden, W.E.
Modelling of coulometric sensor-actuator systems based on ISFETs with a porous actuator covering the gate 7
- Luque de Castro, M.D., see Fernández-Romero, J.M. 99
- Lyle, S.J.
— and Yassin, S.S.
Polarographic studies of metal ion complexes of Ampicillin and Amoxycillin 225
- Maksimoviene, A., see Kulys, J. 53
- Marshall, G.D., see Barnes, D.E. 283
- Martínez Calatayud, J., see Garcia Mateo, J.V. 275
- Matsushita, T., see Fujiwara, M. 293
- Meyerhoff, M.E., see Liu, D. 37
- Michigami, Y.
—, Kuroda, Y., Ueda, K. and Yamamoto, Y.
Determination of urinary fluoride by ion chromatography 299
- Mizutani, F.
—, Yabuki, S. and Katsura, T.
Amperometric enzyme electrode with fast response to glucose using a layer of lipid-modified glucose oxidase and Nafion anionic polymer 201
- Muratsugu, M., see Kurosawa, S. 209
- Nemoto, E., see Kurosawa, S. 209
- Nielsen, J., see Carlsen, M. 117
- Oesterhelt, D., see Jockers, R. 185
- Ogawa, Y., see Kurosawa, S. 209
- Okada, K., see Watanabe, K. 59
- Olin, Å., see Johansson, K. 129
- Olthuis, W., see Luo, J. 7
- Örnemark, U., see Johansson, K. 129
- Otto, M., see Förster, E. 109
- Parvoli, G., see Sturaro, A. 163
- Pérez-Bendito, D., see Förster, E. 109
- Petrukhin, O.M., see Borzitsky, J.A. 125
- Przybylko, A.R.M., see Thomas, C.L.P. 179
- Qu, L.
— and Jin, W.
Adsorption voltammetry of the gallium-morin system 65
- Rapsomanikis, S., see Cai, Y. 243
- Rechnitz, G.A., see Leech, D. 25
- Rodríguez Martín, V.
— and Jiménez de Blas, O.

- Numerical treatment of titrations with the formation of a reasonably stable complex: titration of thiocyanate with Hg(II) 367
- Rosés, M.
— and Bosch, E.
Linear solvation energy relationships in reversed-phase liquid chromatography. Prediction of retention from a single solvent and a single solute parameter 147
- Saito, M.
Influence of operating parameters on ion intensity in glow discharge mass spectrometry 327
- Schmid, R.D., see Jockers, R. 185
- Selves, J.-L., see Cristante, M. 303
- Shimazu, H., see Iwamoto, E. 231
- Silva, M., see Förster, E. 109
- Smit, H.C., see Van den Bogaert, B. 71, 87
- Snook, R.D., see Thomas, C.L.P. 179
- Sone, T., see Abe, S. 141
- Stephen, W.I.
— and Islam, M.A.
3,5,6-Trisubstituted 1,2,4-triazines as analytical reagents. Part I. Compounds containing the ferrioxal functional group or iron(II)-methine chromophore 335
— and Islam, M.A.
3,5,6-Trisubstituted 1,2,4-triazines as analytical reagents. Part II. Compounds containing the cuproine functional group 347
- Sturaro, A.
—, Parvoli, G., Doretto, L., Zanchetta, S., Allegri, G. and Battiston, G.
Simultaneous determination of trace metals in human hair by dynamic ion-exchange chromatography 163
- Tanaka, M., see Fujiwara, M. 293
- Taylor, M.J.C., see Barnes, D.E. 283
- Thomas, C.L.P.
— and Alder, J.F.
Effect of relative humidity on the performance of a platinum-lead denuder for the adsorption of nitrobenzene 171
—, Alder, J.F., Fielden, P.R., Przybylko, A.R.M., Snook, R.D. and Watson, A.F.R.
Precision humidifier for dynamic test atmosphere generators 179
- Tian, B., see Wang, J. 1
- Ueda, K., see Michigami, Y. 299
- Urusov, Yu.I., see Borzitsky, J.A. 125
- Vadgama, P., see Christie, I.M. 191
- Valcárcel, M., see Fernández-Romero, J.M. 99
- Van den Bogaert, B.
—, Boelens, H.F.M. and Smit, H.C.
Evaluation and correction of signal model errors in a matched filter for the quantification of chromatographic data 71
—, Boelens, H.F.M. and Smit, H.C.
Quantification of chromatographic data using a matched filter: robustness towards noise model errors 87
- Van der Linden, W.E., see Luo, J. 7
- Van Staden, J.F., see Barnes, D.E. 283
- Wachtveitl, J., see Jockers, R. 185
- Walt, D.R.
—, Gabor, G. and Goyet, C.
Multiple-indicator fiber-optic sensor for high-resolution pCO₂ sea water measurements 47
- Wang, J.
— and Lu, J.
Ultrace measurements of selenium by cathodic stripping voltammetry in the presence of rhodium 219
— and Tian, B.
Screen-printed electrodes for stripping measurements of trace mercury 1
- Wang, L., see Kulyts, J. 53
- Watanabe, K.
—, Okada, K. and Katsu, T.
Determination of methamphetamine in urine in situ using a methamphetamine-sensitive membrane electrode 59
- Watson, A.F.R., see Thomas, C.L.P. 179
- Wildhagen, D.
— and Krivan, V.
Determination of platinum in environmental and geological samples by radiochemical neutron activation analysis 257
- Wytttenbach, A., see Langenauer, M. 253
- Yabuki, S., see Mizutani, F. 201
- Yamamoto, Y., see Michigami, Y. 299
- Yamashoji, Y., see Fujiwara, M. 293
- Yang, X.J.
— and Guan, J.S.
Application of inductively coupled plasma atomic emission spectrometry for the certificate analysis of uranium certified reference material: determination of trace impurity elements in U₃O₈ by extraction chromatography 237
- Yassin, S.S., see Lyle, S.J. 225
- Yokota, K., see Iwamoto, E. 231
- Zanchetta, S., see Sturaro, A. 163

PUBLICATION SCHEDULE FOR 1993

	S'92	O'92	N'92	D'92	J	F	M	A	M	J	J	A
Analytica Chimica Acta	267/1 267/2	268/1 268/2	269/1 269/2	270/1 270/2	271/1 271/2	272/1 272/2 273/1-2	274/1 274/2	275/1-2 276/1	276/2 277/1	277/2 278/1 278/2	279/1 279/2	280/1 280/2
Vibrational Spectroscopy		4/1			4/2		4/3					

INFORMATION FOR AUTHORS

Manuscripts. The language of the journal is English. English linguistic improvement is provided as part of the normal editorial processing. Authors should submit three copies of the manuscript in clear double-spaced typing on one side of the paper only. *Vibrational Spectroscopy* also accepts papers in English only.

Abstract. All papers and reviews begin with an Abstract (50–250 words) which should comprise a factual account of the contents of the paper, with emphasis on new information.

Figures. Figures should be prepared in black waterproof drawing ink on drawing or tracing paper of the same size as that on which the manuscript is typed. One original (or sharp glossy print) and two photostat (or other) copies are required. Attention should be given to line thickness, lettering (which should be kept to a minimum) and spacing on axes of graphs, to ensure suitability for reduction in size on printing. Axes of a graph should be clearly labelled, along the axes, outside the graph itself. All figures should be numbered with Arabic numerals, and require descriptive legends which should be typed on a separate sheet of paper. Simple straight-line graphs are not acceptable, because they can readily be described in the text by means of an equation or a sentence. Claims of linearity should be supported by regression data that include slope, intercept, standard deviations of the slope and intercept, standard error and the number of data points; correlation coefficients are optional. Photographs should be glossy prints and be as rich in contrast as possible; colour photographs cannot be accepted. Line diagrams are generally preferred to photographs of equipment.

Computer outputs for reproduction as figures must be good quality on blank paper, and should preferably be submitted as glossy prints.

Nomenclature, abbreviations and symbols. In general, the recommendations of the International Union of Pure and Applied Chemistry (IUPAC) should be followed, and attention should be given to the recommendations of the Analytical Chemistry Division in the journal *Pure and Applied Chemistry* (see also *IUPAC Compendium of Analytical Nomenclature, Definitive Rules, 1987*).

References. The references should be collected at the end of the paper, numbered in the order of their appearance in the text (*not* alphabetically) and typed on a separate sheet.

Reprints. Fifty reprints will be supplied free of charge. Additional reprints (minimum 100) can be ordered. An order form containing price quotations will be sent to the authors together with the proofs of their article.

Papers dealing with vibrational spectroscopy should be sent to: Dr J.G. Grasselli, 150 Greentree Road, Chagrin Falls, OH 44022, U.S.A. Telefax: (+ 1-216) 2473360 (Americas, Canada, Australia and New Zealand) or Dr J.H. van der Maas, Department of Analytical Molecule Spectrometry, Faculty of Chemistry, University of Utrecht, P.O. Box 80083, 3508 TB Utrecht, The Netherlands. Telefax: (+ 31-30) 518219 (all other countries).

No part of this publication may be reproduced, stored in a retrieval system or transmitted in any form or by any means, electronic, mechanical, photocopying, recording or otherwise, without the prior written permission of the publisher, Elsevier Science Publishers B.V., Copyright and Permissions Dept., P.O. Box 521, 1000 AM Amsterdam, The Netherlands.

Upon acceptance of an article by the journal, the author(s) will be asked to transfer copyright of the article to the publisher. The transfer will ensure the widest possible dissemination of information.

Special regulations for readers in the U.S.A.—This journal has been registered with the Copyright Clearance Center, Inc. Consent is given for copying of articles for personal or internal use, or for the personal use of specific clients. This consent is given on the condition that the copier pays through the Center the per-copy fee for copying beyond that permitted by Sections 107 or 108 of the U.S. Copyright Law. The per-copy fee is stated in the code-line at the bottom of the first page of each article. The appropriate fee, together with a copy of the first page of the article, should be forwarded to the Copyright Clearance Center, Inc., 27 Congress Street, Salem, MA 01970, U.S.A. If no code-line appears, broad consent to copy has not been given and permission to copy must be obtained directly from the author(s). All articles published prior to 1980 may be copied for a per-copy fee of US \$2.25, also payable through the Center. This consent does not extend to other kinds of copying, such as for general distribution, resale, advertising and promotion purposes, or for creating new collective works. Special written permission must be obtained from the publisher for such copying.

No responsibility is assumed by the publisher for any injury and/or damage to persons or property as a matter of products liability, negligence or otherwise, or from any use or operation of any methods, products, instructions or ideas contained in the material herein.

Although all advertising material is expected to conform to ethical (medical) standards, inclusion in this publication does not constitute a guarantee or endorsement of the quality or value of such product or of the claims made of it by its manufacturer.

This issue is printed on acid-free paper.

PRINTED IN THE NETHERLANDS

CHEMICAL SENSOR TECHNOLOGY

Volume 4

edited by **S. Yamauchi**, National Rehabilitation Center for the Disabled, Tokorozawa, Japan

This volume is the fourth in a series of annual reviews on progress in the research and technology of chemical sensors.

New principles, new devices, and the detailed mechanism of various chemical sensors are described. Chemical sensors continue to grow rapidly in importance, encompassing a broad spectrum of technologies covering safety, pollution, fuel economy, medical engineering and industrial processes.

More than half the chapters in this volume are relevant to biosensing, a strategic field for medical and health care equipment, especially in geriatric medicine.

Because biochemical substances play major roles in physiological processes such as metabolism, excitation and contraction of skeletal muscle, and neurotransmission, chemical sensing of the related biochemical substances will eventually become indispensable.

Each chapter is written by an expert active in the front lines of chemical sensor research. Not only is the technological essence of the subject provided, but also the background and philosophy, an evaluation of achievements to date and problems to be dealt with. Each topic is described in sufficient depth to be useful to researchers worldwide.

Contents: Development of the TGS Gas Sensor (*A. Chiba*). Some Basic Aspects of Semiconductor Gas Sensors (*N. Yamazoe, N. Miura*). Silicon Technologies for Sensor Fabrication (*W. Mokwa*). Characterization of Oxygen Adsorbates on Semiconductive Oxides (*M. Iwamoto*). Miniaturization of Catalytic Combustion Sensors (*H. Futata*). Solid Electrolyte Potentiometric Oxygen Gas Sensors (*C.M. Mari, G.B. Barbi*). NASICON: a Sensitive Membrane for Ion Analysis (*P. Fabry, E. Siebert*). Characterization of Poly(dimethyldiallyl-ammonium chloride) and its Application to Electrochemical Sensors (*R.S. Tieman, K.L. Rauen, W.R. Heineman, E.W. Huber*). Biosensors with Microvolume Reaction Chambers (*L. Bousse, J.C. Owicki, J.W. Parce*). Enzyme Sensor Utilizing an Immobilized Mediator (*F. Mizutani, S. Yabuki*). Piezoelectric Biosensors

(*G.J. Bastiaans*). Sensitization of Dielectric Surfaces by Chemical Grafting Application to ISFETs and ENFETs (*P. Clechet, N.J. Renault, C. Martelet*). High Sensitive Immunosensor Employing Surface Photovoltage Technique (*T. Katsube, H. Uchida*). Non-invasive Monitoring of Glucose in Blood (*J. Kimura, T. Kuriyama, M. Kikuchi, T. Arai*). Biosensing System for Odor Compounds Using Plants (*H. Matsuoka*). Index.

1992 xviii + 270 pages
Price: US \$191.50 / Dfl. 335.00
ISBN 0-444-98680-4

Coedition with and distributed in Japan by Kodansha Scientific Ltd.

ORDER INFORMATION

For USA and Canada
ELSEVIER SCIENCE PUBLISHERS
Judy Weislogel
P.O. Box 945
Madison Square Station,
New York, NY 10160-0757
Tel: (212) 989 5800
Fax: (212) 633 3880

In all other countries
ELSEVIER SCIENCE PUBLISHERS

P.O. Box 211
1000 AE Amsterdam
The Netherlands
Tel: (+31-20) 5803 753
Fax: (+31-20) 5803 705

US\$ prices are valid only for the USA & Canada and are subject to exchange fluctuations; in all other countries the Dutch guild price (Dfl.), is definitive. Books are sent postfree if prepaid.



ELSEVIER
SCIENCE PUBLISHERS



0003-2670(19930315)274:2-1-F

711/414\141\0001-00